

N 7 1 - 2 5 2 4 9

NASA CR 118265

NATIONAL AERONAUTICS AND SPACE ADMINISTRATION

Bibliography 39-12

*Publications
of the
Jet Propulsion Laboratory:
July Through December 1970*

CASE FILE
COPY

JET PROPULSION LABORATORY
CALIFORNIA INSTITUTE OF TECHNOLOGY
PASADENA, CALIFORNIA

May 15, 1971

NATIONAL AERONAUTICS AND SPACE ADMINISTRATION

Bibliography 39-12

*Publications
of the
Jet Propulsion Laboratory:
July Through December 1970*

JET PROPULSION LABORATORY
CALIFORNIA INSTITUTE OF TECHNOLOGY
PASADENA, CALIFORNIA

May 15, 1971

Prepared Under Contract No. NAS 7-100
National Aeronautics and Space Administration

Foreword

The JPL Bibliography describes and indexes the formalized technical reporting for a 12-month period that resulted from scientific and engineering work performed, or managed, by the Jet Propulsion Laboratory. However, Bibliography 39-12 includes only the six months of reporting released July through December 1970 in order to change the publication schedule from a fiscal to a calendar year basis.

Four classes of publications are included:

- (1) Technical Reports (32 series), in which the information is complete for a specific accomplishment and is intended for a wide audience. Technical Reports can be either new reports or reprints of certain articles published in the open literature.
- (2) Technical Memorandums (33 series), in which the information is complete for a specific accomplishment but is intended for a limited audience to satisfy unique requirements.
- (3) Articles from three volumes of the Space Programs Summary (37 series). Each volume's collection of articles presents a periodical survey of current accomplishments in the subject area covered by that volume, namely:
 - Volume I. *Flight Projects*
 - Volume II. *The Deep Space Network*
 - Volume III. *Supporting Research and Advanced Development*
- (4) Open literature articles that were not selected for reprint release as Technical Reports.

The publications are indexed by: (1) author, (2) publication type and number, and (3) subject. A descriptive entry appears under the name of each author of each publication; an abstract is included with the entry for the primary (first-listed) author. Unless designated otherwise, all publications listed are unclassified.

JPL personnel can obtain loan copies of formal documents cited from the JPL Library. Personnel of outside organizations can obtain information copies of documents cited by addressing a written request to the Technical Information and Documentation Division Support Section, Attention: Mr. Leo R. Lunine, Jet Propulsion Laboratory, 4800 Oak Grove Drive, Pasadena, California 91103. If documents are out of print, an alternate source for the material will be given to the requester.

Contents

Author Index	1
Publication Index	111
Major Categories Used in Subject Index	119
Subject Index	120

Author Index

ABEL, J.

A001 Attitude Control and Structural Response Interaction

J. Abel

Technical Report 32-1461, November 15, 1970

This report presents an assessment of the problem of the interaction between the structural or elastic response of a spacecraft and the attitude control system dynamics. A general discussion of the problem modes of interaction provides a means of classifying a given spacecraft with respect to the interaction problem. A model spacecraft system is studied and some parameters characterizing the interactions are identified. The question of system stability in the mathematical sense is discussed and the idea of a definition of a practical stability criterion is presented. This concept is applied to the model spacecraft system. Some comments on the adequacy of present methods of evaluating the significance of interactions between attitude control systems and structures are given with particular regard to the concept of frequency separation.

ABHYANKAR, K. D.

A002 An Interferometric Approach to the Measurement of Optical Polarization

A. L. Fymat and K. D. Abhyankar

Appl. Opt., Vol. 9, No. 5, pp. 1075-1081, May 1970

For abstract, see Fymat, A. L.

ACTON, C. H., JR.

A003 Television Image Processing for Navigation

C. H. Acton, Jr.

Support Research and Advanced Development, Space Programs Summary 37-63, Vol. III, pp. 103-105, June 30, 1970

An optical-approach guidance navigation experiment was performed on the *Mariner* Mars 1969 mission. The experiment used spacecraft engineering data and science TV pictures to estimate the spacecraft trajectory relative to Mars during Mars approach. The spacecraft-centered direction to the center of Mars was used as an observable in this navigation process. This article discusses the algorithms used to estimate the location of the center of the Mars image in the digitized TV pictures.

ADAMS, M.

A004 Improved Solar Cell Contact-Interconnect Feasibility Study

M. Adams

Supporting Research and Advanced Development, Space Programs Summary 37-64, Vol. III, pp. 80-87, August 31, 1970

This study was conducted to evaluate new materials and design approaches to the problems of structural mounting and electrical interconnection encountered in the fabrication of silicon solar cell arrays. The primary objective was to reduce the cost of fabrication. Nine commercial thick-film inks and seven organic metal resins were evaluated in a program to determine whether thick-film screenable contacts could be used to form the contact patterns on solar cells. The results of this study indicated that an unfluxed aluminum ink was the only material that appears to have promise as a contact material. A prototype submodule of a solar array was constructed using screen-on-aluminum ink for contacts and a novel dielectric epoxy resin wrap-around technology permitting both N and P contacts to be made on the back side of the cell. The electrical interconnection and structural mounting were accomplished simultaneously by bonding the cells to a "printed circuit" substrate with conductive epoxy resins.

AKLONIS, J. J.

A005 A Generalization of the Boltzmann Superposition Principle

J. Moacanin, J. J. Aklonis, and R. F. Landel

Supporting Research and Advanced Development, Space Programs Summary 37-63, Vol. III, pp. 207-209, June 30, 1970

For abstract, see Moacanin, J.

AKSNES, K.

A006 A Second-Order Artificial Satellite Theory Based on an Intermediate Orbit

K. Aksnes

Technical Report 32-1507, November 1, 1970

An analytical second-order theory is developed for the motion of a satellite of an oblate planet whose gravitational potential includes the second, third, and fourth

zonal harmonics. It is assumed that J_2 is a small quantity of the first order and that J_3 and J_4 are of the second order.

The secular and the periodic perturbations are obtained to the third and to the second order, respectively. The former are contained in the Delaunay variables l'' , g'' , h'' , which are linear functions of the time, while the latter are given as additions to the Hill variables i'' , r'' , G'' , u'' , h'' in the form of trigonometric series with constant coefficients.

The theory is distinguished by a relative simplicity and compactness of the final algorithm achieved by the use of the following special devices and techniques: (1) an intermediate orbit, (2) Hori's perturbation method, and (3) the Hill variables.

A comparison with the results of numerical integration of the equations of motion indicates that the theory is capable of predicting the position of a near-earth satellite to better than one meter over one hundred revolutions.

AKYUZ, F. A.

A007 Natural Coordinate Systems: An Automatic Input Data Generation Scheme for a Finite-Element Method

F. A. Akyuz

Technical Report 32-1486 (Reprinted from *Nucl. Eng. Des.*, Vol. 11, No. 2, pp. 195-207, March 1970)

A description of a scheme for automatic input data generation for a finite-element method is presented. The basic algorithm is based on a suitable classification of the topological properties of complex geometrical configurations in one-, two-, or three-dimensional space. The algorithm provides for an automatic means of discretization for continuous domains of any form by using the concept of natural coordinate systems; this concept is introduced in this article. Depending on the complexity of the geometrical form and the diversity of the field quantities associated with different regions in the domain considered or on its boundary, the solution domain is divided into subdomains. Each subdomain has homogeneous field properties and reasonably convex form. The field quantities and geometrical properties associated with each region and the connectivity information of the adjacent subdomains are provided by the user as input. The generation of the mesh, computations of nodal coordinates, and the distribution of the field properties to each finite element are automatically performed. Examples from stress analysis are given.

ALLEN, J. E.

A008 [DSN] Monitor System

J. E. Allen

The Deep Space Network, Space Programs Summary 37-65, Vol. II, pp. 6-13, September 30, 1970

The Deep Space Network (DSN) Monitor System provides the capability to determine failures to the facility subsystem level and distribute data to the DSN Tracking Telemetry, Command, and Operations Control Systems. This article describes the DSN Monitor System for the Mark III era, with emphasis on the monitor criteria data set generation. The interface between the monitor system and the other DSN systems at both the system level and the facility level is described.

ALLEN, L. H.

A009 Operation of the Surveyor Television System in the Photon-Integration Mode

L. H. Allen and P. M. Salomon

J. SMPTE (Society of Motion Picture and Television Engineers), Vol. 79, No. 7, pp. 615-620, July 1970

The *Surveyor* television system was designed to obtain panoramic images of the lunar terrain from a spacecraft-landed position. The televised images provided photometric and photogrammetric information about the lunar surface, in addition to serving as the feedback loop necessary to complete other onboard scientific experiments. A photon-integration mode of vidicon camera operation was included in the *Surveyor* television system to provide the necessary increase in sensitivity to obtain television images during lunar sunset and earthshine-illuminated operations. By utilizing the unique image-storage capabilities of a slow-scan vidicon, exposures of as long as 30 min in duration were possible. Scene luminance levels on the order of 0.008 fL provided usable vidicon target exposures. The principal limitation of integration time was found to be the rate of dark current buildup. Accurate pre-launch camera calibration provided the necessary camera characteristic data to allow the resultant television pictures to be corrected for dark current and other vidicon-induced distortions.

AMOROSE, R. J.

A010 DSN Telemetry Systems Operations Group

R. J. Amorose

The Deep Space Network, Space Programs Summary 37-63, Vol. II, pp. 3-6, May 31, 1970

The Deep Space Network (DSN) Telemetry Systems Operations Group, which is comprised of two teams of real-time and non-real-time analysts, is responsible

for supervising the performance of the DSN Telemetry System. The DSN telemetry analysts monitor critical points throughout the telemetry system in real time to evaluate system performance. In the event of telemetry system anomalies, corrective courses of action are recommended. A description of the analysis function and the services provided by the Operations Group are given.

ANDERSON, J. D.

A011 Celestial Mechanics Experiment for Mariner Mars 1971

J. Lorell, J. D. Anderson, and I. I. Shapiro (Massachusetts Institute of Technology)
Icarus: Int. J. Sol. Sys., Vol. 12, No. 1, pp. 78–81, January 1970

For abstract, see Lorell, J.

ANDERSON, T. O.

A012 Digital Transition Tracking Symbol Synchronizer for Low SNR Coded Systems

W. J. Hurd and T. O. Anderson
Technical Report 32-1488 (Reprinted from *IEEE Trans. Communication Technology*, Vol. COM-18, No. 2, pp. 141–147, April 1970)

For abstract, see Hurd, W. J.

A013 Digital Acquisition and Detection: Minimum Switching Network for Generating the Weight, in Binary Notation, of a Binary Vector

T. O. Anderson
The Deep Space Network, Space Programs Summary 37-64, Vol. II, pp. 33–35, August 31, 1970

Implementation of the weight function, in binary notation, of a binary vector finds numerous applications in Deep Space Network coding systems. It applies not only to the encoders and decoders of both block codes and convolutional codes, but also to coding systems used in searching for good codes. This article discusses the most common implementation of this function, as well as other possible implementations. The implementation described here features maximum speed of operation with a minimum amount of hardware. The proposed switching network is entirely modular in its structure; only a single type of module is used in an iterative pattern. The module is described in detail, the modular structure is discussed, and an example of a 24-bit network is shown. The module network can be proven to be theoretically optimum for a minimum-hardware, minimum-propagation-time network using a single type of module in an iterative pattern.

ANDREWS, G. R.

A014 Polaroid Quick-Look System

R. D. Brandt and G. R. Andrews
Supporting Research and Advanced Development, Space Programs Summary 37-62, Vol. III, pp. 22–25, April 30, 1970

For abstract, see Brandt, R. D.

ARNETT, J. C.

A015 Evaluation of 26–32 AWG Wire for Outer Planet Mission Applications

J. C. Arnett
Technical Memorandum 33-463, December 1, 1970

Tests were performed establishing dimensional, physical, electrical, and handling characteristics of small-gage wire for outer planet mission applications. Environmental tests in vacuum and low temperature were made to evaluate exposure-related degradation effects. The most promising candidates for electronic packaging applications on future spacecraft were selected.

ARNOLD, J. R.

A016 Gamma Ray Spectroscopic Measurements of Mars

A. E. Metzger and J. R. Arnold (University of California, San Diego)
Appl. Opt., Vol. 9, No. 6, pp. 1289–1303, June 1970

For abstract, see Metzger, A. E.

ARTHUR, E.

A017 Spectral Observations of Jupiter in the Frequency Interval 18.5–24.0 GHz: 1968

D. E. Jones (Brigham Young University), B. L. Meredith, and E. Arthur
Pub. Astron. Soc. Pacific, Vol. 82, No. 484, pp. 122–125, February 1970

For abstract, see Jones, D. E.

ASHLOCK, J. C.

A018 Quasi-Linearity of Digital Record/Reproduce Process on Magnetic Tape Recorders

J. C. Ashlock
Supporting Research and Advanced Development, Space Programs Summary 37-62, Vol. III, pp. 203–206, April 30, 1970

A new phenomenon of digital tape recorders termed “quasi-linearity” is described and discussed, and the

conditions necessary for its existence are examined. The significance of this phenomenon in digital tape recording is indicated. It is shown that, by employing a decision theoretic approach, the quasi-linearity phenomenon can be used to derive the structure of the optimum bit detector for use in reconstructing a binary bit stream from the signal of the playback heads. In addition, a simple, attractive bit detector is described and discussed in detail.

ATKINSON, G.

A019 Magnetospheric Flows and Their Time Dependence

T. Unti and G. Atkinson

Supporting Research and Advanced Development, Space Programs Summary 37-62, Vol. III, p. 53, April 30, 1970

For abstract, see Unti, T.

A020 Auroral Arcs: Result of the Interaction of a Dynamic Magnetosphere with the Ionosphere

G. Atkinson

J. Geophys. Res., Space Physics, Vol. 75, No. 25, pp. 4746-4755, September 1, 1970

A model of auroral arcs is presented. It is assumed that the magnetic field lines into the auroral oval are loaded with kev electrons, that precipitating auroral electrons locally constitute a net field-aligned current, and that currents close in the outer magnetosphere by polarization currents. The model predicts that a flux tube convecting through the oval will undergo a highly nonlinear oscillation that produces standing waves, the auroral arcs. The conditions to be satisfied are (1) Ohm's law in the ionosphere, (2) electron number conservation in the ionosphere, (3) electric current continuity, (4) the tendency for electric fields to map between ionosphere and magnetosphere. The physics of condition 4 is not understood, but it is probable that arc-like solutions exist for several models. A specific model, including perfect mapping of electric fields, is studied. The solutions to this model closely resemble the arcs. Predicted in agreement with observation are arc thickness, inter-arc spacing, and the electric field behavior. The thickness and the spacing are functions of both the amplitude of the oscillation and the physical properties of the system. However, thickness times spacing is a function of the physical properties only, and the thickness divided by the spacing is a function of amplitude only. Presumably these and other quantitative relationships can be checked by observations.

AVIŽIENIS, A.

A021 Digital Fault Diagnosis by Low-Cost Arithmetical Coding Techniques

A. Avižienis

Technical Report 32-1476, August 1, 1970

Error-detecting and correcting codes may be employed to diagnose (i.e., detect and locate) logic faults in a digital computer concurrently with its normal operation. Arithmetic error codes must be used if the same code is to be used in the entire computer. A class of arithmetic codes with a low-cost check algorithm is analyzed which possesses partial fault location properties. Complete fault location (i.e., single error correction) is then attained by multiple encodings. The results are applied to both residue and product (or An) arithmetic error codes.

A022 Reliability Analysis and Architecture of a Hybrid-Redundant Digital System: Generalized Triple Modular Redundancy With Self-Repair

F. P. Mathur and A. Avižienis (University of California, Los Angeles)

Technical Report 32-1490 (Reprinted from Proceedings of the American Federation of Information Processing Societies Conference, Atlantic City, New Jersey, May 5-7, 1970, Vol. 36, pp. 375-383)

For abstract, see Mathur, F. P.

BACK, L. H.

B001 Acceleration and Cooling Effects in Laminar Boundary Layers—Subsonic, Transonic, and Supersonic Speeds

L. H. Back

AIAA J., Vol. 8, No. 4, pp. 794-802, April 1970

The structure of laminar boundary layers is investigated analytically over a large range of values of flow acceleration, surface cooling, and flow speeds. For flow of a perfect gas over an isothermal surface, the transformed boundary-layer equations with the similarity assumption were solved numerically for values of the acceleration parameter β up to 20, a value not uncommon to transonic flow in supersonic nozzles and for flat-faced bodies placed in supersonic flow, as well as for values of the surface-to-total-gas enthalpy g_w ranging from 0 (severely cooled surface) to 1. The solutions were inverted and shown in the physical plane, where the velocity and total enthalpy profiles depend upon the flow speed or compressibility parameter S in addition to β and g_w . Friction and heat-transfer parameters, as well as thicknesses associated

with the boundary layer, are also shown. In general, the effects of acceleration, cooling, and flow speed are significant, but the dependence of the heat-transfer parameter on $\bar{\beta}$ and g_w is weak when g_w is small. Application of the similarity solutions to accelerated flow of real gases for which viscosity is not proportional to temperature and for which the Prandtl number is not unity is discussed.

B002 Effect of Wall Cooling on the Mean Structure of a Turbulent Boundary Layer in Low-Speed Gas Flow

L. H. Back, R. F. Cuffel, and P. F. Massier

Int. J. Heat Mass Transfer, Vol. 13, No. 6, pp. 1029–1047, June 1970

The influence of wall cooling on the mean structure of a turbulent boundary layer in low-speed gas flow is discussed in terms of measured velocity and temperature profiles and friction coefficients, and comparisons are made with existing semi-empirical analyses of turbulent boundary layers. The measurements were made in an air flow through the entrance region of a smooth, isothermal tube where the free-stream velocity variation was negligible. Satisfactory agreement was found between the magnitude of the increase of the friction coefficient with cooling and values predicted from: (1) a reference temperature concept, (2) Spalding and Chi's empirical correlation, and (3) Cole's transformation theory in which an appropriate value of the viscosity-temperature exponent lies between 0.7 and 1.0. Measured velocity and temperature profiles when represented in terms of u^+ , T^+ and y^+ depended on a cooling parameter β , indicated by theory. Fair agreement was found between measured and predicted profiles involving Prandtl's mixing length and Coles' transformation theories.

BADIN, R.

B003 Holography Application Study to Pressure Vessel Flaw Detection

G. Morse, A. Knoell, and R. Badin

Supporting Research and Advanced Development, Space Programs Summary 37-64, Vol. III, pp. 100–101, August 31, 1970

For abstract, see Morse, G.

B004 Holographic Interferometry Application to Shell Structures

J. C. Chen and R. Badin

Supporting Research and Advanced Development, Space Programs Summary 37-64, Vol. III, pp. 101–106, August 31, 1970

For abstract, see Chen, J. C.

BANES, R.

B005 Heat-Sterilizable Battery Development

R. Banes

Supporting Research and Advanced Development, Space Programs Summary 37-62, Vol. III, pp. 142–153, April 30, 1970

The program to develop heat-sterilizable Ag-Zn cells has progressed so that engineering models of a primary 70-A-h cell are capable of 100% cycles following severe vibration and 6-mo open-circuit stand, and secondary 25-A-h cells capable of ninety 60% cycles have performed satisfactorily following sterilization and 8-mo stand. A modification has been made to the fabrication technique of the negative plate for the high-impact cell design to eliminate the sintering that caused loss of strength in the substrate. In the development of the 400-cycle cell, it has been shown that only the ratio of active material in the positive and negative plates is a significant parameter in the cycle testing.

BARTERA, R. E.

B006 Application of Imposed Magnetic Fields to Compact-Arc Lamps

C. G. Miller and R. E. Bartera

Supporting Research and Advanced Development, Space Programs Summary 37-63, Vol. III, pp. 161–166, June 30, 1970

For abstract, see Miller, C. G.

B007 Solar Simulators at the Jet Propulsion Laboratory

R. E. Bartera, H. N. Riise, and C. G. Miller

Appl. Opt., Vol. 9, No. 5, pp. 1068–1074, May 1970

The large JPL solar simulation systems are unique in their ability to furnish well-collimated light over large areas with good uniformity and high efficiency/intensity. These systems furnish simulated solar irradiance to 10-ft (3-m) and 25-ft (7.6-m) space simulation chambers. The existing facilities are described, and some potential improvements are discussed. Some results of a high-intensity lamp development program are included.

BATELAAN, P. D.

B008 A Noise-Adding Radiometer for Use in the DSN

P. D. Batelaan, R. M. Goldstein, and C. T. Stelzried

The Deep Space Network, Space Programs Summary 37-65, Vol. II, pp. 66–69, September 30, 1970

The communication requirements for deep space missions necessitate the use of high-gain antennas and

sensitive receivers on the ground. Because of their unusually good sensitivity, these receiving systems are also well-suited to radio astronomy applications. However, most gain compensation techniques normally employed for radio astronomy, such as the Dicke scheme, would degrade the communication capability of a Deep Space Network (DSN) receiver. A radiometer which is compatible with the DSN communication requirements is described in this article. With this radiometer, the effect of gain instability is eliminated by a noise injection technique. Included are a block diagram, experimental recordings, and performance comparisons (both theoretical and experimental) with a total power radiometer.

BAUMAN, A. J.

B009 Fluorometric Examination of the Returned Lunar Fines From Apollo 11

J. H. Rho, A. J. Bauman, T. F. Yen (University of Southern California), and J. Bonner (California Institute of Technology)
Proceedings of the Apollo 11 Lunar Science Conference, Houston, Texas, January 5-8, 1970, Vol. 2, pp. 1929-1932

For abstract, see Rho, J. H.

BEATTY, R. W.

B010 Comparisons of Waveguide Losses Calibrated by the DC Potentiometer, AC Ratio Transformer, and Reflectometer Techniques

T. Y. Otoshi, C. T. Stelzried, B. C. Yates (National Bureau of Standards), and R. W. Beatty (National Bureau of Standards)
IEEE Trans. Microwave Theory and Techniques, Vol. MTT-18, No. 7, pp. 406-409, July 1970

For abstract, see Otoshi, T. Y.

BEAUDET, R. A.

B011 Skeletal Molecular Structure of *closo*-2,3-Dicarbahexaborane(6) From Microwave Spectral Studies

R. A. Beudet (University of Southern California) and R. L. Poynter
J. Chem. Phys., Vol. 53, No. 5, pp. 1899-1905, September 1, 1970

The microwave spectra of 13 isotopic species of *closo*-2,3-dicarbahexaborane(6) have been studied. From these results, the cage structure of this molecule has been determined, and the accuracy of the molecular structure has been evaluated. The bond lengths determined were:

Bond	Length, Å
B(1)-B(6)	2.434 ± 0.005
C(2)-B(4)	2.297 ± 0.005
B(1)-B(4)	1.721 ± 0.015
B(4)-B(5)	1.752 ± 0.005
B(4)-C(3)	1.605 ± 0.005
C(2)-C(3)	1.540 ± 0.005
B(1)-C(2)	1.627 ± 0.015

The measured dipole moment was 1.50 ± 0.03 D.

BEHM, J. W.

B012 Study of the Effects of Heat Sterilization and Vacuum Storage on the Ignition of Solid Propellant Rockets

L. Strand, J. A. Mattice, and J. W. Behm
Supporting Research and Advanced Development, Space Programs Summary 37-63, Vol. III, pp. 196-206, June 30, 1970

For abstract, see Strand, L.

BEJCZY, A. K.

B013 State Determination for Disturbed Limit Cycle Operations via Nonlinear Filtering

A. K. Bejczy
Supporting Research and Advanced Development, Space Programs Summary 37-62, Vol. III, pp. 170-175, April 30, 1970

A stochastic van der Pol system observed through noisy linear measurements is investigated to determine the state of the related limit cycle operation by nonlinear filtering techniques. Two nonlinear filter algorithms are constructed: one from the maximum principle least-squares scheme and one from a postulated scheme. For the latter filter, the gains are constants determined by the requirement of minimizing the steady-state variance of the filter error; for this scheme, the filter's performance is evaluated by deterministic techniques. Two computed and digitally simulated cases are presented for implementing the filter algorithms on a flight computer when increased reliability in the spacecraft attitude-control system might warrant the application of nonlinear filtering. The maximum principle least-squares filter yields somewhat better performance than the minimum steady-state variance constant gain filter. Considering the involved constraints and approximations, however, the performance of the latter filter can be regarded as satisfactory.

B014 The Reverse Goddard Problem

A. K. Bejczy

Paper 69-868, AIAA (American Institute of Aeronautics and Astronautics) Guidance, Control, and Flight Mechanics Conference, Princeton, New Jersey, August 18–20, 1969

Fuel-optimal and time-optimal finite amplitude retrothrust control programs are obtained for nonlifting bodies subject to drag. Particularly, vertical and gravity-turn ballistic trajectories are investigated for the terminal conditions of soft landing. The optimization problems are formulated as Mayer-type problems in the Calculus of Variations, and are treated by applying the Pontryagin Maximum Principle. The possibility of singular extremal controls as well as the general behavior of the switching functions are investigated in some details. The computational aspects of the two-point boundary value problems associated with the canonical equations of optimal controls are elaborated.

Numerical results for a Mars landing problem are presented. The fuel-optimal and time-optimal retrothrust controls exhibit significant superiority over other types of controls in the computed cases. The main results are as follows: (1) The fuel-optimal and the time-optimal solutions of the formulated control problems are identical. This, somewhat surprising, result is interpreted in terms of the integrated time history of the atmospheric drag. (2) The fuel-optimal and time-optimal solutions of the formulated control problems are of the bang-bang type, composed of only two sections in the optimal control sequence. In particular, it is proved that, for vertical trajectories, the fuel-optimal retrothrust control program always is of the bang-bang type, and for gravity-turn ballistic trajectories, conditions are presented for which the fuel-optimal retrothrust control may differ from a bang-bang type of control.

BENESH, M.

B015 Extraterrestrial Convergent Photogrammetric Mapping System—An Error Analysis

M. Benesh

Technical Memorandum 33-455, December 1, 1970

An effort to define specific photogrammetric parameters that could be incorporated into an extraterrestrial television mapping system through investigations of convergent photogrammetric stereomodels is described. Also described are error analyses of direct and external relative orientation, and practical tests that investigated: (1) aspects of television image quality and its

resulting influence upon mapping accuracy, and (2) the design of an effective analytical method for complex interior orientation calibration.

BERDAHL, C. M.

B016 Two Blackbody Radiometers of High Accuracy

J. M. Kendall, Sr., and C. M. Berdahl

Appl. Opt., Vol. 9, No. 5, pp. 1082–1091, May 1970

For abstract, see Kendall, J. M., Sr.

BERMAN, A. L.

B017 A New Tropospheric Range Refraction Model

A. L. Berman

The Deep Space Network, Space Programs Summary 37-65, Vol. II, pp. 140–153, September 30, 1970

This article describes a new tropospheric range refraction model. Previously, the dry component of range and range rate refraction (signal retardation component) was assumed to be a linear function of surface refractivity. This appears to be a result of assuming an isothermal atmospheric model and then failing to consider the functional dependence required of the “scale height” by that assumption. Consideration of the hydrostatic equation and the gas law led inescapably to the conclusion that range refraction (at least at reasonable elevation angles) is linearly dependent upon surface refractivity. The derivation of the functional basis of the “dry” component, a method of integrating the “wet” component, and an error analysis of the model are presented in this article.

BERMAN, P. A.

B018 Radiation Damage in Lithium-Doped Silicon

P. A. Berman

Supporting Research and Advanced Development, Space Programs Summary 37-62, Vol. III, pp. 134–136, April 30, 1970

Investigations have been undertaken to obtain information on the behavior of radiation-induced defects in lithium-doped silicon. Studies were made to determine the effects of high-energy electron and neutron irradiation and of various annealing treatments on the minority carrier lifetime. To determine the nature of the radiation-induced defects, investigations were carried out that utilized electron spin resonance measurements, infrared spectroscopy, and minority carrier lifetime measurements as a function of temperature.

BLINN, J. C., III

B019 Multispectral Remote Sensing of an Exposed Volcanic Province

J. G. Quade (University of Nevada), P. E. Chapman (University of Nevada), P. A. Brennan (University of Nevada), and J. C. Blinn III

Technical Memorandum 33-453, June 15, 1970

For abstract, see Quade, J. G.

BOETTGER, H. G.

B020 Pyrolysis of Natural Products: Identification of Products From Nucleotide Pyrolysis by High Resolution Mass Spectrometry

H. G. Boettger and A. M. Kelly

Supporting Research and Advanced Development, Space Programs Summary 37-63, Vol. III, pp. 10-13, June 30, 1970

Experiments are described in which the behavior of RNA and DNA polymers, nucleotide and nucleoside monomers as well as the free bases has been investigated under thermal analysis conditions. Mass spectrometry by itself and in conjunction with gas chromatography has been used to identify the degradation products. Characteristic compounds, i.e., the corresponding purine or pyrimidine bases, are formed at 120 to 200°C, but fail to pass through the gas chromatograph. At 500°C, low molecular weight products of no structural significance are formed.

BOGNER, R. S.

B021 Battery Storage Optimization and Design Studies

R. S. Bogner and R. E. Patterson

Technical Memorandum 33-462, December 15, 1970

Sealed Ag-Zn cells with five different separator systems from four different vendors, and one group of Ag-Cd cells, were tested to evaluate their capability of maintaining a predictable output after long periods of inactivity. Electrolyte concentration was included as a variable in two of the cell designs. The cells were grouped into sets of three for storage at six different temperatures and four different time intervals. Extrapolation of rate capacity loss data at low temperature storage (0 to -20°C) indicates that after ten years of storage most of the cell designs would deliver 75% of their original capacity. Cells with the RAI-116 separator system showed the best charge retention. Cells of the one Ag-Cd design did not maintain charge retention as well as most of the Ag-Zn cells.

B022 Development of a Long-Life, High Cycle Life, 30-A-h, Sealed AgO-Zn Battery

R. E. Patterson and R. S. Bogner

Supporting Research and Advanced Development, Space Programs Summary 37-62, Vol. III, pp. 138-142, April 30, 1970

For abstract, see Patterson, R. E.

BONNER, J.

B023 Fluorometric Examination of the Returned Lunar Fines From Apollo 11

J. H. Rho, A. J. Bauman, T. F. Yen (University of Southern California), and J. Bonner (California Institute of Technology)

Proceedings of the Apollo 11 Lunar Science Conference, Houston, Texas, January 5-8, 1970, Vol. 2, pp. 1929-1932

For abstract, see Rho, J. H.

BORNCAMP, F.

B024 A Proposed Method of Counting Doppler With the Digital Tracking Subsystem

F. Borncamp

The Deep Space Network, Space Programs Summary 37-63, Vol. II, pp. 112-116, May 31, 1970

The Digital Tracking Subsystem (DTS) provides the first opportunity to use data smoothing techniques to minimize high-frequency doppler noise and provide a better estimate of the true phase of the received signal at the time of sampling. This proposal assumes the doppler counter will be sampled at a rate of 100 times per second, while the maximum output rate and/or permanent storage rate would be 10 samples per second. Thus, the samples that reside within ± 0.04 s of the points on the integer tenth of seconds could be used to form an uncorrelated or at least non-overlapping set of improved estimates of the phase on the integer tenths of the second. This technique is easy to implement in the DTS since it consists of single integer multiplications on each sub-sample and then a summation of terms. The resultant improvement is a lowering of the one-sigma noise on the doppler estimates to $\approx 50\%$ of the original value.

BOWERS, M. T.

B025 An Ion Cyclotron Resonance Study of the Ion-Molecule Reactions in Hydrogen-Methane Mixtures

M. T. Bowers and D. D. Elleman

Supporting Research and Advanced Development, Space Programs Summary 37-62, Vol. III, pp. 32-36, April 30, 1970

The principal ion-molecule reactions in hydrogen-methane mixtures are reported, along with the pressure

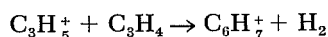
dependence of the $\text{CD}_4\text{H}^+/\Sigma\text{C}(\text{H},\text{D})_3^+$ ratio as a function of H_2 pressure in a $\text{CD}_4\text{-H}_2$ mixture. To explain the details of the pressure dependence, reactions of both excited $[\text{H}_3^+]^*$ and deactivated H_3^+ with CD_4 are postulated. $[\text{H}_3^+]^*$ forms CD_3^+ and CD_2H^+ primarily via a direct mechanism, while H_3^+ first forms $[\text{CD}_4\text{H}^+]^*$, which is subsequently collisionally stabilized or decomposes to CD_3^+ and CD_2H^+ .

B026 Analysis of Ion-Molecule Reactions in Allene and Propyne by Ion Cyclotron Resonance

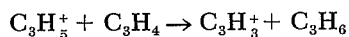
M. T. Bowers (University of California, Santa Barbara), D. D. Elleman, R. M. O'Malley (The University, Sheffield, England), and K. R. Jennings (The University, Sheffield, England)

J. Phys. Chem., Vol. 74, No. 13, pp. 2583-2589, 1970

Thermal energy product distributions and their energy dependencies for the C_3H_4^+ ions in allene and propyne are determined using ion cyclotron resonance (ICR). Reaction sequences for the C_3H_3^+ , C_3H_2^+ , and C_3H^+ primary ions are also determined from double resonance results. These data are compared with the medium-pressure mass spectral data of Myher and Harrison taken at a 3.4-eV ion exit energy. Significant differences between the ICR and medium-pressure product distributions are observed. Double resonance results indicate that the discrepancies arise mainly from the difference in energy of the reactant ions in the two techniques. In addition, at thermal energies, secondary C_3H_5^+ ions undergo the condensation reaction



and *do not* undergo the hydride ion abstraction reaction



This latter reaction was observed by Myher and Harrison in their higher-energy experiments. Isotopic mixing experiments indicate that a *four-centered* intermediate is important in many of the condensation reactions of allene and propyne.

BRANDT, R. D.

B027 Polaroid Quick-Look System

R. D. Brandt and G. R. Andrews

Supporting Research and Advanced Development, Space Programs Summary 37-62, Vol. III, pp. 22-25, April 30, 1970

This article describes the design philosophy and hardware implementation of a device that generates a Polaroid print directly from a computer. The Polaroid print is available approximately 1.5 min after print initiation. The device eliminates the normal waiting

period for film development and thus decreases the time required for "image processing" whenever the next process is determined by information from the photographic print of the previous process.

BRECKENRIDGE, W. G.

B028 Mariner Mars 1969 Approach Guidance Demonstration

T. C. Duxbury and W. G. Breckenridge

Supporting Research and Advanced Development, Space Programs Summary 37-64, Vol. III, pp. 72-73, August 31, 1970

For abstract, see Duxbury, T. C.

B029 Defining a Spacecraft-Based Navigation System

W. G. Breckenridge and T. C. Duxbury

Astronaut. Aeronaut., Vol. 7, No. 5, pp. 44-49, May 1970

The stringent navigation requirements for proposed outer-planet missions make even the projected ability of a solely earthbased system marginal, and so have emphasized the need for an onboard system. The addition of spacecraft-based data to the navigation process significantly improves the target-centered estimate of the spacecraft trajectory, especially when the target planet does not significantly influence spacecraft motion. A better trajectory estimate means, in effect, better control of the spacecraft trajectory, better pointing of science instruments, ability to make trajectory corrections during less critical periods, and higher over-all probability of mission success. In multiple-outer-planet missions the greater trajectory control from onboard navigation would permit reducing the fraction of spacecraft weight allocated for trajectory correction by as much as 25%.

This article discusses various facets of spacecraft-based navigation data, primarily for application to the outer-planet missions, and describes the results of a navigation demonstration—the processing of spacecraft-based science and engineering data from *Mariner* Mars 1969.

BRENNAN, P. A.

B030 Multispectral Remote Sensing of an Exposed Volcanic Province

J. G. Quade (University of Nevada), P. E. Chapman (University of Nevada), P. A. Brennan (University of Nevada), and J. C. Blinn III

Technical Memorandum 33-453, June 15, 1970

For abstract, see Quade, J. G.

BRERETON, R. G.

- B031 A Miniaturized Absolute Gravimeter for Terrestrial, Lunar, and Planetary Research**
R. G. Brereton, B. H. Chovitz (United States Coast and Geodetic Survey), W. M. Greene (Marshall Space Flight Center), O. K. Hudson (Marshall Space Flight Center), R. A. Lytleton (St. John's College), and R. D. Regan (United States Geology Survey)
Supporting Research and Advanced Development, Space Programs Summary 37-62, Vol. III, pp. 1-5, April 30, 1970

The design and application of a new type of gravimeter is discussed. The instrument utilizes a laser light source and the principles of a Michelson interferometer to measure the acceleration caused by gravity of a small free-fall body over a measured path. The instrument is expected to measure the absolute value of g to 1 part in 10^7 or better.

- B032 Automated Post-Missions for the Lunar Roving Vehicle**
R. G. Brereton
Supporting Research and Advanced Development, Space Programs Summary 37-62, Vol. III, pp. 5-8, April 30, 1970

For maximum utilization of *Apollo* hardware, some possible post-mission uses for the lunar roving vehicle, which will be left at the *Apollo* lunar site when the astronauts return to earth, are considered. Discussions are presented on whether this vehicle can be used in an automated mode and, if so, what changes are necessary and what scientific advantage would be gained by its use. The concept for a very simple automated rover and priorities for modification of this simple rover are described.

- B033 Mission Objectives for a Lunar Roving Vehicle**
R. G. Brereton
Supporting Research and Advanced Development, Space Programs Summary 37-64, Vol. III, pp. 1-3, August 31, 1970

Field tasks are defined for lunar roving vehicles in a lunar science program on the bases of function, utility, or mission requirements. Field geology and traverse geophysics experiments are required to answer fundamental questions about the moon. The feasibility of a lunar roving vehicle exploration system must be determined by additional testing.

- B034 Desert Stream Channels Resembling Lunar Sinuous Rilles**
J. D. Burke, R. G. Brereton, and P. M. Muller

Nature, Vol. 225, No. 5239, pp. 1234-1236, March 28, 1970

For abstract, see Burke, J. D.

BRINKMANN, R. T.

- B035 Electron Impact Excitation of N_2**
R. T. Brinkmann and S. Trajmar
Supporting Research and Advanced Development, Space Programs Summary 37-62, Vol. III, pp. 47-53, April 30, 1970

An experimental and theoretical study was made of the excitation of gaseous molecular nitrogen under electron bombardment. Differential electron-impact energy-loss spectra were obtained at scattering angles from 0 to 80 deg; incident energies of 20, 30, 40, 60, and 80 eV; and energy losses from 0 to 19 eV. Resolution was typically 0.10 eV. The resulting cross sections were put on an approximate absolute scale by normalizing to available total collision probability measurements. At higher incident energies, various forms of the Born approximation were assumed. A computer program was written that uses the Monte Carlo method to calculate the energy deposited in the various states as a function of incident energy and distance from the source. Branching ratios and quenching efficiencies were assumed, and the resultant emission intensities were calculated.

- B036 Departures From Jeans' Escape Rate for H and He in the Earth's Atmosphere**
R. T. Brinkmann
Planet. Space Sci., Vol. 18, No. 4, pp. 449-478, April 1970

It has long been recognized that thermal, or gravitational, escape must perturb the velocity distribution function of an escaping species; thus, Jeans' classic escape rate cannot be strictly correct. The magnitude of the appropriate correction has remained unknown. Three recent statistical (Monte Carlo) investigations of this problem have produced such discordant correction factors as to prompt yet another such study, reported here. Major differences in approach are: (1) realistic atom-atom elastic scattering cross-sections are used instead of an isotropic approximation, and (2) program efficiency is increased dramatically by studying the virtual trajectories of atoms missing from the atmosphere instead of the real atoms comprising the atmosphere. Excellent agreement is achieved with one of the previous investigations; the escape rates of hydrogen and helium from the earth's atmosphere are typically 70-75 and 97-99% of Jeans' rate, respectively.

BROKL, S.

B037 Digital Acquisition and Detection: Numerical Interactive Controller

S. Brokl

The Deep Space Network, Space Programs Summary 37-64, Vol. II, pp. 35-38, August 31, 1970

The numerical interactive controller (NIC) described here gives additional versatility to the digital video display system. It provides X-Y positional information to the operator to allow him to modify displayed data. The NIC is designed primarily to solve the user interface problem for two-dimensional processing of range-doppler data or for real-time data evaluation by experimenters as required in the Space Flight Operations Facility Mark III. The NIC is compatible with SDS 900-series computers and can be used wherever X-Y positional information is needed.

BROUCKE, R. A.

B038 On the Matrizant of the Two-Body Problem

R. A. Broucke (University of California, Los Angeles)

Astron. Astrophys., Vol. 6, No. 2, pp. 173-182, August 1970

A general theory for the construction of the matrizant of the two-body problem or any other completely integrable dynamic system is developed in this article. This theory essentially constructs the fundamental matrix of the variational equations and then shows how its inverse is obtained. The matrizant is in this way decomposed into a product of two matrices. Three interesting forms of decomposition are developed in detail; they correspond to the classical orbit elements, the "Set-Three" elements, and the "Set-One" elements. The matrices thus developed have essentially two main applications: computation of perturbations and differential correction of orbits with observations. The results include the partial derivatives of the velocity components and thus make possible the applications to radar doppler observations.

B039 How to Assemble a Keplerian Processor

R. Broucke (University of California, Los Angeles)

Celest. Mech., Vol. 2, No. 1, pp. 9-20, May 1970

This article describes how a set of computer programs has been constructed to perform the literal series expansions of the two-body problem. The different steps of the approach are outlined, from the basic generation of fundamental Kepler functions with the aid of Bessel series to the construction of derived Kepler

functions by elementary Poisson series operations. The different tests and checks that have been made are also described. The most extensive test application of the package of programs, the expansion of the lunar disturbing function, is included.

BROWN, D. W.

B040 Planetary Ranging Demodulator

D. W. Brown

The Deep Space Network, Space Programs Summary 37-64, Vol. II, pp. 71-74, August 31, 1970

The planetary ranging demodulator originally implemented in 1967 at the Mars Deep Space Station has been redesigned and rebuilt to enhance operational and performance characteristics. Significant engineering improvements have been incorporated in the equipment, which will soon be returned to the field for use during *Mariner Mars 1969 Extended Mission* and *Mariner Mars 1971* support. The modifications made to the demodulator are described in this article.

BUCHANAN, H. R.

B041 Polarization Converter

H. R. Buchanan

The Deep Space Network, Space Programs Summary 37-63, Vol. II, pp. 44-47, May 31, 1970

The polarization incompatibility between the *Pioneer* space probe antennas and the Deep Space Instrumentation Facility (DSIF) antennas brought about the development of a polarization converter. A relatively simple device has been devised which can be easily and quickly installed in front of the DSIF antenna feedhorn. This device effectively converts the normally circular polarization of the DSIF feed to linear polarization, which is compatible with the *Pioneer* space probes. A nominal 3-dB improvement in downlink and uplink signal strength has resulted.

BUNCE, R. C.

B042 Block IV Receiver Automatic Carrier Acquisition

R. C. Bunce

The Deep Space Network, Space Programs Summary 37-65, Vol. II, pp. 107-116, September 30, 1970

A new method to automatically acquire spacecraft down-link carriers for the Block IV receiver-exciter subsystem is described in this article. The design combines the frequency-sweep capability of a programmed local oscillator with an automatic acquisition detector.

The design of the acquisition detector is described in detail, and considerations leading to the choice of design parameters are derived. The mathematical expressions involved are, in general, transcendental, and machine calculation and plot are used extensively. Theoretical results are verified by comparison with actual waveforms obtained during a feasibility study. The theory is applied to obtain the numbers used for the Block IV acquisition system hardware design and operation.

BUNKER, E. R., JR.

B043 Large-Scale Hybrid Prototype—Method of Functionally Checking Hybrid Layouts Prior to Processing

E. R. Bunker, Jr.

Supporting Research and Advanced Development, Space Programs Summary 37-63, Vol. III, pp. 140-143, June 30, 1970

At the present time, the functional evaluation of a hybrid electronic circuit can only be achieved by going through the whole sequence of operations used to produce a functioning module. Usually several iterations are required before all the errors and possible crosstalk effects are eliminated.

A novel approach to check the hybrid layout prior to processing is to fabricate a functioning module the same size as the initial art work. Conductor patterns are fabricated on a pyrex sheet to scale from adhesive-backed copper tape, with insulating tape of the proper thickness and electrical parameters used for cross-overs. Conventional, active, and passive components, such as transistors, capacitors, composition resistors, etc., electrically equivalent to the microminiature components to be installed on the final hybrid, but of conventional discrete component size, are soldered in place. Then the prototype is connected into the subsystem for functional test. Two circuits, one simple and one complex, have been fabricated and are undergoing tests.

BURKE, J. D.

B044 Desert Stream Channels Resembling Lunar Sinuous Rilles

J. D. Burke, R. G. Brereton, and P. M. Muller
Nature, Vol. 225, No. 5239, pp. 1234-1236, March 28, 1970

Several stream channels in the Mojave Desert geographic province of southern California are on alluvial slopes where windblown sand is present, so the inter-

mittent streams emerging from canyons are forced to transport fine sand in addition to their normal burden of alluvium. The meandering channels are then partly covered by more windblown sand, much of it resting at the angle of repose typical for desert dunes. Thus, all shapes are gently rounded, and the channel banks are hidden, except for occasional outcrops of loose or weakly consolidated sand, gravel, and angular cobbles. These stream beds look quite unlike ordinary desert washes, but are strikingly similar to certain sinuous rilles on the moon. Some of the lunar rilles seem to have been formed by fluid flow, but what the fluid was is unknown. Two of the desert rilles have been examined to determine their means of formation in an attempt to learn more about the means of formation of the lunar rilles. The results are presented in this article.

BUTMAN, S.

B045 Coding and Synchronization Research: Interplex—An Efficient Two-Channel Telemetry System for Space Exploration

S. Butman and U. Timor

Supporting Research and Advanced Development, Space Programs Summary 37-62, Vol. III, pp. 57-60, April 30, 1970

A new scheme for a two-channel coherent communication system is presented. In the existing system, there is a power loss due to intermodulation that is, in general, greater than the power available in the low-rate channel. The new system increases the power available to the data channels and makes the power loss negligible. The resulting modulation angles satisfy $\theta_1 \leq 90$ deg, $\theta_2 \leq 45$ deg, but not necessarily $\theta_1 + \theta_2 \leq 90$ deg. However, even if it is required to have $\theta_1 + \theta_2 \leq 90$ deg, the new system still leads to significantly improved performance.

B046 Coding and Synchronization Research: Optimization of Acquisition Time for Sequential Ranging System

S. Butman and J. Molinder

Supporting Research and Advanced Development, Space Programs Summary 37-62, Vol. III, pp. 60-62, April 30, 1970

The best allocation of time between phase estimation and component acquisition is determined numerically under the constraint that equal integration times are used for all but the high-frequency component. The optimum performance under these constraints is approximately 1 dB worse than the performance if the exact phase reference were known at the start.

B047 On the Receiver Structure for a Single-Channel, Phase-Coherent Communication System

M. K. Simon and S. Butman

Supporting Research and Advanced Development,
Space Programs Summary 37-62, Vol. III, pp. 103–108,
April 30, 1970

For abstract, see Simon, M. K.

B048 Coding and Synchronization Research: Efficient Multichannel Space Telemetry

S. Butman and U. Timor

Supporting Research and Advanced Development,
Space Programs Summary 37-63, Vol. III, pp. 34–37,
June 30, 1970

The Interplex modulation scheme for two-channel telemetry is extended to n , channels. By properly choosing the modulation indices, the power loss due to intermodulation can be minimized. This loss can no longer be made equal to zero (as for $n = 2$); however, in the case of one high rate data channel and several low rate channels, the loss is negligible.

B049 Coding and Synchronization Research: Decision Rules for a Two-Channel Deep-Space Telemetry System

S. Butman, J. E. Savage (Brown University), and U. Timor

Supporting Research and Advanced Development,
Space Programs Summary 37-63, Vol. III, pp. 38–41,
June 30, 1970

Optimum and suboptimum decision rules are examined for a telemetry system in which the modulation consists of phase modulation with two orthogonal phase functions. Coherent demodulation is assumed and two statistically dependent communication channels are created. An optimum decision rule that uses this statistical dependence is examined as well as two rules which use this dependence partially. One of these rules is the appropriate one to use when the channel conditions are those which prevailed in the *Mariner* Mars 1969 system. This rule, however, is far superior to that which is now used.

B050 Space Station Unified Communication: Suppressed-Carrier Two-Channel Interplex Modulation System

U. Timor and S. Butman

Supporting Research and Advanced Development,
Space Programs Summary 37-64, Vol. III, pp. 27–31,
August 31, 1970

For abstract, see Timor, U.

B051 Rank-Order Statistics for Optimum Detection of Binary Signals in the Presence of White Noise and DC Drift

S. Butman

IEEE Trans. Information Theory, Vol. IT-16, No. 3,
pp. 348–351, May 1970

It is well-known that the bit-by-bit threshold detector is optimum for detecting binary pulses (of amplitude ± 1) in white noise. In practice, however, this detector is often accompanied by a high-pass filter designed to remove any unknown dc that may be generated in the receiver, because the presence of the dc would bias the threshold away from the optimum value. This, in turn, causes the detector to make many errors whenever a long (relative to the time constant of the high-pass filter) sequence of 1 or -1 occur in the data, since the filter rejects such low-frequency signals.

Admittedly, the probability of occurrence of such sequences in the data decreases exponentially with length for an independent and equiprobable pulse stream and can be neglected in most practical systems. Nevertheless, the device is no longer theoretically optimum, and it is of interest to find the structure of the optimum detector for the case of unknown dc as well as white noise.

The optimum (maximum-likelihood) detector for extracting any binary sequence (of length K) from additive gaussian white noise and an unknown dc bias is derived in this article. It is shown that this detector must order the received noise-contaminated sequence so as to detect economically. Since the ordering of K real numbers requires at least $K \log_2 K$ binary operations, this detector must be at least $\log_2 K$ times as fast (or $\log_2 K$ times as complex) as the simple bit-by-bit detector. It is, therefore, doubtful that this considerably more complex receiver will find any practical use.

CAMERON, R. E.

C001 Microbiology, Ecology and Microclimatology of Soil Sites in Dry Valleys of Southern Victoria Land, Antarctica

R. E. Cameron, J. King, and C. N. David

Antarctic Ecology: Volume 2, pp. 702–716,
Academic Press, Inc., New York, 1970

The investigation of Antarctic dry valleys has been undertaken in preparation for attempts to detect life in extraterrestrial environments. These valleys are useful study areas prior to searching for life in Martian soils because of low temperatures, low humidities, diurnal freeze-thaw cycles even during daylight hours, low annual precipitation, desiccating winds, high sublimation and evaporation, high radiation, low magnetic

field, absence of higher life forms, and the irregular distribution and low abundance of soil micro-organisms. For the study reported here, five sites were established for approximately 1-wk periods during austral summers 1966–1967 and 1967–1968 in McKelvey, Victoria, Taylor, Wheeler, King, and David Valleys. Environmental measurements of soil and air temperature, relative humidity, dew point, wind direction and velocity, solar and environmental radiation flux, net thermal exchange, evaporation rate, light intensity, barometric pressure, and cloud cover were made either continuously or every 3 h. Additional sites in these and other dry valleys were investigated during both summers, and approximately 150 samples were collected from 75 sites. Samples were collected from the surface to depths of hard, icy permafrost (ice-cemented soil), using aseptic techniques developed for sampling, handling, and processing of desert soils.

Soil physical, physico-chemical, and chemical analyses were performed for many of the samples, including mineralogy; mechanical analysis; bulk density; porosity; reflectivity; *in situ* moisture and moisture constants; gases; weight loss on ignition; cation exchange capacity; buffer capacity; pH; Eh; electrical conductivity; elemental abundance; ionic concentrations; and inorganic and organic C, H, and N and their ratios. Abundance and distribution of general and specific groups of soil micro-organisms were determined by direct inoculation of soil onto agar plates or by spread plate and dilution culture techniques designed for the investigation and study of low abundances of desert soil micro-flora. Tests were performed at various temperatures (2 to 55°C) for aerobic, microaerophilic, and anaerobic bacteria; lactose fermenters; nitrate reducers; and coliforms. Additional media were used to detect and enumerate actinomycetes (streptomycetes), fungi, and algae. The results of the investigation are presented in this report.

C002 Antarctic Soil Algal Crusts: Scanning Electron and Optical Microscope Study

R. E. Cameron and J. R. Devaney

Trans. Am. Microsc. Soc., Vol. 89, No. 2, pp. 264–273, April 1970

Two algal soil crusts from South Victoria Land, Antarctica were chosen for study with the scanning electron microscope, and a comparison study was made with the light transmission microscope. Soils were investigated microscopically without treatment, and following incubation in moist chambers and in dilution cultures. By scanning electron microscopy, algae were readily discerned in association with soil particles as flowing and entwined masses which bound soil particles

together, but individual species were usually not readily identified within community associations. Structure of trichomes was obscured by sheath material, but some naked trichomes were observed. The algal crust components were primarily closely related oscillatoroid blue-green algae: *Schizothrix calcicola* (Ag.) Gom., *S. arenaria* (Berk.) Gom., and *S. rubella* Gom. Globose colonies of *Nostoc commune* Vauch. were observed by both scanning electron microscopy and light microscopy. A rarely encountered form of *N. commune* was observed as *Hydrocoryne spongiosa* Schw. The only green alga present was *Chlorella vulgaris* Beij. It was concluded that the scanning electron microscope is a new and valuable tool in the investigation of microbial associations of a soil algal community, but the light transmission microscope is still useful for routine identification of the soil algal components.

CAMPBELL, R. W.

C003 RTG Radiation Test Laboratory

R. W. Campbell and M. Reier

Supporting Research and Advanced Development, Space Programs Summary 37-62, Vol. III, pp. 145–148, April 30, 1970

This article presents an overview of the progress in the radioisotope thermoelectric generator (RTG) radiation test laboratory over the last 6-mo period. The gamma-ray spectrum analysis of a 1.5-W (thermal) plutonium-fueled SNAP-15A (System for Nuclear Auxiliary Power 15A) heat source has been completed, and analysis of the SNAP-27 gamma-ray spectrum is under way. Work in the area of laboratory facilities has included the fabrication and use of a source for the radiation simulation of a 1575-W (thermal) PuO₂ fuel capsule assembly. The calibration of the liquid organic scintillator for neutron spectrometry has been completed. Extensive work has been done in the determination of the monoenergetic gamma-ray and neutron response for a Geiger–Mueller tube and a variety of solid-state detectors, including both surface-barrier and lithium-drifted types.

CAPEN, C. F.

C004 Martian Blue-Clearing During 1967 Apparition

C. F. Capen

Icarus: Int. J. Sol. Sys., Vol. 12, No. 1, pp. 118–127, January 1970

The occurrences of Martian blue-clearing during a 20-month observational patrol are tabulated and summarized. Periods of clearing were more numerous

and stronger during the 1967 apparition than during 1965. The percentage of nights in which some form of clearing was detected was 48.5% of the total nights of quality violet-blue observations. Blue-clearings were noted 175 days before opposition and 349 days after opposition.

CAPODICI, S.

C005 Design of a Thick-Film Microcircuit DC-to-DC Converter

H. Wick and S. Capodici (General Electric Co.)
Supporting Research and Advanced Development,
Space Programs Summary 37-64, Vol. III, pp. 64-67,
August 31, 1970

For abstract, see Wick, H.

CAPUTO, R. S.

C006 Multi-Hundred-Watt Radioisotope Thermoelectric Generator Radiant Interchange Factors

R. S. Caputo
Supporting Research and Advanced Development,
Space Programs Summary 37-63, Vol. III, pp. 86-93,
June 30, 1970

The radiative thermal interaction is evaluated between the multi-hundred-watt radioisotope thermoelectric generators (MHW-RTGs) and the Thermoelectric Outer-Planet Spacecraft. The study is made for RTG-spacecraft positions that exist from pad operation through orbital deployment. The RTG arrangement used is the two-in-tandem, two-in-parallel arrangement. The geometric view factors from the RTGs to the surrounding objects are calculated, and determination is made of the overall radiation interchange factors of the RTGs. These data are also transformed for use as input for a transient performance RTG computer code.

CARD, D. C.

C007 [DSN] System Simulation Models

D. C. Card
The Deep Space Network, Space Programs Summary 37-65,
Vol. II, pp. 4-6, September 30, 1970

The Deep Space Network (DSN) can be considered a complex communications network system that handles many distinct types of traffic. As a supporting system to space flight projects, the DSN operates under requirements and objectives reflected by the various mis-

sion profiles. This article describes the application of a Monte Carlo simulation program, the general-purpose Simulation System program, as an analysis and design tool in the DSN system analysis area. This program is a powerful tool because it has been designed for the modeling and simulation of traffic flow systems, and because its high-level language permits rather direct interpretation of system flow diagrams into coded blocks for program execution.

CARL, C.

C008 Approximate Analysis of Command Lock Detector Performance

C. Carl
Supporting Research and Advanced Development,
Space Programs Summary 37-63, Vol. III, pp. 51-58,
June 30, 1970

An approximate analysis of a coherent, additive gaussian noise channel lock detector preceded by a band-pass limiter is presented. The analysis covers the error-rate performance for both the signal-plus-noise and noise-only input conditions. Results are given for various values of the input bandwidth-bit time product and the detector threshold. A comparison with experimental data shows good agreement with the analytic results over the range of practical interest.

CARLS, L. W.

C009 Results of the Near Infrared Multidetector Grating Spectrometer Study

L. W. Carls and P. W. Schaper
Supporting Research and Advanced Development,
Space Programs Summary 37-63, Vol. III, pp. 1-5,
June 30, 1970

The results of the study task for the Near Infrared Multidetector Grating Spectrometer for the *Nimbus F* spacecraft are summarized. The task consisted of two approaches: (1) to arrive at a conceptual design for the instrument, and (2) to demonstrate a system of data utilization for the experiment.

CARLSON, R. W.

C010 Curves of Growth of Autoionizing Spectral Lines With Application to the 3s-4p Transition in Argon

A. Chutjian and R. W. Carlson (University of
Southern California)
J. Opt. Soc. Am., Vol. 60, No. 9, pp. 1204-1208,
September 1970

For abstract, see Chutjian, A.

CARPENTER, J.

C011 DSS 51 Antenna Mechanical Subsystem Upgrade

J. Carpenter, V. Lobb, A. Nicula, and D. Nelson
The Deep Space Network, Space Programs Summary 37-64,
Vol. II, pp. 98–104, August 31, 1970

The antenna mechanical subsystem upgrade at the Johannesburg Deep Space Station (DSS 51) was implemented to restore the original specification agreement relative to the addition of the declination wheel electronics house, provide for the use of acquisition patterns and snap-on tests, increase tracking coverage, and attain a stiffer structure for S-band tolerances and thereby achieve compatibility with the four-legged antennas at the Weemala, Robledo, and Cebreros Deep Space Stations. The work included: (1) addition of structural members for rigidity, (2) replacement of hydraulic drive units, (3) replacement of structural bolts to minimize joint slippage, (4) optical measurement and resetting of the cassegrain system, and (5) special testing and adjustments of the servo system to obtain a more perfect balance between the electronics and hydraulics. The upgrade effort is described in this article.

CASPERSON, R. D.

C012 Overseas 210-ft-diam Antenna Project

R. D. Casperson and W. W. Lord
The Deep Space Network, Space Programs Summary 37-65,
Vol. II, pp. 154–158, September 30, 1970

This article reports on the progress made on the two overseas 210-ft-diam antenna projects. The fabrication and construction of the antenna structural-mechanical subsystem and the design and construction of the power generation, distribution, and facility subsystems are described. These antennas, one in Australia and one in Spain, coupled with the 210-ft-diam prototype antenna operational at the Mars Deep Space Station in California, will comprise the three-station subnetwork of the Deep Space Instrumentation Facility.

CASELL, P. L.

C013 Plasma-Immersion-Probe Tube in Metal-Ceramic Envelope

K. Shimada and P. L. Cassell
Supporting Research and Advanced Development,
Space Programs Summary 37-62, Vol. III, pp. 153–157,
April 30, 1970

For abstract, see Shimada, K.

CHADWICK, H. D.

C014 Estimating the Phase of a Sample Signal with Minimum Mean-Square Error

H. D. Chadwick
Supporting Research and Advanced Development,
Space Programs Summary 37-62, Vol. III, pp. 99–103,
April 30, 1970

In a digital implementation of a phase-coherent receiver, the input signal, together with additive noise, is sampled at the receiver input. If the sampled input is correlated with each of the possible discrete phase positions of a replica of the transmitted signal, a set of correlation values is obtained, the maximum of which gives a discrete estimate of the true phase position. Such an estimate is subject to quantization error, which can be reduced by increasing the input sampling rate. Because the correlation values are all determined from the same input samples, they are not statistically independent and the variance of the phase estimate itself increases as the sampling rate is increased. In this article, the sampling rate that gives rise to the minimum overall mean-square phase error is computed as a function of the input signal-to-noise ratio.

C015 The Error Probability of a Wide-Band FSK Receiver in the Presence of Multipath Fading

H. D. Chadwick
Supporting Research and Advanced Development,
Space Programs Summary 37-62, Vol. III, pp. 113–118,
April 30, 1970

Calculations are made for the probability of error of a wide-band frequency-shift-keyed (FSK) receiver of the type used in relay links when multipath reflections off the planetary surface cause signal fading. The error probability is found for both low and high fading bandwidths and for small and large reflected path delays.

C016 The Equivalence of Rank Permutation Codes to a New Class of Binary Codes

H. D. Chadwick and I. S. Reed (University of Southern California)
IEEE Trans. Information Theory, Vol. IT-16, No. 5,
pp. 640–641, September 1970

An equivalence between the rank permutation codes and a new class of binary codes has been observed. A binary code may be generated by direct transformation of a permutation code. The binary codes are usually nonlinear and may be decoded by the inverse transformation and rank correlation of the equivalent permutation.

CHAMBERLAIN, R. G.

C017 On Forming a Consensus of Individual Preferences or Consolidation of Pecking Orders

R. G. Chamberlain

Supporting Research and Advanced Development, Space Programs Summary 37-64, Vol. III, pp. 170-172, August 31, 1970

The problem of combining several individual preference patterns into a single preference pattern for the society composed of those individuals is considered. Numerical techniques for producing such a consensus are often suggested. They almost invariably fail due to an attempt to produce results containing more information than is present in the input. It is suggested in this article that if *ignorance* is identified as a valid relationship, it is possible to find a consensus that contains no more and no less information than can be inferred from the individual patterns. Rules for finding this consensus are not given.

CHAPMAN, P. E.

C018 Multispectral Remote Sensing of an Exposed Volcanic Province

J. G. Quade (University of Nevada), P. E. Chapman (University of Nevada), P. A. Brennan (University of Nevada), and J. C. Blinn III

Technical Memorandum 33-453, June 15, 1970

For abstract, see Quade, J. G.

CHEN, C. J.

C019 Drift Velocities of Electrons in the Positive Column of a Neon Discharge

M. Sugawara and C. J. Chen

J. Appl. Phys., Vol. 41, No. 8, pp. 3442-3445, July 1970

For abstract, see Sugawara, M.

CHEN, J. C.

C020 Nonlinear Vibration of an Infinite Long Circular Cylinder [February-March 1970]

J. C. Chen

Supporting Research and Advanced Development, Space Programs Summary 37-62, Vol. III, pp. 182-187, April 30, 1970

Equations of motion of a large amplitude vibration of a thin-walled infinitely long circular cylinder have been derived. These nonlinear equations are reduced to a sequence of linear equations by perturbation methods that can be solved by the existing technique.

C021 Nonlinear Vibration of an Infinite Long Circular Cylinder [June-July 1970]

J. C. Chen

Supporting Research and Advanced Development, Space Programs Summary 37-64, Vol. III, pp. 96-100, August 31, 1970

A large amplitude vibration of a thin-walled infinite long circular cylinder has been analyzed by the perturbation method. The stability of the response is investigated by using the known results of Mathieu's equation. A comparison between the analysis and the existing experimental results is made. This perturbation method is proposed for the systematic approach to a nonlinear vibration of general structural systems.

C022 Holographic Interferometry Application to Shell Structures

J. C. Chen and R. Badin

Supporting Research and Advanced Development, Space Programs Summary 37-64, Vol. III, pp. 101-106, August 31, 1970

This article summarizes some recent applications of holographic interferometry to vibration and buckling problems in spacecraft structures. Time-average holography was applied to study the vibration mode shapes of a cantilevered thin-walled circular cylindrical shell. A double exposure technique was used to study the pre-buckling imperfection growth. In all cases, the results showed good agreement with the theory and demonstrated the capabilities of holographic interferometry for studies of shell structures.

CHOVITZ, B. H.

C023 A Miniaturized Absolute Gravimeter for Terrestrial, Lunar, and Planetary Research

R. G. Brereton, B. H. Chovitz (United States Coast and Geodetic Survey), W. M. Greene (Marshall Space Flight Center), O. K. Hudson (Marshall Space Flight Center), R. A. Lytleton (St. John's College), and R. D. Regan (United States Geology Survey)

Supporting Research and Advanced Development, Space Programs Summary 37-62, Vol. III, pp. 1-5, April 30, 1970

For abstract, see Brereton, R. G.

CHUTJIAN, A.

C024 Curves of Growth of Autoionizing Spectral Lines With Application to the 3s-4p Transition in Argon

A. Chutjian and R. W. Carlson (University of Southern California)

J. Opt. Soc. Am., Vol. 60, No. 9, pp. 1204-1208, September 1970

Curves of growth are calculated for autoionizing transitions having the Beutler-Fano form of absorption cross section. Both graphs and tabulated values of the curves are presented. The curve-growth analysis is applied to the $3s-4p$ transition in argon at 466 Å. The line parameters Γ , q , and ρ^2 obtained by fitting the theoretical and experimental equivalent widths are in good agreement with other high-resolution values. The curve-of-growth technique thus appears to be an attractive method for determining the parameters of autoionizing features. The application of this technique to make path-length or particle-density measurements in, for example, a King furnace or a plasma is also discussed.

CLARK, B. G.

C025 High-Resolution Observations of Compact Radio Sources at 13 Centimeters

K. I. Kellermann (National Radio Astronomy Observatory), B. G. Clark (National Radio Astronomy Observatory), D. L. Jauncey (Cornell University), M. H. Cohen (California Institute of Technology), D. B. Shaffer (California Institute of Technology), A. T. Moffet (California Institute of Technology), and S. Gulkis
Astrophys. J., Vol. 161, No. 3, pp. 803-809, September 1970

For abstract, see Kellermann, K. I.

CLAYTON, R. M.

C026 Injector Hydrodynamics Effects on Baffled-Engine Stability

R. M. Clayton
Supporting Research and Advanced Development, Space Programs Summary 37-62, Vol. III, pp. 272-279, April 30, 1970

Initial experimental results of an investigation of the effects of injector hydrodynamic properties on the effectiveness of baffles for the control of dynamic stability in liquid rocket engines are summarized. Dynamic stability characteristics are determined for a research combustor that utilizes an injector with large hydraulic impedance, where a four-blade array of baffles with axial lengths greater than 2.4 in. are shown to be highly effective in providing stability to both induced and spontaneous high-amplitude combustion disturbances. Baffles shorter than 2.4 in. failed to stabilize the combustor. Damping times for the stable configurations were of the order of 10 ms and did not vary significantly with injector operating conditions (mixture ratios) or baffle lengths between 2.4 and 5.4 in. (the maximum length tested). For inadequate-length baffles, the amplitude of combus-

tion resonance increased with progressively shorter baffles, showing the important relationship between axial combustion distribution and baffle length.

COHEN, M. H.

C027 High-Resolution Observations of Compact Radio Sources at 13 Centimeters

K. I. Kellermann (National Radio Astronomy Observatory), B. G. Clark (National Radio Astronomy Observatory), D. L. Jauncey (Cornell University), M. H. Cohen (California Institute of Technology), D. B. Shaffer (California Institute of Technology), A. T. Moffet (California Institute of Technology), and S. Gulkis
Astrophys. J., Vol. 161, No. 3, pp. 803-809, September 1970

For abstract, see Kellermann, K. I.

CONEL, J. E.

C028 Microwave Emission From Granular Silicates: Determination of the Absorption Coefficient From Plate Measurements and the Effects of Scattering

J. E. Conel
Technical Memorandum 33-458, October 15, 1970

Microwave brightness temperature measurements (1.4-37 GHz) from plane layers of granulated silicate materials backed by a perfectly reflecting metal plate are used to determine the mass absorption coefficient, attenuation length, and effective values of electrical conductivity and loss tangent. The important experimental finding is that the mass absorption coefficient is independent of frequency but highly dependent on moisture content. From this one determines that the effective conductivity increases with frequency, and that the loss tangent is independent of frequency in this frequency range. Computed values of these quantities are in rough numerical agreement with extrapolated laboratory values on other silicate materials. The effects of scattering, using elementary solutions of the equation of radiative transfer, are described.

C029 Coloring of Synthetic and Natural Lunar Glass by Titanium and Iron

J. E. Conel
Supporting Research and Advanced Development, Space Programs Summary 37-62, Vol. III, pp. 26-31, April 30, 1970

Synthetic glass prepared from lunar rock 10020 is distinctly dark reddish-brown in contrast to the fresh unfused material that is dark gray. Mössbauer analysis shows a ratio of $\text{Fe}^{+3}/\text{total Fe}$ of 0.04 and no Fe_2O_3 .

Other red and brown natural lunar glasses have high iron and titanium contents and no ferric iron. Coloring mechanisms for glass involving *d*-orbital electronic transitions in Fe^{+2} and Ti^{+3} are found unsuitable for producing required absorption in the blue. Calculations show that a wide variety of colors may conceivably be produced by scattering from colloidal iron or ilmenite spheres suspended in silicate glass, but the required scatterers have not been directly identified in lunar or other glasses. A charge transfer (ligand-metal) mechanism involving ionic forms of titanium (Ti^{+4}) and perhaps iron is suggested as a possible alternative for coloring of lunar glass.

C030 A New Method for Determining SiO_2 Abundance in Silicate Glass From Powder Film Transmission Measurements in the Infrared

J. E. Conel

Supporting Research and Advanced Development, Space Programs Summary 37-63, Vol. III, pp. 7-9, June 30, 1970

The Christiansen frequency of a substance is conveniently determined from transmission measurements on thin ($\sim 30 \mu\text{m}$) films of powder with particle sizes on the order of $10 \mu\text{m}$ or greater in diameter. This frequency is defined by the position of maximum transmission and represents the frequency of minimum scattering for the (average) complex refractive indices of the materials involved. Transmission measurements on silicate glasses prepared from naturally occurring igneous rocks and the plagioclase mineral series have revealed a striking relationship between Christiansen frequency and SiO_2 abundance. The data illustrates a simple, rapid method for semiquantitative determination of silica abundances in synthetic rock and mineral glasses and the crystalline material from which they were prepared.

C031 Spectral Reflectance and Albedo of Apollo 11 Lunar Samples: Effects of Irradiation and Vitrification and Comparison With Telescopic Observations

J. E. Conel and D. B. Nash

Proceedings of the Apollo 11 Lunar Science Conference, Houston, Texas, January 5-8, 1970, Vol. 3, pp. 2013-2023

Spectral reflectance ($0.23\text{--}2.5 \mu\text{m}$) and albedo ($0.4\text{--}0.7 \mu\text{m}$) measurements were made on fresh powders of rock 10020 before and after both proton irradiation and vitrification. Doses of 2 keV protons, equivalent to 20,000 yr exposure to the solar wind, reduced the albedo from 20 to 18%, while artificial vitrification reduced it to 8%. Vitrification is thus a possible lunar darkening mechanism.

The crystalline and glassy materials studied show important differences in spectral reflectivity. Rock powder of 10020 is characterized by prominent absorption features near $1.0 \mu\text{m}$ and $2.2 \mu\text{m}$, and relatively strong reflection in the blue, all attributed to pyroxene. Synthetic glass, on the other hand, has broad absorption bands at $1.02 \mu\text{m}$ and $1.8 \mu\text{m}$ and strong reflection near $0.7 \mu\text{m}$. Weak structure near $0.95 \mu\text{m}$ in the spectrum of lunar fines arises mostly from pyroxene.

Lunar rocks and fines and synthetic lunar glass are used to interpret qualitatively color differences for some bright and dark areas of the moon's surface obtained by McCord and others. Reflectance ratios in the visible spectrum are interpreted to indicate that bright craters are covered in part by crystalline rock or crushed debris derived therefrom, and dark areas by material similar to Tranquillitatis fines.

COOPER, M. A.

C032 The Effect of Steric Compression on Proton-Proton, Spin-Spin Coupling Constants. Further Evidence and Mechanistic Considerations

M. A. Cooper and S. L. Manatt

J. Am. Chem. Soc., Vol. 92, No. 15, pp. 4646-4652, July 29, 1970

Analyses of the nuclear magnetic resonance (NMR) spectra of 1,4-dimethylnaphthalene, 1,4-di-*t*-butylnaphthalene, and benzo[*c*]-phenanthrene are presented. These results confirm earlier suggestions that NMR spin-spin coupling constants involving a proton in a sterically compressed situation exhibit appreciably different magnitudes from couplings found in less crowded but otherwise similar environments. A detailed discussion of the mechanisms producing these changes in the case of three-bond, *ortho* couplings ($^3J_{\text{HH}}$) is given, and it is shown that the behavior of $^3J_{\text{HH}}$ in overcrowded molecules is consistent with the occurrence of strain-relieving distortions in molecular geometry such as have been independently proposed on theoretical grounds. The use of NMR coupling constants as qualitative measures of strain-induced deformations in overcrowded aromatic molecules is discussed.

C033 Proton NMR Spectra of Cyclopentadiene, 1,3-Cyclohexadiene, 1,3-Cyclooctadiene, and 1,2-Dihydronaphthalene

M. A. Cooper, D. D. Elleman, C. D. Pearce, and S. L. Manatt

J. Chem. Phys., Vol. 53, No. 6, pp. 2343-2352, September 15, 1970

The proton nuclear magnetic resonance (NMR) coupling constants between vinyl protons in cyclopentadiene (I), 1,3-cyclohexadiene (II), and 1,3-cycloocta-

diene (III) have been obtained by analyses of the spectra of the latter protons when the methylene protons were decoupled. An analysis of the full spectrum of I has also been achieved. Analysis of the spectrum of 1,2-dihydronaphthalene (IV) was undertaken both to obtain a value of $^3J_{HH}$ across the olefinic double bond, and to compare certain of its coupling constants with those from our previous work on indene. The long-range coupling constants between vinyl protons in the planar molecule I and nearly planar II are significantly different from those in the nonplanar III. The differences are discussed in terms of the conformations of these molecules, and the importance of these results for testing theories of long-range coupling constants is pointed out.

COSTOGUE, E. N.

C034 Solar Electric Propulsion System Tests

E. V. Pawlik, E. N. Costogue, J. D. Ferrera, and T. W. Macie
Technical Report 32-1480, August 15, 1970

For abstract, see Pawlik, E. V.

C035 Solar Electric Propulsion System Evaluation

E. V. Pawlik, E. N. Costogue, J. D. Ferrera, and T. W. Macie
J. Spacecraft Rockets, Vol. 7, No. 8, pp. 968-976,
August 1970

For abstract, see Pawlik, E. V.

COYNER, J. V., JR.

C036 Parametric Study of the Performance Characteristics and Weight Variations of Large-Area Roll-Up Solar Arrays

J. V. Coyner, Jr. and R. G. Ross, Jr.
Technical Report 32-1502, December 15, 1970

An analysis has been conducted to determine the relationships between the performance characteristics (power-to-weight ratio, blanket tension, structural member section dimensions, and resonant frequencies) of large-area roll-up solar arrays of the single-boom, tensioned-substrate design. The study includes the determination of the size and weight of the base structure supporting the boom and blanket and the determination of the optimum width, blanket tension, and deployable boom stiffness needed to achieve the minimum-weight design for a specified frequency for the first mode of vibration. A computer program has been used to generate a set of plots that provide optimum structural sizing and estimated weights for arrays with blanket areas ranging from 100 to 400 ft² and for first-mode natural frequencies ranging from 0.03 to 0.7 Hz. Use of these plots enables a quick evaluation of the potential merits of a proposed roll-up array.

CRAMER, P. W., JR.

C037 Large Spacecraft Antennas: Performance Comparison of Focal Point and Cassegrain Antennas for Spacecraft Applications

P. W. Cramer, Jr.

Supporting Research and Advanced Development, Space Programs Summary 37-62, Vol. III, pp. 80-87,
April 30, 1970

The RF performances of focal point and cassegrain parabolic reflector antennas are compared. The design of each type is optimized with respect to the focal-length-to-diameter ratio, edge illumination, aperture blockage, etc., and the results are presented in a form helpful in designing and analyzing such antennas. The X-band performances of the two configurations are then compared for antenna diameters of 7 to 30 ft. It is found that the focal point configuration is better for diameters less than approximately 11 ft and the cassegrainian configuration is better for larger diameters.

CRAWFORD, W. E.

C038 Solar Electric Spacecraft Thrust Vector Control System Mechanization

W. E. Crawford and G. E. Fleischer

Supporting Research and Advanced Development, Space Programs Summary 37-62, Vol. III, pp. 164-166,
April 30, 1970

A new mechanization of the solar electric propulsion spacecraft translator (or gimbal) axis controller is described. Controller feedback compensation is derived directly from the actuator drive signal (voltage-controlled oscillator output) rather than actuator output position. As a result, feedback signal-to-noise ratio is significantly improved. System gain values are determined that achieve control response equivalent (for the noise-free case) to that for the original mechanization concept.

C039 Solar Electric Propulsion System Technology Project Thrust Vector Control Electronics

W. E. Crawford

Supporting Research and Advanced Development, Space Programs Summary 37-64, Vol. III, pp. 75-77,
August 31, 1970

The thrust vector control electronics hardware will be used to support the solar electric propulsion system technology (SEPST) effort which is directed toward a system feasibility demonstration scheduled for calendar years 1970-1971. This article describes the electronic hardware in detail and also briefly describes the electric propulsion ion engine mechanical configuration.

CROSBY, J. R.

C040 Temperature Control Materials Technology

J. R. Crosby and T. F. Moran
Supporting Research and Advanced Development,
Space Programs Summary 37-62, Vol. III, pp. 179-180,
April 30, 1970

A calorimeter for measuring the thermal properties of multilayer insulation has been constructed, calibrated, and placed in operation. Calorimeter tests on various thermal shields have shown that reproducibility of data is $\pm 2.5\%$. Currently, a comparison of thermal performances of the thermal shield configurations used on the *Mariner* Mars 1969 and the *Mariner* Mars 1971 systems is being made.

A preliminary investigation on the formation of non-condensable gases in water/metal heat pipes was performed. Metals evaluated included various stainless-steel alloys, nickel, titanium, beryllium-copper, copper, brass, and bronze alloys. With the exception of the copper and several of the bronze alloys, all samples showed a significant generation of hydrogen gas occurring.

C041 Multilayer Insulation Testing

J. R. Crosby
Supporting Research and Advanced Development,
Space Programs Summary 37-64, Vol. III, pp. 79-80,
August 31, 1970

A calorimeter for measuring the thermal properties of multilayer insulation is in operation, and tests on various thermal shield configurations show that the reproducibility of data is $\pm 2.5\%$. Currently, a comparison of thermal performance between the thermal shield configurations used on the *Mariner* Mars 1969 and the *Mariner* Mars 1971 systems is being made. Based on an equal number of layers, the data show the thermal insulation characteristics of the *Mariner* Mars 1971 shield to be approximately 20% better than those of the *Mariner* Mars 1969 shield. In addition, examination of the data shows that the optimum amount of overlap to use on a *Mariner* Mars 1971 shield seam is on the order of 5 to 6 in. Finally, the effective emittance of a 3.5-ft² cylindrical section of the *Mariner* Mars 1971 shield using a 16-in.-long axial seam with a 5-in. overlap was determined to be 0.0028.

CROW, R. B.

C042 1.0002-MHz Frequency Synthesizer

R. B. Crow
The Deep Space Network, Space Programs Summary 37-63,
Vol. II, pp. 42-45, May 31, 1970

A stable frequency synthesizer has been developed to furnish the transmit coder clock (1.0002 MHz) and

the reference for the clock doppler detector (1.0000 MHz) for the Planetary Ranging System. The prime requirement for this module is to maintain stability between the 1.000- and 1.0002-MHz outputs. Drift between these two outputs appears as drift in range. An improvement of 50 to 1 was achieved by careful attention to component drift and the design of the phase-locked loop used in the 1.0002-MHz frequency synthesizer module.

C043 DSIF Multiple-Mission Command System

R. Crow, S. Friesema, J. Wilcher, and J. Woo
The Deep Space Network, Space Programs Summary 37-63,
Vol. II, pp. 77-94, May 31, 1970

Progress continues on the design and hardware-software development for the Deep Space Instrumentation Facility (DSIF) Multiple-Mission Command System reported earlier. An engineering model of the command modulator assembly (CMA) has been constructed and is undergoing evaluation tests. To evaluate the performance of the CMAs when coupled to the telemetry and command processor computers, a Multiple-Mission Command Demonstration-Test Program has been written. This program will also be used for system-integration tests when the CMAs are implemented. Included in this article are descriptions and theory of operation on each of the CMA digital subassemblies and CMA analog equipment.

CUDDIHY, E. F.

C044 Investigation of Sterilizable Battery Separator Membranes [June-July 1970]

E. F. Cuddihy, D. E. Walmsley, and J. Moacanin
Supporting Research and Advanced Development,
Space Programs Summary 37-64, Vol. III, pp. 136-138,
August 31, 1970

Silver-zinc flight batteries employ, as a separator membrane, a thin film of crosslinked polyethylene unto which has been grafted poly(potassium acrylate). These membranes are exposed during service to a strongly caustic 40% KOH electrolyte which is also a strong oxidizing environment caused by the presence of dissolved silver ion. This article provides an update on the continuing studies concerned with the stability and permanence of the membrane in this strong oxidative-caustic environment. Particularly, data and interpretation are given for a kinetic study of the loss from the film of poly(potassium acrylate) and the simultaneous accumulation within the film of deposits of metallic silver and silver oxide. Also included are some pre-

liminary results on the changes in cell resistance caused by the aging of the separators in the battery electrolyte environment.

CUFFEL, R. F.

C045 Performance of a Supersonic Nozzle with a 75-deg Convergent Half-Angle and a Small Throat Radius of Curvature

R. F. Cuffel and P. F. Massier

Supporting Research and Advanced Development, Space Programs Summary 37-64, Vol. III, pp. 149-152, August 31, 1970

Thrust, flow coefficient, and specific impulse were evaluated experimentally for a nozzle that had a convergent half-angle of 75 deg, a divergent half-angle of 15 deg, and a ratio of throat radius of curvature to throat radius of 0.25. The throat diameter was 1.6 in. The flow coefficient was found to be 0.951, and, at the exit of the nozzle (expansion area ratio = 2.3), the thrust ratio was 0.941 and the specific impulse ratio was 0.99.

C046 Effect of Wall Cooling on the Mean Structure of a Turbulent Boundary Layer in Low-Speed Gas Flow

L. H. Back, R. F. Cuffel, and P. F. Massier

Int. J. Heat Mass Transfer, Vol. 13, No. 6, pp. 1029-1047, June 1970

For abstract, see Back, L. H.

CURKENDALL, D. W.

C047 Planetary Navigation: The New Challenges

D. W. Curkendall

Astronaut. Aeronaut., Vol. 7, No. 5, pp. 26-29, May 1970

Effective space navigation in the 1970s will rely upon a tenfold improvement in radio navigation, dramatically narrowed planetary ephemerides, onboard planet sensing, and sophisticated navigation filters. Various aspects of the new challenges in planetary navigation are discussed.

C048 Earthbased Tracking and Orbit Determination—Backbone of the Planetary Navigation System

D. W. Curkendall and R. R. Stephenson

Astronaut. Aeronaut., Vol. 7, No. 5, pp. 30-36, May 1970

Throughout the 1960s, the Deep Space Network—with major complexes in Spain, South Africa, Australia, and the United States—has served as the principal

tracking instrument for nearly all U.S. interplanetary and unmanned lunar spaceflight programs. This article gives an up-to-date account of the Deep Space Network, the inherent accuracy limitations of the data it can gather, and the relationship between data accuracy and the ability to determine the orbit of a deep-space probe.

DALLAS, S. S.

D001 Prediction of the Position and Velocity of a Satellite After Many Revolutions: The Differential Equations of Motion

S. S. Dallas

The Deep Space Network, Space Programs Summary 37-63, Vol. II, pp. 24-29, May 31, 1970

A set of normalized differential equations of motion that govern the motion of a solar-powered satellite are derived. The perturbative accelerations consist of those due to oblateness of the central body, solar gravity, and aerodynamic drag.

DANIELSON, G. E., JR.

D002 Environmental Testing and Calibration of the Mariner Mars 1969 Television System

G. E. Danielson, Jr., and P. M. Salomon

Paper 69-994, AIAA (American Institute of Aeronautics and Astronautics)/ASTM (American Society for Testing Materials)/IES (Institute of Environmental Sciences) 4th Space Simulation Conference, Los Angeles, California, September 8-10, 1969

The environmental test and calibration program for the *Mariner Mars 1969* television system was designed to duplicate the full range of conditions inherent in launch, transit, and encounter maneuvers, and to provide sufficient system calibration data to define the performance characteristics of the system in the Mars-encounter environment. Environmental testing included the full range of mechanical stress tests as well as extended periods of system operation in a thermal vacuum. Photometric and geometric calibration data were obtained for each picture-element location in the television scene format. Major variations in system performance were due to the temperature dependence of the vidicon sensor characteristics. Special environmental tests and data reduction techniques were developed to isolate and individually measure these parameter changes. Calibration-data storage requirements were satisfied by employing magnetic video tape for real-time recording of system performance, while computer reduction of the resultant video tape defined the parameter variation of interest on a picture-element-by-picture-element basis. The details

of the environmental test and calibration program are described, as is the system performance measured during the tests.

DAVAR, M.

D003 Potentialities of a New Class of Anticlotting and Antihemorrhagic Polymers

T. F. Yen (University of Southern California, California State College), M. Davar (University of Southern California, California State College), and A. Rembaum
J. Macromol. Sci.—Chem., Vol. A4, No. 3, pp. 693–714, May 1970

For abstract, see Yen, T. F.

DAVID, C. N.

D004 Microbiology, Ecology and Microclimatology of Soil Sites in Dry Valleys of Southern Victoria Land, Antarctica

R. E. Cameron, J. King, and C. N. David
Antarctic Ecology: Volume 2, pp. 702–716, Academic Press, Inc., New York, 1970

For abstract, see Cameron, R. E.

DAVIS, J. P.

D005 Preliminary Nuclear Criticality Studies for a Thermionic Reactor With Uninsulated Externally Fueled Diodes

T. Papazoglou, H. Gronroos, and J. P. Davis
Supporting Research and Advanced Development, Space Programs Summary 37-62, Vol. III, pp. 256–259, April 30, 1970

For abstract, see Papazoglou, T.

DAWE, R. H.

D006 TOPS Electronic Packaging and Cabling

R. H. Dawe
Supporting Research and Advanced Development, Space Programs Summary 37-63, Vol. III, pp. 143–149, June 30, 1970

The objectives for Thermoelectric Outer-Planet Spacecraft (TOPS) electronic packaging and cabling are to apply proven principles to develop a lighter weight, low-stress, high-density, packaging system. The principles that have been used for the packaging system are reviewed and various configurations considered. The approach taken is to provide single side access plug-in assemblies utilizing new miniature high-

density connectors. The assemblies are utilized in conjunction with an integrated structure providing flexible packaging arrangements and having high structural and thermal efficiencies.

DAYMAN, B., JR.

D007 Aerodynamics of Vehicles in Tubes

B. Walker and B. Dayman, Jr.
Supporting Research and Advanced Development, Space Programs Summary 37-62, Vol. III, pp. 216–218, April 30, 1970

For abstract, see Walker, B.

DEDE, C.

D008 Pressure Dependence of Carbon Trioxide Formation in the Gas-Phase Reaction of O(¹D) With Carbon Dioxide

W. B. DeMore and C. Dede
J. Phys. Chem., Vol. 74, No. 13, pp. 2621–2625, 1970

For abstract, see DeMore, W. B.

DeMORE, W. B.

D009 Rates and Mechanism of Alkyne Ozonation

W. B. DeMore
Supporting Research and Advanced Development, Space Programs Summary 37-63, Vol. III, pp. 14–22, June 30, 1970

The rates and products of the reactions of acetylene, methylacetylene, dimethylacetylene, and ethylacetylene with ozone have been studied in a long-path infrared cell at $21 \pm 1^\circ\text{C}$. The acetylene rate constant agrees well with the Arrhenius parameters for that reaction which were previously measured by a different method. Within experimental error, the ozonation rates of the substituted acetylenes are identical to that of acetylene at 21°C . The results provide further support for the previously derived high A-factor for the acetylene ozonation relative to alkenes, and thus tend to raise some question regarding the concerted reaction mechanism for 1,3 cycloaddition reactions, of which the ozonation reactions are one type.

Product formation in the gas phase alkyne ozonations is postulated to stem from unimolecular fission of an acid anhydride intermediate, the latter being the primary, albeit short-lived, reaction product. Diketone formation was observed in every case, but there is evidence that formation of that product was a side reaction on the walls. It is pointed out that the precursor of the anhydride intermediate is essentially

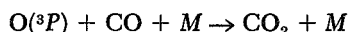
a zwitterionic structure, analogous to the Criegee zwitterion produced in alkene ozonations.

D010 The Efficiency of CO₃ Formation in the Mars and Venus Atmospheres

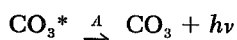
W. B. DeMore

J. Geophys. Res., Space Physics, Vol. 75, No. 25, pp. 4898–4899, September 1, 1970

Recent publications have emphasized the difficulty of explaining the photochemical balances of the Mars and Venus atmospheres by the simple recombination reaction



Alternative mechanisms of CO oxidation have therefore been proposed. According to one of these, CO₃ is produced by radiative stabilization:



where the constant *A* is the transition probability for the stabilizing radiation. Subsequent oxidation of CO by CO₃ thus completes the CO₂ reformation, and the over-all process does not involve any three-body steps.

Quantitative evaluation of the CO₃ scheme has been hampered by a lack of basic laboratory evidence, especially with regard to the pressure dependence of CO₃ formation. A series of laboratory measurements dealing with CO₃ has been completed, and certain applications of that work to the planetary atmospheres are described here.

D011 Pressure Dependence of Carbon Trioxide Formation in the Gas-Phase Reaction of O(¹D) With Carbon Dioxide

W. B. DeMore and C. Dede

J. Phys. Chem., Vol. 74, No. 13, pp. 2621–2625, 1970

The reaction $\text{O}(^1\text{D}) + \text{CO}_2 + \text{M} \rightarrow \text{CO}_3 + \text{M}$ has been studied at -30° over the pressure range of 100–2500 psi. The method involved photolysis (2537 Å) of O₃–CO₂ mixtures pressurized with He or Ar. Detection of CO₃ was based on the fact that its formation is accompanied by removal of atomic oxygen, which in turn is reflected by a decrease in the O₃ concentration. Blank experiments using N₂ instead of CO₂ showed that other paths for loss of atomic oxygen were relatively negligible. Although CO₃ formation was detected by this method, the dominant process at all pressures was quenching of O(¹D) to O(³P), which evidently proceeds *via* a CO₃^{*} intermediate: $\text{O}(^1\text{D}) + \text{CO}_2 \rightarrow \text{CO}_3^* \rightarrow \text{CO}_2 + \text{O}(^3\text{P})$. The observed pres-

sure dependence of CO₃ formation indicates that the lifetime of CO₃^{*} before predissociation to CO₂ + O(³P) is about 10^{–11} to 10^{–12} s.

DERR, L. J.

D012 Advanced Development of a Multiple-Cathode Electron Gun

L. J. Derr

Supporting Research and Advanced Development, Space Programs Summary 37-62, Vol. III, pp. 90–92, April 30, 1970

A multiple-cathode electron gun is being developed for linear-beam electron tubes to improve the operating life of spacecraft transmitters that can be used for the outer-planet missions of the 1970s. This development seeks to extend the 3- to 4-yr operating capability of present electron tubes to as much as 12 yr. In this article, the mechanical models of the gun are described. Environmental tests performed on these models have demonstrated the feasibility of moving, positioning, and operating a multiple-cathode disc within a vacuum environment.

DEVANEY, J. R.

D013 Antarctic Soil Algal Crusts: Scanning Electron and Optical Microscope Study

R. E. Cameron and J. R. Devaney

Trans. Am. Microsc. Soc., Vol. 89, No. 2, pp. 264–273, April 1970

For abstract, see Cameron, R. E.

DEVINE, C. J.

D014 Chebyshev Polynomial Expansions of Emden Functions

C. J. Devine and E. W. Ng

Supporting Research and Advanced Development, Space Programs Summary 37-64, Vol. III, pp. 13–16, August 31, 1970

This article reports on the generation of truncated Chebyshev polynomial approximations to the solution of the Lane–Emden equation

$$\frac{d^2y}{dx^2} + \frac{2}{x} \frac{dy}{dx} + y^\nu = 0, \quad x = 0, y = 1, \frac{dy}{dx} = 0$$

for values of $\nu = 1.0(0.1)4.5$, which will allow evaluation of the solution $f(x)$ at any point x in the range of $0 \leq x \leq x_0$.

DE WINTER, F.

D015 Thermoelectric Properties of 80-at. % Silicon—20-at. % Germanium Alloy as a Function of Time and Temperature

V. Raag and F. de Winter

Supporting Research and Advanced Development, Space Programs Summary 37-62, Vol. III, pp. 125–127, April 30, 1970

For abstract, see Raag, V.

DOBROTIN, B.

D016 Mariner Limit Cycles and Self-Disturbance Torques

B. Dobrotin, E. A. Laumann, and D. Prelewicz (California Institute of Technology)

J. Spacecraft Rockets, Vol. 7, No. 6, pp. 684–689, June 1970

Details of the *Mariner* attitude control system limit cycle operation during cruise are presented. Limit cycle operation is shown to vary from the ideal case to single side operation. The data are analyzed to determine the form of the variation and to seek an explanation. The results show that there is a bias torque of several dyne-cm which changes at the end of a limit cycle, coinciding with the firing of an attitude control jet. Diagrams illustrate the various limit-cycle operations and the changes encountered. Because *Mariner V* had a balanced sun profile, the solar bias was low and it appeared that much of the disturbance torque was self-generated. An analysis of the attitude control jets demonstrated that a sizable torque could be generated by leakage through the attitude control valves. Experimental data obtained confirmed this suspicion.

DORE, M. A.

D017 Gamma Radiation Characteristics of Plutonium Dioxide Fuel

P. J. Gingo and M. A. Dore

Technical Report 32-1481, June 15, 1970

For abstract, see Gingo, P. J.

D018 Gamma Ray and Neutron Analysis for a 15-W(th) Pu²³⁸O₂ Isotopic Heater

M. A. Dore

Supporting Research and Advanced Development, Space Programs Summary 37-63, Vol. III, pp. 93–97, June 30, 1970

Gamma ray and neutron spectra, dose rates, and flux levels are determined by Monte Carlo methods for

all space in the vicinity of a 15-W(th) Pu²³⁸O₂ isotopic heater of the type used on the *Apollo* Passive Seismic Experiment Package. Heaters of similar design are anticipated for possible inclusion on the Thermoelectric Outer-Planet Spacecraft; utilization of this particular design for this preliminary analysis allows comparison with results previously determined by Mound Laboratories. Five fuel ages, from 0 to 18 yr, are considered, assuming nominal (i.e., 1.2 ppm Pu²³⁸ and 0.204% O¹⁸) fuel, to allow meaningful comparison with previous results. Excellent agreement (<5% difference) is obtained for 10- to 18-yr-old fuel for all locations except very near the surface of the heater, where the results obtained are about 12% higher than those of Mound. One possible explanation for this discrepancy is that the value given by Mound was extrapolated from measurements at larger distances, perhaps based upon 1/r² fall-off, in which case a lower than actual value would result. Since the actual fuel was not 10 to 18 yr old, a small though consistent error in the source strengths used is indicated.

DORROH, W. E., JR.

D019 Attitude Control of a TOPS-Based Outer Planet Orbiter Spacecraft

W. E. Dorroh, Jr.

Supporting Research and Advanced Development, Space Programs Summary 37-63, Vol. III, pp. 111–114, June 30, 1970

The Thermoelectric Outer-Planet Spacecraft (TOPS) attitude control subsystem requires few changes for use on the outer planet orbiter spacecraft of the 1980s. The subsystem functional requirements, vehicle moments of inertia, and mass expulsion impulse requirements are approximately the same as for TOPS, and the gravity gradient effects from the planets are minimal. The only major change required is in the autopilot required to control the throttling of the liquid-fuel vernier engines, as opposed to the gimbaled autopilot of a single liquid-fuel engine for TOPS.

D020 Strategies and Systems for Navigation Corrections

W. E. Dorroh, Jr., and T. H. Thornton, Jr.

Astronaut. Aeronaut., Vol. 7, No. 5, pp. 50–55, May 1970

The desire to navigate unmanned spacecraft accurately to the planets makes it necessary to consider using navigation corrections—usually small flightpath changes achieved by applying one or more velocity impulses at certain times along the trajectory. The theory of interplanetary navigation corrections has been developed over the past decade together with

spacecraft hardware and the operational software to implement it in various space missions, such as the *Mariner* series.

This article considers the evolution of the corrections which have been used for space navigation and the chief approaches to control hardware.

DUXBURY, T. C.

D021 Mariner Mars 1969 Approach Guidance Demonstration

T. C. Duxbury and W. G. Breckenridge
Supporting Research and Advanced Development,
Space Programs Summary 37-64, Vol. III, pp. 72-73,
August 31, 1970

This article describes the status of the *Mariner* Mars 1969 approach guidance demonstration. Telemetered data from the *Mariner* spacecraft (*Mariners VI* and *VII*) were used with earth-based doppler data to estimate the trajectories of both spacecraft in near-real-time operations. The demonstration represented the first effort to use spacecraft-based data from an interplanetary spacecraft for the purpose of navigation. The demonstration has laid the ground work for future interplanetary missions requiring spacecraft-based navigation data by demonstrating the feasibility of using this data type, within mission time constraints, to successfully produce trajectory estimates.

D022 Defining a Spacecraft-Based Navigation System

W. G. Breckenridge and T. C. Duxbury
Astronaut. Aeronaut., Vol. 7, No 5, pp. 44-49,
May 1970

For abstract, see Breckenridge, W. G.

D023 A Spacecraft-Based Navigation Instrument for Outer Planet Missions

T. C. Duxbury
J. Spacecraft Rockets, Vol. 7, No. 8, pp. 928-933,
August 1970

This article presents the results of an analytical study of various spacecraft-based data that could be used to improve solely earth-based navigational accuracies when approaching or orbiting outer planets. Measuring the celestial directions to outer planet natural satellites can supply the needed navigational data. The satellite motion can define the celestial direction to the center-of-mass of the outer planet-satellite system more accurately than can be determined from viewing the planet itself. An instrument similar to science television cameras used on the *Mariner* Mars missions would be suited to produce this spacecraft-based data by view-

ing satellites and reference stars simultaneously. A description of an instrument producing these measurements (accurate to better than 5 arc-sec) and the applicability of these spacecraft-based data to a Grand Tour mission are also presented.

EASTON, R.

E001 A Highly Reliable Interface Circuit for Driving FET Switching Trees

R. Easton and E. Hilbert
Supporting Research and Advanced Development,
Space Programs Summary 37-62, Vol. III, pp. 206-211,
April 30, 1970

This article describes a driver circuit for interfacing between transistor-transistor logic and field-effect transistor (FET) switching trees. It was designed for use in switching analog signals in the measurement processor of the Thermoelectric Outer Planet Spacecraft data handling subsystem. The principal objectives of the design are to minimize power dissipation and to maximize reliability.

EISENBERGER, I.

E002 Communication Statistics: Finite-Sample Quantile Estimation

I. Eisenberger
The Deep Space Network, Space Programs Summary 37-65,
Vol. II, pp. 47-50, September 30, 1970

Quantile estimators of the unknown parameters of a normal distribution have been previously derived on the basis of the asymptotic normal distribution of the quantiles used. This article reports the results of an investigation of the effects of a finite sample size on the bias and efficiency of some of the estimators. The exact moments of the quantiles and estimators are computed for sample sizes of $n = 50, 100$, and 200 . The results show that, even for n as small as 50 , the estimators that were considered can be useful. This closes a gap in the theory of quantiles for efficient estimation and detection of signals.

ELLEMAN, D. D.

E003 An Ion Cyclotron Resonance Study of the Ion-Molecule Reactions in Hydrogen-Methane Mixtures

M. T. Bowers and D. D. Elleman
Supporting Research and Advanced Development,
Space Programs Summary 37-62, Vol. III, pp. 32-36,
April 30, 1970

For abstract, see Bowers, M. T.

E004 An Ion Cyclotron Resonance Study of the Ion-Molecule Reactions in Methane-Ammonia Mixtures

W. T. Huntress, Jr., and D. D. Elleman
J. Am. Chem. Soc., Vol. 92, No. 12, pp. 3565-3573,
June 17, 1970

For abstract, see Huntress, W. T., Jr.

E005 Proton NMR Spectra of Cyclopentadiene, 1,3-Cyclohexadiene, 1,3-Cyclooctadiene, and 1,2-Dihydronaphthalene

M. A. Cooper, D. D. Elleman, C. D. Pearce, and S. L. Manatt
J. Chem. Phys., Vol. 53, No. 6, pp. 2343-2352,
September 15, 1970

For abstract, see Cooper, M. A.

E006 Analysis of Ion-Molecule Reactions in Allene and Propyne by Ion Cyclotron Resonance

M. T. Bowers (University of California, Santa Barbara),
D. D. Elleman, R. M. O'Malley (The University, Sheffield,
England), and K. R. Jennings (The University, Sheffield,
England)
J. Phys. Chem., Vol. 74, No. 13, pp. 2583-2589, 1970

For abstract, see Bowers, M. T.

EMERSON, R. F.

E007 Loop Stress Diminution

R. M. Goldstein, R. F. Emerson, W. L. Sjogren, and L. Sydnor
The Deep Space Network, Space Programs Summary 37-64,
Vol. II, pp. 61-67, August 31, 1970

For abstract, see Goldstein, R. M.

FARMER, C. B.

F001 High-Dispersion Spectroscopic Studies of Mars: III. Preliminary Results of 1968-1969 Water-Vapor Studies

R. A. Schorn, C. B. Farmer, and S. J. Little (University
of Texas)
Icarus: Int. J. Sol. Sys., Vol. 11, No. 3,
pp. 283-288, November 1969

For abstract, see Schorn, R. A.

FERRERA, J. D.

F002 Solar Electric Propulsion System Tests

E. V. Pawlik, E. N. Costogue, J. D. Ferrera, and T. W. Macie
Technical Report 32-1480, August 15, 1970

For abstract, see Pawlik, E. V.

F003 Valve Evaluation Program for Use in Nitrogen Attitude Control Gas Systems

J. D. Ferrera

Supporting Research and Advanced Development,
Space Programs Summary 37-62, Vol. III, pp. 158-160,
April 30, 1970

Future spacecraft missions, currently in the planning stage, will place more severe requirements on pneumatic system components than those currently existing for the *Mariner* series. A program has been developed to find and evaluate pneumatic valves that will satisfy the new requirements. Valves from 5 of the more than 20 companies surveyed are described, as well as the various phases of the test program.

F004 Solar Electric Propulsion System Evaluation

E. V. Pawlik, E. N. Costogue, J. D. Ferrera, and T. W. Macie
J. Spacecraft Rockets, Vol. 7, No. 8, pp. 968-976,
August 1970

For abstract, see Pawlik, E. V.

FISHER, J. G.

F005 Mesh Materials for Deployable Antennas

J. G. Fisher

Supporting Research and Advanced Development,
Space Programs Summary 37-62, Vol. III, pp. 176-179,
April 30, 1970

Mechanical characteristics desirable in a furlable spacecraft antenna reflective surface are discussed. Results of an evaluation of two types of mesh material are presented. The first type consisted of a square-weave Dacron mesh plated with electroless copper and protected by a dip-applied silicone overcoat. The second type was a tricot-knit mesh made of Chromel-R wires and coated with electroless gold. Of the two types, the tricot-knit was found to have better mechanical characteristics. Both types suffered from flaking of their respective electroless coatings.

F006 Development of a Conical-Gregorian High Gain Antenna

J. G. Fisher

Supporting Research and Advanced Development,
Space Programs Summary 37-63, Vol. III, pp. 124-128,
June 30, 1970

The conical-Gregorian antenna concept has several theoretical advantages over conventional parabolic reflector types. Among these are the potential elimination of "reverse pillowing" due to chording of mesh surfaces in rib-and-mesh designs, by furling with a simple bending of the reflector surface. First development efforts toward the practical design and

construction of a conical-Gregorian antenna are described. Two models were produced: one a rigidified assembly for RF testing, and the other for experiments in furling. Problems arising in the construction of these antennas, and steps taken toward their solution, are discussed.

FITZGERALD, D. J.

F007 Ion Thruster Hollow Cathode Studies

E. V. Pawlik and D. J. Fitzgerald
Supporting Research and Advanced Development,
Space Programs Summary 37-64, Vol. III, pp. 146-149,
August 31, 1970

For abstract, see Pawlik, E. V.

FLANAGAN, F. M.

F008 Deep Space Network Support of the Manned Space Flight Network for Apollo: 1962-1968

F. M. Flanagan, P. S. Goodwin, and N. A. Renzetti
Technical Memorandum 33-452, Vol. I, July 15, 1970

This memorandum summarizes the development, engineering, and implementation activities of the NASA Deep Space Network (DSN) in support of the NASA Manned Space Flight Network (MSFN), managed by the Goddard Space Flight Center, for the *Apollo* Project from 1960 through 1968. A detailed account is presented of the operational support provided for the *Apollo* 4-8 missions. In the field of *Apollo* telecommunications, the state-of-the-art of the unified S-band system is traced through the development at JPL of the receiver/exciter and ranging subsystems implemented in both the DSN and MSFN.

FLEISCHER, G. E.

F009 Solar Electric Spacecraft Thrust Vector Control System Mechanization

W. E. Crawford and G. E. Fleischer
Supporting Research and Advanced Development,
Space Programs Summary 37-62, Vol. III, pp. 164-166,
April 30, 1970

For abstract, see Crawford, W. E.

FOX, K.

F010 Construction of Tetrahedral Harmonics

K. Fox and I. Ozier (North American Rockwell Corporation)
J. Chem. Phys., Vol. 52, No. 10, pp. 5044-5056,
May 15, 1970

Explicit, detailed, and convenient algorithms have been developed for constructing tetrahedral harmonics

for arbitrary J . These functions are expressed as linear combinations of spherical harmonics and also of symmetric top functions. A projection-operator technique was used to produce projected functions that transform according to the rows of the irreducible matrix representations of T_d . In general, the set of projected functions so constructed may be linearly dependent. The *idempotence* of the projection operators was invoked to show that *all* the required *orthonormal* tetrahedral harmonics can be produced by the diagonalization of the projection-operator matrices. The elements of these matrices are given explicitly for arbitrary J . Alternative procedures, including the Gram-Schmidt method, for the orthogonalization of the projected functions are treated briefly, with special emphasis on the use of these matrix elements. The "symmetry-adapted functions" involve the $d_{K',K}^J(\pi/2)$, and a recursion relation is presented that facilitates an accurate and rapid calculation of these constants. An important new sum rule useful in calculations of integrated intensities is derived, using the idempotence property. Various physical applications are discussed.

FREDRICKS, R. W.

F011 OGO 5 Observations of Quasi-Trapped Electromagnetic Waves in the Solar Wind

F. L. Scarf (Space Sciences Laboratory), R. W. Fredricks (Space Sciences Laboratory), I. M. Green (Space Sciences Laboratory), and M. Neugebauer
J. Geophys. Res., Space Phys., Vol. 75, No. 19,
pp. 3735-3750, July 1, 1970

For abstract, see Scarf, F. L.

FREY, W.

F012 Multiple Mission Telemetry 1971 Configuration

W. Frey, R. Petrie, R. Greenberg, J. McInnis, and R. Wengert
The Deep Space Network, Space Programs Summary 37-63,
Vol. II, pp. 63-77, May 31, 1970

Increased telemetry data-handling requirements placed on the Deep Space Instrumentation Facility (DSIF) to support future flight projects have necessitated an update of the DSIF multiple mission telemetry (MMT) system. The update will allow the DSIF to (1) handle higher telemetry data rates, (2) operate on block-coded data, and (3) process more telemetry data channels simultaneously. This article reports on the progress being made on the block decoder and symbol synchronizer assemblies, and includes information on the telemetry and command data-handling subsystem, the MMT test rack, subcarrier demodulator assemblies, the new high-speed data wide-band data input-output assembly, and mission-independent software.

FRIESEMA, S.

F013 DSIF Multiple-Mission Command System

R. Crow, S. Friesema, J. Wilcher, and J. Woo
The Deep Space Network, Space Programs Summary 37-63,
Vol. II, pp. 77-94, May 31, 1970

For abstract, see Crow, R.

FUZIE, R. E.

F014 DSIF Network Maintenance Facility: Reference Standards Frequency and Timing Laboratory

R. E. Fuzie
The Deep Space Network, Space Programs Summary 37-63,
Vol. II, pp. 101-107, May 31, 1970

The Reference Standards Laboratory of the Deep Space Instrumentation Facility (DSIF) Network Maintenance Facility operates a Frequency and Timing Laboratory for the DSIF that provides precise frequency and time references to the National Bureau of Standards and the United States Naval Observatory. The Frequency and Timing Laboratory is comprised of (1) the laboratory measurement chain, (2) the very low frequency monitoring and measuring system, and (3) the DSIF tick generation and distribution system. This article describes the operation of the Frequency and Timing Laboratory including equipment configuration and the role of each of its major sections in furnishing precision frequency and time to the DSIF.

FYMAT, A. L.

F015 An Interferometric Approach to the Measurement of Optical Polarization

A. L. Fymat and K. D. Abhyankar
Appl. Opt., Vol. 9, No. 5, pp. 1075-1081, May 1970

Following a discussion of the desirability of determining the variation of polarization with frequency in planetary spectra, the possibility of measuring the intensity and state of polarization of optical radiation by means of the high-resolution Fourier spectroscopic method is discussed. In the proposed experimental arrangement, a two-beam interferometer is used with a polarizer in each beam. After recombination, the emergent radiation is analyzed with a linear polarizer. It is shown that the interferograms obtained in this way contain information about the four Stokes parameters of the incident radiation. The polarizers introduce an asymmetry in the interferograms requiring full (exponential) transforms for retrieval of the desired data. The effects of the finite range of path difference and the variation of its zero point with frequency are considered, and evaluation of the corre-

sponding phase error with a proper choice of the polarizer settings is discussed. The formalism also takes into account the residual polarization introduced by the beam splitter and the differential transmission of the two beams. Generally, three independent interferograms are needed for determining the phase error and the four Stokes parameters. Some simple arrangements are described in which the two beams are both either linearly or circularly polarized.

GARCIA, E.

G001 Simulation Conversion Assembly

E. Garcia
The Deep Space Network, Space Programs Summary 37-64,
Vol. II, pp. 88-95, August 31, 1970

The simulation conversion assembly, an assembly of the Deep Space Instrumentation Facility telemetry and command data handling subsystem, is described. This assembly has been designed to provide the deep space stations with a mission-independent spacecraft telemetry simulation capability and will be used in support of spacecraft projects and for test and calibrations of the stations' multiple-mission telemetry equipment.

GARTHWAITE, K.

G002 Quantitative Confirmation of Planetary Defects in the Lunar Theory by Spectral Decomposition

J. D. Mulholland, K. Garthwaite, and D. B. Holdridge
Supporting Research and Advanced Development,
Space Programs Summary 37-64, Vol. III, p. 169,
August 31, 1970

For abstract, see Mulholland, J. D.

GEORGEVIC, R. M.

G003 Analytic Expressions for the Partial Derivatives of Observables With Respect to the Robertson's Relativistic Parameters

R. M. Georgevic
Supporting Research and Advanced Development,
Space Programs Summary 37-64, Vol. III, pp. 162-168,
August 31, 1970

Using the Robertson isotropic line element, closed-form analytic expressions for partial derivatives of the observables, range and range rate, are derived with respect to the parameters β and γ , in terms of the true anomaly of the osculating motion. The parameters β and γ are two of the three constants that appear in Robertson's general static, spherically symmetric, isotropic line element; the third parameter, α , is taken to be unity.

GILCHRIEST, C. E.

G004 The Probability Density Function of a Hardware Performance Parameter

C. E. Gilchrist and M. K. Tam (Tam Research Associates)
Technical Memorandum 33-439, September 1, 1970

A study of the probability density function of a hardware performance parameter delivered by a contractor to a specification is presented. Because sufficient data were not available to estimate this probability density function experimentally, it was necessary to derive *a priori* probability density functions from assumed axioms determined from an investigation of contractor motivation and behavior. From these axioms, the problem was formulated and solved in the form of a calculus of variations problem with integral and inequality constraints.

Numerous examples are presented in which various strategies of contractor manipulation were used. The conclusions based on these examples are that incentive contracting is not an effective tool, and that close surveillance of the contractor is the most effective means for obtaining a hardware parameter to a specification.

GINGO, P. J.

G005 Gamma Radiation Characteristics of Plutonium Dioxide Fuel

P. J. Gingo and M. A. Dore
Technical Report 32-1481, June 15, 1970

An extensive investigation was performed to characterize the net gamma ray source intensity and spectrum for PuO_2 fuel. All major sources were considered, including the gamma radiation from plutonium isotopes and their decay products exclusive of ^{236}Pu , radioactive decay of ^{236}Pu and daughter nuclides, and alpha-particle interaction with the isotope ^{18}O . These sources were tabulated for 20 energy groups ranging from 1 keV to 7 MeV. For each of the age-dependent composite source spectra so determined, gamma ray fluxes were calculated for three different thicknesses of fuel in a typical PuO_2 -fueled capsule. These gamma fluxes were determined at the capsule surface, as well as at several exterior points.

GLUCKLICH, J.

G006 Strain-Energy Size Effect

J. Glucklich
Technical Report 32-1438, August 15, 1970

The effect of the physical size of a specimen upon the *initiation* of fracture of materials is in accordance with statistics of flaw distribution. The effect of size upon *total* fracture is as above, plus the effect during

stable crack propagation. Stability of cracking can be because of (1) energy dissipation, (2) load relaxation, or (3) crack orientation. Only (1) reflects a material property. The *energy-dissipation stability* is affected by the strain-energy content (and therefore by size) in such a way that the higher the energy, the earlier this stability transforms to instability. Consequently, the larger the specimen, the lower the breaking stress and the ductility that accompanies the cracking. A possible explanation is presented in terms of dynamic effects caused by an excess in the energy released over the energy absorbed. These dynamic effects influence the stability of the propagating crack in a manner in which the size of the specimen plays a dominant part.

The behavior of three broad groups of materials is examined from the viewpoint of crack stability. These are *ductile* (mainly soft metals), *semiductile* (materials such as concrete and gypsum), and *brittle* (glass). The conditions favoring instability are listed, and the various materials are classified in accordance with their position relative to a transition size. Examples of the effects of size in various materials are cited, and it is shown that existing theories are unable to explain all of the observations, either qualitatively or quantitatively. The proposed theory of a strain-energy size effect seems to fill these gaps satisfactorily.

It is speculated that, in general, every material has two constants that fully describe its resistance to fracture: γ' and G_i . These involve the critical strain-energy release rate G_c . Here, γ' is the limiting value of $\frac{1}{2} G_c$ when size increases to infinity; G_i is the limiting value of G_c when size decreases to zero. In practice, γ' controls the initiation of cracking and G_c (not G_i) controls the onset of instability. Whereas γ' is independent of specimen size, a study should be made of the size dependence of G_c . Evidently γ' is also the true design criterion for very large, ductile members, and G_i is the design criterion for very small, brittle elements.

Transition-size curves are proposed (in analogy to transition-temperature curves), and the positions of the transition for some materials are roughly indicated.

GOLDSTEIN, R. M.

G007 Loop Stress Diminution

R. M. Goldstein, R. F. Emerson, W. L. Sjogren, and L. Sydnor
The Deep Space Network, Space Programs Summary 37-64, Vol. II, pp. 61-67, August 31, 1970

An experiment was performed on the *Pioneer VI* spacecraft to demonstrate the reductions in spacecraft

receiver loop stress made possible by the use of a programmed up-link. The theory was verified by the data obtained. Such a technique is necessary in outer-planet flybys because of the rapid frequency accelerations. The experimental procedure, the receiver/transmitter, the ephemeris-tuned oscillator, and usage in orbit determination are discussed in this article.

- G008 A Noise-Adding Radiometer for Use in the DSN**
P. D. Batelaan, R. M. Goldstein, and C. T. Stelzried
The Deep Space Network, Space Programs Summary 37-65,
Vol. II, pp. 66-69, September 30, 1970

For abstract, see Batelaan, P. D.

- G009 A Radar Snapshot of Venus**
R. M. Goldstein and H. Rumsey, Jr.
Science, Vol. 169, No. 3949, pp. 974-977,
September 4, 1970

A radar brightness map of Venus has been obtained for a fairly extensive equatorial region ($13,500 \times 7,500$ km). The resultant resolution of 80 km is the best yet achieved for Venus. The bright feature Alpha shows up very clearly, and much of its detail is revealed. There is also a host of interesting radar-bright and radar-dark objects. The procedures used and the resultant map are described in this article.

GOODWIN, P. S.

- G010 Deep Space Network Support of the Manned Space Flight Network for Apollo: 1962-1968**
F. M. Flanagan, P. S. Goodwin, and N. A. Renzetti
Technical Memorandum 33-452, Vol. I, July 15, 1970

For abstract, see Flanagan, F. M.

GOSLINE, R. M.

- G011 DSS 13 Operations**
E. B. Jackson and R. M. Gosline
The Deep Space Network, Space Programs Summary 37-63,
Vol. II, p. 42, May 31, 1970

For abstract, see Jackson, E. B.

GOSS, W. C.

- G012 Advanced Development Electrostatic Image Dissector**
W. C. Goss
Supporting Research and Advanced Development,
Space Programs Summary 37-63, Vol. III, pp. 114-115,
June 30, 1970

A second-generation electrostatic image dissector is being developed for use in the *Mariner* spacecraft attitude-control star tracker. Major improvements are planned in the areas of fabrication yield ratio, dimensional control, leakage currents, temperature tolerance, and tolerance of low-pressure gas environments.

- G013 The Mariner Spacecraft Star Sensors**

W. C. Goss

Appl. Opt., Vol. 9, No. 5, pp. 1056-1067, May 1970

The development history of the star sensors used on the *Mariner* spacecraft is traced, and design and performance details are described. The electro-optically controlled sensor, which was developed for the 1964 Mars mission, was modified for the 1967 Venus mission to withstand the intense planetary illumination. The sensor was further modified for the 1969 Mars mission to survive the more severe launch environment and to provide greater capability for automatic search, identification, and tracking. Special star simulation and stray-light test techniques are discussed.

GOTTLIEB, P.

- G014 Average Access Times for a Magnetic Disk Storage Device**

P. Gottlieb and H. Lass

Supporting Research and Advanced Development,
Space Programs Summary 37-62, Vol. III, pp. 285-289,
April 30, 1970

The mean distances that single or multiple read-write heads must travel in executing an instruction on a magnetic disk storage device have been computed previously, but only in numerical form. Analytic expressions for these distances as a function of the number of tracks and the number of heads are derived. An analytic expression for the variance of the distance traveled by a single read-write head is also derived. Since the head travel time is (approximately) linearly proportional to the mean travel distance, the analytic expressions for these distances should be useful for designing a disk file system.

GOULD, R. W.

- G015 Numerical Study of Collisional Effects on Spatial Ion-Wave Echoes**

K. Nishikawa and R. W. Gould (California Institute of Technology)

Phys. Fluids, Vol. 13, No. 7, pp. 1883-1885, July 1970

For abstract, see Nishikawa, K.

GREEN, I. M.

- G016 OGO 5 Observations of Quasi-Trapped Electromagnetic Waves in the Solar Wind**
F. L. Scarf (Space Sciences Laboratory), R. W. Fredricks (Space Sciences Laboratory), I. M. Green (Space Sciences Laboratory), and M. Neugebauer
J. Geophys. Res., Space Phys., Vol. 75, No. 19, pp. 3735–3750, July 1, 1970

For abstract, see Scarf, F. L.

GREENBERG, R.

- G017 Multiple Mission Telemetry 1971 Configuration**
W. Frey, R. Petrie, R. Greenberg, J. McInnis, and R. Wengert
The Deep Space Network, Space Programs Summary 37-63, Vol. II, pp. 63–77, May 31, 1970

For abstract, see Frey, W.

GREENE, W. M.

- G018 A Miniaturized Absolute Gravimeter for Terrestrial, Lunar, and Planetary Research**
R. G. Brereton, B. H. Chovitz (United States Coast and Geodetic Survey), W. M. Greene, (Marshall Space Flight Center), O. K. Hudson (Marshall Space Flight Center), R. A. Lytleton (St. John's College), and R. D. Regan (United States Geology Survey)
Supporting Research and Advanced Development, Space Programs Summary 37-62, Vol. III, pp. 1–5, April 30, 1970

For abstract, see Brereton, R. G.

GREENWOOD, R. F.

- G019 Solar Cell Standardization**
R. F. Greenwood
Supporting Research and Advanced Development, Space Programs Summary 37-62, Vol. III, pp. 131–132, April 30, 1970

Solar cells calibrated on high-altitude balloons and recovered are used as intensity reference standards during performance testing of solar cells and solar arrays under terrestrial sunlight or artificial light source conditions. Present plans call for a series of three balloon flights to be conducted during June and July 1970 in the vicinity of Minneapolis, Minnesota. Interested NASA and government agencies have been invited to participate in the cooperative solar cell standardization effort.

GREER, R. T.

- G020 Luminescence Properties of Apollo 11 Lunar Samples and Implications for Solar-Excited Lunar Luminescence**
D. B. Nash and R. T. Greer
Proceedings of the Apollo 11 Lunar Science Conference, Houston, Texas, January 5–8, 1970, Vol. 3, pp. 2341–2350

For abstract, see Nash, D. B.

GRIPPI, R. A., JR.

- G021 Design, Fabrication, and Testing of the Applications Technology Satellite Apogee Motor Insulation**
R. A. Grippi, Jr.
Technical Memorandum 33-341, September 15, 1970

The Jet Propulsion Laboratory has completed the design, development, formal qualification, and flight phases of the *Applications Technology Satellite (ATS)* solid propellant apogee motor program. This report describes in detail the design concept, type of material, fabrication, and performance of the titanium motor chamber insulation system. The motor is insulated with Gen-Gard V-52, which is a material formulated of polybutadiene–acrylonitrile rubber, hydrated silica, asbestos fiber, reinforcing resin, plasticizer, antioxidant, and processing and vulcanizing agents. To develop and confirm the insulation design, numerous motor chambers were instrumented with thermocouples on the external surface to obtain temperature data during and after motor firing. The temperature results of these tests are presented for units instrumented in the motor development and qualification phase. On December 7, 1966, November 6, 1967, and August 12, 1969, the JPL apogee motors placed the *ATS-B*, *ATS-C*, and *ATS-E* satellites into synchronous equatorial orbit.

GRONROOS, H.

- G022 Preliminary Nuclear Criticality Studies for a Thermionic Reactor With Uninsulated Externally Fueled Diodes**
T. Papazoglou, H. Gronroos, and J. P. Davis
Supporting Research and Advanced Development, Space Programs Summary 37-62, Vol. III, pp. 256–259, April 30, 1970

For abstract, see Papazoglou, T.

- G023 Design of Reactor Simulator for Thermionic Diode Kinetics Experiment**
H. Gronroos
Supporting Research and Advanced Development,

Space Programs Summary 37-62, Vol. III, pp. 263-271,
April 30, 1970

The methods employed to develop a reactor simulator for the thermionic diode kinetics experiment are described. Analog computers are programmed so that the experiment with the computers in the loop matches the dynamic characteristics of a selected model thermionic reactor powerplant. The programmed equations and data applicable for the experimental assembly are given. Three simulator versions of different degrees of complexity are described.

G024 Reactor Simulator Runs With Thermionic Diode Kinetics Experiment

H. Gronroos

Supporting Research and Advanced Development,
Space Programs Summary 37-63, Vol. III, pp. 215-222,
June 30, 1970

The operation of the thermionic diode kinetics experiment with a nuclear reactor simulator in the loop is described. Two cases from the most recent series of runs are discussed and their response trajectories are shown. A brief account of the modifications presently being incorporated into the experiment is also given. One of the two cases discussed illustrates the open-loop (i.e., no reactor controller) response to an electric load change. The other case shows the event during a simulated reactor start-up run.

GROTCH, S. L.

G025 Matching of Mass Spectra When Peak Height Is Encoded to One Bit

S. L. Grotch

Anal. Chem., Vol. 42, No. 11, pp. 1214-1222,
September 1970

The problem of the identification of low resolution mass spectra has been approached from the viewpoint of statistics and information theory. The mass spectral peak heights of 3000 different organic compounds were quantized to only two levels; a "0" denoting no peak, a "1" a peak above a specified transition. All spectral patterns of three groups of 1000 spectra were compared pairwise and the distribution of mismatches was calculated. A theoretical analysis permits the accurate prediction of the mean and variance of this matching distribution from the statistics of each spectral group. These results indicate that mass spectral patterns are highly specific signatures even when encoded to only one bit. The relationship between the information content of spectra and the matching results is also explored.

GULKIS, S.

G026 High-Resolution Observations of Compact Radio Sources at 13 Centimeters

K. I. Kellermann (National Radio Astronomy Observatory),
B. G. Clark (National Radio Astronomy Observatory),
D. L. Jauncey (Cornell University), M. H. Cohen (California Institute of Technology), D. B. Shaffer (California Institute of Technology), A. T. Moffet (California Institute of Technology), and S. Gulkis
Astrophys. J., Vol. 161, No. 3, pp. 803-809,
September 1970

For abstract, see Kellermann, K. I.

GUPTA, K. K.

G027 High-Impact Dynamic Response Analysis of Nonlinear Structures

K. K. Gupta

Technical Report 32-1498, November 15, 1970

An efficient and generalized digital computer method is presented for determining the dynamic response of nonlinear structures of simple geometric configuration subjected to high-impact loading. A finite element matrix displacement approach utilizing quadrilateral shell elements, in conjunction with a step-by-step integration procedure employing Runge-Kutta extrapolation techniques, has been adopted for the present analysis.

The related procedure yields reliable results for simple structural forms, e.g., rectangular and cylindrical panels, and requires only moderate computer storage and solution time. Numerical results are presented for the analysis of relevant structures subjected to high impact, simulating free landing on a planetary surface.

The program is written in FORTRAN V language to run on the UNIVAC 1108 computer under the EXEC 8 operating system; the source deck consists of about 1800 cards. The physical program, IMAN (IMPact ANALysis), is available from the Computer Software Management and Information Center (COSMIC), the NASA agency for the distribution of computer programs.

HAMILTON, G.

H001 The Recording of SDA Outputs for Mariner Mars 1971

G. Hamilton

The Deep Space Network, Space Programs Summary 37-65,
Vol. II, pp. 116-117, September 30, 1970

The necessity for recording subcarrier demodulator assembly (SDA) outputs is discussed. Included in the article are descriptions of the problems concerning analog recording of the outputs, signal specifications

of the outputs pertinent to magnetic tape recording, and the FM multiplexing scheme chosen, as well as a data path block diagram for the *Mariner* Mars 1971 Project.

HAMILTON, T. W.

H002 Coursing Accurately to the Giant Outer Planets and Their Moons

T. W. Hamilton and J. F. Jordan

Astronaut. Aeronaut., Vol. 7, No. 5, pp. 66–70, May 1970

The late 1970s present a very favorable lineup of the outer planets that will not reoccur for much the better part of two centuries. This favorable configuration makes possible multiple-planet *ballistic* "Grand Tours." In these ballistic flights, the only propulsion applied after departure from earth would make small correction maneuvers. Outerplanet missions in the 1980s, however, may use electric-propulsion systems that operate continuously over portions of the flight. Navigation problems in both kinds of missions are discussed in this article.

HAND, P. J.

H003 TOPS Inertial Reference Unit

P. J. Hand

Supporting Research and Advanced Development, Space Programs Summary 37-63, Vol. III, pp. 122–123, June 30, 1970

The Thermoelectric Outer-Planet Spacecraft (TOPS) attitude-control system baseline is to be all digital. An all digital inertial reference unit (IRU) is therefore being designed which will employ gyros requiring active temperature control. To minimize the power consumption resulting from this approach, a low-thermal-loss IRU design concept is being evaluated. Tests indicate that a controlled-thermal-loss design rather than a minimum-loss design is required. These tests are discussed and plots of gyro input power versus temperature are shown for both atmospheric and vacuum conditions.

HARDY, J.

H004 Large Spacecraft Antennas: Use of Efficiency Program to Calculate Feed Defocusing Loss

A. Ludwig and J. Hardy

Supporting Research and Advanced Development, Space Programs Summary 37-62, Vol. III, pp. 87–89, April 30, 1970

For abstract, see Ludwig, A.

H005 Spacecraft Antenna Research: Preliminary RF Test of Conical Gregorian Antenna

A. C. Ludwig and J. Hardy

Supporting Research and Advanced Development, Space Programs Summary 37-63, Vol. III, pp. 42–46, June 30, 1970

For abstract, see Ludwig, A. C.

HARRISON, B. K.

H006 General Relativistic Axially Symmetric Rotating Perfect Fluids

B. K. Harrison

Supporting Research and Advanced Development, Space Programs Summary 37-63, Vol. III, p. 14, June 30, 1970

New formulations and simplifications of the equations for general relativistic axially symmetric rotating perfect fluids have been found.

H007 Simplified Equations for Relativistic Rotating Perfect Fluids With Axial Symmetry

B. K. Harrison

Phys. Rev., Pt. D: Part. Fields, Vol. 1, No. 8, pp. 2269–2271, April 15, 1970

The general relativistic equations for a stationary axially symmetric rotating perfect fluid, in a comoving coordinate system, are presented in an elegant general form. The coordinates can then be chosen in any of several ways to further simplify the equations. One choice reduces the number of independent metric functions to three.

HARTLEY, R. B.

H008 Apollo Mission Support [by DSN, May–June 1970]

R. B. Hartley

The Deep Space Network, Space Programs Summary 37-64, Vol. II, pp. 7–11, August 31, 1970

The support provided by the Deep Space Network (DSN) to the Manned Space Flight Network (MSFN) during the abortive *Apollo 13* mission is described. Support was provided from the three 85-ft-antenna DSN/MSFN Wing stations, the 210-ft-antenna Mars Deep Space Station, the Ground Communications Facility, and the Space Flight Operations Facility. Permission and mission activities are discussed, and a brief mission description is included.

HAUDENSCHILD, C.

H009 Multi-Phase Ammonia Water System

C. Haudenschild

Supporting Research and Advanced Development, Space Programs Summary 37-64, Vol. III, pp. 4-9, August 31, 1970

Equations are fitted to tabular laboratory data available for ammonia water systems. The equations relate temperature, concentration, and partial pressures over solution, solid hydrate, solid water, and solid ammonia. The freezing curve, in the form of an equation for temperature as a function of concentration, is given for the phase boundary of each region. Finally, a phase diagram displaying all equations is produced.

HAYES, B. M.

H010 SFOF Mariner Mars 1971 Mission Support Area

B. M. Hayes

The Deep Space Network, Space Programs Summary 37-64, Vol. II, pp. 107-108, August 31, 1970

A mission support area for the *Mariner Mars 1971* Project has been constructed in the Space Flight Operations Facility (SFOF) at JPL. The architectural and electrical designs were determined by the requirements and various mission objectives of the project. The design of the mission support area is described, and a floor plan is included.

HAYS, L. G.

H011 Thermal Conductance of Alumina-Nickel Interfaces at Elevated Temperatures

L. G. Hays

Int. J. Heat Mass Transfer, Vol. 13, No. 8, pp. 1293-1297, August 1970

The thermal conductance in vacua between an alumina surface at 1100°C and a nickel surface at 55-90°C was determined experimentally over a range of contact pressures. The added resistance due to a mono-layer of zirconia microspheres between these surfaces was also measured. The results show the predicted dependency of conductance upon contact pressure, but the absolute magnitudes were from $\frac{1}{2}$ to $\frac{1}{4}$ of the theoretical magnitudes.

H012 Surface Damage from High-Velocity Flow of Lithium

L. G. Hays

J. Mater., Vol. 5, No. 3, pp. 666-683, September 1970

High-velocity impact and flow of liquid metals on surfaces is a problem area in many advanced power gen-

erating systems. In liquid metal magnetohydrodynamic or turbine power systems flow may occur at velocities which are an order of magnitude greater than those for which corrosion tests have been conducted previously. Prediction of the lifetime of these power systems, therefore, is dependent on having information on liquid metal corrosion processes at high velocities, which is not currently available.

An experiment was performed to measure the corrosion of two materials—columbium-1% zirconium alloy and yttrium oxide—by a lithium stream flowing in a test section at velocities of 19, 34, and 48.5 m/s. The corrosion specimens were flat blocks which had part of their surface in contact with the liquid-metal stream.

After 109 h at 1143°C, the yttria specimens were dissolved completely. After an additional 391 h at 1073°C, the maximum depth of material removal from the columbium alloy was measured to be about 3, 5, and 7 μm in the fully developed flow regions of the respective velocity sections. These values correspond to the depths calculated from the empirical turbulent mass transfer relations for simple dissolution if the temperature coefficient of solubility is taken to be 1.2×10^{-9} g-columbium/g-lithium °C and if the diffusivity of columbium in lithium is calculated by the Einstein-Stokes equation. For a normally behaved solute-solvent combination, this value of temperature coefficient of solubility would result in an absolute value of solubility at 1100°C of 1 to 5 ppm by weight. The measured variation of material loss with lithium velocity followed the dependency predicted by these mass transfer relations, indicating a diffusion-limited process is occurring.

The physical character of the columbium alloy surfaces in various stages of dissolution was determined by examination with a scanning electron microscope. These micrographs show the progressive development of a lattice of cavities, due probably to preferential attack of some grain faces followed by hydrodynamic effects. These cavities appear to be sufficiently deep to cause accelerated erosion if they were to occur in a region where liquid impact were occurring also.

HEER, E.

H013 Optimum Structural Design Based on Reliability Analysis

M. Shinozuka (Columbia University), J.-N. Yang, and E. Heer
Technical Report 32-1496 (Reprinted from *Proceedings of the Eighth International Symposium on Space Technology and Science, Tokyo, Japan, August 25-30, 1969, pp. 245-258*)

For abstract, see Shinozuka, M.

H014 On the Maximum Dynamic Response of Structures and Proof Testing

J.-N. Yang and E. Heer

Supporting Research and Advanced Development,
Space Programs Summary 37-64, Vol. III, pp. 91-95,
August 31, 1970

For abstract, see Yang, J.-N.

HEIDENREICH, G.

H015 TOPS Trajectory Correction Engine

G. Heidenreich

Supporting Research and Advanced Development,
Space Programs Summary 37-63, Vol. III, pp. 227-235,
June 30, 1970

Future unmanned space missions, such as the Grand Tour of the outer planets, will require up to nine separate trajectory course corrections with a total burn time of 1500 s. A pressure-fed blowdown system using a monopropellant blend of hydrazine in a catalytic decomposition chamber producing 25-lbf thrust has been chosen as the baseline propulsion system for the Thermoelectric Outer-Planet Spacecraft (TOPS). A series of tests were conducted to determine the effects of multiple cold starts, long-duration (up to 800 s) steady-state burns, and low-temperature incoming propellant. Some preliminary tests were also conducted with a blend of 76% N_2H_4 , 24% $N_2H_5NO_3$. The tests to date indicate that the duty cycle envisioned can be met with state-of-the-art technology using neat hydrazine as the propellant. However, extreme care must be given to both design and testing to insure a high degree of confidence and reliability, since catalytic performance and life is limited. It is determined that considerable development effort will be needed before a higher performing monopropellant can be utilized. Several known problems requiring future investigation are discussed.

H016 TOPS Trajectory Correction Engine Testing

G. Heidenreich

Supporting Research and Advanced Development,
Space Programs Summary 37-64, Vol. III, pp. 153-157,
August 31, 1970

Upcoming flyby missions to the outer planets will require extended and multiple firings of a trajectory correction engine for midcourse maneuvers. The most severe duty cycle for such an engine in terms of number of cold (40-70°F) starts and firing duration would be a mission designed to fly by all five outer planets. This article reports on a series of tests conducted on an existing flight-weight, space-qualified, catalytic monopropellant hydrazine engine. The engine was the tran-

stage attitude control system hydrazine engine developed for the *Titan IIIC*. An engine, which had 380 s of qualification (pulse-mode) tests, was put through a simulated Thermoelectric Outer-Planet Spacecraft (TOPS) mission duty cycle. The testing consisted of seven steady-state firings, ranging in length from 16 to 753 s, and totaling 1270 s. Performance remained good throughout. Chamber pressure roughness near the end of the tests grew to ± 29 psi.

HELLER, J.

H017 DSN Tracking System Operations

J. Heller and R. B. Miller

The Deep Space Network, Space Programs Summary 37-65,
Vol. II, pp. 122-125, September 30, 1970

This article describes the operations of the Deep Space Network (DSN) Tracking Operations Analysis Group in the Mark IIIA era. Most of the functions described are being performed at the present time by manual procedures and with the use of the software available on the IBM 7044/7094 computer system. The design of the IBM 360/75 software is geared towards minimizing manual operations in the accountability and validation of tracking data and towards using computer displays to monitor data flow and system performance. A functional diagram illustrating the Space Flight Operations Facility tracking subsystem software design is included in the article.

HERRERA, G.

H018 Thrust and Plume Measurements Taken on Miniature Nozzles in a Vacuum Chamber

G. Herrera

Supporting Research and Advanced Development,
Space Programs Summary 37-62, Vol. III, pp. 214-216,
April 30, 1970

This article covers the experimental part of the nozzle flow and vacuum exhaust technology task that utilizes the 25-ft Space Simulator and Molsink. The data obtained and the nozzles evaluated are described, as are the test instrumentation, hardware, and procedures.

HILBERT, E.

H019 A Highly Reliable Interface Circuit for Driving FET Switching Trees

R. Easton and E. Hilbert

Supporting Research and Advanced Development,
Space Programs Summary 37-62, Vol. III, pp. 206-211,
April 30, 1970

For abstract, see Easton, R.

HOFFMAN, J. K.

**H020 Evaluation of Recording Tapes for Use in
Spacecraft Magnetic Tape Recorders
[April–May 1970]**

J. K. Hoffman, S. H. Kalfayan, and R. H. Silver
Supporting Research and Advanced Development,
Space Programs Summary 37-63, Vol. III, p. 160,
June 30, 1970

Efforts to solve problems related to reliability of magnetic tape in typical spacecraft recorder applications continue. Tape to magnetic head frictional drag characteristics were investigated under certain environmental conditions. Further evaluation of data and additional testing is in progress.

**H021 Evaluation of Spacecraft Magnetic
Recording Tapes [April–May 1970]**

S. H. Kalfayan, R. H. Silver, and J. K. Hoffman
Supporting Research and Advanced Development,
Space Programs Summary 37-63, Vol. III, pp. 209–214,
June 30, 1970

For abstract, see Kalfayan, S. H.

**H022 Evaluation of Recording Tapes for Use in
Spacecraft Magnetic Tape Recorders
[June–July 1970]**

J. K. Hoffman, S. H. Kalfayan, and R. H. Silver
Supporting Research and Advanced Development,
Space Programs Summary 37-64, Vol. III, p. 119,
August 31, 1970

The second phase of a continuing effort to investigate the characteristics of magnetic recording tape and the tape-to-head interface is discussed.

**H023 Evaluation of Spacecraft Magnetic
Recording Tapes [June–July 1970]**

S. H. Kalfayan, R. H. Silver, and J. K. Hoffman
Supporting Research and Advanced Development,
Space Programs Summary 37-64, Vol. III, pp. 140–145,
August 31, 1970

For abstract, see Kalfayan, S. H.

HOLCOMB, L. B.

**H024 Satellite Auxiliary-Propulsion Selection
Techniques**

L. B. Holcomb
Technical Report 32-1505, November 1, 1970

In order to establish criteria for the selection of attitude- and station-keeping propulsion systems for future satellites and other unmanned spacecraft, current auxiliary propulsion systems were surveyed and parameterized. Thruster systems considered were inert gas, monopropellant hydrazine, vaporizing liquid, electrolysis, Tri-dyne, resistojet, radioisotopic, and subliming solid. Electrostatic and electromagnetic thrusters were also surveyed, but were not included in the detailed study. A generalized auxiliary propulsion system selection technique, based on cost-effectiveness criteria, is presented. Three specific missions are included as examples of the use of the selection criteria: a synchronous satellite, a subsynchronous satellite, and a Grand Tour planetary spacecraft.

HOLDRIDGE, D. B.

**H025 Quantitative Confirmation of Planetary Defects
in the Lunar Theory by Spectral Decomposition**

J. D. Mulholland, K. Garthwaite, and D. B. Holdridge
Supporting Research and Advanced Development,
Space Programs Summary 37-64, Vol. III, p. 169,
August 31, 1970

For abstract, see Mulholland, J. D.

HOLICK, A.

**H026 Minimum Redundancy Transformation Between
Body and Inertial Frame for a Typical
Strapped-Down Inertial Navigation System**

A. Holick
Supporting Research and Advanced Development,
Space Programs Summary 37-62, Vol. III, pp. 166–170,
April 30, 1970

During applications of electrically suspended gyros (ESGs) to long-life spacecraft, it became apparent that the reliability of the ESG could be improved by using the inherent redundancy in an ESG inertial reference, which uses two gyros, each having three pick-offs. These results are applicable to all users of ESGs in strapped-down inertial navigators. Preliminary algorithms are given for implementing the minimum-redundancy transformation between body and inertial frame. It is shown that a three-parameter approach is possible if the angle between the two spin vectors is constant in the interval of interest. There are 18 different operational modes depending upon which 3 measurements are available, each requiring, in general, a different set of equations. The total number of equations to be implemented in the on-board computer can be significantly reduced by adopting an iterative approach and by recognizing certain patterns in indexing the variables.

HOLMES, J. K.

**H027 Coding and Synchronization Research:
Performance of a First-Order Digital
Phase-Locked Loop**

J. Holmes

*Supporting Research and Advanced Development,
Space Programs Summary 37-63, Vol. III, pp. 28-34,
June 30, 1970*

This article develops the exact analysis of an unmodulated digital phase-locked loop for the (modulo 2π reduced) steady-state phase error variance and for the first passage time problem. Also the bit error probability is obtained for the modulated case. The results have been applied to the operation of the newly proposed all-digital, single-channel command system being developed as part of the Thermoelectric Outer-Planet Spacecraft Project.

**H028 Coding and Synchronization Research:
Performance of an All-Digital Command
System Timing Loop**

J. Holmes

*Supporting Research and Advanced Development,
Space Programs Summary 37-64, Vol. III, pp. 17-22,
August 31, 1970*

This article develops the analysis of a pseudonoise code-modulated, first-order digital phase-locked loop. The loop provides coherent detection of a biphasemodulated, single-channel, command system currently under development as part of the Thermoelectric Outer-Planet Spacecraft Project. Three aspects of performance are considered: (1) the stationary timing error variance, (2) the signal-to-noise ratio degradation due to timing jitter, and (3) the bias due to doppler shift.

**H029 On a Solution to the Second-Order
Phase-Locked Loop**

J. K. Holmes

*IEEE Trans. Communication Technology, Vol. COM-18,
No. 2, pp. 119-126, April 1970*

A solution of the stationary, mod- 2π -reduced phase-error probability density function for the second-order phase-lock loop is derived, based on a mean square fit to a certain unknown conditional expectation term. The resulting phase variance obtained from this density function yields an error that is negligible for $\sigma_\phi^2 \leq 1$ and an error no greater than 0.06 rad^2 for signal-to-noise ratios $\geq 2 \text{ dB}$ by comparison with actual measurements, and it appears to be the most accurate to date. The usefulness of the result lies in the fact that an accurate estimate of the phase-error variance for arbitrary parameter values is easily obtained without the use of a computer.

HONG, J. P.

**H030 Pattern Recognition: Invariant Stochastic Feature
Extraction and Classification by the Sequential
Probability Ratio Test—Theory and Experimental
Results for the Two-Class Problem**

J. P. Hong

*Supporting Research and Advanced Development,
Space Programs Summary 37-63, Vol. III, pp. 153-159,
June 30, 1970*

Random lines are used to obtain a feature extraction algorithm in which the extracted features are insensitive to rotation and translation of the pattern within the retina. It is shown that the statistics of the total intersection length of the random line of the pattern is such an invariant feature. The choice of random line intersection length as a feature extractor is an arbitrary one. It is hypothesized that the statistics of the number of intersections which a random line makes with a pattern is also such an invariant feature. Furthermore, it may be less sensitive to the font. This article presents the mechanics necessary to predict the average number of observations that are needed to properly classify unknown letters. The theory presented also allows one to make a tradeoff between the number of required samples and the accuracy of the classification. Experimental results are included which verify the theory.

HORIUCHI, H. H.

**H031 Mariner Mars 1969 Scan Control Subsystem
Design and Analysis**

T. Kerner and H. H. Horiuchi

Technical Report 32-1506, October 30, 1970

For abstract, see Kerner, T.

HORTTOR, R. L.

**H032 Cyclic Search Algorithms for Synchronizing
Maximal Length Linear Shift Register Sequences**

R. L. Horttor

*Supporting Research and Advanced Development,
Space Programs Summary 37-63, Vol. III, pp. 58-63,
June 30, 1970*

This article compares two algorithms for synchronizing one maximal length linear shift register sequence with another one biphasemodulated onto a carrier. A phase-locked loop is used to acquire and track the carrier. One algorithm is the Maximum Likelihood Receiver which examines all possible synchronization times before making a decision. The second is a

sequential algorithm which does not always require a complete search before making a decision. The mean and variance of the search times are calculated from the respective generating functions.

HOUSEMAN, J.

H033 Optimum Mixing of Hypergolic Propellants in an Unlike Doublet Injector Element

J. Houseman

Technical Report 32-1487 (Reprinted from *AIAA J.*, Vol. 8, No. 3, pp. 597-599, March 1970)

The unlike doublet is a common injector element in liquid rocket engines; its function is to produce a spray of well-mixed droplets of fuel and oxidizer. The fluid dynamics of the impingement region of an injector element can be altered appreciably by liquid-phase chemical reactions at the interface of the propellants. This effect can be used to considerable advantage to obtain better mixing of the propellants than would be possible without chemical effects. However, the extent of the liquid-phase reaction must be controlled by careful selection of the injector operating conditions, since too much reaction results in poor mixing of the propellants.

The following possible mechanisms for the formation of gas in the impingement region are now envisioned:

- (1) The liquid-phase reactions produce gaseous products.
- (2) The liquid-phase reactions generate so much heat locally that the propellant begins to boil.
- (3) The fuel and oxidizer jets are separated by a thin film of mixed gas. The reaction in this gas film generates a sufficient amount of heat to vaporize enough oxidizer and fuel on both sides of the film to maintain the film.

A study of these combustion effects in sprays was undertaken to determine the range of applicability of nonreactive spray data to hypergolic propellant systems. An interim objective of this study was to obtain direct experimental data that show the existence of both the penetrated and separated mechanisms of spray formation for hydrazine and nitrogen tetroxide propellants; these data are presented in this article. These different mechanisms have been identified by measuring the chemical composition of the combustion gases resulting from the propellant spray. It is shown that, for small orifices, there is a gradual transition from penetration to separation as the flow rate and chamber pressure are increased. It is proposed that the transi-

tion zone between penetration and separation represents a new optimum mixing condition for hypergolic propellants.

HOWARTH, H. C.

H034 Polarizers and Retardance Plates for a Vector Helium Magnetometer

H. C. Howarth

Supporting Research and Advanced Development, Space Programs Summary 37-62, Vol. III, pp. 12-14, April 30, 1970

The theory of operation of retardance plates and polarizers is described, with typical curves for birefringence of retardance plates included. A method of obtaining an exact $\frac{1}{4}\lambda$ plate from a general retardance plate is presented. Bonding materials and useful design formulas are discussed. The results of this theoretical study are directly applicable to the vector helium magnetometer.

HUBBARD, J. S.

H035 Nature of the Inactivation of the Isocitrate Dehydrogenase From an Obligate Halophile

J. S. Hubbard and A. B. Miller

J. Bacteriol., Vol. 102, No. 3, pp. 677-681, June 1970

The nicotinamide adenine dinucleotide phosphate-specific isocitrate dehydrogenase (ICDH) of *Halo-bacterium cutirubrum* is rapidly inactivated at low NaCl levels. From sucrose gradient analysis, it was estimated that the active ICDH has an $S_{20,w}$ of 5.3 and a molecular weight of 75,000. The inactivation by removal of NaCl causes an unfolding of the protein, yielding a less-compact conformer with an $S_{20,w}$ of 2.0. This inactivation apparently causes internal sulfhydryl groups to be exposed. Over 90% of the initial activity can be restored by dialyzing the inactivated ICDH against 4M NaCl, provided that the exposed sulfhydryl groups are protected with dithiothreitol. The ICDH is permanently inactivated when the sulfhydryl groups are oxidized or alkylated. The alkylation of the inactive ICDH was demonstrated by treatment with ^{14}C -N-ethyl maleimide. Sucrose gradient analysis showed that ^{14}C was bound to a protein with sedimentation properties identical to that of reversibly inactivated ICDH, i.e., an $S_{20,w}$ of 2.0. Much less ^{14}C was bound when active ICDH was treated with ^{14}C -N-ethyl maleimide. The *H. cutirubrum* ICDH resembles other bacterial isocitrate dehydrogenases in being susceptible to concerted feed-back inhibition by oxalacetate and glyoxalate.

HUDSON, O. K.

- H036 A Miniaturized Absolute Gravimeter for Terrestrial, Lunar, and Planetary Research**
R. G. Brereton, B. H. Chovitz (United States Coast and Geodetic Survey), W. M. Greene (Marshall Space Flight Center), O. K. Hudson (Marshall Space Flight Center), R. A. Lyttleton (St. John's College), and R. D. Regan (United States Geology Survey)
Supporting Research and Advanced Development, Space Programs Summary 37-62, Vol. III, pp. 1-5, April 30, 1970

For abstract, see Brereton, R. G.

HUESMANN, L. R.

- H037 Man-Machine Interaction in the Post-1971 SFOF**
L. R. Huesmann
The Deep Space Network, Space Programs Summary 37-65, Vol. II, pp. 126-131, September 30, 1970

In the post-1971 period, the changing nature of space missions will raise some serious problems for man-machine interaction in the Space Flight Operations Facility (SFOF). To remedy these problems, it is proposed in this article that: (1) the onboard computer should be upgraded to assume a portion of the functions previously executed by ground-based machines and decision makers, (2) crucial human decision-making be executed in parallel, (3) the ground-based system be designed to disperse information in a way that improves human reliability and efficiency, and (4) the computing systems assume a greater portion of the decision-making and planning functions. Such alterations should improve the reliability of performance, reduce the time required for a planning cycle, and permit real-time control of some activities.

HULTBERG, J. A.

- H038 Thermal Joint Conductance**
J. A. Hultberg
Supporting Research and Advanced Development, Space Programs Summary 37-62, Vol. III, pp. 198-202, April 30, 1970

This article summarizes the thermal joint conductance work performed by JPL over the last several years. The work performed under NASA grants and JPL contracts monitored at JPL is discussed as to its relationship with the work at JPL. Tests and supporting analyses at JPL to link with the research performed at universities are described.

HUNTRESS, W. T., JR.

- H039 An Ion Cyclotron Resonance Study of the Ion-Molecule Reactions in Methane-Ammonia Mixtures**
W. T. Huntress, Jr., and D. D. Elleman
J. Am. Chem. Soc., Vol. 92, No. 12, pp. 3565-3573, June 17, 1970

The ion-molecule reactions of ions formed by electron impact in methane-ammonia mixtures have been studied by ion cyclotron resonance techniques, and a number of charge transfer, proton transfer, hydrogen atom abstraction, and condensation reactions have been identified. Ion cyclotron resonance single- and double-resonance techniques using mixtures of isotopically substituted methane and ammonia have been combined to identify and sort out the masking effects of exchange reactions in order to study the mechanism of the condensation reaction of methyl cations with ammonia. The condensation is shown to proceed by two distinct channels: one by loss of a hydrogen molecule across the C-N bond, and the other by loss of a hydrogen molecule from the nitrogen end of the intermediate complex. The first process results in an excited $(\text{CH}_2\text{NH}_2^+)^*$ ion, and the second yields the CH_3NH^+ ion. The ratio of the rates of these two reactions is approximately 3.3, and the total rate for the condensation reaction is $2.0 \pm 0.5 \times 10^{-9} \text{ cm}^3/\text{molecule-s}$. The excited $(\text{CH}_2\text{NH}_2^+)^*$ ion undergoes exothermic proton transfer to NH_3 , the proton most likely coming from the carbon end of the molecule. At high pressures, the $(\text{CH}_2\text{NH}_2^+)^*$ ion is deactivated by nonrearrangement collisions. Proton transfer from ground state CH_2NH_2^+ ions to ammonia is endothermic and results in proton loss exclusively from the nitrogen end of the molecule.

- H040 On the Reaction of O^+ With CO_2**
M. Mosesman and W. T. Huntress, Jr.
J. Chem. Phys., Vol. 53, No. 1, pp. 462-463, July 1, 1970

For abstract, see Mosesman, M.

HURD, W. J.

- H041 Digital Transition Tracking Symbol Synchronizer for Low SNR Coded Systems**
W. J. Hurd and T. O. Anderson
Technical Report 32-1488 (Reprinted from IEEE Trans. Communication Technology, Vol. COM-18, No. 2, pp. 141-147, April 1970)

In coded telemetry systems symbol synchronization must be performed at low symbol signal-to-noise ratios (ST/N_0) with negligible degradation from the perfect synchronization case. A digital transition tracking syn-

chronizer which operates with less than 0.03-dB degradation at $ST/N_0 = -3$ dB and at rates of 5.6 bit/s to 250 kbit/s is described.

H042 On Multiple Demand Access Satellite Systems for Speech Communications in Remote Areas

W. J. Hurd

Technical Report 32-1501 (Reprinted from proceedings of the IEEE International Communication Conference, San Francisco, California, June 9–11, 1970, Session 46, pp. 33–40)

Multiple access communications satellites can be used to provide reliable speech communications systems for low-density individual users in remote areas of the world where the best existing means of communications utilize high frequency radio, which is very unreliable. System networks for such applications would consist of a large number of ground stations, each active only a small portion of the time, serviced by one satellite. This paper discusses various multiple access systems, concentrating on those system types believed most practical for the application. Satellite and ground station parameters, and modulation and multiple access methods are considered. The main conclusion is that such a system is technically feasible, but that practicality depends on economic considerations, primarily ground station cost.

INGHAM, J. D.

I001 Functionality of Isobutylene Prepolymers

J. D. Ingham

Supporting Research and Advanced Development, Space Programs Summary 37-64, Vol. III, pp. 138–140, August 31, 1970

This article interrelates various methods of determining unsaturation in poly(isobutylenes) to arrive at more reliable estimates of the concentration of unsaturation or degree of functionality in polymers. It is concluded that the intensity of infrared absorbance at 1630 cm^{-1} can provide good estimates of the degree of functionality. These estimates are probably adequate for the purpose of selecting candidate prepolymers for studies of chain-extension for ultimate incorporation in advanced propellant systems.

JACKSON, E. B.

J001 DSS 13 Operations [March–April 1970]

E. B. Jackson and R. M. Gosline

The Deep Space Network, Space Programs Summary 37-63, Vol. II, p. 42, May 31, 1970

During the period February 16 through April 15, 1970, DSS 13 (Venus Deep Space Station) was fully operational for only two 1-wk periods. The non-operational period was devoted mainly to maintenance and support of the Mars Tri-Cone installation and testing. During the operational period, a mono-static and bi-static planetary radar track was performed on Venus. Frequent pulsar tracks, noise-adding radiometer tests, and clock synchronization transmissions were performed during both operational periods.

J002 DSS 13 Operations [June–July 1970]

E. B. Jackson

The Deep Space Network, Space Programs Summary 37-64, Vol. II, pp. 70–71, August 31, 1970

From mid-April to mid-June 1970, the Venus Deep Space Station (DSS 13) maintained a full schedule of clock synchronization transmissions, continued its support of the program of pulsar observations, and participated in cooperative planetary radar experiments with the Mars Deep Space Station (DSS 14). Additionally, the station supported the *Mariner* Extended Mission Project by taking high-resolution spectrograms of the RF carrier from the *Mariner VI* spacecraft and both the carrier and the first telemetry sideband from the *Mariner VII* spacecraft while the spacecraft were operating in “two-way” mode, with the ground transmitter maintaining the spacecraft receiver in phase lock. This article describes these station operations, as well as the completion of the 100-kW, 2115-MHz transmitter.

J003 Transmitter Phase Modulation as a Result of Beam Voltage Ripple

C. P. Wiggins, E. B. Jackson, and T. W. Rathbun

The Deep Space Network, Space Programs Summary 37-64, Vol. II, pp. 96–97, August 31, 1970

For abstract, see Wiggins, C. P.

J004 DSS 13 Operations [July–August 1970]

E. B. Jackson

The Deep Space Network, Space Programs Summary 37-65, Vol. II, pp. 84–85, September 30, 1970

From mid-June to mid-August 1970, the Venus Deep Space Station (DSS 13) activities included a special clock synchronization experiment, routine pulsar observations for 24 h each week, cooperative planetary radar activities, and continued development of the ephemeris update tracking program. This article describes these activities, as well as the completed installations of the Model IV receiver–exciter and the 100-kW, 2115-MHz transmitter.

JAFFE, P.

- J005 Planetary Entry Flight Dynamic Research**
P. Jaffe
Supporting Research and Advanced Development,
Space Programs Summary 37-62, Vol. III, pp. 218–222,
April 30, 1970

With the evaluation of our knowledge about planetary-entry flight dynamic problems, attention has focused on the difference between planar and nonplanar dynamic stability. Anticipating the need for an experimental nonplanar capability, the JPL wind tunnel free-flight technique was extended into this regime and is now capable of producing extremely high-grade nonplanar data. Two brief tests (the first with the improved system) were recently conducted on blunt 60-deg and sharp 10-deg half-angle cone configurations. This article discusses the testing techniques and presents an interim progress report on the two tests, the results of which are currently being reduced and analyzed.

JAMES, D.

- J006 Outer Planet Telemetry and Command: Exact Power Spectrum of PN Codes**
D. James
Supporting Research and Advanced Development,
Space Programs Summary 37-64, Vol. III, pp. 48–51,
August 31, 1970

This article describes an exact method for finding the power spectrum of a pseudonoise (PN) code-modulated subcarrier for any length PN code and for any number of subcarrier cycles per PN code bit. The method is straightforward, exact, and far less tedious than previous solutions. It is used in the article to compute the spectrum for a PN code used in a digital command system.

JAUNCEY, D. L.

- J007 High-Resolution Observations of Compact Radio Sources at 13 Centimeters**
K. I. Kellermann (National Radio Astronomy Observatory),
B. G. Clark (National Radio Astronomy Observatory),
D. L. Jauncey (Cornell University), M. H. Cohen (California Institute of Technology), D. B. Shaffer (California Institute of Technology), A. T. Moffet (California Institute of Technology), and S. Gulkis
Astrophys. J., Vol. 161, No. 3, pp. 803–809,
September 1970

For abstract, see Kellermann, K. I.

JENNINGS, K. R.

- J008 Analysis of Ion–Molecule Reactions in Allene and Propyne by Ion Cyclotron Resonance**
M. T. Bowers (University of California, Santa Barbara),
D. D. Elleman, R. M. O'Malley (The University, Sheffield, England), and K. R. Jennings (The University, Sheffield, England)
J. Phys. Chem., Vol. 74, No. 13, pp. 2583–2589, 1970

For abstract, see Bowers, M. T.

JET PROPULSION LABORATORY

- J009 Analysis of Surveyor Data**
Jet Propulsion Laboratory
Technical Report 32-1443, June 30, 1969

This report presents some results of the extended postflight analysis of *Surveyor* data for the thermal, physical, and mechanical properties of the lunar surface; the photometric and polarimetric properties of the earth; and the colorimetric measurements of the solar eclipse and earth. Also described are the optical systems and alignment procedures used in the *Surveyor VII* laser pointing test.

- J010 Mariner Mars 1969 Final Project Report: Development, Design, and Test**
Jet Propulsion Laboratory
Technical Report 32-1460, Vol. I, November 1, 1970

This is the first of three volumes of the *Mariner Mars 1969 Final Project Report*. This volume describes the pre-operational activities including planning, development, design, manufacture, and testing. Volume II describes the performance of the mission by flight and earth-based elements during the launch and space-flight phases. Volume III deals with the scientific program, including experiment results.

The *Mariner Mars 1969 Project* was organized around four functional systems: (1) the *Mariner* spacecraft, based on the *Mariner C* design, (2) the *Atlas/Centaur* launch vehicle, (3) the Tracking and Data Acquisition System, and (4) the Mission Operations System. Four spacecraft were prepared: one proof test model, two flight spacecraft, and a spare. The spacecraft were divided into nineteen functional subsystems which were subcontracted by JPL and the launch vehicles were adapted and built by a contractor under the cognizance of the NASA Lewis Research Center.

J011 Proceedings of the Conference on Scientific Applications of Radio and Radar Tracking in the Space Program (Held at the Jet Propulsion Laboratory, Pasadena, California, April 9–10, 1969)

Jet Propulsion Laboratory
(L. Efron and C. B. Solloway, Editors)
Technical Report 32-1475, July 1, 1970

This report is a compilation of the papers presented at the Conference on Scientific Applications of Radio and Radar Tracking in the Space Program, hosted by JPL. Four major topics are discussed: data taking techniques, data processing and modeling techniques, scientific exploitation of the data, and planetary structure and atmosphere.

**JET PROPULSION LABORATORY:
ASTRONICS DIVISION**

**J012 Mariner Mars 1971: Astrionics
[July–August 1970]**

Jet Propulsion Laboratory: Astrionics Division
Flight Projects, Space Programs Summary 37-65, Vol. I,
pp. 23–31, September 30, 1970

The *Mariner* Mars 1971 flight telemetry subsystem performs the data conditioning, multiplexing, encoding, and modulation of spacecraft engineering parameters and the modulation and block coding of science data for transmission to earth. The design requirements, and the design, test, and performance of the mechanization implemented to meet these requirements are described here. Block diagrams of the subsystem are included.

**JET PROPULSION LABORATORY:
DATA SYSTEMS DIVISION**

**J013 Mariner Mars 1971: Data Systems
[March–April 1970]**

Jet Propulsion Laboratory: Data Systems Division
Flight Projects, Space Programs Summary 37-63, Vol. I,
pp. 4–10, May 31, 1970

The development of the mission and test computer system is described in this article. The higher data rates required for *Mariner* Mars 1971 and the need for handle and process as much as possible of the data in real time necessitated additional computing capability to supplement that of the existing two UNIVAC 1219 systems. A dual high-rate data processor consisting of a UNIVAC 1230 computer and peripheral equipment was leased to receive, block decode as necessary, decommutate, and perform all input processing functions on all high-rate data streams. A full UNIVAC 1230/dual UNIVAC 1219 configuration to accom-

modate the simultaneous testing of two flight spacecraft and the system test complex data streams available to the mission and test computer system are illustrated.

The Mission Operations System is responsible for development of the mission-dependent computer programs required for mission operations, simulation, and spacecraft checkout, except for the mission-dependent software in the Deep Space Instrumentation Facility telemetry and command processor. The *Mariner* Mars 1971 Mission Operations System software system operates in the UNIVAC 1108 or IBM 360/75 Space Flight Operations Facility computers. The presently defined programs, the program functions, and the computer in which each program is currently planned to operate are also described here.

**J014 Mariner Mars 1971: Data Systems
[May–June 1970]**

Jet Propulsion Laboratory: Data Systems Division
Flight Projects, Space Programs Summary 37-64, Vol. I,
pp. 3–7, July 31, 1970

The mission and test video (MTV) system is used primarily to receive digital video data from the mission and test computer (MTC) system and to produce photographic negatives, prints, and enlargements by the use of film recorders and photoprocessing systems. The data are recorded by the MTC system during spacecraft system tests or system-level calibrations of the television subsystem. The MTV system is a development of the *Surveyor* television ground data-handling system, which was modified to handle digital data and otherwise increased in scope to process and display the *Mariner* Mars 1969 flyby video data. Additional expansion and development are underway since the volume of video data processing required for the orbital operations phase of the *Mariner* Mars 1971 missions is expected to be vastly increased over that required for the *Mariner* Mars 1969 missions. Descriptions of the system and of the photographic product are included in this article.

**JET PROPULSION LABORATORY:
ENGINEERING MECHANICS DIVISION**

**J015 Mariner Mars 1971: Engineering Mechanics
[March–April 1970]**

Jet Propulsion Laboratory: Engineering Mechanics Division
Flight Projects, Space Programs Summary 37-63, Vol. I,
pp. 24–34, May 31, 1970

Most of the structure, cabling, and mechanical devices subsystem equipment for the *Mariner* Mars 1971 proof test model has been delivered to the Spacecraft Assembly Facility. Engineering mechanics activities

are now concentrated on the completion of flight equipment and the support of efforts to eliminate problem areas in the subsystems. Reported here are the procurement of integrated circuits, design and fabrication of the solar panel deployment and damper mechanism, vibration testing of the development test model, and space simulator testing of the temperature control model.

**J016 *Mariner Mars 1971: Engineering Mechanics*
[May–June 1970]**

Jet Propulsion Laboratory: Engineering Mechanics Division
Flight Projects, Space Programs Summary 37-64, Vol. I,
pp. 21–25, July 31, 1970

The television shutter materials and mechanisms used on the *Mariner Mars 1971* spacecraft are based on the successful design employed on the *Mariner Mars 1969* spacecraft. A major design change was the employment of a double lip on one of the shutters to improve the light stopping capability of the shutters in the closed position. Two failures occurred during the developmental testing of the shutters for the narrow-angle television camera. The failures occurred at -50°C and were due to fatigue of the mating leading edges of the shutter blades. The failure analysis and the materials, process, and design changes resulting from it are described in this article.

Also presented are the results of a spacecraft flight loads analysis. *Mariner Mars 1971* flight-induced adapter loads (shear and moment at the spacecraft field joint) were estimated using the acceleration time histories from various missions employing *Atlas/Centaur* launch vehicles. The method consisting of deriving a mathematical model of the *Mariner Mars 1971* spacecraft with the flight data to determine the required inertia loads. This effort, which resulted in revised structural design criteria, was instrumental in allowing the use of residual *Mariner Mars 1969* equipment.

**J017 *Viking, Orbiter System: Engineering Mechanics*
[May–June 1970]**

Jet Propulsion Laboratory: Engineering Mechanics Division
Flight Projects, Space Programs Summary 37-64, Vol. I,
pp. 34–41, July 31, 1970

The temperature control effort for the *Viking* orbiter system consists of both the design and development of hardware items, such as louvers, blankets, and heaters, and the effective use of these tools to achieve an acceptable overall or system thermal design. The first portion of this article discusses the thermal design from the point of view of the entire system heat bal-

ance; this design will later form the basis for the detail design of specific parts of the spacecraft.

Engineering mechanics effort for the project includes the design, fabrication, and, in many cases, use of the mechanical ground handling and assembly equipment. Although many of these activities are still in the planning stage, the basic ground handling philosophy has been selected, and general techniques have been outlined for the major activities.

The second portion of this article briefly discusses the ground handling design approach and assembly and test sequences and equipment, indicating departures from previous practices. Although handling of the entire *Viking* spacecraft is not a JPL responsibility, combined operations that involve the orbiter and other major hardware items must be considered.

**J018 *Mariner Mars 1971: Engineering Mechanics*
[July–August 1970]**

Jet Propulsion Laboratory: Engineering Mechanics Division
Flight Projects, Space Programs Summary 37-65, Vol. I,
pp. 42–55, September 30, 1970

Mariner Mars 1971 propulsion support structure problems have involved a low-strength beryllium tube, local ring buckling, cracked/failed upper bipod fittings on center and end trusses, failed upper truss fittings, cracked W-truss upper fitting, beryllium strut fracture, cracked lower pressurant support fittings, and cracked threads around threaded inserts. A solar panel deployment/damper mechanism problem was a less-than-minimum critical damping at lower specification temperatures during simulated $\frac{1}{4}$ -g motor firings. These problems and their solutions are described in this article.

Also discussed are the design and operation of the medium-gain antenna RF plug assembly. This assembly attenuates the radiated energy that impinges on the *Centaur* forward electronics platform prior to separation.

A decision was made to launch the spacecraft with the ullage gas at low pressure inside the propellant tank bladders. As a result, tests were made to determine the effects of ullage gas placement on the fluid dynamics of the propellant tank. The implementation and results of these tests are reported.

Results are also presented for investigations of two separate cracked solder joint problems: one in the inertial electronics subassembly in which an electrical open was recorded, and the other involving both the flight command subsystem and the data storage electronics subsystem.

**JET PROPULSION LABORATORY:
ENVIRONMENTAL SCIENCES DIVISION**

**J019 Mariner Venus-Mercury 1973: Environmental
Sciences [July-August 1970]**

Jet Propulsion Laboratory: Environmental Sciences Division
Flight Projects, Space Programs Summary 37-65, Vol. 1,
pp. 57-58, September 30, 1970

High-intensity solar simulation will be required to perform developmental testing of instruments on the *Mariner Venus-Mercury 1973* spacecraft that will be exposed to solar radiation. The radiation intensity level expected is 5.4 times that at earth or 700 W/ft². The tests described in this article were conducted in the 10-ft space simulator using a small collimating mirror to produce a small high-intensity beam. The purposes of these tests were to: (1) determine the uniformity of intensity throughout the beam using the existing integrating lenses, which are not geometrically optimized for the optical system thus developed; and (2) gain experience in the operation of instrumentation exposed to high-intensity solar radiation.

**JET PROPULSION LABORATORY:
GUIDANCE AND CONTROL DIVISION**

**J020 Mariner Mars 1971: Guidance and Control
[March-April 1970]**

Jet Propulsion Laboratory: Guidance and Control Division
Flight Projects, Space Programs Summary 37-63, Vol. 1,
pp. 10-24, May 31, 1970

During the *Mariner Mars 1971* solar panel shadow analysis program, a shadow-casting computer program was used to provide a set of plots at 5-deg increments in both directions of yaw, and an initial analysis was made of the effect on the solar panel output power. The first portion of this article describes a follow-up effort wherein photographs were taken of a spacecraft model to help confirm the initial data obtained and to determine what additional points might be necessary to more accurately define the geometry of the shadows cast.

Under the constraint for satisfactory television picture-taking, only two or three scan platform position changes are required. During these, disturbing torques are applied to the spacecraft as a result of the law of conservation of momentum. The effects of these disturbing torques on the *Mariner Mars 1971* attitude-control subsystem are determined. Also described are the results of an analysis to determine the effects on attitude-control gas consumption from scan platform motion during the orbital phase of the mission. Gas storage requirements based on the most current definition of the vehicle configuration and the mission

requirements that affect gas consumption are also examined.

Illustrations are provided for the initial and modified Canopus-sensor/attitude-control-electronics circuitry. Recently conducted integration tests of the attitude-control subsystem, which are also described in this article, revealed an anomalous logic state of the subsystem not anticipated during the design phase. The logic equations were thus modified to correct this condition, and the hardware was reworked to reflect the changes to the logic.

The final portion of the article describes a circuit incorporated into the laboratory and system test sets to stabilize the autopilot for test purposes and to prevent driving the engine gimbal actuators to their mechanical stops.

**J021 Mariner Venus-Mercury 1973: Guidance and
Control [March-April 1970]**

Jet Propulsion Laboratory: Guidance and Control Division
Flight Projects, Space Programs Summary 37-63, Vol. 1,
pp. 40-44, May 31, 1970

The *Mariner Venus-Mercury 1973* power subsystem is planned to be of *Mariner Mars 1971* design, modified for operation in the vicinity of Mercury and for a revised power profile. The reasons for these changes and a preliminary description of the overall power subsystem, including a functional block diagram and a weight breakdown, are presented in this article.

**J022 Viking, Orbiter System: Guidance and Control
[March-April 1970]**

Jet Propulsion Laboratory: Guidance and Control Division
Flight Projects, Space Programs Summary 37-63, Vol. 1,
pp. 61-65, May 31, 1970

An improvement in the functional sequence associated with roll axis control has been designed for incorporation on the *Viking* attitude-control subsystem. The proposed sequence eliminates some unnecessary roll search modes. The attitude-control subsystem does not immediately initiate a spacecraft roll search mode upon loss of Canopus, thus affording ground controllers time to override the automatic features of the sequence if circumstances call for it. This article describes the attitude-control sequence for Canopus reacquisition.

Also described are the attitude-control subsystem status register and the scan subsystem mechanization. The status register replaces the event register of the *Mariner*-type spacecraft. The scan subsystem mechanization involves a proposed modification to the *Mariner Mars 1971* scan control that results in some hardware economies and in improved operational flexibility.

**J023 *Mariner Mars 1971: Guidance and Control*
[May–June 1970]**

Jet Propulsion Laboratory: Guidance and Control Division
Flight Projects, Space Programs Summary 37-64, Vol. I,
pp. 10–21, July 31, 1970

This article presents the results of an analysis and computer simulation of the *Mariner Mars 1971* attitude-control subsystem in the commanded turn mode of operation. The work was performed to verify the new design and to assess the overall performance of the attitude-control subsystem for this control mode.

The *Mariner Mars 1971* spacecraft uses the same celestial references for attitude control as did the *Mariner Mars 1969* spacecraft, i.e., the sun for pitch and yaw and the star Canopus for roll. All of the design modifications made to the *Mariner Mars 1969* Canopus tracker for use on the *Mariner Mars 1971* spacecraft have been demonstrated to improve tracker performance characteristics or reduce manufacturing difficulties. A description of the various modifications to the Canopus tracker is presented. Also described are the modified Sun sensors, which include a cruise sensor, an acquisition sensor, and a sun gate. These are structurally simplified forms of the *Mariner Mars 1969* sensors and, due to structural differences between the spacecraft, are located in different positions on the spacecraft.

**J024 *Viking, Orbiter System: Guidance and Control*
[May–June 1970]**

Jet Propulsion Laboratory: Guidance and Control Division
Flight Projects, Space Programs Summary 37-64, Vol. I,
pp. 31–34, July 31, 1970

The *Viking* spacecraft orbital trajectory is such that the planet will pass between the spacecraft and the sun once each orbit. The duration of sun occultation will extend from a few minutes to as much as 2 h. To maintain attitude control during this period, the gyros will control the spacecraft in the inertial mode of operation. A proposed method to achieve this mode of operation is to detect occultation through the use of the sun gate in conjunction with the acquisition and cruise sun sensors. A signal from these sensors will be used to initiate inertial control of the spacecraft. The mechanization, sun sensor characteristics, gyro “inertial start” requirements and performance, and orbital considerations are discussed in this article.

**J025 *Mariner Mars 1971: Guidance and Control*
[July–August 1970]**

Jet Propulsion Laboratory: Guidance and Control Division
Flight Projects, Space Programs Summary 37-65, Vol. I,
pp. 9–23, September 30, 1970

The *Mariner Mars 1971* mission requirements necessitated several changes to the *Mariner Mars 1969* power subsystem design. The major modification is a new battery consisting of 26 nickel–cadmium cells. Other modifications in the power subsystem conditioning electronics, including the battery charger, 30-Vdc regulator, power source and logic, power distribution, and power subsystem telemetry, are described in this article.

The scan actuator design is identical to that for the *Mariner Mars 1969* spacecraft, except for a minor change in the mounting configuration. This change and the present status of the actuators are discussed, and the scan actuator is illustrated.

Also discussed are the operation of the attitude-control subsystem and the sun acquisition performance while the solar panels are in their latched configuration. Sun acquisition performance with latched solar panels is of concern for the late launch opportunities where spacecraft separation will occur in a sunlit condition.

An autopilot system using a 300-lbf gimbaled bipropellant rocket engine powered by hypergolic fuels will control the spacecraft in its midcourse maneuver and later into orbit about Mars. Orientation about each of the two axes of the gimbaled engine is controlled by an electromechanical linear actuator. Since the functional requirements for the actuators were identical, it was possible to design one actuator to be interchangeable on either axis. The design requirements and the actuator design, testing, and performance are described.

The last portion of this article concerns the various design studies and the resulting design for the reaction control assembly, which provides the actuating torques required for spacecraft attitude control. Each *Mariner*-series spacecraft has carried two identical half gas systems consisting basically of a high-pressure storage vessel, a pressure-reducing regulator, a low-pressure distribution system, and six jet valve nozzle assemblies.

**J026 *Viking, Orbiter System: Guidance and Control*
[July–August 1970]**

Jet Propulsion Laboratory: Guidance and Control Division
Flight Projects, Space Programs Summary 37-65, Vol. I,
pp. 60–66, September 30, 1970

The *Viking* orbiter system power profile was revised to include a 2% allocation of power required for operation off the solar panel maximum power point, a 42-W subsystem contingency, and refinements to some subsystems. The preliminary power profile is presented in this article. A solar panel discussion includes the power versus voltage curves for Trajectory A (launch on August 16, 1975; arrival on August 1, 1976) and Trajectory B (launch on August 19, 1975; arrival on September 2, 1976). Battery charging is also discussed.

The reaction control assembly will be essentially a *Mariner*-type, dual-redundant, cold-nitrogen thruster system. The primary changes from the *Mariner* design result from considerations of spacecraft geometry, increased spacecraft inertias, and environmental requirements. A description of this assembly is presented.

Also discussed are the design and tests of the electronic integrator used in the inertial reference unit for the attitude-control subsystem. This integrator is a redesign of that used for the *Mariner* Mars 1971 spacecraft. Three such integrators are used in conjunction with three single-degree-of-freedom gyros to provide angular position information during the inertial-hold mode of spacecraft attitude control.

JET PROPULSION LABORATORY: MARINER MARS 1971 PROJECT

J027 *Mariner* Mars 1971: Project Description and Status [March–April 1970]

Jet Propulsion Laboratory: *Mariner* Mars 1971 Project
Flight Projects, Space Programs Summary 37-63, Vol. I,
pp. 1–3, May 31, 1970

The primary objective of the *Mariner* Mars 1971 Project is to place two spacecraft in orbit around Mars that will be used to perform scientific experiments directed toward achieving a better understanding of the physical characteristics of that planet. An engineering objective is to demonstrate the ability of the spacecraft to perform orbital operations in an adaptive mode wherein information from one orbital pass is used to develop the operations plan for subsequent orbital passes. Specific mission objectives, the spacecraft, its scientific experiments, and management responsibilities for the project are briefly described. Status information includes documentation, computer program completions, and proof-test-model, temperature-control-model, and propulsion-engineering-test-model operations. The television team matrix is illustrated.

J028 *Mariner* Mars 1971: Project Description and Status [May–June 1970]

Jet Propulsion Laboratory: *Mariner* Mars 1971 Project
Flight Projects, Space Programs Summary 37-64, Vol. I,
pp. 1–3, July 31, 1970

The primary objective of the *Mariner* Mars 1971 Project is to place two spacecraft in orbit around Mars that will be used to perform scientific experiments directed toward achieving a better understanding of the physical characteristics of that planet. An engineering objective is to demonstrate the ability of the spacecraft to perform orbital operations in an adaptive

mode wherein information from one orbital pass is used to develop the operations plan for subsequent orbital passes. Specific mission objectives, the spacecraft, its scientific experiments, and management responsibilities for the project are briefly described. The television team matrix is illustrated.

J029 *Mariner* Mars 1971: Project Description [July–August 1970]

Jet Propulsion Laboratory: *Mariner* Mars 1971 Project
Flight Projects, Space Programs Summary 37-65, Vol. I,
pp. 1–3, September 30, 1970

The primary objective of the *Mariner* Mars 1971 Project is to place two spacecraft in orbit around Mars that will be used to perform scientific experiments directed toward achieving a better understanding of the physical characteristics of that planet. An engineering objective is to demonstrate the ability of the spacecraft to perform orbital operations in an adaptive mode wherein information from one orbital pass is used to develop the operations plan for subsequent orbital passes. Specific mission objectives, the spacecraft, its scientific experiments, and management responsibilities for the project are briefly described.

JET PROPULSION LABORATORY: MARINER VENUS–MERCURY 1973 PROJECT

J030 *Mariner* Venus–Mercury 1973: Project Description and Status [March–April 1970]

Jet Propulsion Laboratory: *Mariner* Venus–Mercury 1973 Project
Flight Projects, Space Programs Summary 37-63, Vol. I,
pp. 39–40, May 31, 1970

The primary objective of the *Mariner* Venus–Mercury 1973 Project is to launch one spacecraft to conduct exploratory investigations of the planet Mercury's environment, atmosphere, surface, and body characteristics and to obtain environmental and atmospheric data on the planet Venus, with first priority assigned to the Mercury investigations. The secondary objectives are to perform interplanetary experiments en route to Mercury and to obtain experience with the gravity-assist mission mode. Preliminary project planning is described.

J031 *Mariner* Venus–Mercury 1973: Project Description [July–August 1970]

Jet Propulsion Laboratory: *Mariner* Venus–Mercury 1973 Project
Flight Projects, Space Programs Summary 37-65, Vol. I,
p. 56, September 30, 1970

The primary objective of the *Mariner* Venus–Mercury 1973 Project is to launch one spacecraft in October

1973 to obtain environmental and atmospheric data for the planet Venus in February 1974 and to conduct exploratory investigations of the planet Mercury's environment, atmosphere, surface, and body characteristics some 7 wk later, with first priority assigned to the Mercury investigations. The secondary objectives are to perform interplanetary experiments enroute to Mercury and to obtain experience with the gravity-assist mission mode. The spacecraft, its scientific experiments, and preliminary project planning are described.

JET PROPULSION LABORATORY: PROPULSION DIVISION

J032 Mariner Mars 1971: Propulsion [March–April 1970]

Jet Propulsion Laboratory: Propulsion Division
Flight Projects, Space Programs Summary 37-63, Vol. I,
pp. 34–38, May 31, 1970

The *Mariner* Mars 1971 propulsion subsystem must perform a midcourse maneuver near earth and four or more maneuvers near Mars. An electrically operated bipropellant valve and a gaseous nitrogen pressure regulator will nominally prevent fluid leakage during non-firing periods. Concern over the possible leakage of these components during the 6-mo duty cycle resulted in the incorporation of three groups of pyrotechnic-actuated valves in the system. For a nominal sequence, the first midcourse maneuver and the four maneuvers near Mars are treated as two maneuver sets. The pressurant and propellant lines will nominally be opened and closed before and after each set. A fifth valve in each line provides redundancy and/or extended mission capability. A failure-mode analysis of the propulsion-subsystem sequence is described in this article.

J033 Mariner Mars 1971: Propulsion [May–June 1970]

Jet Propulsion Laboratory: Propulsion Division
Flight Projects, Space Programs Summary 37-64, Vol. I,
pp. 26–29, July 31, 1970

The *Mariner* Mars 1971 propulsion subsystem uses nitrogen gas pressurization for both fuel and oxidizer propellant tanks. Each propellant tank has a pressurant relief valve that terminates in a tee with two opposed nozzles. The relief valve vents pressurant gas if pressures reach 290 to 330 psid. Unbalanced torque produced on the spacecraft during venting is minimized by selective pairing of nozzles.

Reported here are the results of: (1) an analysis of deflected flow from the thermal blanket, which is asymmetrical with respect to the vent tee assembly, and (2) an analysis to estimate the increase in pressure at the Canopus sensor. The latter analysis was important, since pressures of the order of 2×10^{-6} psia can support an arc/corona discharge within the sensor. Two pressurant relief valve vent nozzles were flow-tested to determine the maximum unbalanced thrust produced when the nozzles are vented through a tee assembly.

J034 Mariner Mars 1971: Propulsion [July–August 1970]

Jet Propulsion Laboratory: Propulsion Division
Flight Projects, Space Programs Summary 37-65, Vol. I,
pp. 31–42, September 30, 1970

Following a brief description of the *Mariner* Mars 1971 propulsion subsystem, a description of the design, operation, testing, and performance of the pressurant relief valve is presented. The primary purpose of this valve is to vent off high-pressure gases in the event of gas regulator failure, thereby avoiding possible rupture of the lightweight thin-shell propellant tanks. This valve is basically that used in both the *Apollo* service module and lunar excursion module, modified for the *Mariner* Mars 1971 operating pressures and to incorporate certain design improvements.

Also discussed is an analysis of pressurant gas solubility in the propellant tanks. Plots are presented for both oxidizer tank and fuel tank predicted propellant saturation, pressure, and bubble volume as functions of time.

The scan latch subsystem is a prepressurized gaseous nitrogen system that, when actuated, will unlatch the planetary platform to accurately point the scientific instrument payload. Its manifold assembly consists of a normally closed explosive valve to control the start of flow, a ball-type fill valve, and a flow manifold block. Various modifications made to the *Mariner* Mars 1969 design and the problems that necessitated these modifications are described.

Liquid propellant expulsion Teflon bladder bags have failed due to the formation of tears and cracks near an aluminum seal ring that forms the mouth of the bag. Solvent sensitivity, biaxial stresses, fatigue, and crystallinity were identified as the factors believed to be critical in contributing to the failures. Detailed studies of these factors for the standard laminate bladder bags are being conducted. The last portion of this article reports the results of the solvent sensitivity study. Also discussed are results obtained on a new experimental material designated "co-dispersion laminate."

**JET PROPULSION LABORATORY:
SPACE SCIENCES DIVISION**

**J035 Viking, Orbiter System: Space Sciences
[March–April 1970]**

Jet Propulsion Laboratory: Space Sciences Division
Flight Projects, Space Programs Summary 37-63, Vol. I,
pp. 46–48, May 31, 1970

A high-resolution spectrometer has been selected for the *Viking* orbiter system science package to determine the amount and distribution of water vapor in the Martian atmosphere. The instrument is to operate in the $1.4\text{-}\mu$ region with a spectral resolution of no more than 0.5 cm^{-1} . As described in this article, ray-trace analyses were performed on nine monochromator configurations. The configuration selected was a Littrow double-pass with parabolic collimating mirror and corner return prism. Illustrations of the instrument are provided.

**J036 Mariner Mars 1971: Space Sciences
[May–June 1970]**

Jet Propulsion Laboratory: Space Sciences Division
Flight Projects, Space Programs Summary 37-64, Vol. I,
pp. 7–10, July 31, 1970

The image processing laboratory (IPL) is used in the processing of video data from the *Mariner* Mars 1971 television subsystem. As part of the calibration of the subsystem, the IPL must obtain video data from it during bench calibration tests. It was decided to transfer these data from the bench checkout equipment to the IPL directly over a hardwire link and into the IBM 360/44 computer. The bench checkout equipment also contains a tape recorder, thus providing an additional method of obtaining the data. This data acquisition concept is sufficiently similar to that for the *Mariner* Mars 1969 subsystem to allow the hardware built for it to be modified to add a *Mariner* Mars 1971 mode of operation. The basic data acquisition system has also been provided with the added capability of receiving digitized video from a slow-scan television subsystem. The hardware and the associated software for each of the data acquisition modes are described here.

**J037 Mariner Mars 1971: Space Sciences
[July–August 1970]**

Jet Propulsion Laboratory: Space Sciences Division
Flight Projects, Space Programs Summary 37-65, Vol. I,
pp. 3–8, September 30, 1970

The vidicon used in the *Mariner* Mars 1971 television subsystem is a specialized version of a common photoconductive sensor. Its key component is a target consisting of a transparent conductive coating on an

optically flat faceplate covered by a thin film of a photo-sensitive semiconductor material. Described in this article is the vidicon screening program established for the *Mariner* Mars 1971 Project. This program has been used in selecting reliable vidicons for space flight and to increase understanding of the performance characteristics of the slow-scan vidicon used in the *Mariner* Mars 1969 and 1971 television subsystems.

**JET PROPULSION LABORATORY:
TELECOMMUNICATIONS DIVISION**

**J038 Viking, Orbiter System: Telecommunications
[March–April 1970]**

Jet Propulsion Laboratory: Telecommunications Division
Flight Projects, Space Programs Summary 37-63, Vol. I,
pp. 48–61, May 31, 1970

The *Viking* orbiter radio frequency subsystem will be of *Mariner* Mars 1971 design, with the incorporation of a redundant receiver proposed as the only major change. As with the *Mariner* radio subsystems, this subsystem will provide the communications and tracking link between the orbiter and the Deep Space Instrumentation Facility. The receiver and duplexer subassemblies, exciter subassembly, control unit, traveling-wave-tube amplifiers, microwave components, S-/X-band experiment interface, and redundant receivers are discussed in this article, and a block diagram of the radio frequency subsystem is provided.

Also described in this article is the *Viking* orbiter relay system, which will provide receiving and detection capability for communications via a UHF lander-to-orbiter link. The relay system includes the relay radio subsystem, telemetry subsystem, and antenna subsystem. Discussions are included for each of these subsystems, as well as for relay link requirements, performance estimates, and beacon considerations.

**JET PROPULSION LABORATORY:
VIKING PROJECT**

**J039 Viking: Project Description and Status
[March–April 1970]**

Jet Propulsion Laboratory: Viking Project
Flight Projects, Space Programs Summary 37-63, Vol. I,
pp. 45–46, May 31, 1970

The primary objective of the *Viking* Project is to send two vehicles to the planet Mars to perform scientific experiments directed toward enhancing current knowledge about the physical characteristics of the planet, particularly its capability for supporting life and possible evidence of life. The launches are currently anticipated during 1975. Each vehicle will consist of an orbiter system being developed by JPL and a

lander system being developed by the Martin-Marietta Corp. A gas chromatograph/mass spectrometer for the lander system is being developed by JPL. Langley Research Center has overall management responsibility for the project. The specific objectives for the orbiter system and the lander system are described. Status information includes commonality studies with the *Mariner* Venus-Mercury 1973 Project Office and navigation studies.

**J040 Viking: Project Description and Status
[May-June 1970]**

Jet Propulsion Laboratory: *Viking Project
Flight Projects, Space Programs Summary 37-64, Vol. I,*
pp. 30-31, July 31, 1970

The primary objective of the *Viking* Project is to send two vehicles to the planet Mars to perform scientific experiments directed toward enhancing current knowledge about the physical characteristics of the planet, particularly its capability for supporting life and possible evidence of life. The launches are currently anticipated during 1975. Each vehicle will consist of an orbiter system being developed by JPL and a lander system being developed by the Martin-Marietta Corp. A gas chromatograph/mass spectrometer for the lander system is being developed by JPL. Langley Research Center has overall management responsibility for the project. The specific objectives for the orbiter system and the lander system are described. Status information includes cost estimation activities and commonality studies between the *Mariner* Venus-Mercury 1973 and *Viking* orbiter 1975 missions.

**J041 Viking: Project Description and Status
[July-August 1970]**

Jet Propulsion Laboratory: *Viking Project
Flight Projects, Space Programs Summary 37-65, Vol. I,*
pp. 59-60, September 30, 1970

The primary objective of the *Viking* Project is to significantly advance current knowledge of the planet Mars by direct measurements in the atmosphere and on the surface and by observations of the planet during approach and from orbit. Particular emphasis will be placed on obtaining information concerning biological, chemical, and environmental factors relevant to the existence of life on the planet at this time or some time in the past or the potentials for the development of life in the future. Two spacecraft, each consisting of an orbiter system and a lander system, are planned for launch during the 1975 opportunity. The orbiter system is being developed by JPL; Langley Research Center is responsible for the lander system, being developed under contract by the Martin-Marietta Corporation. Langley Research Center also has overall

management responsibility for the project. The specific objectives for the orbiter system and the lander system are described. Status information includes documentation and engineering breadboard testing and integration.

JONES, D. E.

**J042 Spectral Observations of Jupiter in the
Frequency Interval 18.5-24.0 GHz: 1968**

D. E. Jones (Brigham Young University), B. L. Meredith,
and E. Arthur
Pub. Astron. Soc. Pacific, Vol. 82, No. 484, pp. 122-125,
February 1970

There is continuing interest in observations of Jupiter that pertain to the composition and structure of the upper regions of the Jovian atmosphere. This article reports the results of observations in the frequency range 18.5-24.0 GHz near the opposition of 1968. The observations were made with the 30-ft cassegrain radio telescope at the Venus Deep Space Station. The results are in excellent agreement with those of Law and Staelin obtained during the opposition of 1966, suggesting the reality of the previously observed discrepancy between predicted and measured brightness temperatures for this frequency interval.

JORDAN, J. F.

**J043 Coursing Accurately to the Giant Outer Planets
and Their Moons**

T. W. Hamilton and J. F. Jordan
Astronaut. Aeronaut., Vol. 7, No 5, pp. 66-70,
May 1970

For abstract, see Hamilton, T. W.

JUVINALL, G. L.

J044 Model Pore Electrode Studies

G. L. Juvinall
Supporting Research and Advanced Development,
Space Programs Summary 37-62, Vol. III, pp. 136-138,
April 30, 1970

Studies of the electrolytic oxidation of silver model pore electrodes have been performed at Brigham Young University under contract to JPL. Accurately controlled pores were produced by confining bundles of silver wires in specially designed holders. Experimental data show that the current density varies as electrolytic oxidation proceeds into the electrode pores and that a cyclic variation in potential occurs under

constant current conditions. These results are discussed in some detail.

J045 Electrochemical Cells Incorporating Liquid Amalgam Electrodes

G. L. Juvinall

Supporting Research and Advanced Development, Space Programs Summary 37-64, Vol. III, pp. 67-69, August 31, 1970

Work done at the Idaho State University under JPL contract has resulted in the fabrication of electrochemical cells which combine liquid potassium amalgam electrodes with silver and nickel electrodes, respectively. Preliminary open-circuit voltage and stand life data are presented. Construction details of the cells are also included.

KALFAYAN, S. H.

K001 Long-Term Aging of Elastomers: Stress Relaxation of SBR With Thiophenol

R. Rakutis and S. H. Kalfayan

Supporting Research and Advanced Development, Space Programs Summary 37-62, Vol. III, pp. 242-244, April 30, 1970

For abstract, see Rakutis, R.

K002 Evaluation of Recording Tapes for Use in Spacecraft Magnetic Tape Recorders [April-May 1970]

J. K. Hoffman, S. H. Kalfayan, and R. H. Silver

Supporting Research and Advanced Development, Space Programs Summary 37-63, Vol. III, p. 160, June 30, 1970

For abstract, see Hoffman, J. K.

K003 Evaluation of Spacecraft Magnetic Recording Tapes [April-May 1970]

S. H. Kalfayan, R. H. Silver, and J. K. Hoffman

Supporting Research and Advanced Development, Space Programs Summary 37-63, Vol. III, pp. 209-214, June 30, 1970

The values of the dynamic frictional forces between magnetic recording tapes and magnetic heads were determined under various conditions. Three tapes (3M 990, 3M 20250, and CEC W-4) were evaluated at 25 and 55°C and at speeds of 0.133 and 0.333 in./s under dry and humid conditions. The performance of these tapes under such conditions is discussed. The object of the investigation is to explain the stick-slip and seizure phenomenon observed in magnetic tape recorders used in spacecraft.

K004 Evaluation of Recording Tapes for Use in Spacecraft Magnetic Tape Recorders [June-July 1970]

J. K. Hoffman, S. H. Kalfayan, and R. H. Silver

Supporting Research and Advanced Development, Space Programs Summary 37-64, Vol. III, p. 119, August 31, 1970

For abstract, see Hoffman, J. K.

K005 Long-Term Aging of Elastomers: Kinetics of Oxidation of SBR by Infrared Spectroscopy

R. Rakutis, R. H. Silver, and S. H. Kalfayan

Supporting Research and Advanced Development, Space Programs Summary 37-64, Vol. III, pp. 125-130, August 31, 1970

For abstract, see Rakutis, R.

K006 Evaluation of Spacecraft Magnetic Recording Tapes [June-July 1970]

S. H. Kalfayan, R. H. Silver, and J. K. Hoffman

Supporting Research and Advanced Development, Space Programs Summary 37-64, Vol. III, pp. 140-145, August 31, 1970

The adhesion of a typical magnetic tape to magnetic heads used in spacecraft was studied under various time and temperature conditions. Investigations included the effects of degassing the tape, removal of oxide-binder layer and tape speed on sticking and/or coefficient of friction. It was shown that sticking is dependent on contact time and temperature, and that degassing alleviates the adhesion problem. Tests at various speeds indicated that the coefficient of friction of the tape (3M 20250) was an exponential function of the speed.

K007 Effects of Simulated Venusian Atmosphere on Polymeric Materials

S. H. Kalfayan and R. H. Silver

J. Spacecraft Rockets, Vol. 7, No. 5, pp. 634-636, May 1970

Polymeric materials (plastics and rubbers) serve as electrical and thermal insulators, protective and structural materials, vibration dampeners, adhesives, etc., on spacecraft and planetary landing probes. In 1967, *Venera 4* entered the Venus atmosphere and sent back information about temperature, pressure, and atmospheric composition as it descended to the surface, and *Mariner V* flew by Venus and sent back atmospheric data, among other information. This article presents results of exposure of polymeric materials to a simulation of the Venusian atmosphere, which was

reported to be composed as follows (in weight percentages): CO₂, 90 ± 10 (probably >90); O₂, 0.4–1.6 (probably ~1); N₂, <7 (probably <2.5); and H₂O, 0.1–0.7. The effects of the simulated "Venus" atmosphere are compared with those of air and nitrogen at 550°F and 18 atm.

KATOW, M. S.

K008 30-ft-diam Reflector Upgrade Study

M. S. Katow

The Deep Space Network, Space Programs Summary 37-65, Vol. II, pp. 70–72, September 30, 1970

The tipping assembly of the 30-ft-diam antenna at the Venus Deep Space Station, which is an example of a practical arrangement of trusses using rigid bars, was analyzed for possible improvement in the gravity distortion mode by use of a passive compensator (spring).

The analytical results presented in this article show that the rms distortion for the symmetric (zenith look, gravity off-to-on) loading case can be reduced from 0.017 to 0.002 in. without affecting the anti-symmetric distortion of 0.002 in. However, additional bracings for wind loading may be desirable.

KELLERMANN, K. I.

K009 High-Resolution Observations of Compact Radio Sources at 13 Centimeters

K. I. Kellermann (National Radio Astronomy Observatory), B. G. Clark (National Radio Astronomy Observatory), D. L. Jauncey (Cornell University), M. H. Cohen (California Institute of Technology), D. B. Shaffer (California Institute of Technology), A. T. Moffet (California Institute of Technology), and S. Gulkis
Astrophys. J., Vol. 161, No. 3, pp. 803–809, September 1970

Two antennas of the NASA Deep Space Network at Goldstone, California, and Canberra, Australia, have been used as elements of an interferometer. The baseline length is 10592 km, or 81×10^6 wavelengths ($\lambda = 13.1$ cm). Sources larger than 0".001 are well resolved. Fifty-six sources show clear interference fringes, which indicate the presence of structure on a scale of 0".001 or less. Five sources appear to be completely unresolved; seven others probably have a relatively simple structure and are assigned an angular size. The other 44 have more complex structure. Twenty-four sources are reported as showing no fringes, and a lower limit to their diameter is given. It is estimated that about 15% of the stronger sources at decimeter wavelengths have appreciable structure 0".002 or smaller in angular size.

KELLY, A. M.

K010 Pyrolysis of Natural Products: Identification of Products From Nucleotide Pyrolysis by High Resolution Mass Spectrometry

H. G. Boettger and A. M. Kelly

Supporting Research and Advanced Development, Space Programs Summary 37-63, Vol. III, pp. 10–13, June 30, 1970

For abstract, see Boettger, H. G.

KENDALL, J. M., JR.

K011 Supersonic Boundary Layer Transition Studies

J. M. Kendall, Jr.

Supporting Research and Advanced Development, Space Programs Summary 37-62, Vol. III, pp. 43–47, April 30, 1970

Experimental results are presented concerning the flow fluctuations existing in laminar boundary layers on supersonic wind tunnel test models. The overall growth of these fluctuations, culminating in transition to turbulence, is found to be substantially greater than that predicted by the boundary layer stability theory. It is shown that the fluctuations are forced by the sound field of the tunnel stream. Speculation is made on the mechanism of forcing.

KENDALL, J. M., SR.

K012 Two Blackbody Radiometers of High Accuracy

J. M. Kendall, Sr., and C. M. Berdahl

Appl. Opt., Vol. 9, No. 5, pp. 1082–1091, May 1970

Two cavity-type radiometers have been developed, based on first principles, having the capability of measuring an irradiance with an indicated error 0.3%. The prerequisites for this accuracy are a measured aperture area, a measurement of electric voltages, and an effective absorptance of its blackbody cavity from 0.998 to 0.999 throughout the ultraviolet, visible, and infrared spectral ranges. The first cavity-type radiometer is designed to operate only in a vacuum of <10⁻⁵ torr and to measure intensities from 10 to 300 mW/cm². By using this radiometer in an evacuated cold chamber, an experimental determination of the Stefan-Boltzmann constant is obtained at a value that differs from the theoretical value by 0.3%, which indicates the degree of confidence that can be expected in measurements made with blackbody cavity radiometers. The second type of radiometer is designed to operate in either air or vacuum. Although its aperture opening is windowless, it is unaffected by wind. The range of intensities accurately measurable is from about 10 to 800 mW/cm²; the indicated accuracy is also 0.3%.

KERNER, T.

K013 Mariner Mars 1969 Scan Control Subsystem Design and Analysis

T. Kerner and H. H. Horiuchi

Technical Report 32-1506, October 30, 1970

The scan platform control system designed for the *Mariner* Mars 1969 spacecraft is described. The platform, which acts as a mounting base for the science instruments, has two deg-of-freedom about a set of spacecraft fixed coordinates. The system controls the platform movement and position. This report covers the detailed system design, the servo analysis, and the system error analysis.

KINDER, W.

K014 Real-Time Selection and Validation of Telemetry Data in the SFOF

W. Kinder and W. Kizner

The Deep Space Network, Space Programs Summary 37-65, Vol. II, pp. 118-121, September 30, 1970

An historical appraisal of telemetry data validation techniques was undertaken for the adoption of an automatic real-time algorithm utilizing the new IBM 360/75 computer plant in the Space Flight Operations Facility (SFOF). This article describes an interim algorithm for incorporation into the 1971-era telemetry system, the possible application of discriminant analysis to data validation, and possible future work with discriminant analysis for the evaluation of the telemetry system partial status observables.

KING, J.

K015 Microbiology, Ecology and Microclimatology of Soil Sites in Dry Valleys of Southern Victoria Land, Antarctica

R. E. Cameron, J. King, and C. N. David

Antarctic Ecology: Volume 2, pp. 702-716, Academic Press, Inc., New York, 1970

For abstract, see Cameron, R. E.

KIRK, D. E.

K016 A Dual-Mode Routing Algorithm for an Autonomous Roving Vehicle

D. E. Kirk (Naval Postgraduate School) and L. Y. Lim

Technical Report 32-1484 (Reprinted from *IEEE Trans. Aerospace and Electronic Systems*, Vol. AES-6, No. 3, pp. 290-294, May 1970)

A dual-mode algorithm for routing an unmanned autonomous roving vehicle designed to explore the un-

certain terrain of other planets is presented. The algorithm consists of a global mode, which uses dynamic programming and terrain information available from photo reconnaissance data to determine a nominal optimal path, and a local mode, which routes the vehicle around obstacles whose presence, location, and extent are not known in advance. Gaussian probability density functions are used to simulate terrain for examples that illustrate the performance of the algorithm.

KISSANE, W.

K017 Welded Joint Integrity Study

V. Lobb and W. Kissane

The Deep Space Network, Space Programs Summary 37-64, Vol. II, pp. 79-86, August 31, 1970

For abstract, see Lobb, V.

K018 Clock-Sync Antenna Installation at the U.S. Naval Observatory

W. Kissane

The Deep Space Network, Space Programs Summary 37-64, Vol. II, pp. 97-98, August 31, 1970

The mechanical installation of a clock-sync receiving antenna at the U. S. Naval Observatory in Washington, D.C. is described. As a result of this installation, this government facility is now capable of receiving coded timing signals from the 30-ft-diameter-antenna Venus Deep Space Station transmitter.

KIZNER, W.

K019 Real-Time Selection and Validation of Telemetry Data in the SFOF

W. Kinder and W. Kizner

The Deep Space Network, Space Programs Summary 37-65, Vol. II, pp. 118-121, September 30, 1970

For abstract, see Kinder, W.

KLAUS, R. L.

K020 Theoretical Arguments Supporting the Instantaneous Burning Rate Measurements for Solid Propellants During Depressurization Made at JPL

R. L. Klaus

Supporting Research and Advanced Development, Space Programs Summary 37-63, Vol. III, pp. 169-173, June 30, 1970

Measurements of the instantaneous burning rates of solid propellants during a depressurization transient

have indicated that during the early part of the transient, the instantaneous burning rate is greater than that of a steadily burning propellant at the same pressure. This result contradicts former theoretical predictions. New theoretical arguments are advanced to support the observed phenomena by considering the effect of a finite step-function decrease in system pressure. It is shown that in this case the propellant always extinguishes and that in the early part of the transient, the surface temperature, and hence instantaneous burning rate, is always greater than the corresponding steady value. It is also shown how these results apply to finite depressurization rates.

K021 An Improved Newton-Raphson Algorithm for Finding the Roots of Equations for Solid Propellant Combustion Studies

R. L. Klaus and S. Wilson

Supporting Research and Advanced Development, Space Programs Summary 37-63, Vol. III, pp. 173-175, June 30, 1970

An improved Newton-Raphson algorithm for finding roots of equations is described. If a root is present within a specified interval, the algorithm is guaranteed to find it regardless of the shape of the curve within the interval. Moreover, the method of interval shrinking which is used guarantees that the root will be found to within the specified tolerance. As the calculation proceeds, it is tested to determine whether convergence is being attained at least as fast as by the method of interval halving; if not, the algorithm shifts to interval halving until such time as the Newton-Raphson method converges more rapidly. The algorithm has been coded for a computer in FORTRAN and tested.

K022 Basic Equations in the Mathematical Modeling of the Gas Phase of a Burning Solid Propellant

R. L. Klaus

Supporting Research and Advanced Development, Space Programs Summary 37-63, Vol. III, pp. 175-184, June 30, 1970

The basic equations that describe the gas phase of a burning solid propellant are derived and their behavior from both a mathematical and physical standpoint is discussed. In the case of a semi-infinite flame (which applies when no ignition stimulus is being applied at the edge of the flame), it is shown that boundary conditions at the solid-gas interface are themselves sufficient to completely determine the problem. An attempt to apply boundary conditions at the gas side may result in an ill-posed problem. In order to consider ignition stimuli in the form of a

heat flux to the flame on the gas side, a finite flame is also considered. This case permits the inclusion of two additional boundary conditions at the edge of the flame.

KLEINROCK, L.

K023 Discretionary Research: A Simple Sequence-Permutation Method

L. Kleinrock

Supporting Research and Advanced Development, Space Programs Summary 37-62, Vol. III, pp. 75-79, April 30, 1970

An extremely simple permutation encoder-decoder system for use in a speech disguiser is described. The decoder is essentially a copy of the encoder, and both are easily implemented.

K024 Discretionary Research: Uniform Permutation of Sequences

L. Kleinrock

Supporting Research and Advanced Development, Space Programs Summary 37-64, Vol. III, pp. 32-43, August 31, 1970

A series configuration of simple coders is analyzed. Experimental results show that this configuration is inadequate for effective speech scrambling. A ternary tree structure is then proposed and studied; this configuration yields a uniform distribution of shift length which is a desired property for permuting samples of speech.

KLOC, I.

K025 Vehicle Mobility Tests: Soft Soil Slopes

I. Kloc

Supporting Research and Advanced Development, Space Programs Summary 37-62, Vol. III, pp. 188-192, April 30, 1970

This exploratory testing program evaluates vehicle mobility performance on soft, level, and sloping terrains. Specific information is given about vehicle characteristics, soil material, equipment, instrumentation, and an analysis of test results. The basic objectives of these tests are to: (1) obtain vehicle performance data for soft steep slopes for potential lunar applications, considering low soil-wheel contact pressures of less than 0.75 psi and small sinkages; (2) establish criteria for planning representative single wheel tests on slopes; and (3) guide the formulation of a mathematical soil-wheel interaction model for horizontal and sloping terrains.

KNOELL, A. C.

K026 Development of Advanced Composite Liquid Propulsion Pressure Vessels

A. C. Knoell

Supporting Research and Advanced Development,
Space Programs Summary 37-62, Vol. III, pp. 181-182,
April 30, 1970

This article reports progress relating to the design development of boron-epoxy liquid propulsion tanks. The effects of buckling, thermal shock, and space environment on tank designs are assessed, and a materials test and evaluation program and critical design problem areas are described.

K027 Holography Application Study to Pressure Vessel Flaw Detection

G. Morse, A. Knoell, and R. Badin

Supporting Research and Advanced Development,
Space Programs Summary 37-64, Vol. III, pp. 100-101,
August 31, 1970

For abstract, see Morse, G.

KOERNER, M. A.

K028 Effect of Premodulation Filtering on the Correlation and Error Signals in a Pseudonoise Receiver

M. A. Koerner

Supporting Research and Advanced Development,
Space Programs Summary 37-64, Vol. III, pp. 51-59,
August 31, 1970

Spread spectrum techniques are commonly used in communication and radio tracking systems to suppress interfering signals. The effectiveness of the spreading will be limited by the frequency response of the channel through which the wide-band signal must be transmitted. This article examines the effect of premodulation filtering in a system where the frequency spreading is achieved by multiplying a phase-modulated carrier with a binary-valued (± 1) signal. The receiver uses two observables, the correlation $C(\hat{\tau})$ and the error signal $E(\hat{\tau})$, to synchronize a locally generated replica with the binary modulation carried by the received signal. Equations are presented for evaluating $C(\hat{\tau})$ and $E(\hat{\tau})$ for predemodulation filters which are either Butterworth or Tchebycheff low-pass filters, or the high-pass, band-pass, or band-reject filters which can be synthesized from these low-pass filters using simple frequency transformations.

KOLBLY, R. B.

K029 Switched-Carrier Experiments

R. B. Kolbly

The Deep Space Network, Space Programs Summary 37-65,
Vol. II, pp. 81-84, September 30, 1970

The Deep Space Instrumentation Facility has a requirement, in support of the *Viking* Project, for simultaneous transmission of two carriers from one antenna. These carriers would be separated by approximately 5 MHz and carry ranging modulation. The power level required is a minimum of 40 kW in each carrier and its associated sidebands. The 400-kW transmitter can supply this easily if excitation is supplied at the two frequencies, but past experience and test data have shown that intermodulation products in the receiver passband well above threshold are generated by this approach. These products are generated whenever two carriers exist in the nonlinear klystron; there is even evidence that they may be generated in the waveguide equipment or the antenna structure.

If the excitation could be switched so that the klystron and antenna see only one carrier at a time, these products would not be generated. This article describes initial experiments to investigate the feasibility of time-sharing a klystron amplifier between two uplink channels in order to simultaneously track two spacecraft. Design of a suitable diode switch is described.

K030 Waveguide Switch Protector

R. B. Kolbly

The Deep Space Network, Space Programs Summary 37-65,
Vol. II, pp. 105-106, September 30, 1970

The waveguide switches used by the Deep Space Instrumentation Facility are driven by a gear-reduced dc motor, with no power supplied to the motor armature with the switch in its operating position. If, for any reason, the motor operates with the switch rotor "hung up," the motor will destroy itself. A fuse is provided, but it is required to protect several switches and does not reliably protect an individual switch motor. This article describes a device to protect the waveguide switches from failure due to overload of the drive motor. This protection is achieved by detection of the amount of time the motor is receiving power and removal of the power if the time is excessive, while signaling the operator at the same time.

KRUG, A.

K031 Long-Term Life Test of the Spare Mariner Venus 1967 Power Subsystem Hardware

A. Krug

Supporting Research and Advanced Development,
Space Programs Summary 37-62, Vol. III, p. 145,
April 30, 1970

The long-term life testing of the *Mariner* Venus 67 spare power subsystem hardware is under way. During functional testing of the flight hardware and checkout

of the test procedure, two failures were noted involving 1N459A-type diodes. The circuits in which these diodes were used are electrically unrelated and are physically located in separate cases. Analysis of the failed parts indicated that electrical overstress was the cause in both instances, but the source of the electrical overstress has not been identified.

KUPPERMANN, A.

K032 Vibrational Excitation of H₂ by Low- and Medium-Energy Electrons

S. Trajmar, D. G. Truhlar (California Institute of Technology), J. K. Rice (California Institute of Technology), and A. Kuppermann (California Institute of Technology) *Supporting Research and Advanced Development, Space Programs Summary 37-62, Vol. III, pp. 36-43, April 30, 1970*

For abstract, see Trajmar, S.

K033 Electron Scattering by H₂ With and Without Vibrational Excitation: III. Experimental and Theoretical Study of Inelastic Scattering

S. Trajmar, D. G. Truhlar (California Institute of Technology), J. K. Rice (California Institute of Technology), and A. Kuppermann (California Institute of Technology) *J. Chem. Phys., Vol. 52, No. 9, pp. 4516-4533, May 1, 1970*

For abstract, see Trajmar, S.

KURTZ, D. W.

K034 DSS 14 Antenna Wind Loading Measurements

D. W. Kurtz
The Deep Space Network, Space Programs Summary 37-63, Vol. II, pp. 35-37, May 31, 1970

In order to supplement existing design information, a test has been proposed to obtain direct wind load measurements from the 210-ft antenna at DSS 14 (Mars Deep Space Station). Strain gage instrumented force panels will be mounted in the antenna surface and local pressure across the disk will be obtained. Integration of these data will yield the aerodynamic coefficients for comparison and correlation with existing wind tunnel data. These results should help in resolving some of the problems and scaling effects involved in current wind load predictions.

K035 Compilation of Wind Tunnel Coefficients for Parabolic Reflectors

R. Levy and D. Kurtz
The Deep Space Network, Space Programs Summary 37-63, Vol. II, pp. 36-42, May 31, 1970

For abstract, see Levy, R.

LAESER, R. P.

L001 Mariner Mars 1971 Mission [Support, by DSN, March-April 1970]

R. P. Laeser
The Deep Space Network, Space Programs Summary 37-63, Vol. II, pp. 11-14, May 31, 1970

An operational system for support of the *Mariner Mars 1971* S-band occultation experiment is being implemented by the Deep Space Network (DSN) and includes elements at three deep space stations and at the Space Flight Operations Facility. A functional description of the system is presented along with supporting information on the experiment itself.

L002 Mariner Mars 1971 Mission Support [by DSN, May-June 1970]

R. P. Laeser
The Deep Space Network, Space Programs Summary 37-64, Vol. II, pp. 4-7, August 31, 1970

The Deep Space Network (DSN) testing program leading to *Mariner Mars 1971* support is constrained by project requirements, DSN testing philosophy, DSN training requirements, and implementation schedules. This article demonstrates how satisfaction of these constraints will be maximized in a minimum-time test program.

L003 Mariner Mars 1971 Mission Support [by DSN, July-August 1970]

R. P. Laeser
The Deep Space Network, Space Programs Summary 37-65, Vol. II, pp. 19-23, September 30, 1970

The calibration of radio metric data [generated by the Deep Space Network (DSN) while tracking a spacecraft] to compensate for the effects of propagation phenomena and the variations of a deep space station location in space is a DSN responsibility in some cases; in other cases, the DSN provides analytic calibration assistance to each supported project. This effort, called Tracking System analytic calibration, has been formalized for support starting with the *Mariner Mars 1971* Project. This article describes how Tracking System analytic calibration will provide the necessary accuracy, especially through the calibration of tropospheric and charged-particle effects, to meet the *Mariner Mars 1971* requirements.

LA FRIEDA, J.

L004 Space Station Unified Communication: Optimum Modulation Indexes and Maximum Data Rates for the Interplex Modem

J. La Frieda

Supporting Research and Advanced Development,
Space Programs Summary 37-64, Vol. III, pp. 23-27,
August 31, 1970

This article is concerned with the determination of the optimum modulation indexes, and the corresponding maximum rate-to-bandwidth ratios for the two-channel PSK-PM interplex modem, when the bit error probabilities of the data channels are equal. The results, which are presented in the form of design curves, are of practical interest, since the interplex modem yields significantly improved performance over the existing two-channel telemetry system.

LANDEL, R. F.

L005 A Generalization of the Boltzmann Superposition Principle

J. Moacanin, J. J. Aklonis, and R. F. Landel
Supporting Research and Advanced Development,
Space Programs Summary 37-63, Vol. III, pp. 207-209,
June 30, 1970

For abstract, see Moacanin, J.

L006 Synthesis and Properties of a New Class of Potential Biomedical Polymers

A. Rembaum, S. P. S. Yen, R. F. Landel, and
M. Shen (University of California, Berkeley)
J. Macromol. Sci.—Chem., Vol. A4, No. 3, pp. 715-738,
May 1970

For abstract, see Rembaum, A.

LASS, H.

L007 Average Access Times for a Magnetic Disk Storage Device

P. Gottlieb and H. Lass
Supporting Research and Advanced Development,
Space Programs Summary 37-62, Vol. III, pp. 285-289,
April 30, 1970

For abstract, see Gottlieb, P.

LAUE, E. G.

L008 The Measurement of Solar Spectral Irradiance at Different Terrestrial Elevations

E. G. Laue
Sol. Energy, Vol. 13, No. 1, pp. 43-57, April 1970

The increasing world population and the increasing complexity of civilization require improved efficiency in the utilization of natural resources. Solar energy is the primary determinate of our environment, and an understanding of the nature of its irradiance is fundamental in the control or modification of human and

biological ecology. Recent improvements in filter radiometry have resulted in the realization of simple, sturdy instruments facilitating spectral irradiance determinations, in wavelength bands as narrow as 100 nm, throughout the solar spectrum. Application of these instruments, utilizing jet rocket aircraft, has extended our knowledge of the solar spectral irradiance at altitudes up to 80 km. This paper describes the methods necessary to obtain such spectral data and presents some ground-based summaries and, in particular, new results of concurrent measurements made at 1.3 and 2.3 km; the meteorological interpretation is indicated. Since knowledge of the variation of such radiant energy fluxes at various locations on the earth's surface is meager, it is difficult to assess the potential application. Initial efforts might entail, as a minimum requirement, a three-channel bandpass system monitoring the total, ultraviolet, and infrared irradiances. Data from this system could provide useful information concerning the local aerological situation.

LAUMANN, E. A.

L009 Mariner Limit Cycles and Self-Disturbance Torques

B. Dobrotin, E. A. Laumann, and D. Prelewicz (California Institute of Technology)
J. Spacecraft Rockets, Vol. 7, No. 6, pp. 684-689,
June 1970

For abstract, see Dobrotin, B.

LAYLAND, J. W.

L010 Combinatorial Communication: An Upper Bound on the Free Distance of a Tree Code

J. Layland and R. McEliece
Supporting Research and Advanced Development,
Space Programs Summary 37-62, Vol. III, pp. 63-64,
April 30, 1970

An upper bound on the free distance (minimum distance) of an arbitrary binary tree code of finite memory is obtained. This extends a previous result in which the code was assumed to be convolutional, systematic, and of rate $1/v$ for some integer $v \geq 2$. In addition, it is shown how these bounds can sometimes be tightened in the important special case of convolutional codes.

L011 Information Systems: Synchronizability of Constraint Length Convolutional Codes and a Heuristic Code-Construction Algorithm

J. W. Layland
The Deep Space Network, Space Programs Summary 37-64, Vol. II, pp. 41-44, August 31, 1970

This article presents the simulated bit error probabilities for optimum decoding of convolutional codes at constraint lengths three to ten. At a design point of 5×10^{-3} bit error probability, the best constraint length, considering both the code performance gain and decoder complexity, is found to be small, $K = 4$ or 5.

The codes presented were constructed using a hill-climbing algorithm operating on an approximate bit error probability criterion. The algorithm is far faster than a global search of possible codes. Where a comparison exists, the codes constructed by this algorithm exhibit better performance at the bit error probabilities currently of interest in Deep Space Instrumentation Facility communications than do codes constructed by global search using other performance measures. The main conclusion is that these codes represent a saving of 0.6 dB over "Green Machine" decoding of biorthogonal codes at an error rate of 10^{-3} with the complexity of the decoder held constant.

L012 Information Systems: Performance of Short Convolutional Codes

J. W. Layland

The Deep Space Network, Space Programs Summary 37-64, Vol. II, pp. 44-50, August 31, 1970

This article studies the problem of acquiring branch synchronization for the decoding of convolutional codes by Viterbi's optimal decoding algorithm. Simulations of this algorithm have shown that it is self-synchronizing once branch synchronization has been established. In most cases, branch synchronization can be established by examination of the decoder state likelihoods, but this cannot always be guaranteed. For example, the all-zeros data sequence produces an all-zeros code sequence for which branch synchronization can never be identified. Techniques for endowing a convolutional code with guaranteed synchronizability are examined, with results which are predominantly negative for the higher rate codes of greatest interest to the Deep Space Instrumentation Facility. However, assuming that the data source is suitably random, simulation results reported herein show that branch synchronization can be identified by examining the decoder state likelihoods over several hundred branches of the code tree.

L013 Information Systems: Multiple-Mission Sequential Decoder—Comparing Performance Among Three Rate $\frac{1}{2}$, $K = 32$ Codes

J. W. Layland

The Deep Space Network, Space Programs Summary 37-64, Vol. II, pp. 50-52, August 31, 1970

This article compares the performance of three rate $\frac{1}{2}$, constraint length 32 convolutional codes when decoded by the multiple-mission sequential decoder. The first two codes are the systematic and non-systematic quick look codes under consideration for *Pioneers F* and *G*. The third code is also non-systematic. The erasure probabilities for all three codes are virtually identical and significantly greater than the error probability of any of them. The error probability of the systematic code is much higher than that of the quick look non-systematic code, which is slightly higher than the error probability of the non-systematic code without the quick look property. The computations were performed using the multiple-mission sequential decoder with a changed metric.

LEONARD, W. D.

L014 Spacecraft-RTG Thermal Interface Considerations

W. D. Leonard

Supporting Research and Advanced Development, Space Programs Summary 37-62, Vol. III, pp. 127-131, April 30, 1970

The effect on radioisotope thermoelectric generator (RTG) temperatures and performance due to the interaction between units mounted on parallel axes was evaluated for various spacings between RTGs. The possible advantages of inserting a reflector or reradiator between the RTGs to minimize the interaction effects were also evaluated. It was found that, for RTG separation distances of 20 in. or greater, the interaction effects were tolerable. The use of a reflector or reradiator interposed between the RTGs does not significantly reduce the effect for the same spacing between RTGs.

Methods of providing the thermal control subsystem with heat from the RTG were also evaluated. Of the various schemes examined, it appears that a heat exchanger conductively coupled to a common mounting point for the four RTGs would result in the least perturbation upon the RTGs. Thus, from a thermal viewpoint, no serious reason seems to exist that would preclude the use of a two-axis, side-by-side arrangement of the RTGs on the Thermoelectric Outer-Planet Spacecraft.

L015 Multi-Hundred-Watt Radioisotope Thermoelectric Generator Transient Performance

W. D. Leonard and O. S. Merrill

Supporting Research and Advanced Development, Space Programs Summary 37-63, Vol. III, pp. 80-86, June 30, 1970

The transient performance of two possible multi-hundred-watt radioisotope thermoelectric generator (MHW-RTG) concepts has been evaluated over the critical period from launch to launch plus 5 h. The analysis considered the effect of radiation interchange factors for the RTG. One of the RTG concepts was found to be capable of supplying 100% of the power required during the entire launch phase. In the other concept, useful power was not delivered until approximately 45 min after launch, and 100% of the needed power was not delivered until about 85 min after launch. The latter system must be supplemented with 260 W-h of battery power until the RTGs can assume the full load.

LEPPLA, F. B.

L016 DSIF Monitor System Development

F. B. Leppla

The Deep Space Network, Space Programs Summary 37-64, Vol. II, p. 87, August 31, 1970

The Deep Space Instrumentation Facility (DSIF) Monitor System being developed as part of the Deep Space Network Monitor System is described. In order to meet functional requirements for the 1971 era, the DSIF software will be modified extensively. The DSIF hardware capabilities will be expanded to provide for 4800-bit/s high-speed data input and output. A remote terminal will be added to the station equipment for monitor display purposes.

LEVY, R.

L017 Compilation of Wind Tunnel Coefficients for Parabolic Reflectors

R. Levy and D. Kurtz

The Deep Space Network, Space Programs Summary 37-63, Vol. II, pp. 36-42, May 31, 1970

Loading data from wind tunnel tests on parabolic reflectors are compiled and summarized in tabular and plotted format. Non-dimensional force and moment coefficients are provided over complete ranges of azimuth and elevation angles for four practical combinations of focal length/diameter, focal length/depth, and surface porosity ratios.

L018 Thirty-Degree Reflector Mockup Study: Comparisons of Measured and Predicted Deflections

R. Levy

The Deep Space Network, Space Programs Summary 37-64, Vol. II, pp. 74-79, August 31, 1970

Field measurements of deflections due to applied loads are compared with the analytical predictions for a

full-sized 30-deg central angle sector of an 85-ft-diameter reflector. Descriptions of the structure and analytic model, data generation, data fitting, and data processing are included.

L019 A Method for Selecting Antenna Rigging Angles to Improve Performance

R. Levy

The Deep Space Network, Space Programs Summary 37-65, Vol. II, pp. 72-76, September 30, 1970

Given the half path-length surface deviations from the best-fitting parabola for only two gravity loading positions, a new closed-form computational procedure will give the best-fit rms surface deviation at any arbitrary antenna elevation attitude. This procedure, described in this article, greatly facilitates the selection of antenna rigging angle to minimize the peak rms deviation or to optimize RF performance with respect to an elevation-attitude weighting function.

LEWYN, L. L.

L020 Gamma Ray Spectrometer for Apollo 16

L. L. Lewyn

Supporting Research and Advanced Development, Space Programs Summary 37-62, Vol. III, pp. 9-12, April 30, 1970

A gamma ray spectrometer has been developed for two lunar flights, beginning with *Apollo 16*. The spectrometer will be used to measure the natural and solar-induced lunar gamma ray flux in the 0.2- to 10-MeV range from the orbiting *Apollo* service module. The development and operational characteristics of this instrument are described in this article.

LIM, L. Y.

L021 A Dual-Mode Routing Algorithm for an Autonomous Roving Vehicle

D. E. Kirk (Naval Postgraduate School) and L. Y. Lim
Technical Report 32-1484 (Reprinted from *IEEE Trans. Aerospace and Electronic Systems*, Vol. AES-6, No. 3, pp. 290-294, May 1970)

For abstract, see Kirk, D. E.

LIN, H. S.

L022 TOPS Attitude Control Reliability Study

H. S. Lin

Supporting Research and Advanced Development, Space Programs Summary 37-63, Vol. III, pp. 106-109, June 30, 1970

The effects of imperfect sensing and switching on system reliability for the Thermoelectric Outer-Planet

Spacecraft (TOPS) Attitude Control System are being studied. General formulas of the reliability function are derived. The reliability of the system is expressed in terms of the failure rate of the operating unit, the failure rate of the standby unit, and the probabilities of proper operation of failure detectors and switching mechanism. For the constant failure rates, special cases are solved.

LINDSEY, W. C.

L023 Hybrid Carrier and Modulation Tracking Loops

W. C. Lindsey

Supporting Research and Advanced Development, Space Programs Summary 37-62, Vol. III, pp. 108-113, April 30, 1970

The tracking loops described in this article exploit the coherency of the observed data sidebands at the carrier frequency for improvements in phase-coherent tracking, telemetry, and command system performance. The loop is motivated by one aspect of generalized harmonic analysis, namely, the so-called cross-spectrum. The basic idea is to use the power in the composite received signal (sidebands including cross-modulation components) to enhance the signal-to-noise ratio in the carrier tracking loop, thereby reducing the noisy reference loss and ultimately the subcarrier reference jitter, the symbol sync jitter, and the error probability of the data detector. The modulation from the extracted sidebands is removed in such a way that the coherence power in the data sidebands can be used for tracking at the carrier frequency.

LINNES, K. W.

L024 Mariner Mars 1969 Extended Operations

[Mission Support, by DSN, July-August 1970]

K. W. Linnes

The Deep Space Network, Space Programs Summary 37-65, Vol. II, pp. 14-19, September 30, 1970

As described in this article, the Deep Space Network (DSN) has supported the *Mariner* Mars 1969 Extended Operations Mission with the 210-ft-diam-antenna Mars Deep Space Station, a new experimental high-power transmitter, a new experimental sequential acquisition ranging system, and the 85-ft-diam-antenna Echo and Cebreros Deep Space Stations. The tracking coverage of this unique equipment has enabled meeting of the objectives of the mission to test relativistic gravitational theories, measure solar coronal and interplanetary electron density profiles, demonstrate a highly accurate ranging system at 2.6 AU, and determine the utility and accuracy of the differenced range versus integrated doppler (DRVID) method of charged-particle cali-

bration of metric radio tracking data. The support was provided during the critical period of superior conjunction of the *Mariner VI* and *VII* spacecraft around April 29 and May 10, 1970. Doppler and ranging data were obtained within 2 deg of the Sun.

LITTLE, S. J.

L025 High-Dispersion Spectroscopic Studies of Mars: III. Preliminary Results of 1968-1969 Water-Vapor Studies

R. A. Schorn, C. B. Farmer, and S. J. Little (University of Texas)

Icarus: Int. J. Sol. Sys., Vol. 11, No. 3, pp. 283-288, November 1969

For abstract, see Schorn, R. A.

LIU, A. S.

L026 Variational Equations Derived From the Herrick Variation of Parameters Method

A. S. Liu

J. Astronaut. Sci., Vol. XVII, No. 4, pp. 185-217, January-February 1970

The partial derivatives of the position and velocity of a spacecraft with respect to an arbitrary set of initial conditions can be obtained by solving the variational equations derived from Cowell's equations of motion. A similar set of variational equations can be derived from other forms of the equation of motion, such as the Herrick variation of parameters method. The matrix which results from solving this latter set of variational equations is one whose elements are the partial derivatives of osculating orbital parameters at time t with respect to osculating orbital parameters at initial time t_0 .

This paper tabulates the variational equations derived from the Herrick variation of parameters method, and the results of a numerical solution are presented for the case of the minor planet number 1566, Icarus, during its recent encounter with the earth. It was found that the departures from conic conditions in the partial derivatives occur rapidly during an encounter of a minor planet with a perturbing body. The deviations from conic conditions amount to 1% for the case of Icarus. Plots resulting from the numerical solutions are presented.

LOBB, V. B.

L027 Welded Joint Integrity Study

V. Lobb and W. Kissane

The Deep Space Network, Space Programs Summary 37-64, Vol. II, pp. 79-86, August 31, 1970

A 30-deg test segment of an 85-ft-antenna reflector and backup was constructed for use in researching possible future antenna changes, maintenance procedures, welding distortions, and thermal changes. Seventy thermocouples were installed. One thermocouple was installed at each intersection of the members of the test structure (joint of the computer model) for use in measuring temperature changes in the test structure.

A theodolite equipped with an optical micrometer was used to measure structure changes, using 31 targets installed on the panels at the test structure's surface joints. In addition, 49 targets installed in one of the surface panels were measured to determine thermal distortion.

Four daily measurements were taken for the structure and panel targets and structure temperatures to analyze effects of solar heating on various finishes and structure connections and to find the weld distortions in the structure caused by welding of the test structure's joints. The data reduction of field data to engineering rms was performed on computers using a JPL-developed program.

The results of this research show that welding distortions are minor, and welding is an effective way to eliminate bolted structure creep. In addition, the results give structure temperature ranges for various finishes, thermal rms ranges, creep effect, cyclic effect, and paint effects and form a basis for determining thermal allowances.

L028 Antenna Acceleration: Impact Damage Modifications

V. Lobb

The Deep Space Network, Space Programs Summary 37-64, Vol. II, p. 97, August 31, 1970

A deceleration-impact damage investigation revealed structural clip damage and failures developing in the hour-angle wheel counterweight cage support areas of the Pioneer, Echo, Woomera, and Johannesburg Deep Space Stations. From this investigation, a change was instigated to modify all the antennas in the Deep Space Network. The first impact damage modification done as an engineering change order was accomplished at the Weemala Deep Space Station. The work was performed as a joint effort of the cognizant operations and cognizant development engineers. This was done to provide a training period for this modification that would enable the cognizant operations engineers to implement the modification at the Robledo and Cebreros Deep Space Stations in late-1970. The modification procedures are outlined.

L029 DSS 51 Antenna Mechanical Subsystem Upgrade

J. Carpenter, V. Lobb, A. Nicula, and D. Nelson

The Deep Space Network, Space Programs Summary 37-64, Vol. II, pp. 98-104, August 31, 1970

For abstract, see Carpenter, J.

L030 Low-Frequency Low-Level Stress Reversals on an Assembly of Bolted Joint Specimens

V. B. Lobb

The Deep Space Network, Space Programs Summary 37-65, Vol. II, pp. 77-81, September 30, 1970

In previous joint integrity research, JPL found that the inorganic zinc coating used as a corrosion barrier on the 210-ft-diam antennas broke down on the contact surfaces when undergoing stress reversals. To ensure that this desirable coating could be used without joint slippage, research was initiated to determine which design parameter and stress level would warrant use of inorganic zinc-painted coatings on specimens undergoing low-cycle, low-load complete stress reversals. Bolted structural assemblies with plain mill scale faying surfaces were assigned the role of a control surface by which the inorganic zinc-painted surface was to be compared. This research investigated the effect of surface conditions, bolt design, bolt strength level, and applied stress versus joint slip displacement. Another objective of the program was to confirm previous stress reversal studies concerning the effect of load level and the type of fastener. The research program and the test procedures and results are described in this article.

LORD, H. C., III

L031 Retention Coefficients and Thermal Release Profiles of Ion-Injected Argon From Silicates and Iron

H. C. Lord III

Canad. J. Phys., Vol. 48, No. 12, pp. 1472-1479, June 15, 1970

Thermal release profiles and retention coefficients of injected argon ions were investigated as functions of substrate composition and prior ion-irradiation history. Samples of forsterite, enstatite, oligoclase, obsidian, and cold-rolled steel were irradiated with various sequences of 1-keV H⁺, 4-keV He⁺, and 40-keV Ar⁺. The release temperature of the maximum argon concentration was found to be a function of incident Ar⁺ dose and pre-irradiation history, but not substrate composition. The hydrogen or helium pre-irradiation converted the volume diffusion argon release to a low-temperature defect diffusion release. An increase in the incident dose of Ar⁺ ions resulted in an increase in the percentage of the argon released by defect diffusion and a decrease in the argon retention coefficient.

LORD, W. W.

L032 Overseas 210-ft-diam Antenna Project

R. D. Casperson and W. W. Lord

The Deep Space Network, Space Programs Summary 37-65,
Vol. II, pp. 154-158, September 30, 1970

For abstract, see Casperson, R. D.

LORELL, J.

L033 Celestial Mechanics Experiment for Mariner Mars 1971

J. Lorell, J. D. Anderson, and I. I. Shapiro (Massachusetts Institute of Technology)

Icarus: Int. J. Sol. Sys., Vol. 12, No. 1, pp. 78-81,
January 1970

A spacecraft experiment is described. This experiment is expected to test the theory of general relativity, improve the Martian ephemeris, and provide new gravimetric data for Mars. The anticipated measurements will be obtained from the radio tracking system used to navigate the *Mariner* Mars 1971 orbiter.

LOVELOCK, J. E.

L034 Palladium-Hydrogen System: Efficient Interface for Gas Chromatography-Mass Spectrometry

P. G. Simmonds, G. R. Shoemaker, and J. E. Lovelock

Anal. Chem., Vol. 42, No. 8, pp. 881-885,
July 1970

For abstract, see Simmonds, P. G.

L035 The Palladium Generator-Separator-A Combined Electrolytic Source and Sink for Hydrogen in Closed Circuit Gas Chromatography

J. E. Lovelock, P. G. Simmonds, and G. R. Shoemaker

Anal. Chem., Vol. 42, No. 9, pp. 969-973,
August 1970

An electrolytic cell with a hollow palladium alloy cathode is known as a source of high pressure, ultra-pure hydrogen. An extension of the principles involved has been used to construct a practical device to serve as a combined source and sink for hydrogen. The cell electrolyzes water to generate hydrogen at the cathode of the cell in sufficient quantity to transport a gaseous sample through a gas chromatographic column. The hydrogen is subsequently removed at the anode of the cell, prior to the gas chromatographic detector. When the cathode and anode are connected through a gas chromatographic column, the cell operates at 100% electrolytic efficiency for the generation and removal of hydrogen. This device provides a

means of sample enrichment and facilitates special gas chromatographic techniques such as flow and pressure programming.

LUDWIG, A. C.

L036 Large Spacecraft Antennas: Use of Efficiency Program to Calculate Feed Defocusing Loss

A. Ludwig and J. Hardy

Supporting Research and Advanced Development,
Space Programs Summary 37-62, Vol. III, pp. 87-89,
April 30, 1970

An existing JPL computer program may be used to facilitate computation of axial defocusing loss for parabolic reflector antennas. Results are computed for various cases, including the Thermoelectric Outer-Planet Spacecraft high-gain antenna, and are compared to a more exact solution.

L037 Spacecraft Antenna Research: Preliminary RF Test of Conical Gregorian Antenna

A. C. Ludwig and J. Hardy

Supporting Research and Advanced Development,
Space Programs Summary 37-63, Vol. III, pp. 42-46,
June 30, 1970

The design and RF test results of a prototype conical Gregorian antenna are presented. The test data demonstrate that the performance of the antenna is consistent with the optical principle assumed in the design. The antenna also performs well in monopulse mode of operation and when the subreflector is less than six wavelengths in diameter.

LUTWACK, R.

L038 Heat-Sterilizable Battery Development [June-July 1970]

R. Lutwack

Supporting Research and Advanced Development,
Space Programs Summary 37-64, Vol. III, pp. 69-71,
August 31, 1970

Several aspects of the program to develop heat-sterilizable batteries are reported. The Ni-Cd cell development program has ended; the technology has been achieved for heat-sterilizable cells with capacity, efficiency, and energy density properties comparable to unsterilizable cells. Considerable information has been obtained for the design of impact-resistant Ni-Cd cells. The development of a remotely activated, Ag-Zn battery has been completed; tests on three batteries have revealed a high gas pressure problem, although the power goals of the task were achieved. Studies of the permeability characteristics of an AMF C-103 mem-

brane using NaCl solutions have been used to correlate experimental data with the mathematical descriptions from steady-state thermodynamics. In an investigation of transient current phenomena, it has been shown that the experimental data fit the theoretical prediction very well for current interruption but that the correspondence is very poor for current buildup and that the combined effects of convection and pulse charging result in the reduction of the charging time by 80% if the pulse current is at least 10 times the steady-state diffusion-limiting current.

LYTTLETON, R. A.

L039 On the Internal Structures of Mercury and Venus

R. A. Lyttleton

Technical Report 32-1439 (Reprinted from *Astrophys. Space Sci.*, Vol. 5, No. 1, pp. 18-35, September 1969)

Recent radar measures of the radius and mass of Mercury imply a composition for the planet containing about 60% iron. One or other of two conclusions seems inescapable: either that Mercury is a highly exceptional object among terrestrial planets, or that all measures to date of the planet involve substantial systematic error. In either case the situation is such that independent checking of the radius and mass of Mercury by some entirely different means has become of the greatest importance to planetary physics and cosmogony.

The recent radar and other determinations of the solid radius of Venus imply an internal structure similar to that of the earth, namely a liquid core surrounded by a solid mantle and outer-shell zone. The theory also implies that the temperatures within Venus should be slightly higher than at the corresponding parts of the earth. The proportion of mass in the core of Venus (about 25% of the whole) is entirely consistent with the phase-change hypothesis as to its nature, as of course is also the absence of any liquid or iron core in both Mars and the moon. On the older iron-core hypothesis, Venus with considerably less iron content by mass than the earth, and Mars and the moon with none, would all present problems in different degrees to account for the differences of composition.

If Venus began as an all-solid planet, the initial radius would have been about 6300 km, and the total amount of surface reduction to date owing to contraction of the planet would have been almost 40 million km², and as a proportion of the total area only slightly less than the contraction of the earth. The theory thus predicts the existence of folded and thrustured mountain-systems of terrestrial type at the surface of Venus.

L040 A Miniaturized Absolute Gravimeter for Terrestrial, Lunar, and Planetary Research

R. G. Brereton, B. H. Chovitz (United States Coast and Geodetic Survey), W. M. Greene (Marshall Space Flight Center), O. K. Hudson (Marshall Space Flight Center), R. A. Lyttleton (St. John's College), and R. D. Regan (United States Geology Survey)

Supporting Research and Advanced Development, Space Programs Summary 37-62, Vol. III, pp. 1-5, April 30, 1970

For abstract, see Brereton, R. G.

L041 The Structures of the Terrestrial Planets

R. A. Lyttleton

Advances in Astronomy and Astrophysics, Vol. 7, pp. 83-145. Academic Press, Inc., New York, 1970

It would seem probable that the study of the internal structure of the planets should concentrate first upon the 99.99% or more of the mass at present inaccessible to direct observations. The same holds even more strongly for planets other than the earth, for, as yet, only the outer solid surface can be observed and sometimes not even that. It is plain both from their masses and mean densities that the four inner planets and the moon taken as a group can be regarded in an overall sense as having different physical structures and compositions from the group formed by the great outer planets. The structures of this terrestrial group (Mercury, Venus, earth, moon, and Mars) are discussed in detail in this article.

MACIE, T. W.

M001 Solar Electric Propulsion System Tests

E. V. Pawlik, E. N. Costogoe, J. D. Ferrera, and T. W. Macie
Technical Report 32-1480, August 15, 1970

For abstract, see Pawlik, E. V.

M002 Solid-State Switching Matrix for Solar Electric Propulsion

T. W. Macie

Technical Memorandum 33-461, December 15, 1970

To reconnect an ion thruster from one power conditioner to another, a mechanical switching matrix is presently utilized. The current study compares the mechanical solution to a solid-state solution using thyristors. The comparison of the two systems is based on a discussion and analysis of the following parameters: (1) configuration, (2) thyristor characteristics, (3) losses, (4) heat radiators, (5) total weight, and (6) reliability. Comparative conclusions are in terms of weight, size, reliability, and efficiency of the two systems. The study also includes an Appendix outlining

the tradeoffs relating to choice of thyristors as a further effort of system optimization.

M003 Power Conditioner Evaluation: Circuit Problems and Cures (SEPST III—Breadboard 1)

T. W. Macie and T. D. Masek

Supporting Research and Advanced Development,
Space Programs Summary 37-62, Vol. III, pp. 245–250,
April 30, 1970

Integration of the breadboard power conditioner BB-1, developed for the Solar Electric Propulsion System Technology (SEPST) Program, with a JPL oxide-cathode ion thruster is described. The power conditioner was tested and evaluated, circuit problems were identified, and corrective measures were taken. The 500-h uninterrupted closed-loop operation without any failures demonstrated that the cures were adequate, and sufficient confidence was gained in the performance and reliability of the circuit design to warrant its acceptance.

M004 Solar Electric Propulsion System Evaluation

E. V. Pawlik, E. N. Costogoe, J. D. Ferrera, and T. W. Macie
J. Spacecraft Rockets, Vol. 7, No. 8, pp. 968–976,
August 1970

For abstract, see Pawlik, E. V.

MANATT, S. L.

M005 The Effect of Steric Compression on Proton–Proton, Spin–Spin Coupling Constants. Further Evidence and Mechanistic Considerations

M. A. Cooper and S. L. Manatt

J. Am. Chem. Soc., Vol. 92, No. 15, pp. 4646–4652,
July 29, 1970

For abstract, see Cooper, M. A.

M006 Proton NMR Spectra of Cyclopentadiene, 1,3-Cyclohexadiene, 1,3-Cyclooctadiene, and 1,2-Dihydronaphthalene

M. A. Cooper, D. D. Elleman, C. D. Pearce, and S. L. Manatt
J. Chem. Phys., Vol. 53, No. 6, pp. 2343–2352,
September 15, 1970

For abstract, see Cooper, M. A.

MARSH, E. L.

M007 The Nonlinear Equations of Motion for a Solar-Electric Powered Spacecraft

E. L. Marsh

Supporting Research and Advanced Development,
Space Programs Summary 37-63, Vol. III, pp. 115–122,
June 30, 1970

The nonlinear equations of attitude motion are presented for a solar-electric spacecraft. Flexibility of the solar panels is accounted for in the equations. The hybrid coordinates method of Likins is used for analyzing the dynamic interaction of the flexible solar arrays. Also included are the dynamics associated with the translation of the solar-electric engine cluster.

MARSH, H. E., JR.

M008 Low-Modulus Propellant for Case-Bonded, End-Burning Motors

H. E. Marsh, Jr., and D. Udlock

Supporting Research and Advanced Development,
Space Programs Summary 37-63, Vol. III, pp. 184–188,
June 30, 1970

A low-modulus propellant for use in fully case-bonded end-burning motors has been developed and demonstrated. This development was achieved by employing a new binder formulating technique based on polymer network theory. The low modulus was obtained by adjusting the network polymer formation within the propellant binder by means of chain termination. The chain termination was accomplished by the introduction of a monofunctional binder ingredient, which effectively lowers the polymer crosslink concentration, resulting in a highly extensible propellant binder.

The properties of this binder make possible propellants with controllable physical properties over a wide range. This has allowed the design of a fully case-bonded end-burning motor with a propellant which is elastic enough to withstand the triaxial strains imposed upon it and yet is rigid enough so that it will not deform under its own weight. Preliminary tests with a flight-weight motor containing 800 lb of propellant have been successful.

MASEK, T. D.

M009 Plasma Properties and Performance of Mercury Ion Thrusters

T. D. Masek

Technical Report 32-1483, June 15, 1970

The objectives of this report are: (1) to present a description of the electron bombardment ion thruster operation and show the relationship of the plasma to this operation, (2) to show a method for computing the discharge power per beam ion from the plasma properties for comparison with the measured value, (3) to interpret the variations of discharge power per beam ion with variations in operating conditions in terms of the plasma properties, and (4) to interpret the results of recent thruster improvement studies in

terms of the effect of thruster configuration on the plasma properties.

Langmuir probe measurements in conventional 15- and 20-cm-diameter thrusters using mercury are presented. The 15-cm-diameter thruster, of 1962 vintage, was operated at high flowrates (650-mA equivalent mercury flowrate) for comparison with previous lower-flowrate data and to establish reference thruster plasma characteristics. Measurements made in an improved 20-cm-diameter thruster are used to show the effects of operating conditions on the plasma and for comparison with the reference thruster characteristics.

A modified form of the Bohm stable sheath criterion is shown to apply for computing ion fluxes. The use of this criterion, along with calculations of ion production rates and electron fluxes, permits a more accurate and comprehensive picture of discharge losses than has been obtained previously.

M010 Sizing a Solar Electric Thrust Subsystem

T. D. Masek

Technical Report 32-1504, November 15, 1970

The analysis presented in this report provides a simple method for determining the approximate mass and dimensions of a solar electric thrust subsystem. Each system element is discussed in terms of mass, and efficiency or power. Results are presented as a function of the power into the power conditioning units. The dependence of the size on a given mission is shown to be a function of thrust cutoff distance and thruster throttling capability.

M011 Power Conditioner Evaluation: Circuit Problems and Cures (SEPST III-Breadboard 1)

T. W. Macie and T. D. Masek

Supporting Research and Advanced Development,
Space Programs Summary 37-62, Vol. III, pp. 245-250,
April 30, 1970

For abstract, see Macie, T. W.

MASON, P. V.

M012 Superconducting Josephson Junctions Fabricated on Anodized Tantalum Substrates

P. V. Mason and H. B. Thacker

Supporting Research and Advanced Development,
Space Programs Summary 37-62, Vol. III, pp. 212-213,
April 30, 1970

Superconducting Josephson junctions have been successfully fabricated using wet anodization of tantalum. The fabrication technique and electrical properties of the resulting junctions are described.

MASSIER, P. F.

M013 Performance of a Supersonic Nozzle with a 75-deg Convergent Half-Angle and a Small Throat Radius of Curvature

R. F. Cuffel and P. F. Massier

Supporting Research and Advanced Development,
Space Programs Summary 37-64, Vol. III, pp. 149-152,
August 31, 1970

For abstract, see Cuffel, R. F.

M014 Effect of Wall Cooling on the Mean Structure of a Turbulent Boundary Layer in Low-Speed Gas Flow

L. H. Back, R. F. Cuffel, and P. F. Massier

Int. J. Heat Mass Transfer, Vol. 13, No. 6, pp. 1029-1047,
June 1970

For abstract, see Back, L. H.

MATHUR, F. P.

M015 Reliability Analysis and Architecture of a Hybrid-Redundant Digital System: Generalized Triple Modular Redundancy With Self-Repair

F. P. Mathur and A. Avizienis (University of California, Los Angeles)

Technical Report 32-1490 (Reprinted from *Proceedings of the American Federation of Information Processing Societies Conference, Atlantic City, New Jersey, May 5-7, 1970*, Vol. 36, pp. 375-383)

A digital computer is said to be fault-tolerant when it can carry out its programs correctly in the presence of logic faults (defined as any deviations of the logic variables in a computer from the design values). Protective redundancy in the computer system provides the means to make its operation fault-tolerant. It consists of additional programs, additional circuits, and additional time of operation that would not be necessary in a perfectly fault-free system. Many systems with hardware redundancy share the common problem of a "hard core." This "hard core" consists of logic circuits that must continue to function in real time in order to assure the proper fault detection and recovery of the entire system.

The results of a general study of the architecture and reliability analysis of a new class of digital systems that are suitable to serve as the "hard core" of fault-tolerant computers are reported here. These systems are called hybrid-redundant systems and consist of the combination of a multiplexed system with majority voting (providing instant internal fault-masking) and of standby spare units (providing an extended

mean life over the purely multiplexed system). The new quantitative results demonstrate that hybrid systems possess advantages over purely multiplexed systems in the relative improvement of reliability and mean life with respect to a nonredundant reference system.

MATTICE, J. A.

M016 Study of the Effects of Heat Sterilization and Vacuum Storage on the Ignition of Solid Propellant Rockets

L. Strand, J. A. Mattice, and J. W. Behm
Supporting Research and Advanced Development, Space Programs Summary 37-63, Vol. III, pp. 196-206, June 30, 1970

For abstract, see Strand, L.

McCLURE, J. P.

M017 GCF Wideband Digital Data System

J. P. McClure
The Deep Space Network, Space Programs Summary 37-65, Vol. II, pp. 102-103, September 30, 1970

The Ground Communications Facility (GCF) will install a 50-kbit/s wideband digital data capability between the Space Flight Operations Facility, the Mars Deep Space Station, and the JPL Compatibility Test Area. This new capability, as described in this article, will become operational in the fall of 1970 and will initially be used in support of the *Mariner* Mars 1971 missions. The wideband system will permit simultaneous transmission of two digital video streams of 16 kbits/s.

McELIECE, R. J.

M018 Combinatorial Communication: Ramsey Bounds for the Coefficients of Internal Stability of Graph Products

R. J. McEliece and H. Taylor
Supporting Research and Advanced Development, Space Programs Summary 37-62, Vol. III, pp. 62-63, April 30, 1970

The best possible upper bound for the coefficient of internal stability of product graphs that depends only on the coefficients of the factors is presented. This result, when translated into the language of coding, gives the best possible upper bound on the size of the largest zero-error probability code of block length n , say, in terms of the largest such codes for block lengths less than n .

M019 Combinatorial Communication: An Upper Bound on the Free Distance of a Tree Code

J. Layland and R. McEliece
Supporting Research and Advanced Development, Space Programs Summary 37-62, Vol. III, pp. 63-64, April 30, 1970

For abstract, see Layland, J.

M020 Combinatorial Communication: Hide and Seek, Data Storage, and Entropy

R. McEliece and E. Posner
Supporting Research and Advanced Development, Space Programs Summary 37-63, Vol. III, pp. 23-28, June 30, 1970

This article shows that the worst-case probability distribution on a compact data source typically forces a minimum average word length for storage within a given fidelity which is no better than what could be realized if no advantage were taken of the probability law whatever. This minimum turns out to be the logarithm of the reciprocal of the value of a hide and seek game played on the data source.

M021 On the Symmetry of Good Nonlinear Codes

R. J. McEliece
IEEE Trans. Information Theory, Vol. IT-16, No. 5, pp. 609-611, September 1970

It is shown that there are arbitrarily long "good" (in the sense of Gilbert) binary block codes that are preserved under very large permutation groups. This result contrasts sharply with the properties of linear codes: it is conjectured that long cyclic codes are bad and known that long affine-invariant codes are bad.

McGINNESS, H. D.

M022 New Cable Wrap-Up System for 210-ft-diam Antenna

H. D. McGinness
The Deep Space Network, Space Programs Summary 37-63, Vol. II, pp. 53-56, May 31, 1970

The installation of the structural components of the cable wrap-up system is described. A comparison between the actual configuration at full wrap-up and the predicted configuration is presented.

McINNIS, J.

M023 Multiple Mission Telemetry 1971 Configuration

W. Frey, R. Petrie, R. Greenberg, J. McInnis, and R. Wengert
The Deep Space Network, Space Programs Summary 37-63, Vol. II, pp. 63-77, May 31, 1970

For abstract, see Frey, W.

McLYMAN, W. T.

M024 Integrated Toggle Relay Driver

W. T. McLyman

Supporting Research and Advanced Development,
Space Programs Summary 37-62, Vol. III, pp. 143–145,
April 30, 1970

The use of a thick-film, integrated-circuit relay driver to replace the welded-module discrete component type used in the *Mariner* Mars 1971 spacecraft is discussed. The integrated-circuit construction reduced the volume by a factor of 10 and the weight by a factor of 7. Three integrated circuits have been built and tested with excellent results.

MELBOURNE, W. G.

M025 Brute-Force Least-Squares Estimation

W. G. Melbourne and C. B. Solloway

Supporting Research and Advanced Development,
Space Programs Summary 37-62, Vol. III, pp. 282–285,
April 30, 1970

In certain parameter estimation problems, it is common practice to fix the values of particular parameters and find the best least-squares estimate of the remaining parameters as functions of these fixed values. The process is continued by varying the fixed values until a minimum least-squares fit is obtained. One then has a joint best estimate of all the parameters.

It is shown that the brute-force least-squares method yields the same result as the simultaneous least-squares solution for all the parameters. Moreover, it is shown that the covariance matrix of the particular parameters used to generate the brute-force method is simply related to the matrix describing the quadratic form that is minimized. It is this latter result that does not seem to be widely recognized. The brute-force, least-squares method yields an optimistic value for the covariance matrix of the remaining parameters in general, but does not directly yield any information on the cross-covariance between the two sets.

M026 Planetary Ephemerides

W. G. Melbourne

Astronaut. Aeronaut., Vol. 7, No. 5, pp. 38–43,
May 1970

Recognizing that future missions would set more stringent navigational requirements, JPL undertook a serious effort, beginning in 1966, to improve the accu-

racy of the planetary ephemerides stored on tape by using optical observations, planetary radar-bounce measurements, and radio-tracking data from the planetary-encounter phase of the *Mariner* spacecraft. The accuracies of the planetary ephemerides produced since that time and those currently being produced at JPL are discussed in this article. An initial goal of the current effort is for Jovian planet ephemerides accurate to 0.1 arc sec.

MENICHELLI, V. J.

M027 Nondestructive Testing of Insensitive Electroexplosive Devices by Transient Techniques

L. A. Rosenthal (Rutgers University) and V. J. Menichelli
Technical Report 32-1494, July 15, 1970

For abstract, see Rosenthal, L. A.

M028 Nondestructive Testing of 1-W, 1-A Electro-Explosive Devices [February–March 1970]

V. J. Menichelli

Supporting Research and Advanced Development,
Space Programs Summary 37-62, Vol. III, pp. 228–233,
April 30, 1970

By pulsing an electro-explosive device with a safe-level constant current, the electrothermal behavior of the bridgewire–explosive interface can be examined. The resistance change of the bridgewire, due to heating, provides a signal that describes the heat sinking to the explosive and enclosure. Deviations from a normal trace must be treated with suspicion, and a nondestructive testing procedure is possible. Three techniques for obtaining electrothermal data of the bridgewire–explosive interface are presented.

M029 Initiation of Explosives by Laser Energy

V. J. Menichelli and L. C. Yang

Supporting Research and Advanced Development,
Space Programs Summary 37-63, Vol. III, pp. 167–169,
June 30, 1970

Primary high explosives and some metal/metal-oxide mixtures are easily initiated by pulsed laser energy in the free running mode. Secondary high explosives are not easily initiated except under very special conditions. The shock phenomenon, associated with Q-switched lasers, may be strong enough to start a detonation in the less sensitive secondary high explosives. This technique is being studied and some preliminary results are reported.

MEREDITH, B. L.

M030 Spectral Observations of Jupiter in the Frequency Interval 18.5–24.0 GHz: 1968

D. E. Jones (Brigham Young University), B. L. Meredith, and E. Arthur
Pub. Astron. Soc. Pacific, Vol. 82, No. 484, pp. 122–125, February 1970

For abstract, see Jones, D. E.

MERRILL, O. S.

M031 Multi-Hundred-Watt Radioisotope Thermoelectric Generator Transient Performance

W. D. Leonard and O. S. Merrill
Supporting Research and Advanced Development, Space Programs Summary 37-63, Vol. III, pp. 80–86, June 30, 1970

For abstract, see Leonard, W. D.

METZGER, A. E.

M032 Gamma Ray Spectroscopic Measurements of Mars

A. E. Metzger and J. R. Arnold (University of California, San Diego)
Appl. Opt., Vol. 9, No. 6, pp. 1289–1303, June 1970

A gamma ray spectrometer placed in orbit around Mars is expected to yield significant compositional data which can be related to the evolution of that planet. Components of the observable gamma ray flux come from the Martian surface, galactic and intergalactic space, and the spacecraft itself. The flux can be detected by a scintillation crystal or solid state detector, either of which combines efficiency of detection with energy resolution, and returns information to the earth as a pulse height distribution in order to detect characteristic energy line structure. The data will be evaluated for evidence of elemental differentiation with reference to terrestrial, meteoritic, solar, and lunar abundances. A lengthy mission will allow the surface of Mars to be mapped in a search for possible correlations between composition and topography or albedo.

MEYER, R.

M033 Frequency Generation and Control: The Measurement of Phase Jitter

R. Meyer and A. Sward
The Deep Space Network, Space Programs Summary 37-64, Vol. II, pp. 55–58, August 31, 1970

A phase jitter measurement system has lowered the observable noise level to 1.2 μ deg rms/root Hz

through the use of Schottky barrier diode mixers and the development of a low noise dc amplifier. Phase noise was found to be reduced by negative feedback and unrelated to noise figure. This article describes the system, its performance, and the measurements that have been made.

MILLER, A. B.

M034 Nature of the Inactivation of the Isocitrate Dehydrogenase From an Obligate Halophile

J. S. Hubbard and A. B. Miller
J. Bacteriol., Vol. 102, No. 3, pp. 677–681, June 1970

For abstract, see Hubbard, J. S.

MILLER, C. G.

M035 Design Considerations for Accelerated Radiation Tests

C. G. Miller and R. H. Parker
Supporting Research and Advanced Development, Space Programs Summary 37-62, Vol. III, pp. 223–227, April 30, 1970

Accelerated tests of cumulative radiation damage to components of spacecraft planned for outer-planet missions are considered. The amount of acceleration that can be used is limited by three factors: (1) unrealistic component heating by the accelerated rate, (2) safety considerations from extremely strong radiation sources, and (3) non-uniformity of field when sources are brought too close to the test object. Practical and desirable limits to the three effects are given.

M036 Application of Imposed Magnetic Fields to Compact-Arc Lamps

C. G. Miller and R. E. Bartera
Supporting Research and Advanced Development, Space Programs Summary 37-63, Vol. III, pp. 161–166, June 30, 1970

Sealed xenon compact-arc lamps are used as light sources for JPL solar simulators. The factors influencing arc lamp brightness and operation are given. To improve performance, some of these factors may be influenced by using magnetic fields imposed on the arc during operation. The use of imposed magnetic fields have resulted in improved lamp performance through: (1) increased anode heat-carrying capacity, (2) increased cathode current density during operation, (3) increased power delivered into the imaged area of the arc, and (4) increased stability of banks of lamps in operation.

M037 Solar Simulators at the Jet Propulsion Laboratory

R. E. Bartera, H. N. Riise, and C. G. Miller
Appl. Opt., Vol. 9, No. 5, pp. 1068–1074, May 1970

For abstract, see Bartera, R. E.

M038 Interactions Between Radiation Fields From Radioisotope Thermoelectric Generators and Scientific Experiments on Spacecraft

C. G. Miller and V. C. Truscillo
Nucl. Appl. Technol., Vol. 9, No. 5, pp. 722–735,
November 1970

A study was made to determine the extent of the interference that may be expected in the operation of spacecraft science instruments when the spacecraft carries a radioisotope thermoelectric generator.

Suitable analytical models were developed to predict the effects of the radiation spectrum on the various selected components. The gamma radiation was expressed as a 20-group structure between the energies of 40 keV and 10 MeV; the detectors selected for detailed evaluation were Geiger–Mueller tubes, continuous-channel electron multipliers, and silicon surface barrier detectors.

The conclusions were that with reasonable separation between the radioisotope thermoelectric generator and the sensitive science components (~15-ft) individual detectors would require a pound or less of shielding material in order that an acceptable spurious counting rate would be achieved. For a typical spacecraft payload, including such experiments as the cosmic-ray telescope, trapped radiation detector, and a low-energy proton and electron differential energy analyzer, <10 lb of shielding would be required. Recommendations for developmental methods that could lead to means to reduce this amount of shielding were also made.

MILLER, R. B.

M039 DSN Tracking System Operations

J. Heller and R. B. Miller
The Deep Space Network, Space Programs Summary 37-65,
Vol. II, pp. 122–125, September 30, 1970

For abstract, see Heller, J.

MOACANIN, J.

M040 A Generalization of the Boltzmann Superposition Principle

J. Moacanin, J. J. Aklonis, and R. F. Landel
Supporting Research and Advanced Development,
Space Programs Summary 37-63, Vol. III, pp. 207–209,
June 30, 1970

In previous work a mathematical representation was developed for the stress relaxation or creep behavior of an elastomer undergoing scission reactions. These results have been extended so that arbitrary time-dependent deformations could be treated. A convolution integral was derived. In absence of chemical reaction, this integral reduces to the classical statement of the Boltzmann superposition principle.

M041 Investigation of Sterilizable Battery Separator Membranes [June–July 1970]

E. F. Cuddihy, D. E. Walmsley, and J. Moacanin
Supporting Research and Advanced Development,
Space Programs Summary 37-64, Vol. III, pp. 136–138,
August 31, 1970

For abstract, see Cuddihy, E. F.

MOFFET, A. T.

M042 High-Resolution Observations of Compact Radio Sources at 13 Centimeters

K. I. Kellermann (National Radio Astronomy Observatory),
B. G. Clark (National Radio Astronomy Observatory),
D. L. Jauncey (Cornell University), M. H. Cohen (California
Institute of Technology), D. B. Shaffer (California Institute
of Technology), A. T. Moffet (California Institute of
Technology), and S. Gulkis
Astrophys. J., Vol. 161, No. 3, pp. 803–809,
September 1970

For abstract, see Kellermann, K. I.

MOLINDER, J.

M043 Coding and Synchronization Research: Optimization of Acquisition Time for Sequential Ranging System

S. Butman and J. Molinder
Supporting Research and Advanced Development,
Space Programs Summary 37-62, Vol. III, pp. 60–62,
April 30, 1970

For abstract, see Butman, S.

M044 Digital Telemetry and Command: Mean-Square Error and Bias of Phase Estimator for the JPL Sequential Ranging System

J. Molinder
The Deep Space Network, Space Programs Summary 37-64,
Vol. II, pp. 27–28, August 31, 1970

The JPL sequential ranging system uses the first and third harmonics of the high-frequency squarewave to

estimate the phase of the incoming signal. This estimate is then used as a reference for the remaining lower frequency components. In this article, plots of the conditional mean-square error and the bias in the estimate are given. A plot of the bias under no-noise conditions is included.

MONDT, J. F.

M045 A 70-kWe Thermionic Reactor Electric Propulsion Spacecraft

J. F. Mondt

Supporting Research and Advanced Development, Space Programs Summary 37-62, Vol. III, pp. 250-255, April 30, 1970

This article discusses the integration of an externally fueled reactor power subsystem into an electric propulsion spacecraft with a large length-to-diameter ratio. A *Titan/Centaur* launch vehicle would be used for launching the 12,000-lb spacecraft to earth escape velocity. The electric propulsion system would boost the spacecraft to the outer planets. The initial spacecraft mass consists of 2075 lb of net spacecraft, 3760 lb of mercury propellant, and a 4990-lb electric propulsion system.

MOORE, J. W.

M046 Navigational Approaches to Planetary Orbiters and Rovers

J. W. Moore, W. J. O'Neil, and G. D. Pace

Astronaut. Aeronaut., Vol. 7, No. 5, pp. 56-64, May 1970

Placing a spacecraft in orbit about a planet represents the next logical step in exploring the inner solar system. An orbiter will bring even smaller closest approach distances, high-resolution mapping over the greater portion of the planet's surface, and long-term measurements of specific areas to detect temporal changes. For example, the two *Mariner* Mars 1971 missions, planned for a closest approach of about 1500 km, are designed to record and transmit detailed pictures of 70% of the Martian surface and repeatedly view selected areas over a period of three months—with a total information return of 70×10^9 bits. More intimate planetary inspection will necessitate a landing capsule. This article concerns the navigation aspects of both orbiter and lander missions: orbit insertion and subsequent trim corrections, capsule descent, and extended post-landing capsule navigation.

MORAN, T. F.

M047 Temperature Control Materials Technology

J. R. Crosby and T. F. Moran

Supporting Research and Advanced Development, Space Programs Summary 37-62, Vol. III, pp. 179-180, April 30, 1970

For abstract, see Crosby, J. R.

MORRIS, G.

M048 Digital Acquisition and Detection: Digital Frequency Doubler

G. Morris

The Deep Space Network, Space Programs Summary 37-65, Vol. II, pp. 40-42, September 30, 1970

A digital frequency doubler is described which uses only three integrated circuits and six discrete components. This frequency doubler, a broad-band device, can perform with input frequencies up to 10 MHz. At all frequencies, the output pulses have constant width. Waveshaping is provided to convert the input sine wave into fast rise-time pulses to drive digital circuits.

MORSE, G.

M049 Holography Application Study to Pressure Vessel Flaw Detection

G. Morse, A. Knoell, and R. Badin

Supporting Research and Advanced Development, Space Programs Summary 37-64, Vol. III, pp. 100-101, August 31, 1970

Preliminary efforts to use optical holography for flaw detection in pressure vessels pointed up the need for an analytic study to parametrically evaluate types of vessels for which this method is useful. This study is currently underway. The effect of vessel material constants on fringe density for thin- and thick-walled cylinders and spheres is being evaluated, and results will be tested experimentally.

MOSESMAN, M.

M050 On the Reaction of O^+ With CO_2

M. Mosesman and W. T. Huntress, Jr.

J. Chem. Phys., Vol. 53, No. 1, pp. 462-463, July 1, 1970

The reaction of O^+ with CO_2 to form the O_2^+ ion has been studied by a number of workers. A recent investigation by Schilderout and Franklin suggested that an additional channel is available in the reaction at O^+ kinetic energies sufficient to overcome the endothermicity of the charge transfer reaction:





This conclusion followed from the observation that the O_2^+ production rate constant was appreciably less than the O^+ loss rate constant for kinetically excited O^+ ions. Schilderout and Franklin proposed Reaction (2) to explain their observations but were unable to measure any increase in CO_2^+ ions from (2) since the CO_2^+ ion is the major primary ion in the spectrum. Reported here is the concurrent detection of both Reactions (1) and (2) using a unique combination of ion cyclotron resonance pulse ejection and double resonance techniques.

MUDGWAY, D. J.

M051 DSN Support for Viking [March–April 1970]

D. J. Mudgway

The Deep Space Network, Space Programs Summary 37-63, Vol. II, p. 14, May 31, 1970

The Deep Space Network (DSN) Interface Design Handbook has been released and is intended for use by all flight projects as a standard source of advanced technical information describing the DSN interfaces with the projects in telecommunications, data processing, and simulation. Telecommunications interfaces are considered in the context of a full 210-ft subnet, together with the existing but enhanced 85-ft subnet. Data processing interfaces are considered in terms of the Mark III Space Flight Operations Facility systems, subsystems, and assemblies; the simulation section introduces the concept of tracking, telemetry, and command mathematical software models.

MUELLER, P. A.

M052 Control Analysis of an Ion Thruster With Programed Thrust

P. A. Mueller and E. V. Pawlik

J. Spacecraft Rockets, Vol. 7, No 7, pp. 837–842, July 1970

Results of an analysis and a digital computer simulation of various control loops for ion thruster control are presented. The concept considered for controlling the thrust of an ion thruster over a 2-to-1 range in output power is to vary the propellant flowrate as both the specific impulse and propellant utilization are maintained at constant values. Thrusters employing oxide cathodes and utilizing mercury as propellant are analyzed extensively with a detailed digital computer simulation. It is necessary to use nonoptimum efficiency thruster to obtain a stable system when a propellant flow rate meter is not used. The use of a propellant flow rate meter makes higher thruster efficiencies usable in a stable configuration.

MULHALL, B. D.

M053 Charged-Particle Calibration System Analysis

B. D. Mulhall

The Deep Space Network, Space Programs Summary 37-64, Vol. II, pp. 13–21, August 31, 1970

The major competing schemes considered for tracking system analytic calibration activities in the charged particle media are described and evaluated on the basis of operational considerations and measurement resolution. The various charged-particle calibration techniques may be grouped into two types: (1) those requiring a specific hardware implementation on the spacecraft (e.g., dual-frequency, differential-phase, DRVID, and S-band faraday rotation measurements), and (2) those independent of any spacecraft hardware (e.g., VHF faraday rotation, back-scattering, and ionosonde measurements).

M054 The Ionospheric Electron Content as Determined From Faraday Rotation Measurements of an Earth Satellite and Deep-Space Probe

B. D. Mulhall and C. T. Stelzried

The Deep Space Network, Space Programs Summary 37-64, Vol. II, pp. 21–24, August 31, 1970

Faraday rotation measurements were made at the Venus Deep Space Station by a polarimeter monitoring the *Pioneer VII* deep-space probe, transmitting at 2.3 GHz. At the same time, during the fall of 1968, faraday rotation measurements were made at Stanford University, observing the *Applications Technology Satellite 1 (ATS-1)* geostationary satellite beacon at 137 MHz. Both measurements were converted to columnar electron content. The *ATS-1* electron content measurements, made at a constant elevation and azimuth, were adjusted or mapped to the *Pioneer* ray path that passed through the earth's ionosphere at varying elevation and azimuth by correcting for differences in local time, path length through the ionosphere, and geomagnetic latitude. In this article, the two measurements are compared, and the differences between them are discussed.

M055 Evaluation of the Ionospheric Model

B. D. Mulhall

The Deep Space Network, Space Programs Summary 37-64, Vol. II, pp. 25–27, August 31, 1970

The ionospheric model used to predict the diurnal behavior of the earth's ionosphere for the purpose of computing its effect on navigation was evaluated by the following procedure. The model was fitted to the ionospheric data from 1967, 1968, and 1969, and the average values of the resulting model parameters were computed. These average values were used in a

composite model, which was then employed on the *Mariner V* 1967 mission. The resulting navigational errors—the error caused by the total ionospheric effect versus the effect remaining after the model was employed—are compared to indicate the effectiveness of the model. The results of this evaluation indicate that the present model improves the navigational accuracy in declination and is not effective in correcting errors in right ascension.

M056 The Effect of the Diurnal Variation of the Earth's Ionosphere on Interplanetary Navigation

B. D. Mulhall and K. L. Thuleen

The Deep Space Network, Space Programs Summary 37-65, Vol. II, pp. 35–39, September 30, 1970

Described in this article is a parametric study to determine the effects of the diurnal variation of the charged particles in the earth's ionosphere on interplanetary spacecraft navigation. Model ionospheres representing diurnal variations for different seasons and solar cycle phases were used to estimate the ionospheric effect. The seasonal and solar cycle variations in the model parameters were determined by fitting the model to actual ionospheric measurements. The sun–earth–probe angle was varied to represent various mission geometries.

MULHOLLAND, J. D.

M057 Quantitative Confirmation of Planetary Defects in the Lunar Theory by Spectral Decomposition

J. D. Mulholland, K. Garthwaite, and D. B. Holdridge

Supporting Research and Advanced Development, Space Programs Summary 37-64, Vol. III, p. 169, August 31, 1970

Spectral analysis has been performed on the residuals of a numerical integration of lunar motion compared with a source theory over a 50-yr interval. All of the significant local maxima in the spectral power density correspond closely with planetary perturbation periods, providing quantitative confirmation of the qualitative and somewhat conjectural identification of such features reported earlier.

MULLEN, P. G.

M058 High-Speed Data, SFOF Outbound Communication

P. G. Mullen

The Deep Space Network, Space Programs Summary 37-65, Vol. II, p. 101, September 30, 1970

A new capability being developed to transmit high-speed data from the Space Flight Operations Facility

(SFOF) computers to distant sites via the Ground Communications Facility is described in this article. This effort has necessitated JPL in-house development of a high-speed-data converter and certain interface switching between the 360/75 computers and the block multiplexer in the Ground Communications Facility.

MULLER, P. M.

M059 Desert Stream Channels Resembling Lunar Sinuous Rilles

J. D. Burke, R. G. Brereton, and P. M. Muller

Nature, Vol. 225, No. 5239, pp. 1234–1236, March 28, 1970

For abstract, see Burke, J. D.

M060 Lunar Gravimetrics

P. M. Muller and W. L. Sjogren

Space Research X, pp. 975–983, North-Holland Publishing Co., Amsterdam, 1970

Reduction of *Lunar Orbiter* radio tracking data has made possible the construction of a high-resolution gravimetric map of the lunar earthside hemisphere between longitudes ± 100 deg and latitudes ± 60 deg. The gravitational variations have been determined to a precision of 10 mgal, and a resolution of 100 km (equivalent to a 50th-order spherical harmonic expansion). This new analysis has utilized all of the suitable *Lunar Orbiter* data (226 orbits, 20,000 doppler observations), has resulted in extraction of nearly all the gravimetric information possible with the method (the doppler fit is down to the 0.3 mm-sec⁻¹ noise level), and has demonstrated consistency through agreement between the polar and equatorial *Lunar Orbiters*.

The study has revealed large (50–250 mgal) mass concentrations (“mascons”) centered in each of the ringed seas (Imbrium, Serenitatis, Crisium, Nectaris, Humorum, Aestuum, and Orientale). This 1:1 correspondence between mascons and ringed seas suggests a definite relationship between the two phenomena. Therefore, an analysis of the current implications of the new observations is presented here. For example, the hypothesis that huge lava flows are responsible for the lunar mare material must explain the presence of large gravitational highs in the depressed basins, a fact which may be breathing more life into the theory that the mare material consists of sedimentary deposits left by lunar seas now vanished. The debate stimulated by the preliminary work has led to this more complete analysis and to the presentation of the results in their most basic form (observed accelerations along the earth–probe vector) for the direct utilization of the scientific community at large.

NASH, D. B.

N001 Spectral Reflectance and Albedo of Apollo 11 Lunar Samples: Effects of Irradiation and Vitrification and Comparison With Telescopic Observations

J. E. Conel and D. B. Nash

Proceedings of the Apollo 11 Lunar Science Conference, Houston, Texas, January 5-8, 1970, Vol. 3, pp. 2013-2023

For abstract, see Conel, J. E.

N002 Luminescence Properties of Apollo 11 Lunar Samples and Implications for Solar-Excited Lunar Luminescence

D. B. Nash and R. T. Greer

Proceedings of the Apollo 11 Lunar Science Conference, Houston, Texas, January 5-8, 1970, Vol. 3, pp. 2341-2350

Luminescence measurements of Tranquillity samples indicate that energy efficiencies for laboratory excitation by protons and ultraviolet radiation are in the range 10^{-6} or below; natural and induced thermoluminescence is even weaker. If these samples are typical, lunar surface luminescence cannot occur at reported levels. Comparison of proton luminescence spectra from the exterior and interior of rocks and fine fragments provides evidence of solar wind impingement on the moon's surface.

NELSON, D.

N003 DSS 51 Antenna Mechanical Subsystem Upgrade

J. Carpenter, V. Lobb, A. Nicula, and D. Nelson

The Deep Space Network, Space Programs Summary 37-64, Vol. II, pp. 98-104, August 31, 1970

For abstract, see Carpenter, J.

NERHEIM, N. M.

N004 Experimental Measurements of Some ArII Transition Probabilities and a Comparison of Published Values

N. M. Nerheim and H. N. Olsen (Plasma Sciences Laboratories)

J. Quant. Spectrosc. Radiat. Transfer, Vol. 10, No. 7, pp. 755-773, July 1970

Transition probabilities of a number of ArII lines have been determined experimentally from observing a 1.1 atm free-burning arc. Techniques used in previous work were modified to allow observation of lines in the UV spectral region. Previous work was extended to include lines with both $4p$ and $4d$ upper energy levels that cover a range of 5.6 eV and the results compared with both theoretical and available experimental values. In addition, the ArII transition probabilities found in the literature are compared by

estimating the temperature differences that may be attributed solely to the differences in the transition probabilities.

NEUGEBAUER, M.

N005 OGO 5 Observations of Quasi-Trapped Electromagnetic Waves in the Solar Wind

F. L. Scarf (Space Sciences Laboratory), R. W. Fredricks

(Space Sciences Laboratory), I. M. Green (Space Sciences Laboratory), and M. Neugebauer

J. Geophys. Res., Space Phys., Vol. 75, No. 19, pp. 3735-3750, July 1, 1970

For abstract, see Scarf, F. L.

NG, E. W.

N006 Some Mathematical and Computational Properties for the Incomplete Gamma Functions

E. W. Ng

Supporting Research and Advanced Development, Space Programs Summary 37-64, Vol. III, pp. 10-12, August 31, 1970

The mathematical properties of the incomplete gamma functions that are most pertinent to the computation of these functions are discussed. Various trade-offs are mentioned for the implementation of a general-purpose algorithm.

N007 Chebyshev Polynomial Expansions of Emden Functions

C. J. Devine and E. W. Ng

Supporting Research and Advanced Development, Space Programs Summary 37-64, Vol. III, pp. 13-16, August 31, 1970

For abstract, see Devine, C. J.

N008 Certification of Algorithm 385 [S13] Exponential Integral $Ei(x)$ (Kathleen A. Paciorek, *Comm. ACM* 13 (July 1970) 444-445)

E. W. Ng

Comm. ACM (Association for Computing Machinery), Vol. 13, No. 7, p. 449, July 1970

This algorithm computes, for $x \geq 0$,

$$Ei(x) = \int_{-\infty}^x \frac{e^t}{t} dt$$
$$-E_1(x) = Ei(-x)$$

The algorithm was compiled and executed without any modification on a UNIVAC-1108 computer. It was tested against a reference subprogram QE1E1, which computes $Ei(x)$ in extended precision using a

package of subroutines in 70-bit (about 21 decimal) arithmetic. The subprogram QE1EI, written by the author, computes $Ei(x)$ from truncated Chebyshev series for negative x and from Taylor and asymptotic expansions for positive x .

For the seven intervals of x as indicated in this algorithm, tests were made of the algorithm against QE1EI, which was considered as producing the "correct" function values. Each interval was partitioned into 1000 subintervals of equal length, and, in each subinterval, one test value of x was selected using a uniform pseudorandom number generator. The results of the tests are described in this article.

NICULA, A.

N009 DSS 51 Antenna Mechanical Subsystem Upgrade

J. Carpenter, V. Lobb, A. Nicula, and D. Nelson
The Deep Space Network, Space Programs Summary 37-64,
 Vol. II, pp. 98-104, August 31, 1970

For abstract, see Carpenter, J.

NISHIKAWA, K.

N010 Numerical Study of Collisional Effects on Spatial Ion-Wave Echoes

K. Nishikawa and R. W. Gould (California Institute of Technology)
Phys. Fluids, Vol. 13, No. 7, pp. 1883-1885, July 1970

Collisional effects on the second-order spatial ion-wave echo are studied numerically. General agreement is obtained with the experimental results of Ikezi, Takahashi, and Nishikawa. A critical argument is raised against the validity of the small collision approximation.

N011 Second-Order Perturbed Distribution Associated With the Plasma Wave Echo

K. Nishikawa
Phys. Fluids, Vol. 13, No. 9, pp. 2420-2422, September 1970

As discussed herein, the perturbed distribution which contributes a plasma wave echo shows an oscillatory behavior with different phases and amplitudes before and after the echo. The difference in amplitude is found to be negligibly small, except for very special cases.

NISHIMURA, T.

N012 A Dynamic Programming Approach to Optimal Stochastic Orbital Transfer Strategy

T. Nishimura and C. G. Pfeiffer (TRW Systems)
J. Spacecraft Rockets, Vol. 7, No. 4, pp. 398-404, April 1970

The optimal stochastic orbit transfer strategy is defined as the sequence of guidance corrections that will minimize a statistical measure of final error, subject to the constraint that the total correction capability expended be less than a specified number. The dynamic programming algorithm is employed to solve this problem. The numerical difficulty of storing the many values of the optimized performance index corresponding to every discrete value of the state variables is overcome by representing the performance surface only in the neighborhood of local minima. The computer program designed to solve this problem is described, and some numerical results applicable to a space mission of a Mars orbiter are presented.

NORMAN, R. A.

N013 Correction Factors for Near Field Horn Antenna Gain Measurements

R. A. Norman
The Deep Space Network, Space Programs Summary 37-63,
 Vol. II, pp. 34-35, May 31, 1970

Spherical wave function theory is used in the calculation of the near field gain variation of a dual-mode conical horn. The near field gain values are calculated for the two-horn insertion loss gain measurement technique.

NORTON, D. J.

N014 Heat-Sterilizable Capsule Spin Motors

D. J. Norton
 Technical Report 32-1469 (Reprinted from *J. Spacecraft Rockets*, Vol. 7, No. 1, pp. 81-84, January 1970)

This article reports an investigation of the use of heat-sterilized solid-propellant motors for the spin stabilization of planetary landing capsules. Since there were no existing motors of the proper size that could be heat-sterilized, a spin motor whose grain weight and geometry could be accurately controlled was designed. The hardware employed was used originally as a despin motor for a Jupiter missile re-entry nose cone program. The grain was an internal- and external-burning, cartridge-loaded cylinder. This design permitted accurate machining, rapid burning of the required mass of propellant, and a relatively neutral pressure-time history. The propellant utilized, an Aerojet formulation, was shown to be a high-modulus, heat-sterilizable formulation useful in accurate machining of highly reproducible charges.

The capsule deflection maneuver is accomplished by a sequence of events, all of which influence the total pointing error. The first step occurs as the spacecraft and capsule are separated. Ideally, the spin-up of the

capsule should take place immediately to prevent a buildup of error caused by the tip-off rate resulting from nonuniformities in the spring constants and the unlatching sequence. However, there must be some separation distance between the capsule and the spacecraft before the spin motors are ignited to prevent unwanted forces and heating rates on the spacecraft due to plume impingement. Only those errors associated with these separation and spin-up phases were considered in this investigation.

The sterilized spin-motor firings indicate that the differences in total impulse and average pressure can be maintained at or below the 1% level. To minimize the spin-up pointing error for given spin motors, the distance between the plane of the spin motor and the center of gravity, as well as the initial tip-off rate, should be kept to a minimum. Significant increases in pointing error result from unequal motor temperatures, even if total impulses are the same. For the geometry under consideration, increasing nozzle expansion ratio and spin motor canting angle do not significantly reduce the plume impingement effects.

OLSEN, H. N.

O001 Experimental Measurements of Some ArII Transition Probabilities and a Comparison of Published Values

N. M. Nerheim and H. N. Olsen (Plasma Sciences Laboratories)

J. Quant. Spectrosc. Radiat. Transfer, Vol. 10, No. 7, pp. 755-773, July 1970

For abstract, see Nerheim, N. M.

O'MALLEY, R. M.

O002 Analysis of Ion-Molecule Reactions in Allene and Propyne by Ion Cyclotron Resonance

M. T. Bowers (University of California, Santa Barbara), D. D. Elleman, R. M. O'Malley (The University, Sheffield, England), and K. R. Jennings (The University, Sheffield, England)

J. Phys. Chem., Vol. 74, No. 13, pp. 2583-2589, 1970

For abstract, see Bowers, M. T.

ONDRASIK, V. J.

O003 A Solution for the Tropospheric Zenith Range Correction Using a Single Pass of Differenced Doppler Data

V. J. Ondrasik

The Deep Space Network, Space Programs Summary 37-63, Vol. II, pp. 16-22, May 31, 1970

The ability to solve for the tropospheric zenith range correction is analyzed using a single pass of differenced doppler data and a very simple tropospheric model. To improve upon the accuracy obtainable from surface weather measurements requires use of data below an elevation angle of 10 deg. However, the problems associated with using such low elevation angle data probably preclude the determination of zenith tropospheric corrections from differenced doppler data.

O004 The Effects of a Variable h_{\max} on the Mapping of Zenith Ionospheric Corrections to Lower Elevation Angles

V. J. Ondrasik

The Deep Space Network, Space Programs Summary 37-63, Vol. II, pp. 21-24, May 31, 1970

Ionospheric corrections computed using elevation angle mappings based firstly on a Chapman model with constant parameters and secondly on a Chapman model with a variable h_{\max} (height of maximum electron density) are compared. For the example considered, the corrections may differ by as much as 0.5 m in range and 1.4×10^{-3} Hz in doppler.

O005 Variations in the Zenith Tropospheric Range Effect Computed From Radiosonde Balloon Data

V. J. Ondrasik and K. L. Thuleen

The Deep Space Network, Space Programs Summary 37-65, Vol. II, pp. 25-35, September 30, 1970

For many years, it has been recognized that the passage of a tracking signal through the troposphere will significantly corrupt the data used in determining the orbit of a distant spacecraft. At the present time, a tropospheric refractivity model, which is independent of time, is being used in attempts to reduce the tropospheric errors. In this article, some idea of the temporal behavior of errors in radio tracking data due to the troposphere is obtained by calculating the tropospheric zenith range effect from measured refractivity profiles collected during 1967. In addition, a cursory examination of the surface weather measurements is undertaken to see if it may be worthwhile to try to predict the variations of zenith range effect from such measurements.

O'NEIL, W. J.

O006 Navigational Approaches to Planetary Orbiters and Rovers

J. W. Moore, W. J. O'Neil, and G. D. Pace

Astronaut. Aeronaut., Vol. 7, No. 5, pp. 56-64, May 1970

For abstract, see Moore, J. W.

ORLIK, F. W.

O007 Environmental Testing of the Surveyor Spacecraft at the JPL Environmental Test Laboratory

F. W. Orlik

Recent Advances in Engineering Science: Volume 5, pp. 359–383, Gordon & Breach, Science Publishers, Inc., New York, 1970

The *Surveyor* spacecraft environmental testing program was conducted at the JPL Environmental Test Laboratory (ETL). Most of the testing was done at JPL on-site facilities, but facilities at Edwards Air Force Base and Cape Kennedy were also used. During *Surveyor* activities in the years 1965 through 1967, 19% of all testing in the ETL was directed to the *Surveyor* project and a total of 39 *Surveyor* components and assemblies were tested. This paper describes the ETL facilities used in the program and the test innovations designed to meet the temperature extremes required in *Surveyor* environmental testing. The concluding section of the paper presents some of the outstanding lunar photographs sent back by *Surveyor*.

OTOSHI, T. Y.

O008 Improved RF Calibration Techniques: A Precision Compact Rotary Vane Attenuator

T. Y. Otoshi

The Deep Space Network, Space Programs Summary 37-63, Vol. II, pp. 29–33, May 31, 1970

The results of radio frequency calibrations on a compact H-band rotary vane attenuator are presented. The calibrations consist of (1) 8448-MHz reflection coefficient measurements on the individual component parts of the compact attenuator, and (2) phase and attenuation characteristics of the overall attenuator over the frequency range of 8.0 to 10.0 GHz. Comparison of measured and theoretical values indicate that the compact attenuator theory is valid over a broad band of frequencies.

Sources of error causing deviation from theory have been analyzed. The results are presented in graphic form. It is concluded that when transitions having voltage standing-wave ratios of 1.02 or less are installed on the compact attenuator assembly, the attenuator will obey the modified law within the total probable error limits.

O009 Tracking and Data Acquisition Elements Research: Improved RF Calibration Techniques—Precision Compact Rotary Vane Attenuator

T. Y. Otoshi

The Deep Space Network, Space Programs Summary 37-64, Vol. II, pp. 67–69, August 31, 1970

In previous studies of rotary vane attenuators, the effects of phase shift versus frequency have not been investigated thoroughly. This article presents some experimental data which indicate that the differential phase shift properties are strongly dependent upon the resistive film material on the center vane. It is also shown that, for the limiting case where the resistive material is removed from the center vane, the rotary vane attenuator performs as an accurate low-loss phase shifter or as a very accurate rotary vane attenuator with a total dynamic range of a few hundredths of one decibel.

O010 Improved Calibration Techniques: Realizability Conditions on Reflection Coefficients of Unsymmetrical, Passive, Reciprocal 2-Port Networks

T. Y. Otoshi

The Deep Space Network, Space Programs Summary 37-65, Vol. II, pp. 64–65, September 30, 1970

In the microwave calibrations of a reciprocal 2-port network where the waveguide types on each port are different, it is often difficult or inconvenient to measure the reflection coefficient at each of the ports. This article discusses simple limit formulas that can be used to obtain estimates of the reflection coefficient for the second port when the only known quantities are the reflection coefficient for the first port and the dissipative loss of the 2-port network. It is required that the 2-port network be reciprocal, but no restriction is placed on the lossiness of the network.

O011 Comparisons of Waveguide Losses Calibrated by the DC Potentiometer, AC Ratio Transformer, and Reflectometer Techniques

T. Y. Otoshi, C. T. Stelzried, B. C. Yates (National Bureau of Standards), and R. W. Beatty (National Bureau of Standards) *IEEE Trans. Microwave Theory and Techniques*, Vol. MTT-18, No. 7, pp. 406–409, July 1970

Comparisons are made of the losses of two precision waveguide sections that were calibrated by three independent attenuation measurement methods. The loss measurement systems involved were: (1) the dual-channel system which uses thermistors and a dc potentiometer test set, (2) the dual-channel system which uses barretters and an ac ratio transformer test set, and (3) the National Bureau of Standards reflectometer system which utilizes a quarter-wave short circuit and an IF attenuation standard. Loss values of about 0.05 dB, as calibrated by the three independent methods, typically agreed to within 0.0006 dB. It is believed that the results of these calibrations are representative of the best that can be achieved with current state-of-the-art techniques and available instrumentation for low-loss waveguide measurements.

OZIER, I.

O012 Construction of Tetrahedral Harmonics

K. Fox and I. Ozier (North American Rockwell Corporation)
J. Chem. Phys., Vol. 52, No. 10, pp. 5044–5056,
May 15, 1970

For abstract, see Fox, K.

PACE, G. D.

P001 Navigational Approaches to Planetary Orbiters and Rovers

J. W. Moore, W. J. O'Neil, and G. D. Pace
Astronaut. Aeronaut., Vol. 7, No. 5, pp. 56–64,
May 1970

For abstract, see Moore, J. W.

PAPAZOGLU, T.

P002 Preliminary Nuclear Criticality Studies for a Thermionic Reactor With Uninsulated Externally Fueled Diodes

T. Papazoglou, H. Gronroos, and J. P. Davis
Supporting Research and Advanced Development,
Space Programs Summary 37-62, Vol. III, pp. 256–259,
April 30, 1970

The results of initial nuclear criticality calculations for the JPL externally fueled, uninsulated diode, thermionic reactor design are summarized. The purpose of these analyses was to determine core dimensions, reflector thicknesses, and available reflector control drum worths with sufficient accuracy to support spacecraft design studies. The two-dimensional neutron transport code DOT was used to obtain the data presented. An updated Hansen–Roach 16-group set formed the basic cross-section structure. The results indicate that it is possible to obtain a sufficient control margin with reflector control drums that contain a poison segment. The thermal power distributions show that a small degree of fuel zoning is necessary to obtain a nearly uniform profile.

PARKER, R. H.

P003 Design Considerations for Accelerated Radiation Tests

C. G. Miller and R. H. Parker
Supporting Research and Advanced Development,
Space Programs Summary 37-62, Vol. III, pp. 223–227,
April 30, 1970

For abstract, see Miller, C. G.

PATTERSON, R. E.

P004 Battery Storage Optimization and Design Studies

R. S. Bogner and R. E. Patterson
Technical Memorandum 33-462, December 15, 1970

For abstract, see Bogner, R. S.

P005 Development of a Long-Life, High Cycle Life, 30-A-h, Sealed AgO–Zn Battery

R. E. Patterson and R. S. Bogner
Supporting Research and Advanced Development,
Space Programs Summary 37-62, Vol. III, pp. 138–142,
April 30, 1970

A two-phase development program is under way to demonstrate the capability with sealed AgO–Zn cells for a 6-mo, wet-charged stand during interplanetary travel plus an orbiting life of at least 100 24-h cycles at 50% depth of discharge based on 30-A-h rated capacity. Following 4 mo of charged stand (open-circuit voltages between 1.85 and 1.86 V), 60 50%-depth-of-discharge cycles have been completed on five of the seven Phase I designs. Positive wrapped design 1L EM 470, 4L FSC at 80-oz/in.² pack pressure had the least capacity decay through 50 cycles. Phase II cells (six different designs) have completed two initial cycles and 4 mo of a 6-mo charged stand.

PAWLIK, E. V.

P006 Solar Electric Propulsion System Tests

E. V. Pawlik, E. N. Costogoue, J. D. Ferrera, and T. W. Macie
Technical Report 32-1480, August 15, 1970

The design and experimental evaluation of a solar electric primary propulsion system is described. The system consists of two electron-bombardment ion thrusters complete with the associated thrust vector aligning actuators, a switching network, controller, and a flight-type power conditioner. The system was operated over a 2:1 range in output power. System integration problems such as matching of thruster performance and response to arcing within the thruster and solutions to these problems are described. Short endurance tests of the system were undertaken. Noise within the system was the major lifetime-limiting factor for both the power conditioner and controller.

P007 Ion Thruster Control-Loop Sensitivity

E. V. Pawlik
Supporting Research and Advanced Development,
Space Programs Summary 37-63, Vol. III, pp. 223–226,
June 30, 1970

Electrical parameters of a 20-cm diameter electron-bombardment ion thruster were varied from the nominal set points as the thruster output power and mercury propellant flowrate were regulated by control loops. The effect of variations in the fixed parameters on the indirectly controlled propellant flowrate was determined. It was found that about $\pm 1\%$ regulation was required for the arc chamber current and voltage. A regulation of $\pm 10\%$ was found sufficient for all other parameters.

P008 Ion Thruster Hollow Cathode Studies

E. V. Pawlik and D. J. Fitzgerald
Supporting Research and Advanced Development,
 Space Programs Summary 37-64, Vol. III, pp. 146-149,
 August 31, 1970

An experimental investigation was undertaken to examine the effects of changing hollow cathode geometry on the operation of a 20-cm-diameter ion thruster. Three cathode orifice sizes were investigated as cathode temperature and ion thruster arc chamber losses were measured. Increasing orifice sizes were found to reduce both cathode temperature and arc chamber losses.

P009 Control Analysis of an Ion Thruster With Programed Thrust

P. A. Mueller and E. V. Pawlik
J. Spacecraft Rockets, Vol. 7, No. 7, pp. 837-842,
 July 1970

For abstract, see Mueller, P. A.

P010 Solar Electric Propulsion System Evaluation

E. V. Pawlik, E. N. Costogoe, J. D. Ferrera, and T. W. Macie
J. Spacecraft Rockets, Vol. 7, No. 8, pp. 968-976,
 August 1970

The design and experimental evaluation of a solar-electric primary propulsion system is described. The system consists of two electron-bombardment ion thrusters complete with the associated thrust-vector aligning actuators, a switching network, controller, and a flight-type power conditioner. The system was operated over a 2:1 range in output power. System integration problems such as matching of thruster performance and response to arcing within the thruster and solutions to these problems are described. A 252-h shakedown test and a 298-h endurance test of the system were conducted. Noise within the system was the major lifetime-limiting factor for both the power conditioner and controller.

PEARCE, C. D.

P011 Proton NMR Spectra of Cyclopentadiene, 1,3-Cyclohexadiene, 1,3-Cyclooctadiene, and 1,2-Dihydronaphthalene

M. A. Cooper, D. D. Elleman, C. D. Pearce, and S. L. Manatt
J. Chem. Phys., Vol. 53, No. 6, pp. 2343-2352,
 September 15, 1970

For abstract, see Cooper, M. A.

PERLMAN, M.

P012 Linear m -ary Feedback Shift Registers

M. Perlman
Supporting Research and Advanced Development,
 Space Programs Summary 37-64, Vol. III, pp. 120-124,
 August 31, 1970

A linear m -ary feedback shift register (FSR) is decomposed into parallel linear p -ary FSRs where each p is a distinct prime factor of the integer m . The behavior of a linear p -ary FSR is determined from the divisibility properties of $\phi(x)$ over $GF(p)$, where $\phi(x)$ is the denominator of its generating function. An initial state of a linear m -ary FSR is shown to be on a cycle whose length divides the least-common multiple of the periods of the p -ary FSRs with corresponding initial states.

PETRICK, S. W.

P013 Results of Apollo Gamma Ray Spectrometer Thermal Model Tests

S. W. Petrick
Supporting Research and Advanced Development,
 Space Programs Summary 37-64, Vol. III, pp. 108-112,
 August 31, 1970

To verify the thermal design of the *Apollo* gamma ray spectrometer, a thermal model was built and exposed to thermal conditions at least as severe as those expected during a normal mission. Since the thermal model was not damaged by the extreme temperature conditions and maintained the desired temperature levels during simulated operating conditions, the thermal design is considered to be satisfactory.

PETRIE, R.

P014 Multiple Mission Telemetry 1971 Configuration

W. Frey, R. Petrie, R. Greenberg, J. McInnis, and R. Wengert
The Deep Space Network, Space Programs Summary 37-63,
 Vol. II, pp. 63-77, May 31, 1970

For abstract, see Frey, W.

PFEIFFER, C. G.

P015 A Dynamic Programming Approach to Optimal Stochastic Orbital Transfer Strategy

T. Nishimura and C. G. Pfeiffer (TRW Systems)
J. Spacecraft Rockets, Vol. 7, No. 4, pp. 398–404,
April 1970

For abstract, see Nishimura, T.

PHILLIPS, R. J.

P016 Dipole Antenna Radiation in a Compressible, Anisotropic Electron Plasma Overlying an Imperfectly Conducting Half-Space—Lunar Applications: 1. Formulation of the Solution; 2. Integration and Results

R. J. Phillips and S. H. Ward (University of California, Berkeley)
Radio Sci., Vol. 5, No. 5, pp. 821–839, May 1970

The problem of the electromagnetic response of infinitesimal electric and magnetic dipole sources in a compressible, anisotropic electron plasma overlying a lossy dielectric half-space is solved by integral transform and matrix techniques to assess antenna radiation in the lunar environment. In part 1, the solutions are formulated in terms of Fourier–Bessel integrals operating on matrix quantities. In particular, the field solutions are shown to linear combinations of classical plane-wave modes in a compressible, anisotropic plasma. The introduction of a lossy dielectric half-space yields uncoupled TE and TM modes propagating into the dielectric plus three reflected plasma modes. The modal reflection coefficients represent reflections coupled to all plasma modes.

In part 2, the Fourier–Bessel integrals of part 1 are evaluated by the saddle-point method. By utilizing the arguments of ray optics, an algorithm is devised to find the saddle points by a numerical search procedure on dispersion surfaces. Reflection coefficients show a strong oscillatory structure as a function of frequency in the vicinity of the plasma frequency. This phenomenon is caused by rapid changes in ray convergence and by constructive–destructive interference of reflected modes. Branch-cut contributions yield lateral waves traveling along the dielectric boundary. The dominant lateral wave species is the modified extraordinary (MEX) mode launched by an acoustic-acoustic reflection. Other lateral waves are less important, and, for these species, the position of the observer can go from the propagating zone to the shadow zone as the frequency is increased upward from the plasma frequency.

PHILLIPS, W. M.

P017 Uranium Nitride–Tungsten Compatibility

W. M. Phillips
Supporting Research and Advanced Development,
Space Programs Summary 37-62, Vol. III, pp. 259–263,
April 30, 1970

A compatibility test between uranium mononitride and tungsten was run under thermal gradient conditions at 1800°C. No evidence of chemical reaction was observed; however, grain boundary penetration of the tungsten was observed. Redistribution of the uranium nitride also occurred.

POLANSKY, R. G.

P018 DSN Mark IIIA Simulation Center Development

R. G. Polansky
The Deep Space Network, *Space Programs Summary 37-65*,
Vol. II, pp. 94–96, September 30, 1970

The simulation center subsystem, a part of the Deep Space Network (DSN) Simulation System, has required extensive increase in capability to support the Mark IIIA DSN and future flight projects. Added capabilities are core memory expansion, EMR-6050/UNIVAC-1108 interface, interactive cathode-ray-tube terminals, and programmed input/output receivers and generators. Block diagrams of the subsystem with and without the added capabilities are included.

PORCHÉ, W.

P019 Computerized Receiver and Telemetry SNR Predictions Program

W. Porché
The Deep Space Network, *Space Programs Summary 37-65*,
Vol. II, pp. 133–135, September 30, 1970

The receiver and telemetry signal-to-noise ratio (SNR) predictions program described in this article provides predicted computations of ground receiver signal strength and telemetry SNR on a daily basis. The receiver signal strength is calculated using the space-loss equation, which requires the known range and frequency of the spacecraft. Once the ground receiver signal strength is calculated, the receiver margin, telemetry SNR, and parity error rate or bit error rate for specific bit rates are determined. The program has the additional capability of predicting either single-station telemetry or dual-station telemetry modes.

POSNER, E.

P020 Combinatorial Communications: Epsilon Entropy and Data Compression

E. Posner and E. Rodemich

*Supporting Research and Advanced Development,
Space Programs Summary 37-62, Vol. III, pp. 64-75,
April 30, 1970*

This article discusses efficient data transmission, or "data compression," from the standpoint of the theory of epsilon entropy. The notion of the entropy of a "data source" is defined. This quantity gives a precise measure of the amount of channel capacity necessary to describe a data source to within a given fidelity, epsilon, with probability one, when each separate "experiment" must be transmitted without storage from experiment to experiment. The absolute epsilon entropy of a source, i.e., the amount of capacity needed when storage of experiments is allowed before transmission, is defined. The absolute epsilon entropy is shown to be equal to Shannon's rate distortion function, evaluated for zero distortion, when suitable identifications are made. The main result is that the absolute epsilon entropy and the epsilon entropy have a ratio close to one if they are large. Thus, very little can be saved by storing the results of independent experiments before transmission.

P021 Combinatorial Communication: Hide and Seek, Data Storage, and Entropy

R. McEliece and E. Posner

*Supporting Research and Advanced Development,
Space Programs Summary 37-63, Vol. III, pp. 23-28,
June 30, 1970*

For abstract, see McEliece, R.

POYNTER, R. L.

P022 Skeletal Molecular Structure of closo-2,3-Dicarbaheptaborane(6) From Microwave Spectral Studies

R. A. Beaudet (University of Southern California) and
R. L. Poynter

J. Chem. Phys., Vol. 53, No. 5, pp. 1899-1905,
September 1, 1970

For abstract, see Beaudet, R. A.

PRELEWICZ, D.

P023 Mariner Limit Cycles and Self-Disturbance Torques

B. Dobrotin, E. A. Laumann, and D. Prelewicz (California
Institute of Technology)

J. Spacecraft Rockets, Vol. 7, No. 6, pp. 684-689,
June 1970

For abstract, see Dobrotin, B.

QUADE, J. G.

Q001 Multispectral Remote Sensing of an Exposed Volcanic Province

J. G. Quade (University of Nevada), P. E. Chapman
(University of Nevada), P. A. Brennan (University of
Nevada), and J. C. Blinn III

Technical Memorandum 33-453, June 15, 1970

During July of 1968 a mission was flown, for a second year, over a volcanic province at Mt. Lassen National Park, in support of the NASA Earth Resources Program. Day and night flights were completed with the following instruments operating satisfactorily: two 9-in. by 9-in. metric cameras with black and white and color IR film, an 8-14 μ m IR scanner, four microwave radiometers operating at 8.9, 15.8, 22.2, and 34.0 GHz and a 13.3-GHz radar scatterometer.

Four ground stations were manned during the flights to monitor ground temperatures and moistures. These data were used in conjunction with ground-based radiometers operating at 1.4, 9.3, 13.7, and 37.0 GHz. Prior to the overflights, extensive ground studies (terrametrics), utilizing standard geologic and geophysical techniques, were performed. Some of these studies were reported in greater detail in JPL Technical Memorandum 33-405; however, those pertinent to this report and studies completed this year are reported herein.

Data from the aircraft and ground-based sensors are presented with the relative merits of each sensor discussed along with recommendations for their application.

RAAG, V.

R001 Thermoelectric Properties of 80-at. % Silicon-20-at. % Germanium Alloy as a Function of Time and Temperature

V. Raag and F. de Winter

*Supporting Research and Advanced Development,
Space Programs Summary 37-62, Vol. III, pp. 125-127,
April 30, 1970*

The outer-planet spacecraft being studied at JPL will have electrical power supplied by radioisotope thermoelectric generators. These generators contain silicon-germanium thermoelectric materials that will be expected to perform for periods far in excess of those for which thermoelectric property data are available. Predictions for the time and temperature dependence of these thermoelectric properties are presented and discussed.

RAKUTIS, R.

R002 Long-Term Aging of Elastomers: Stress Relaxation of SBR With Thiophenol

R. Rakutis and S. H. Kalfayan
Supporting Research and Advanced Development,
Space Programs Summary 37-62, Vol. III, pp. 242-244,
April 30, 1970

Continuous and intermittent stress relaxation experiments were performed on dicumyl peroxide-cured styrene-butadiene rubber (SBR) that contained thiophenol. Contrary to expectations, crosslinking occurred, to a large extent, in the presence of this free radical inhibitor.

R003 Long-Term Aging of Elastomers: Kinetics of Oxidation of SBR by Infrared Spectroscopy

R. Rakutis, R. H. Silver, and S. H. Kalfayan
Supporting Research and Advanced Development,
Space Programs Summary 37-64, Vol. III, pp. 125-130,
August 31, 1970

Oxidation of styrene-butadiene rubber (SBR) was investigated by infrared spectroscopy using a specially constructed cell for continuous recording of the spectra of the rubber. Rate data were obtained, in air and oxygen, at temperatures ranging from 110 to 150°C, by following the formation of hydroxyl and carbonyl groups. Energies of activation for both the hydroxyl and carbonyl group formation had an average value of 15 ± 1 kcal from maximum rates and 21 ± 1 kcal from induction periods.

RATHBUN, T. W.

R004 Transmitter Phase Modulation as a Result of Beam Voltage Ripple

C. P. Wiggins, E. B. Jackson, and T. W. Rathbun
The Deep Space Network, Space Programs Summary 37-64,
Vol. II, pp. 96-97, August 31, 1970

For abstract, see Wiggins, C. P.

REED, I. S.

R005 The Equivalence of Rank Permutation Codes to a New Class of Binary Codes

H. D. Chadwick and I. S. Reed (University of Southern California)
IEEE Trans. Information Theory, Vol. IT-16, No. 5,
pp. 640-641, September 1970

For abstract, see Chadwick, H. D.

REGAN, R. D.

R006 A Miniaturized Absolute Gravimeter for Terrestrial, Lunar, and Planetary Research

R. G. Brereton, B. H. Chovitz (United States Coast and Geodetic Survey), W. M. Greene (Marshall Space Flight Center), O. K. Hudson (Marshall Space Flight Center), R. A. Lytleton (St. John's College), and R. D. Regan (United States Geology Survey)
Supporting Research and Advanced Development,
Space Programs Summary 37-62, Vol. III, pp. 1-5,
April 30, 1970

For abstract, see Brereton, R. G.

REICHHARDT, R. W.

R007 Synthesis of a Binary System

R. W. Reichhardt
The Deep Space Network, Space Programs Summary 37-63,
Vol. II, pp. 94-97, May 31, 1970

A set of algorithms has been developed that define a computer program to extract and synthesize the logical structure of a record of binary data. The program, which has been coded in the basic language, is designed for interactive control through a remote terminal. Given a data record of sampled values of a set of binary-valued parameters, the program permits detection and representation of combinatorial relations among the parameters. Functional relations are expressed, in output, as lists of prime implicants.

REID, M. S.

R008 Tracking and Data Acquisition Elements Research: Improved RF Calibration Techniques—System Operating Noise Temperature Calibrations of Low Noise Cones

M. S. Reid and C. T. Stelzried
The Deep Space Network, Space Programs Summary 37-64,
Vol. II, pp. 69-70, August 31, 1970

The system operating noise temperature performance of the low noise cones is reported for the period February through May, 1970. These cones are operated at the Echo, Venus, and Mars Deep Space Stations.

REIER, M.

R009 RTG Radiation Test Laboratory

R. W. Campbell and M. Reier
Supporting Research and Advanced Development,
Space Programs Summary 37-62, Vol. III, pp. 145-148,
April 30, 1970

For abstract, see Campbell, R. W.

R010 Absolute Gamma Ray Intensity Measurements of a SNAP-15A Heat Source

M. Reier

*Supporting Research and Advanced Development,
Space Programs Summary 37-63, Vol. III, pp. 97-102,
June 30, 1970*

A germanium crystal has been used to measure the absolute intensity of gamma rays from the decay of Pu^{238} , Pb^{212} , Bi^{212} , and Tl^{208} in a 1.5-W SNAP-15A (System for Nuclear Auxiliary Power 15A) heat source. In practically all cases, agreement with other measurements is excellent. In addition, the amount of Pu^{236} impurity originally present in the sample can be measured with an accuracy of 4%. It is estimated that the Pu^{236} content in a fuel sample that is several months old can easily be measured with an accuracy of 10%.

REILLY, T. H.

R011 Scientific Objectives for Imaging Experiments at the Outer Planets: A Discussion

T. H. Reilly

Technical Memorandum 33-454, June 15, 1970

This memorandum outlines some scientific objectives for imaging experiments on a flyby of the outer planets Jupiter, Saturn, Uranus, Neptune, and Pluto. Imaging experiments are proposed for atmospheres, satellites and rings, planetary figures, the surface of Pluto, and the asteroid belt. An attempt is made to demonstrate how the proposed experiments would fill gaps in our current knowledge concerning the outer planets. Some functional requirements such as resolution and spectral bandwidth of the imaging system have been identified.

RE MBAUM, A.

R012 Kinetics of Formation of High Charge Density Ionene Polymers [February-March 1970]

A. Rembaum, H. Rile, and R. Somoano

*Supporting Research and Advanced Development,
Space Programs Summary 37-62, Vol. III, pp. 235-240,
April 30, 1970*

The polymerization kinetics of a high charge density polymer (3,4-ionene bromide) were investigated by following the rate of disappearance of dimethylamino groups. The rate of polymerization obeyed the second-order law and increased with concentration, dielectric strength of solvent, and temperature. The rate constant for the system dimethylformamide: methanol (4:1) may be expressed by means of the equation: $K = 3.45 \times 10^6 \exp(-12,300/RT)$. The highest weight-average molecular weight (of the order of

15,000) was obtained at room temperature and at high concentration of reagents. The polymer was found to impart antistatic and bacteriostatic properties to various substrates.

R013 Potentialities of a New Class of Anticlotting and Antihemorrhagic Polymers

T. F. Yen (University of Southern California, California State College), M. Davar (University of Southern California, California State College), and A. Rembaum
*J. Macromol. Sci.-Chem., Vol. A4, No. 3, pp. 693-714,
May 1970*

For abstract, see Yen, T. F.

R014 Synthesis and Properties of a New Class of Potential Biomedical Polymers

A. Rembaum, S. P. S. Yen, R. F. Landel, and M. Shen (University of California, Berkeley)
*J. Macromol. Sci.-Chem., Vol. A4, No. 3, pp. 715-738,
May 1970*

Both low molecular weight compounds and some polyelectrolytes containing quaternary nitrogen atoms in their structure have been known for some time to possess important biological activity. Aliphatic ammonium compounds are used as bacteriocides and muscle relaxants, and quinolinium compounds have recently been found to be excellent antileukemic agents. In addition, a considerable amount of evidence has been accumulated to show that organic ammonium salts combine with heparin, and the resulting complex may be used as a coating to render polymers blood-compatible.

However, the introduction of ammonium groups into the backbone of a polymer exhibiting good mechanical properties offers certain advantages. The present paper describes a synthesis of a new family of polymeric elastomers containing quaternary nitrogen atoms in the polymeric backbone. They may be prepared from the following commercially available materials: (A) polyhydroxy prepolymers reacted with diisocyanates first and then with dimethylamino alcohols, (B) tetramethyl or hexamethylamino alkanes and α,ω -dibromoalkanes, and (C) halo prepolymers formed from diisocyanates reacted with halo alcohols. It is thus possible to obtain a very large number of homo or block elastomers with a variable concentration of positive charges as well as of hydrophilic and hydrophobic segments by A-B, B-C, and C-A reactions.

One of the block polymers obtained from Solithane 113 and dibromopolybutadiene was examined in detail. Heparin was grafted onto its surface by a simple impregnation treatment, and the resulting material was found to be antithrombogenic. Electron scanning

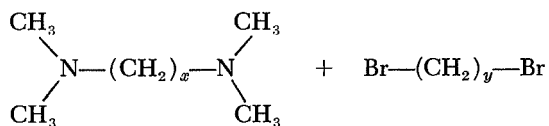
micrographs show that the surface structure of the elastomer was altered by heparinization. Thermograms for a Perkin-Elmer scanning calorimeter exhibited two transitions: one around -80°C , being identified as the glass transition temperature of the polybutadiene blocks, and another very broad transition near room temperature due to the Solithane blocks. Modulus-temperature and modulus-time curves determined by viscoelastic measurements show only the low temperature transition. There is a continuous decrease in modulus with increasing temperature and time above the polybutadiene T_g . It was demonstrated from the WLF plot that the free volume fraction in this range is smaller than in ordinary homopolymers. Above 100°C the modulus drops, indicating the onset of interchange reactions of the polyurethane linkages. Fracture tests of the heparinized and unheparinized polymers indicate that these elastomers have good tensile strength properties.

R015 Kinetics of Formation of High Charge Density Ionene Polymers

A. Rembaum, H. Rile, and R. Somoano

J. Polym. Sci., Pt. B: Polym. Lett., Vol. 8, No. 7, pp. 457-466, July 1970

It was previously shown that the reaction of N,N,N',N' -tetramethyl- α , ω -diaminoalkanes with α , ω -dibromoalkanes



yields a variety of products, depending on the values of the integers x and y . When x and y were less than 3, only monomeric products were formed. The lowest values of x and y leading to the formation of polymers were $x = 2$, $y = 4$; $x = 4$, $y = 2$; $x = 3$, $y = 3$; $x = 4$, $y = 3$; and $x = 3$, $y = 4$. Out of these combinations, only the last two yielded polyelectrolytes of weight average molecular weight greater than 10,000; since these high-charge-density polyelectrolytes (ionene polymers) are of considerable practical importance, the formation of 3,4 ionene bromide was investigated in detail and is reported in this article.

It was found that the rate of polymerization obeyed second-order kinetics and increased with the concentration of reagents as well as with the magnitude of the dielectric constant of the solvent. The polymers obtained at high reagent concentration and at 25°C had a higher intrinsic viscosity than those prepared in dilute solutions or at higher temperatures than 25°C . The high-charge-density ionene polymers are effective

flocculating and electrostatic agents. In addition, they form water-insoluble polyhalides characterized by bacterial growth inhibiting properties.

R016 Electronic Conductivity of Elastomeric Ionenes

R. Somoano, S. P. S. Yen, and A. Rembaum

J. Polym. Sci., Pt. B: Polym. Lett., Vol. 8, No. 7, pp. 467-479, July 1970

For abstract, see Somoano, R.

RENNILSON, J. J.

R017 Uniform Variable Light Sources for Instrument Calibration

H. P. Squyres and J. J. Rennilson

Technical Report 32-1470 (Reprinted from *Appl. Opt.*, Vol. 9, No. 5, pp. 1092-1096, May 1970)

For abstract, see Squyres, H. P.

RENZETTI, N. A.

R018 Tracking and Data System Support for the Pioneer Project: Pioneer VIII. Prelaunch Through May 1968

N. A. Renzetti

Technical Memorandum 33-426, Vol. III, July 15, 1970

The *Pioneer VIII* spacecraft (outward trajectory and heliocentric orbit) employed seven scientific instruments to accumulate information relative to interplanetary high-energy particles, solar phenomena, and plasma. The spacecraft also served as a celestial-mechanics-experiment reference point and carried aloft a "piggy-back" satellite to be used for *Apollo* ground station crew training and mission simulation. The Tracking and Data System (comprised of the Air Force Eastern Test Range, Deep Space Network, Manned Space Flight Network, and NASA Communications Network) tracked the spacecraft from launch through the near-earth and deep space phases of the mission. For near-earth tracking, all Tracking and Data System facilities responded to mission, launch-vehicle, and range requirements. For deep space tracking, the Deep Space Network responded to tracking, telemetry, command, monitoring, simulation, and operations control requirements.

R019 Tracking and Data System Support for the Pioneer Project: Pioneer IX. Prelaunch Through June 1969

N. A. Renzetti

Technical Memorandum 33-426, Vol. IV, November 15, 1970

The *Pioneer IX* mission (inward trajectory and heliocentric orbit) employed seven scientific instruments to

accumulate information relative to interplanetary high-energy particles, solar phenomena, and plasma. The launch vehicle carried aloft a "piggyback" satellite called the *Test and Training Satellite (TETR)* to be used for *Apollo* ground station crew training and mission simulation. The spacecraft also served as a celestial mechanics experiment reference point. In addition, a convolutional coding experiment was conducted. The Tracking and Data System (Air Force Eastern Test Range, JPL Deep Space Network, Manned Space Flight Network, and NASA Communications Network) tracked the spacecraft from launch through the near-earth and deep space phases of the mission. For near-earth tracking, all Tracking and Data System facilities responded to the mission, launch-vehicle, and range requirements. For deep space tracking, the Deep Space Network responded to the tracking, telemetry, command, monitoring, simulation, and operations control requirements.

The *Pioneer E* mission (near the earth for 900 days, then heliocentric) was intended to investigate interplanetary phenomena. After 438 s of flight on August 27, 1969, a destruct signal was transmitted because of a loss of hydraulic pressure in the first stage. This was the fifth spacecraft in the second *Pioneer* generation and the only failure (launch vehicle failed).

R020 Deep Space Network Support of the Manned Space Flight Network for Apollo: 1962-1968

F. M. Flanagan, P. S. Goodwin, and N. A. Renzetti
Technical Memorandum 33-452, Vol. I, July 15, 1970

For abstract, see Flanagan, F. M.

RHEIN, R. A.

R021 Determination of Molecular Weight Distribution of Poly(Isobutylene) by Gel Permeation Chromatography: Procedure and Computer Program

R. A. Rhein
Supporting Research and Advanced Development,
Space Programs Summary 37-62, Vol. III, pp. 240-242,
April 30, 1970

By means of gel permeation chromatography, it was found that molecular weight distributions of poly(isobutylenes) were very nearly identical to those obtained from poly(propylene oxide) standards. A listing and operating procedure for a computer program that uses the retention time (counts) and corresponding heights as input data is described. The computer output is number-average and weight-average molecular weight and a table of weight percent and cumulative weight percent versus molecular weight.

R022 The Molecular-Sieve Catalyzed Polymerization of Isobutylene

R. A. Rhein
Supporting Research and Advanced Development,
Space Programs Summary 37-64, Vol. III, pp. 130-135,
August 31, 1970

As part of a program to investigate solid propellant binders, a study of the polymerization of isobutylene by molecular sieves was undertaken. Molecular sieves were found to polymerize isobutylene to mixtures of dimers, trimers, tetramers, and polymers. The polymers generally were viscous liquids of number-average molecular weight less than 1000, but there were some instances of higher molecular weight polymers formed. Although molecular sieves 3A and 4A did not catalyze the polymerization of isobutylene, polymerization was observed with types 5A, 10X, 13X, SK45, SK100, SK110, SK200, SK310, SK400, SK410, and SK500. The resulting polymers were characterized by infrared spectra. Of the types A, X, Y, and L molecular sieves, the highest polymer yields resulted from type A, although type L produced polymers with a high level of unsaturation, but at very low yields. No polymerization resulted from a molecular sieve of a pore diameter less than 5Å; above 5Å, the degree of polymer unsaturation and polymer molecular weight apparently increased with increasing pore diameter.

The nature of the cation within the molecular sieve influenced the nature of the reaction products. Cationic sites produced the highest polymer yield, but degree of unsaturation was greatest for the Na and K forms. The presence of finely divided metals (Pt, Pd, Ni, Cu, and rare earths) had little apparent effect upon the resulting polymers. Increased reaction time and decreasing sieve particle size (with the exception of the finely divided powder) generally resulted in increasing polymer molecular weight and degree of unsaturation.

RHO, J. H.

R023 Fluorometric Examination of the Returned Lunar Fines From Apollo 11

J. H. Rho, A. J. Bauman, T. F. Yen (University of Southern California), and J. Bonner (California Institute of Technology)
Proceedings of the Apollo 11 Lunar Science Conference, Houston, Texas, January 5-8, 1970, Vol. 2, pp. 1929-1932

Organic solvent extracts of the bulk fine lunar sample have been examined for the presence of porphyrins by spectrofluorometry. Porphyrins were not found in any of the extracts, even under conditions in which less than 10^{-13} moles/g of sample could have been detected. However, a material was found that exhibits absorption peaks at 310 and 350 m μ and fluorescence

peaks at 405 and 690 $m\mu$, the latter with excitation maxima of 360 and 410 $m\mu$ (uncorrected), respectively.

RICE, J. K.

R024 Vibrational Excitation of H₂ by Low- and Medium-Energy Electrons

S. Trajmar, D. G. Truhlar (California Institute of Technology), J. K. Rice (California Institute of Technology), and A. Kuppermann (California Institute of Technology) *Supporting Research and Advanced Development, Space Programs Summary 37-62, Vol. III, pp. 36-43, April 30, 1970*

For abstract, see Trajmar, S.

R025 Electron Scattering by H₂ With and Without Vibrational Excitation: II. Experimental and Theoretical Study of Elastic Scattering

S. Trajmar, D. G. Truhlar (California Institute of Technology), and J. K. Rice (California Institute of Technology) *J. Chem. Phys., Vol. 52, No. 9, pp. 4502-4515, May 1, 1970*

For abstract, see Trajmar, S.

R026 Electron Scattering by H₂ With and Without Vibrational Excitation: III. Experimental and Theoretical Study of Inelastic Scattering

S. Trajmar, D. G. Truhlar (California Institute of Technology), J. K. Rice (California Institute of Technology), and A. Kuppermann (California Institute of Technology) *J. Chem. Phys., Vol. 52, No. 9, pp. 4516-4533, May 1, 1970*

For abstract, see Trajmar, S.

RIEBLING, R. W.

R027 Advanced Combustion Device Development [June-July 1970]

R. W. Riebling *Supporting Research and Advanced Development, Space Programs Summary 37-64, Vol. III, pp. 157-161, August 31, 1970*

Preliminary screening tests of two 200-lbf self-impinging doublet jet injectors with FLOX/B₂H₆ propellants are described. Mixture ratio and B₂H₆ temperature were varied at a nominal stagnation pressure of 105 psia in short-duration sea level firings made with an uncooled copper chamber having a contraction ratio of 5.0 and a characteristic length of 20 in. The

effects of these variables, as well as those of injector design and stratified barrier cooling, on combustion efficiency and solids deposition are discussed.

RIGGS, R. L.

R028 Low Transmitted Power Operation [of DSIF Antennas]

R. L. Riggs *The Deep Space Network, Space Programs Summary 37-65, Vol. II, pp. 136-139, September 30, 1970*

This article discusses a method by which the radiated output power level from a Deep Space Instrumentation Facility (DSIF) antenna may be adjusted while maintaining the transmitter at constant power and bandwidth levels. The constant power output from the transmitter is split into appropriate levels between a dissipative load and the antenna feed horn. Described are two devices that will accomplish the splitting: (1) basically a fixed high-power directional coupler (or combination of couplers), and (2) a high-power microwave power divider that has a capability of being continuously variable. Current instrumentation techniques for monitoring the output power level are not changed with either device, and the overall accuracy of the system is degraded only by the tolerances in the calibration of the added device(s).

RIISE, H. N.

R029 Solar Simulators at the Jet Propulsion Laboratory

R. E. Bartera, H. N. Riise, and C. G. Miller *Appl. Opt., Vol. 9, No. 5, pp. 1068-1074, May 1970*

For abstract, see Bartera, R. E.

RILE, H.

R030 Kinetics of Formation of High Charge Density Ionene Polymers [February-March 1970]

A. Rembaum, H. Rile, and R. Somoano *Supporting Research and Advanced Development, Space Programs Summary 37-62, Vol. III, pp. 235-240, April 30, 1970*

For abstract, see Rembaum, A.

R031 Kinetics of Formation of High Charge Density Ionene Polymers

A. Rembaum, H. Rile, and R. Somoano *J. Polym. Sci., Pt. B: Polym. Lett., Vol. 8, No. 7, pp. 457-466, July 1970*

For abstract, see Rembaum, A.

RINDFLEISCH, T. C.

R032 The Digital Removal of Noise From Video Imagery

T. C. Rindfleisch

*Supporting Research and Advanced Development,
Space Programs Summary 37-62, Vol. III, pp. 18-22,
April 30, 1970*

All physically realizable camera systems introduce noises into the images they record. Digital techniques are described and examples given of the removal of periodic, streak, and spike noises from imagery, based on structural characteristics that distinguish these noises from the video data on which they are superimposed.

RODEMICH, E.

R033 Combinatorial Communications: Epsilon Entropy and Data Compression

E. Posner and E. Rodemich

*Supporting Research and Advanced Development,
Space Programs Summary 37-62, Vol. III, pp. 64-75,
April 30, 1970*

For abstract, see Posner, E.

ROHR, J. A.

R034 STAR Computer Software

J. A. Rohr

*Supporting Research and Advanced Development,
Space Programs Summary 37-63, Vol. III, pp. 150-152,
June 30, 1970*

Software for the STAR (self-testing and repairing) computer is comprised of three types of programs. The first type is used to prepare STAR computer programs. Two versions of the programming subsystem for the STAR computer have been completed: one for the IBM 7094 and one for the UNIVAC 1108. Each consists of an assembler, loader, simulator, and executive control program. An initial version of the second type of program, the operating system, is now being developed. Some programs of the third type, common subroutines and special-purpose applications programs, have already been written. In the future, the operating system will be developed further and more subroutines and applications programs will be written.

ROPER, W.

R035 Spacecraft Adhesives for Long Life and Extreme Environments

W. Roper

*Supporting Research and Advanced Development,
Space Programs Summary 37-63, Vol. III, pp. 128-133,
June 30, 1970*

The present state-of-the-art of high performance adhesives was reviewed to identify those newer adhesive materials which show promise for application in future spacecraft fabrication. The adhesives survey revealed several new polymeric materials which show considerable potential for spacecraft use when both elevated and cryogenic environments are encountered. These include the polyimide, polybenzimidazole, and the polyquinoxaline polymers.

ROSELLI-LORENZINI, F. G.

R036 Two-Dimensional Molecular Gas Leakage Flow

F. G. Roselli-Lorenzini

*Supporting Research and Advanced Development,
Space Programs Summary 37-62, Vol. III, pp. 161-164,
April 30, 1970*

A two-dimensional, molecular flow gas leakage analysis has been performed and a computer program written. The procedure adopted is to compute the leakage port area, using a given set of initial conditions, and then introduce this value into the integral expressions for the pressure in the vessel, the mixture ratios, and the mass flow rate through the port as a function of time. Results obtained using the *Mariner* Mars 1971 scan platform sealed actuator are shown. The results will be extended to a three-dimensional model.

ROSEN, B. W.

R037 A Statistical Theory of Material Strength With Application to Composite Materials

C. Zweben and B. W. Rosen (Material Sciences Corporation)
J. Mech. Phys. Solids, Vol. 18, No. 3, pp. 189-206,
June 1970

For abstract, see Zweben, C.

ROSENTHAL, L. A.

R038 Nondestructive Testing of Insensitive Electroexplosive Devices by Transient Techniques

L. A. Rosenthal (Rutgers University) and V. J. Menichelli
Technical Report 32-1494, July 15, 1970

By pulsing an electroexplosive device with a safe-level constant current and examining the resistance variation of the bridgewire, it is possible to explore the electrothermal behavior of the bridgewire-explosive

interface. The bridgewire, acting as a resistance thermometer, provides a signal that describes the average wire temperature and the heat sinking to the explosive and enclosure. This report describes equipment and observations specific to nondestructive testing of 1-W/1-A no-fire devices.

ROSS, R. G., JR.

R039 Parametric Study of the Performance Characteristics and Weight Variations of Large-Area Roll-Up Solar Arrays

J. V. Coyner, Jr. and R. G. Ross, Jr.

Technical Report 32-1502, December 15, 1970

For abstract, see Coyner, J. V., Jr.

R040 Optimum Shell Design

A. E. Salama and R. G. Ross, Jr.

Supporting Research and Advanced Development, Space Programs Summary 37-63, Vol. III, pp. 134-139, June 30, 1970

For abstract, see Salama, A. E.

RUMSEY, H., JR.

R041 A Radar Snapshot of Venus

R. M. Goldstein and H. Rumsey, Jr.

Science, Vol. 169, No. 3949, pp. 974-977, September 4, 1970

For abstract, see Goldstein, R. M.

SABELMAN, E.

S001 TOPS Thermomechanical Pump

E. Sabelman

Supporting Research and Advanced Development, Space Programs Summary 37-64, Vol. III, pp. 113-118, August 31, 1970

A thermal-powered, two-cylinder piston pump has been devised to replace or augment an electric pump for transport of temperature control fluid on the Thermoelectric Outer-Planet Spacecraft (TOPS). Once started, it operates cyclically, analogous to an electronic astable multivibrator, extracting heat energy from the fluid by means of a vapor pressure expansion system. Two test models, which operated at a fluid input temperature of 200°F and heat sink at 0 to 30°F, were constructed. The longest self-powered oscillation achieved was seven cycles. A successful fast response heat exchanger has been designed, and a digital computer simulation program is presently being completed.

SALAMA, A. E.

S002 Optimum Shell Design

A. E. Salama and R. G. Ross, Jr.

Supporting Research and Advanced Development, Space Programs Summary 37-63, Vol. III, pp. 134-139, June 30, 1970

A unified approach for formulating the problem of optimum shell design satisfying certain design requirements is given and a means of transforming the constrained design problem to an unconstrained minimization problem is discussed. The resulting unconstrained function is simple in form and is devised such that a minimum amount of computational effort is required. The advantages of the form of the suggested function over others described in the literature are discussed.

Two algorithms for unconstrained minimizations are compared. These are the Simplex method of direct search and a gradient technique known as the variable metric method. For the two examples solved, the Simplex method was found to be superior over the variable metric technique.

SALOMON, P. M.

S003 Applications of Slow-Scan Television Systems to Planetary Exploration

P. M. Salomon

J. SMPTE (Society of Motion Picture and Television Engineers), Vol. 79, No. 7, pp. 607-615, July 1970

The design of a spacecraft television system must be selected from many parameters while seeking to optimize performance and reliability with respect to weight and complexity, within the constraints of existing technology. The slow-scan television system employing a vidicon photosensor uses a mechanical shutter which allows the vidicon to effectively store the scene image and perform the readout sequence at a much reduced rate. Digital encoding of the analog video signal prior to recording preserves the high signal-to-noise ratio and eliminates signal degradation in the earth-spacecraft downlink. Future trends are described which involve improvements in sensors, data encoding and storage. Various types of television systems considered for future planetary missions are discussed.

S004 Operation of the Surveyor Television System in the Photon-Integration Mode

L. H. Allen and P. M. Salomon

J. SMPTE (Society of Motion Picture and Television Engineers), Vol. 79, No. 7, pp. 615-620, July 1970

For abstract, see Allen, L. H.

- S005 Environmental Testing and Calibration of the Mariner Mars 1969 Television System**
G. E. Danielson, Jr., and P. M. Salomon
Paper 69-994, AIAA (American Institute of Aeronautics and Astronautics)/ASTM (American Society for Testing Materials)/IES (Institute of Environmental Sciences) 4th Space Simulation Conference, Los Angeles, California, September 8–10, 1969

For abstract, see Danielson, G. E., Jr.

SATO, T.

- S006 Radio Science Support [by DSN, March–April 1970]**
T. Sato and D. Spitzmesser
The Deep Space Network, Space Programs Summary 37-63, Vol. II, pp. 98–101, May 31, 1970

Three proposed experiments received earlier were evaluated and approved by the Radio Astronomy Experiment Selection Panel and three new proposals were received for consideration. Radio science experiments performed at Deep Space Network (DSN) facilities since July 1967 are summarized. Operating times of the 210-ft antenna facility in support of radio science activities during calendar year 1970 are also projected.

- S007 Radio Science Support [by DSN, July–August 1970]**
T. Sato, L. Skjerve, and D. Spitzmesser
The Deep Space Network, Space Programs Summary 37-65, Vol. II, pp. 132–133, September 30, 1970

Described in this article are three proposed experiments that have completed evaluation by the Radio Astronomy Experiment Selection Panel. The SCO-XR1 (on X-ray source in the constellation Scorpio) observations, the trans-Pacific very-long-baseline interferometer experiment, the X-band pulsar observations, and two X-band planetary radar experiments are summarized. These radio-science experiments supported by the Deep Space Network (DSN) were performed during May–July 1970.

SAVAGE, J. E.

- S008 Coding and Synchronization Research: Decision Rules for a Two-Channel Deep-Space Telemetry System**
S. Butman, J. E. Savage (Brown University), and U. Timor
Supporting Research and Advanced Development, Space Programs Summary 37-63, Vol. III, pp. 38–41, June 30, 1970

For abstract, see Butman, S.

- S009 Digital Telemetry and Command: The Asymptotic Complexity of the Green Decoding Procedure**
J. E. Savage (Brown University)
The Deep Space Network, Space Programs Summary 37-64, Vol. II, p. 29, August 31, 1970

Green recently introduced a simple decoding procedure for first-order Reed–Muller codes. This decoding procedure was used to decode the *Mariner Mars 1969* high-rate telemetry.

In this article, the Green procedure is shown to be nearly optimal in the computational work required to decode M code words with a small probability of error on the additive gaussian noise channel. However, the near optimality has been proved only for large M ; for $M = 32$, results are harder to acquire.

- S010 Digital Telemetry and Command: The Effective Computing Power of Computer Memory**
J. E. Savage (Brown University)
The Deep Space Network, Space Programs Summary 37-64, Vol. II, pp. 30–32, August 31, 1970

Any type of computer memory that allows selective reading from storage possesses a computing power; e.g., this is true of the storage in programmable telemetry decoders. In this article, the method for measuring this power is described, and measurements for tape and random access storage are given. In particular, if S is the size of storage and T is the number of computing cycles, it is shown that ST must be large to compute complex functions on general-purpose computers.

- S011 Digital Telemetry and Command: A Collection of Results on Computational Complexity**
J. E. Savage (Brown University)
The Deep Space Network, Space Programs Summary 37-65, Vol. II, pp. 42–47, September 30, 1970

This article discusses: (1) a bound on the maximum time to compute a function, (2) the storage required for autonomous computation, (3) the computation of simple and complex functions, (4) the work potential of a computer, (5) a quantum-mechanical bound on complexity, and (6) the sorting problem. These results on the complexity of computation are tied together by their use of the measure “computational work.” The purpose of this research is to define a method for choosing the best telemetry decoding configuration, but the technique has applicability to other Deep Space Instrumentation Facility uses of computers.

SCARF, F. L.

S012 OGO 5 Observations of Quasi-Trapped Electromagnetic Waves in the Solar Wind

F. L. Scarf (Space Sciences Laboratory), R. W. Fredricks (Space Sciences Laboratory), I. M. Green (Space Sciences Laboratory), and M. Neugebauer
J. Geophys. Res., Space Phys., Vol. 75, No. 19, pp. 3735–3750, July 1, 1970

On April 15, 1968, a flare-associated sudden commencement was detected as *OGO 5* (*Orbiting Geophysical Observatory 5*) was outbound through the bow shock region. Several hours later exceptionally high densities ($N_e > 70/\text{cm}^3$) were encountered, and, when the flux decreased by a moderate factor, large-amplitude 70-kHz noise bursts were sporadically detected on the VLF electric and magnetic sensors. We interpret the oscillations with correlated E and B components as electromagnetic waves that have $n^2 \simeq 1 - (\omega_p^2/\omega^2) < 1$, and direct comparison with the plasma probe density estimate gives an absolute calibration for that instrument. The measured wave amplitudes are also used to evaluate the local density from the relation $n = cB/E$, thus leading to an absolute calibration for the electric dipole within the streaming plasma. We find that all measured or deduced densities are in agreement and are compatible with the interpretation that the correlated noise bursts represent electromagnetic waves with ω near the local plasma resonance frequency. These observations are related to previous measurements of 20- to 30-kHz electric fields in the solar wind (*Zond 3*, *Venus 2*, *Pioneers VIII* and *IX*, and *Luna 11* and *12*), and the problem of distinguishing between electromagnetic waves of this type and electrostatic plasma oscillations is considered.

SCHAPER, P. W.

S013 Results of the Near Infrared Multidetector Grating Spectrometer Study

L. W. Carls and P. W. Schaper
Supporting Research and Advanced Development, Space Programs Summary 37-63, Vol. III, pp. 1–5, June 30, 1970

For abstract, see Carls, L. W.

SCHMIDT, F. W.

S014 Calibrating a Hot Film Anemometer for Low Velocity Measurement in Nonisothermal Flow

B. Zeldin and F. W. Schmidt (Pennsylvania State University)
Rev. Sci. Instr., Vol. 41, No. 9, pp. 1373–1374, September 1970

For abstract, see Zeldin, B.

SCHMIDT, L. F.

S015 Digital Sun Sensor [June–July 1970]

L. F. Schmidt

Supporting Research and Advanced Development, Space Programs Summary 37-64, Vol. III, pp. 77–78, August 31, 1970

A digital sun sensor is being developed to meet the requirements of the Thermoelectric Outer-Planet Spacecraft. The sun's angular position is provided by the sensor in the form of a Gray-coded digital word. The testing of a 6-deg field-of-view breadboard sensor is described, and a discussion of the test results is presented.

SCHNEIDER, W. A.

S016 Hypersonic Blunt-Body Flow of a Radiating Gas at Low Density

W. A. Schneider

Technical Report 32-1451, July 1, 1970

The effect of radiation on hypersonic viscous flow at low densities is studied. Cheng's two-layer flow model (dividing the flow field into a thin shock layer and a thin shock transition zone) is used to simplify the Navier–Stokes equations. Radiation is taken into account by adding an emission term to the energy equation. Because of the low density, self-absorption may be neglected, but nonequilibrium effects become important. Estimates show that vibration, dissociation, and ionization can be assumed to be frozen in the density–velocity regime of interest, but the process of electron excitation has to be investigated on the basis of finite relaxation times. Rate equations for emission due to nonequilibrium radiation from various band systems are derived, and the effect of “collision limiting” is discussed in the light of these equations. The rate constants for the most important molecular band systems in air are determined experimentally. Finally, numerical results for the flow field in the stagnation region and for the heat transfer coefficient are discussed.

SCHORN, R. A.

S017 High-Dispersion Spectroscopic Studies of Mars: III. Preliminary Results of 1968–1969 Water-Vapor Studies

R. A. Schorn, C. B. Farmer, and S. J. Little (University of Texas)
Icarus: Int. J. Sol. Sys., Vol. 11, No. 3, pp. 283–288, November 1969

Recent high-resolution spectra of Mars have confirmed the existence of water vapor in the atmosphere of that planet. New laboratory measurements and improved temperature corrections have resulted in more accurate abundances than obtained previously. In February and March 1969, there was a mean vertical water content of 26 ± 5 precipitable microns in the northern hemisphere at a temperature of 225°K . For the southern hemisphere, the amount was less than $\frac{1}{3}$ of that in the north. Observations from November 1968 through April 1969 give similar results. By August and September 1969, there was less than 5 microns everywhere on the planet. The abundance and temperature estimates discussed here lead to a surprisingly high relative humidity (over 50%), and it is felt by the authors that the possibility of small amounts of liquid water on the planet cannot be dismissed out of hand.

S018 High-Dispersion Spectroscopic Observations of Venus: VI. The Carbon Dioxide Band at 10 362 Å

R. A. Schorn and L. G. Young

Icarus: Int. J. Sol. Sys., Vol. 12, No. 3, pp. 391–401, May 1970

Observations of the 10,362-Å band of carbon dioxide in the spectrum of Venus were made from January through December 1967. The 15 best spectra were combined with spectra obtained several years earlier to derive rotational temperatures. Two methods were used. A linear least-squares fit to a square-root absorption law yielded an average temperature of $240 \pm 19^\circ\text{K}$, while a curve-of-growth technique gave an average temperature of $237 \pm 12^\circ\text{K}$. The rotational temperatures showed no significant variation with the phase angle i of Venus for $26 \leq i, \text{deg} \leq 164$.

SCHREDER, K.

S019 Frequency Generation and Control: Computer-Assisted Acquisition

K. Schreder

The Deep Space Network, Space Programs Summary 37-64, Vol. II, pp. 59–60, August 31, 1970

This article describes a method for acquisition of a received signal near threshold wherein a digital computer is used to determine the offset frequency between the received signal and the local oscillator. The offset frequency can be programmed (dialed) into the voltage-controlled oscillator, and acquisition is accomplished. Results of the simulation on the three most likely received signals using the proposed acquisition method are given.

SCHUMACHER, L. L.

S020 An Analysis of TOPS Science Package Pointing Error Due to Structural Vibration of the Supporting Booms

L. L. Schumacher

Supporting Research and Advanced Development, Space Programs Summary 37-62, Vol. III, pp. 160–161, April 30, 1970

Structural vibrations in the Thermoelectric Outer-Planet Spacecraft (TOPS) can cause excessive science instrument pointing errors. To examine the problem, the dynamic equations of motion were developed and simulated on the UNIVAC 1108 computer. The simulation results indicate that the science instrument pointing error resulting from structural vibration is very small and can be ignored for most applications.

SHAFAER, J. I.

S021 Solid Propellant Spacecraft Motors

J. I. Shafer

Supporting Research and Advanced Development, Space Programs Summary 37-63, Vol. III, pp. 188–196, June 30, 1970

Successful static test firings in 60- and 800-lb flight-weight motors have now shown that the concept of case-bonded end-burning motors, without mechanical stress relief, is technically feasible when the case length-to-diameter ratio is about one. Motors utilized polyether polyurethane propellant zone cured at 140°F under a cure pressure as high as 275 psi (about 93% of the chamber proof pressure). Additional motor processing and firing tests to help determine the boundaries for the concept indicate that the propellant should have unusually low modulus and exceptionally high elongation to avoid buckling in the thin wall case and pullaway at the propellant–insulation interface. A tentative range of values for propellant mechanical properties has been adopted.

SHAFFER, D. B.

S022 High-Resolution Observations of Compact Radio Sources at 13 Centimeters

K. I. Kellermann (National Radio Astronomy Observatory), B. G. Clark (National Radio Astronomy Observatory), D. L. Jauncey (Cornell University), M. H. Cohen (California Institute of Technology), D. B. Shaffer (California Institute of Technology), A. T. Moffet (California Institute of Technology), and S. Gulkis

Astrophys. J., Vol. 161, No. 3, pp. 803–809, September 1970

For abstract, see Kellermann, K. I.

SHAPIRO, I. I.

S023 Celestial Mechanics Experiment for Mariner Mars 1971

J. Lorell, J. D. Anderson, and I. I. Shapiro (Massachusetts Institute of Technology)

Icarus: Int. J. Sol. Sys., Vol. 12, No. 1, pp. 78–81, January 1970

For abstract, see Lorell, J.

SHEN, M.

S024 Synthesis and Properties of a New Class of Potential Biomedical Polymers

A. Rembaum, S. P. S. Yen, R. F. Landel, and

M. Shen (University of California, Berkeley)

J. Macromol. Sci.—Chem., Vol. A4, No. 3, pp. 715–738, May 1970

For abstract, see Rembaum, A.

SHIMADA, K.

S025 Plasma-Immersion-Probe Tube in Metal-Ceramic Envelope

K. Shimada and P. L. Cassell

Supporting Research and Advanced Development, Space Programs Summary 37-62, Vol. III, pp. 153–157, April 30, 1970

A plasma-immersion-probe tube was fabricated in a metal-ceramic envelope in order to study electron-emission properties of various metals, including oxygen-saturated tantalum. The metal structure offers many advantages over glass structures that have been used in the past. The new tube is operable at temperatures as high as 400°C, and all electrodes are demountable. The tube is lined with a ceramic cylinder that provides an insulating wall to contain the plasma.

To demonstrate its feasibility as a plasma device, the tube was equipped with a Langmuir probe and filled with argon at pressures between 1.0 and 0.2 torr. Measurements indicated that the argon plasma density was $4.65 \times 10^{12}/\text{cm}^3$ at the axis of the tube and that the electron temperature was 22,300°K. These results indicate a significant increase in capability over glass plasma-immersion-probe tubes.

SHINOZUKA, M.

S026 Optimum Structural Design Based on Reliability Analysis

M. Shinozuka (Columbia University), J.-N. Yang, and E. Heer

Technical Report 32-1496 (Reprinted from *Proceedings of the Eighth International Symposium on Space Technology and Science*, Tokyo, Japan, August 25–30, 1969, pp. 245–258)

Thermomechanical properties of materials used for the structure of a space vehicle, particularly those of composite materials, exhibit considerable statistical variations. Also, aerospace environments as well as loading conditions involve a number of obvious uncertainties. Both strengths of, and loads on, the aerospace structure should therefore be treated as random variables and the notion of structural reliability should be incorporated into its optimum design. In fact, a number of papers have been published on this subject. Most of these papers, however, did not consider the important fact that major structural components of a space vehicle are usually (proof-load) tested individually or otherwise under simulated environmental conditions before the vehicle is sent on its mission.

In a recent paper, a method of the reliability-based structural optimization was formulated that introduced the level of the proof load as an additional design parameter. It was emphasized that the proof-load test could significantly improve the statistical confidence in the reliability estimate. Also, numerical examples indicated a definite advantage of the proof-load approach in terms of structural savings. The present paper further introduces into the cost formulation the cost of establishing the statistical distribution of strength of the material used for the structure and examines the effect of such a cost on the structural optimization.

SHOEMAKE, G. R.

S027 Palladium-Hydrogen System: Efficient Interface for Gas Chromatography-Mass Spectrometry

P. G. Simmonds, G. R. Shoemaker, and J. E. Lovelock

Anal. Chem., Vol. 42, No. 8, pp. 881–885, July 1970

For abstract, see Simmonds, P. G.

S028 The Palladium Generator-Separator—A Combined Electrolytic Source and Sink for Hydrogen in Closed Circuit Gas Chromatography

J. E. Lovelock, P. G. Simmonds, and G. R. Shoemaker

Anal. Chem., Vol. 42, No. 9, pp. 969–973, August 1970

For abstract, see Lovelock, J. E.

SHUMKA, A.

S029 Thermal Noise in Space-Charge-Limited Solid-State Diodes

A. Shumka

Solid-State Electron., Vol. 13, No. 6, pp. 751–754, June 1970

The spectral intensity S_o for the open-circuit noise voltage and the spectral intensity S_s for the short-circuit noise current and their interrelationship for the thermal noise in a space-charge-limited solid-state diode have been obtained by solving Langevin's equation. These results make it possible to resolve the differences between two existing theories by revealing an invalid assumption in one of them.

SIEGMETH, A. J.

**S030 Pioneer Mission Support
[by DSN, March–April 1970]**

A. J. Siegmeth

The Deep Space Network, Space Programs Summary 37-63, Vol. II, pp. 7–11, May 31, 1970

The Deep Space Network (DSN) is regularly furnishing tracking and data acquisition support for the still-active *Pioneer VI*, *VII*, *VIII*, and *IX* missions. The purpose of this support is to detect and collect telemetry data transmitted by the spacecraft, transmit commands to the spacecraft, and utilize the doppler shift of the two-way coherent S-band carrier for precision spacecraft trajectory determination. This article is concerned only with the telemetry support.

During more than four years of *Pioneer* support, the network has developed an advanced deep-space telecommunications capability encompassing a sizable segment of our solar system. Since 1966, the DSN has implemented several new subsystems in the network, all of which improved the threshold capabilities of the *Pioneer* telemetry support. Seven 85-ft-diam antenna stations were equipped with improved masers, efficient microwave plumbing, linear antenna polarizers, 3-Hz carrier tracking loops, advanced demodulation hardware, and equipment to support the onboard convolutional coding of *Pioneer IX*. Total telemetry signal-to-noise improvements of 8.5 to 10.1 dB were achieved. Both the 85-ft antenna network's *Pioneer* support range and, in a broad sense, the data return from the spacecraft have been almost doubled.

SILVER, R. H.

**S031 Evaluation of Recording Tapes for Use in
Spacecraft Magnetic Tape Recorders
[April–May 1970]**

J. K. Hoffman, S. H. Kalfayan, and R. H. Silver
Supporting Research and Advanced Development,
Space Programs Summary 37-63, Vol. III, p. 160,
June 30, 1970

For abstract, see Hoffman, J. K.

**S032 Evaluation of Spacecraft Magnetic
Recording Tapes [April–May 1970]**

S. H. Kalfayan, R. H. Silver, and J. K. Hoffman
Supporting Research and Advanced Development,
Space Programs Summary 37-63, Vol. III, pp. 209–214,
June 30, 1970

For abstract, see Kalfayan, S. H.

**S033 Evaluation of Recording Tapes for Use in
Spacecraft Magnetic Tape Recorders
[June–July 1970]**

J. K. Hoffman, S. H. Kalfayan, and R. H. Silver
Supporting Research and Advanced Development,
Space Programs Summary 37-64, Vol. III, p. 119,
August 31, 1970

For abstract, see Hoffman, J. K.

**S034 Long-Term Aging of Elastomers: Kinetics of
Oxidation of SBR by Infrared Spectroscopy**

R. Rakutis, R. H. Silver, and S. H. Kalfayan
Supporting Research and Advanced Development,
Space Programs Summary 37-64, Vol. III, pp. 125–130,
August 31, 1970

For abstract, see Rakutis, R.

**S035 Evaluation of Spacecraft Magnetic
Recording Tapes [June–July 1970]**

S. H. Kalfayan, R. H. Silver, and J. K. Hoffman
Supporting Research and Advanced Development,
Space Programs Summary 37-64, Vol. III, pp. 140–145,
August 31, 1970

For abstract, see Kalfayan, S. H.

**S036 Effects of Simulated Venusian Atmosphere
on Polymeric Materials**

S. H. Kalfayan and R. H. Silver
J. Spacecraft Rockets, Vol. 7, No. 5, pp. 634–636,
May 1970

For abstract, see Kalfayan, S. H.

SIMMONDS, P. G.

**S037 Palladium–Hydrogen System: Efficient Interface
for Gas Chromatography–Mass Spectrometry**

P. G. Simmonds, G. R. Shoemaker, and J. E. Lovelock
Anal. Chem., Vol. 42, No. 8, pp. 881–885, July 1970

The property of palladium–silver (25%) tubing to selectively diffuse hydrogen has been used to develop a new type of interface for gas chromatography–mass spectrometry. Optimum efficiency can be maintained at temperatures in excess of 200°C when the separator is placed in an oxidizing atmosphere such as

laboratory air. Catalytic reduction which was anticipated to be a potential handicap of the palladium-silver interface has been investigated and found to be specific for compounds with conjugated unsaturation such as dienes, α,β -unsaturated aldehydes, ketones, and nitriles. The palladium-silver separator was developed for a gas chromatograph-mass spectrometer instrument specifically intended for spaceflight experiments. However, its advantages of possessing a simple and rugged construction, near 100% efficiency, and a quantitative delivery of most sample substances make it attractive for more general use.

S038 The Palladium Generator-Separator—A Combined Electrolytic Source and Sink for Hydrogen in Closed Circuit Gas Chromatography

J. E. Lovelock, P. G. Simmonds, and G. R. Shoemaker
Anal. Chem., Vol. 42, No. 9, pp. 969-973, August 1970

For abstract, see Lovelock, J. E.

S039 Whole Microorganisms Studied by Pyrolysis-Gas Chromatography-Mass Spectrometry: Significance for Extraterrestrial Life Detection Experiments

P. G. Simmonds
Appl. Microbiol., Vol. 20, No. 4, pp. 567-572, October 1970

Pyrolysis-gas chromatography-mass spectrometric studies of two microorganisms, *Micrococcus luteus* and *Bacillus subtilis* var. *niger*, indicate that the majority of thermal fragments originate from the principal classes of bio-organic matter found in living systems such as protein and carbohydrate. Furthermore, there is a close qualitative similarity between the type of pyrolysis products found in microorganisms and the pyrolysates of other biological materials. Conversely, there is very little correlation between microbial pyrolysates and comparable pyrolysis studies of meteoritic and fossil organic matter. These observations will aid in the interpretation of a soil organic analysis experiment to be performed on the surface of Mars in 1975. The science payload of this landed mission will include a combined pyrolysis-gas chromatography-mass spectrometry instrument as well as several "direct biology experiments" which are designed to search for extraterrestrial life.

SIMON, M. K.

S040 On the Receiver Structure for a Single-Channel, Phase-Coherent Communication System

M. K. Simon and S. Butman
Supporting Research and Advanced Development, Space Programs Summary 37-62, Vol. III, pp. 103-108, April 30, 1970

The idea of improving the performance of a standard phase-locked-loop tracking receiver by using the power in the signal sidebands is of interest. Two structures have recently been proposed in the literature that directly make use of this idea in a single-channel, phase-coherent communication system. In this article, these two configurations are shown to be reminiscent of the limiting cases (high and low signal-to-noise ratio) of the receiver that forms the maximum *a posteriori* estimate of the RF phase.

S041 Optimum Modulation Index for a Data-Aided, Phase-Coherent Communication System

M. K. Simon
Supporting Research and Advanced Development, Space Programs Summary 37-63, Vol. III, pp. 63-66, June 30, 1970

The choice of a modulation index which minimizes error probability in a single-channel phase-coherent communication system employing a data-aided tracking loop is considered in this article. It is shown that for a fixed total energy-to-noise ratio and loop bandwidth-symbol time product, a value of modulation factor does indeed exist which minimizes the data detector's probability of error. This minimum error probability performance compares favorably with the case of ideal detection.

S042 The Effect of Limiter Suppression on Command Detection Performance

M. K. Simon
Supporting Research and Advanced Development, Space Programs Summary 37-63, Vol. III, pp. 66-70, June 30, 1970

This article evaluates the error probability penalty paid in the design of present-day vehicle transponders due to passage of the command modulation through a bandpass limiter. Based upon recent theoretical developments relative to bandpass limiters and second-order phase-locked loops, analytical results are given which enable one to compare the performance of the present design with a system which removes the command modulation prior to transmission through the limiter. Also considered is the effect of the bandpass limiter input filter bandwidth on the resulting data detector performance.

S043 An Analysis of the Phase Coherent-Incoherent Output of the Bandpass Limiter

J. C. Springett and M. K. Simon
Supporting Research and Advanced Development, Space Programs Summary 37-63, Vol. III, pp. 70-79, June 30, 1970

For abstract, see Springett, J. C.

SIMON, W.

- S044 Nozzle Exhaust Plumes in a Space Environment**
W. Simon
Supporting Research and Advanced Development,
Space Programs Summary 37-62, Vol. III, pp. 279-281,
April 30, 1970

In the space environment, the interaction of nozzle exhaust gases with spacecraft components causes problems in such diverse areas as flight mechanics, materials and structures, and communications. An experimental and analytical program to predict and characterize the nature of exhaust plumes from nozzles with relatively large internal boundary layer flows has been undertaken. This article summarizes the objectives, plan, and progress of the nozzle flow and vacuum exhaust technology program. Both JPL and contractor efforts are described; a discussion on the nozzles used and the special apparatus required to make plume measurements is also included.

SINGLETON, F. L.

- S045 SFOF Digital Television Assembly**
F. L. Singleton
The Deep Space Network, Space Programs Summary 37-65,
Vol. II, pp. 86-91, September 30, 1970

This article describes the Space Flight Operations Facility (SFOF) digital television (DTV) assembly, a part of the user terminal and display subsystem. This assembly affords 60 channels of television for real-time display of graphic and alphanumeric information. The assembly is fully compatible with the Ground Communications Facility television assembly, allowing distribution of DTV throughout the SFOF. Provision is made for capturing a hard-copy print of any selected format. Each of the 60 channels may selectively display several formats. Modular design will permit future expansion of the DTV assembly.

SJOGREN, W. L.

- S046 Loop Stress Diminution**
R. M. Goldstein, R. F. Emerson, W. L. Sjogren, and L. Sydnor
The Deep Space Network, Space Programs Summary 37-64,
Vol. II, pp. 61-67, August 31, 1970

For abstract, see Goldstein, R. M.

- S047 Lunar Gravimetrics**
P. M. Muller and W. L. Sjogren
Space Research X, pp. 975-983,
North-Holland Publishing Co., Amsterdam, 1970

For abstract, see Muller, P. M.

SKJERVE, L.

- S048 Radio Science Support [by DSN, July-August 1970]**
T. Sato, L. Skjerve, and D. Spitzmesser
The Deep Space Network, Space Programs Summary 37-65,
Vol. II, pp. 132-133, September 30, 1970

For abstract, see Sato, T.

SMITH, J. G.

- S049 Effects of Synchronization Jitter on Relay Performance**
J. G. Smith
Supporting Research and Advanced Development,
Space Programs Summary 37-62, Vol. III, pp. 118-124,
April 30, 1970

Intuitively, it may seem that detecting jittery data with a "clean" bit synchronizer would provide the same steady-state, no-cycle-slip performance as detecting clean data with a jittery bit synchronizer. It is shown that this assumption is invalid in the general case, but valid when successive jitters are completely dependent. This work was motivated by, and applied to, a lander-orbiter-earth relay communication link. The results are in terms of steady-state, no-cycle-slip performance degradation for a gaussian jitter density function.

SMITH, L. S.

- S050 TOPS Attitude-Control Single-Axis Simulator Momentum-Wheel Tachometer Circuit**
L. S. Smith
Supporting Research and Advanced Development,
Space Programs Summary 37-63, Vol. III, pp. 109-111,
June 30, 1970

The characteristics of a Bendix momentum wheel tachometer output are presented. The interfacing logic between the tachometer and the Thermoelectric Outer-Planet Spacecraft (TOPS) attitude-control single-axis simulator digital circuits is discussed.

- S051 TOPS Attitude-Control Single-Axis Simulator Command Telemetry Link**
L. S. Smith
Supporting Research and Advanced Development,
Space Programs Summary 37-64, Vol. III, pp. 74-75,
August 31, 1970

The Thermoelectric Outer-Planet Spacecraft (TOPS) single-axis simulator currently in the buildup stage uses a gas-bearing table which, by necessity, must have very low residual torque. Consequently, the digital attitude-control system located on the table should

receive ground site commands via means producing no mechanical torque. This article describes the capacitive coupling technique being used to deliver digital commands to the table.

SOLLOWAY, C. B.

S052 Brute-Force Least-Squares Estimation

W. G. Melbourne and C. B. Solloway
Supporting Research and Advanced Development,
Space Programs Summary 37-62, Vol. III, pp. 282-285,
April 30, 1970

For abstract, see Melbourne, W. G.

SOMOANO, R.

S053 Kinetics of Formation of High Charge Density Ionene Polymers [February-March 1970]

A. Rembaum, H. Rile, and R. Somoano
Supporting Research and Advanced Development,
Space Programs Summary 37-62, Vol. III, pp. 235-240,
April 30, 1970

For abstract, see Rembaum, A.

S054 Kinetics of Formation of High Charge Density Ionene Polymers

A. Rembaum, H. Rile, and R. Somoano
J. Polym. Sci., Pt. B: Polym. Lett., Vol. 8, No. 7, pp. 457-466,
July 1970

For abstract, see Rembaum, A.

S055 Electronic Conductivity of Elastomeric Ionenenes

R. Somoano, S. P. S. Yen, and A. Rembaum
J. Polym. Sci., Pt. B: Polym. Lett., Vol. 8, No. 7, pp. 467-479,
July 1970

The reaction between N,N,N',N'-tetramethyl- α , ω -diaminoalkanes and α , ω -dihaloalkanes leads under suitable conditions to ionene polymers of weight average molecular weight in the range of 10,000 to 40,000. However, all these polymers consist of crystalline materials exhibiting well-defined X-ray diffraction patterns. Their electrical room temperature resistivity, after reaction with LiTCNQ, was found to be of the order of 10^4 to 10^7 ohm-cm and could be reduced to about 10^2 ohm-cm by addition of neutral tetracyanoquinodimethane (TCNQ).

Because of the great interest in conducting elastomers, a previously used quaternization reaction was applied to commercial "prepolymers" containing oxypropylene as a unit segment. The synthesis was based on the reaction of polypropylene glycol with tolylene diisocya-

nate and subsequent chain extension by means of dimethylamino ethanol and a dihalide. The general reaction scheme permitted the preparation of a series of elastomeric ionenes containing a variable concentration of positive charges located on quaternary nitrogen atoms. The different structure and the relatively low concentration of positive charges in these materials, as compared with those synthesized previously, are responsible for the rubbery properties. The electrical properties of elastomeric ionenes complexed with LiTCNQ are reported here. The study of electrical resistivity as a function of temperature revealed definite breaks in the resistivity temperature curves which could be related to the glass transition temperature of some of the materials.

SPITZMESSER, D.

S056 Radio Science Support [by DSN, March-April 1970]

T. Sato and D. Spitzmesser
The Deep Space Network, Space Programs Summary 37-63,
Vol. II, pp. 98-101, May 31, 1970

For abstract, see Sato, T.

S057 Radio Science Support [by DSN, July-August 1970]

T. Sato, L. Skjerve, and D. Spitzmesser
The Deep Space Network, Space Programs Summary 37-65,
Vol. II, pp. 132-133, September 30, 1970

For abstract, see Sato, T.

SPRINGETT, J. C.

S058 Preliminary System Testing of the Proposed TOPS All-Digital Command Detection Algorithm

J. C. Springett and W. J. Weber
Supporting Research and Advanced Development,
Space Programs Summary 37-62, Vol. III, pp. 93-99,
April 30, 1970

An all-digital command detection/synchronization algorithm has been proposed as a potential solution to the problems of long life and high reliability required by the Thermoelectric Outer-Planet Spacecraft (TOPS) and other outer-planet programs. To assess the potential system performance, an experimental program using computer simulation of the algorithm was undertaken. The results show the detector performance to be within 0.5 dB and the system performance (including RF) to be within 1.5 dB of the theoretical signal-to-noise ratio required to achieve a bit error rate of one in 10^5 trials.

S059 An Analysis of the Phase Coherent-Incoherent Output of the Bandpass Limiter

J. C. Springett and M. K. Simon

Supporting Research and Advanced Development,
Space Programs Summary 37-63, Vol. III, pp. 70-79,
June 30, 1970

Many applications of the bandpass limiter involve coherent demodulation following the limiter. It is shown that as a result of demodulation the signal mean and the noise variance are direct functions of the phase angle between the signal component passed by the bandpass limiter and the coherent reference. As a result, the relationship between the output and input signal-to-noise ratio may be significantly different than that obtained by Davenport for incoherent limiters. A study is also made of the output noise spectral density, and an approximate expression is derived as a function of the input signal-to-noise ratio, reference phase angle, and the characteristics of the input bandpass filter to the limiter. Also discussed is the first-order signal-plus-noise probability density following coherent demodulation.

SQUYRES, H. P.

S060 Uniform Variable Light Sources for Instrument Calibration

H. P. Squyres and J. J. Rennilson

Technical Report 32-1470 (Reprinted from *Appl. Opt.*,
Vol. 9, No. 5, pp. 1092-1096, May 1970)

This paper describes light sources that were developed for use in calibrating cameras for space exploration. The design produces a nearly uniform luminance field whose correlated color temperature ranges from 4000 K to 5000 K in the visible. Luminance of the source may be continuously varied by as much as 500:1 without affecting the uniformity of the field. The sources, consisting basically of two integrating cavities with an iris diaphragm interposed, use xenon light. Luminances as high as 25,000 cd m⁻² are possible. Such sources are used for light-transfer calibration, as well as spectral response of camera systems. After a brief theoretical treatment, the design variations are discussed. Measurement data on these sources indicates that the angular luminance distribution approximates a uniform diffuser within a 50-deg cone.

STAVRO, W.

S061 Possible 1975 Jupiter-Pluto Gravity Assist Trajectories

W. Stavro

Supporting Research and Advanced Development,
Space Programs Summary 37-63, Vol. III, pp. 236-239,
June 30, 1970

A preliminary analysis of a 1975 Jupiter-Pluto mission was performed. A patched conic computer program SPARC was used to search for any possible trajectories. Two kinds of trajectories were found to be possible: (1) those with very high injection energy C_3 and very short launch period (ridge), and (2) those that have Type II Earth-Jupiter legs with very long flight times. Characteristics and plots of these trajectories are given. It is concluded that even though the trajectories are possible the mission is not feasible.

STELZRIED, C. T.

S062 A Faraday Rotation Measurement of a 13-cm Signal in the Solar Corona

C. T. Stelzried

Technical Report 32-1401, July 15, 1970

The goal of this experiment was to further the scientific knowledge of the solar corona by measuring the Faraday rotation of a 2292-MHz continuous wave signal in this plasma.

The *Pioneer VI* spacecraft was launched into a circumsolar orbit on December 16, 1965, and was occulted by the sun in the last half of November, 1968. During the occultation period, the 2292-MHz S-band telemetry carrier wave underwent Faraday rotation due to the interaction of this signal with the plasma and magnetic field in the solar corona. The 210-ft-diam Goldstone Mars station antenna of the Deep Space Network located near Barstow, Calif. was used for the measurement. The antenna feed was modified for automatic polarization tracking for this experiment. This modification is described and the performance evaluated.

Three large-scale transient Faraday rotation phenomena were observed on November 4, 8, and 12. These phenomena typically lasted about 2 h and produced Faraday rotations on the order of 40 deg. Correlation with dekametric solar radio bursts was noted and the implied solar wind velocity estimated.

A steady-state Faraday rotation was observed, commencing at about 10 solar radii on the west limb of the sun. The rotation increased steadily as the ray path approached the sun. At 4 solar radii polarization had rotated over 125 deg. The signal could not be tracked closer to the sun because of the loss in receiver sensitivity caused primarily by the increased system noise temperature. The increase in system noise temperature was due to the antenna side lobes "seeing" the sun. Further loss in sensitivity was due to the spectral broadening of the signal caused by highly random motion of the excited plasma close to the sun. The rotation was of nearly equal magnitude

upon exit on the east limb of the sun but of opposite sense in the outer region.

The steady-state measurement is compared with a theoretical model of the solar corona using a modified Allen-Baumbach electron density and the coronal magnetic field as derived from the Mount Wilson optical solar magnetograph and the *Explorer 33* satellite magnetometer. Although the calculated rotation and the experimental data show general agreement with respect to the magnitude, sense, and timing of the rotation, an improved fit is obtained with an assumed equatorial electron density (in m^{-3})

$$N = 10^{14} \left(\frac{6000}{R^{10}} + \frac{0.002}{R^2} \right), \quad (4 < R < 12)$$

with R in solar radii.

S063 The Ionospheric Electron Content as Determined From Faraday Rotation Measurements of an Earth Satellite and Deep-Space Probe

B. D. Mulhall and C. T. Stelzried

The Deep Space Network, Space Programs Summary 37-64, Vol. II, pp. 21-24, August 31, 1970

For abstract, see Mulhall, B. D.

S064 Tracking and Data Acquisition Elements Research: Improved RF Calibration Techniques—System Operating Noise Temperature Calibrations of Low Noise Cones

M. S. Reid and C. T. Stelzried

The Deep Space Network, Space Programs Summary 37-64, Vol. II, pp. 69-70, August 31, 1970

For abstract, see Reid, M. S.

S065 A Noise-Adding Radiometer for Use in the DSN

P. D. Batelaan, R. M. Goldstein, and C. T. Stelzried

The Deep Space Network, Space Programs Summary 37-65, Vol. II, pp. 66-69, September 30, 1970

For abstract, see Batelaan, P. D.

S066 Precision Microwave Waveguide Loss Calibrations

C. T. Stelzried

IEEE Trans. Instrumentation and Measurement, Vol. IM-19, No. 1, pp. 23-25, February 1970

Precision microwave insertion-loss measurements are an important part of the evaluation and calibration of the JPL-NASA low-noise deep-space communication systems. A study of cooled transmission-line components was initiated with the Rantec Corporation in July 1966; the preliminary work involved WR430 waveguide insertion-loss calibrations using a microwave cavity Q technique. JPL verified the technique

by repeating the calibration using a direct insertion-loss measurement technique between matched components. The JPL measurements are described in detail, and the critical areas identified. The difference between the reported JPL (0.00427 dB) and Rantec (0.00414 dB) measurements of 0.00013 dB is within experimental accuracies and adds to the confidence factor of both measurement techniques.

S067 Comparisons of Waveguide Losses Calibrated by the DC Potentiometer, AC Ratio Transformer, and Reflectometer Techniques

T. Y. Otoshi, C. T. Stelzried, B. C. Yates (National Bureau of Standards), and R. W. Beatty (National Bureau of Standards)
IEEE Trans. Microwave Theory and Techniques, Vol. MTT-18, No. 7, pp. 406-409, July 1970

For abstract, see Otoshi, T. Y.

STEPHENSON, R. R.

S068 Earthbased Tracking and Orbit Determination—Backbone of the Planetary Navigation System

D. W. Curkendall and R. R. Stephenson

Astronaut. Aeronaut., Vol. 7, No. 5, pp. 30-36, May 1970

For abstract, see Curkendall, D. W.

STIMPSON, L. D.

S069 Outer-Planet Infrared Radiometer Cooling

L. D. Stimpson

Supporting Research and Advanced Development, Space Programs Summary 37-62, Vol. III, pp. 192-195, April 30, 1970

An infrared detector cooled to a temperature of 20°K is a potential requirement for outer-planet spacecraft missions. Estimates are made of the heat leaks into the cooled detector from electrical power and from infrared radiation from the planet and the instrument interior, as well as heat conducted in through structural supports and electrical cabling. Based on these estimates, passive radiation alone will be inadequate, and active cooling will be needed.

STIRN, R. J.

S070 Contacts to Photoconducting Cadmium Sulfide

R. J. Stirn

Supporting Research and Advanced Development, Space Programs Summary 37-62, Vol. III, pp. 151-153, April 30, 1970

The stationary high-field-domain analysis of blocking contacts to photoconducting cadmium sulfide has

been extended from 155 to 80°K. No deviation from the previously reported contact behavior (barrier lowering) was found. The measured electric field within the domain showed a maximum in its value at about 180°K, in agreement with some independent calculations. Measurements of the current kinetics upon sudden application of a voltage step were also extended to include several temperatures and light excitation densities under improved experimental conditions. An extension to a previously proposed qualitative model for the barrier lowering is presented.

STRAND, J. N.

S071 Tests of Instruments Proposed for the Scientific Payload of a Lunar Rover

J. N. Strand

Supporting Research and Advanced Development, Space Programs Summary 37-62, Vol. III, pp. 15-18, April 30, 1970

The testing of instruments proposed for the scientific payload of a lunar rover, using the testing philosophy of the Science Experiment Test Laboratory, is discussed. The instruments tested to date include a television camera, a surface sampler, an auger system, and a combination chipper-and-tongs device.

STRAND, L.

S072 Study of the Effects of Heat Sterilization and Vacuum Storage on the Ignition of Solid Propellant Rockets

L. Strand, J. A. Mattice, and J. W. Behm

Supporting Research and Advanced Development, Space Programs Summary 37-63, Vol. III, pp. 196-206, June 30, 1970

A program was conducted to determine the effects of heat sterilization and vacuum storage on the ignition characteristics and performance of typical state-of-the-art solid propellant igniters and igniter materials. The ignition characteristics of a JPL propellant specifically developed to survive heat sterilization cycling were also investigated. The results of various measurements and tests conducted on heat-cycled (three and six heat cycles: 56 h at 275°F per cycle) and vacuum-stored (6 mo at 10^{-7} torr) samples were compared with those for control samples of the same materials. Heat sterilization was found to have small, but measurable, effects on the ignition characteristics of the materials tested. Similar tests on the materials that had undergone vacuum storage did not reveal any distinct effects of the exposure.

SUGAWARA, M.

S073 Drift Velocities of Electrons in the Positive Column of a Neon Discharge

M. Sugawara and C. J. Chen

J. Appl. Phys., Vol. 41, No. 8, pp. 3442-3445, July 1970

Drift velocities of electrons in a gaseous neon plasma have been obtained by measuring the discharge current, radial density profile of electrons, and axial electric field in the positive column of a neon discharge for E/n_a (V-cm²) values ranging between 2.8×10^{-17} and 2.4×10^{-16} at a temperature of 300°K. The data agree very well with that of the previous workers. The validity of the Langmuir probe measurement for the electron densities in this experiment is discussed in detail.

SWARD, A.

S074 Frequency Generation and Control: The Measurement of Phase Jitter

R. Meyer and A. Sward

The Deep Space Network, Space Programs Summary 37-64, Vol. II, pp. 55-58, August 31, 1970

For abstract, see Meyer, R.

S075 Frequency Generation and Control: Analysis of Random Modulation in Amplifier Circuits

A. Sward and G. Thompson

The Deep Space Network, Space Programs Summary 37-65, Vol. II, pp. 50-55, September 30, 1970

The development of the hydrogen maser as a frequency standard for the Deep Space Network requires that the performance of distribution circuitry be re-evaluated. The hydrogen maser output is so nearly an ideal sinusoid that degradation of the signal in an amplifier becomes important. In this article, a theoretical analysis of random amplitude and phase modulation of a sinusoidal carrier is developed. A measure, \mathcal{Q} , of the degradation from the ideal signal is defined. In amplifiers, power spectra with a $1/f$ behavior are of primary interest; for these spectra, the functional behavior of \mathcal{Q} indicates a design criterion to minimize the contributions of undesirable amplitude and phase modulation.

SYDNOR, L.

S076 Loop Stress Diminution

R. M. Goldstein, R. F. Emerson, W. L. Sjogren, and L. Sydnor

The Deep Space Network, Space Programs Summary 37-64, Vol. II, pp. 61-67, August 31, 1970

For abstract, see Goldstein, R. M.

TAHERZADEH, M.

T001 Analytical Calculation of the Neutron Yield From (α, n) Reactions of Low-Z Impurities

M. Taherzadeh

Supporting Research and Advanced Development, Space Programs Summary 37-64, Vol. III, pp. 60-63, August 31, 1970

The neutron yield generated by the interaction of α -particles emitted from the plutonium fuel heat source with low-Z impurities existing in the fuel is presented. Due to the height of the nuclear potential barrier in high-Z impurities for 5.5-MeV α -particles, the expected neutron yield is much smaller than with low-Z materials. The neutron yield per one part per million of the low-Z impurities is given. The total neutron yield due to the combined effects of all the impurities depends upon the fractional weight contribution of each impurity.

TAM, M. K.

T002 The Probability Density Function of a Hardware Performance Parameter

C. E. Gilchrist and M. K. Tam (Tam Research Associates)
Technical Memorandum 33-439, September 1, 1970

For abstract, see Gilchrist, C. E.

TAYLOR, H.

T003 Combinatorial Communication: Ramsey Bounds for the Coefficients of Internal Stability of Graph Products

R. J. McEliece and H. Taylor

Supporting Research and Advanced Development, Space Programs Summary 37-62, Vol. III, pp. 62-63, April 30, 1970

For abstract, see McEliece, R. J.

THACKER, H. B.

T004 Superconducting Josephson Junctions Fabricated on Anodized Tantalum Substrates

P. V. Mason and H. B. Thacker

Supporting Research and Advanced Development, Space Programs Summary 37-62, Vol. III, pp. 212-213, April 30, 1970

For abstract, see Mason, P. V.

THOMPSON, G.

T005 Frequency Generation and Control: Analysis of Random Modulation in Amplifier Circuits

A. Sward and G. Thompson

The Deep Space Network, Space Programs Summary 37-65, Vol. II, pp. 50-55, September 30, 1970

For abstract, see Sward, A.

T006 Frequency Generation and Control: Angle Demodulation Using State-Variable Techniques

G. Thompson

The Deep Space Network, Space Programs Summary 37-65, Vol. II, pp. 55-61, September 30, 1970

Deep space communication receivers for multiple-sideband angle modulation become difficult to analyze as the number of sidebands increases. Analysis that uses state-variable techniques is ideally suited to formulating problems involving large systems of random processes. When applied to sinusoidal angle modulation, the state-variable approach yields a realizable demodulator that is optimum in the minimum-mean-square-error sense at high signal-to-noise ratios. The receiver structure and error covariance above threshold are the direct results of the analysis.

This article applies the state-variable concept to the problem of sinusoidal angle modulation and shows that the resulting receiver is optimum at high signal-to-noise ratios. Two examples are given to illustrate the technique and show its equivalence in the steady state to the Wiener optimum filter.

THORNTON, T. H., JR.

T007 Strategies and Systems for Navigation Corrections

W. E. Dorroh, Jr., and T. H. Thornton, Jr.

Astronaut. Aeronaut., Vol. 7, No. 5, pp. 50-55, May 1970

For abstract, see Dorroh, W. E., Jr.

THULEEN, K. L.

T008 Variations in the Zenith Tropospheric Range Effect Computed From Radiosonde Balloon Data

V. J. Ondrasik and K. L. Thuleen

The Deep Space Network, Space Programs Summary 37-65, Vol. II, pp. 25-35, September 30, 1970

For abstract, see Ondrasik, V. J.

T009 The Effect of the Diurnal Variation of the Earth's Ionosphere on Interplanetary Navigation

B. D. Mulhall and K. L. Thuleen

The Deep Space Network, Space Programs Summary 37-65, Vol. II, pp. 35-39, September 30, 1970

For abstract, see Mulhall, B. D.

TIMOR, U.

**T010 Coding and Synchronization Research:
Interplex—An Efficient Two-Channel Telemetry
System for Space Exploration**

S. Butman and U. Timor

*Supporting Research and Advanced Development,
Space Programs Summary 37-62, Vol. III, pp. 57–60,
April 30, 1970*

For abstract, see Butman, S.

**T011 Coding and Synchronization Research: Efficient
Multichannel Space Telemetry**

S. Butman and U. Timor

*Supporting Research and Advanced Development,
Space Programs Summary 37-63, Vol. III, pp. 34–37,
June 30, 1970*

For abstract, see Butman, S.

**T012 Coding and Synchronization Research: Decision
Rules for a Two-Channel Deep-Space
Telemetry System**

S. Butman, J. E. Savage (Brown University), and U. Timor

*Supporting Research and Advanced Development,
Space Programs Summary 37-63, Vol. III, pp. 38–41,
June 30, 1970*

For abstract, see Butman, S.

**T013 Space Station Unified Communication:
Suppressed-Carrier Two-Channel
Interplex Modulation System**

U. Timor and S. Butman

*Supporting Research and Advanced Development,
Space Programs Summary 37-64, Vol. III, pp. 27–31,
August 31, 1970*

Digital phase-modulated coherent communication systems require, in general, a certain amount of unmodulated signal to track the phase. This RF power reduces the available power for data transmission. In the case of single-channel systems, this loss of data power can be avoided by using the Costas loop or the squaring loop. However, these methods fail in case of two data channels, unless the ratio of powers in the two channels is large. For example, in the Manned Space Station, there are likely to be several high-rate channels of approximately equal power. This article presents a method for tracking the phase of a suppressed carrier two-channel Interplex system. It is shown that the performance is independent of the allocation of data power in the channels, and is superior to unsuppressed carrier systems.

T014 Design of Signals for Analog Communication

U. Timor (University of California, Berkeley)

IEEE Trans. Information Theory, Vol. IT-16, No. 5,
pp. 581–587, September 1970

A method for the design of time-limited and effectively band-limited waveforms for analog communication systems is developed. The design problem is first formulated in the $L_2(0, T)$ space. Nonlinear modulation threshold effects are incorporated directly into the design by introducing constraints in the form of minimum distance between points on the locus. It is shown that all pertinent information can be expressed in terms of the inner product function generated by the locus and its cross derivative. The design is then transformed into a constrained minimization problem in a space of inner product functions. The cases of stationary locus and N -dimensional locus are further investigated.

**T015 An Upper Bound on the Estimation Error in the
Threshold Region**

U. Timor

IEEE Trans. Information Theory, Vol. IT-16, No. 6,
pp. 692–699, November 1970

An upper bound on the estimation error in the threshold region (probability of threshold effect and mean-square error) is obtained for nonlinear pulse modulation systems. The problem is viewed in an N -dimensional Euclidean space. The space of all received signals is divided into two regions, corresponding to the two types of error: weak-noise approximation and threshold effect. The threshold region is geometrically upper bounded by a larger region, and the estimation error is obtained as a sum of incomplete Γ functions. The resulting bounds on the mean-square error were found to be quite close for the cases calculated. An extension of the method to a PPM system is also presented.

TRAJMAR, S.

**T016 Vibrational Excitation of H_2 by Low- and
Medium-Energy Electrons**

S. Trajmar, D. G. Truhlar (California Institute of Technology), J. K. Rice (California Institute of Technology), and A. Kuppermann (California Institute of Technology)
*Supporting Research and Advanced Development,
Space Programs Summary 37-62, Vol. III, pp. 36–43,
April 30, 1970*

The excitation of molecular vibration by electron impact is discussed, with special emphasis on H_2 . Examples of experimental measurements of the elastic

and vibrational excitation cross sections, as well as the calculation of these cross sections by a potential scattering model, are presented. The experimental measurements covered the 7- to 82-eV energy and 0- to 90-deg angular ranges, and calculations were carried out for the 1- to 1000-eV energy range over all angles.

T017 Electron Impact Excitation of N₂

R. T. Brinkmann and S. Trajmar
Supporting Research and Advanced Development,
Space Programs Summary 37-62, Vol. III, pp. 47-53,
April 30, 1970

For abstract, see Brinkmann, R. T.

T018 Vibrational Excitation of N₂ and CO by Electron Impact

W. Williams and S. Trajmar
Supporting Research and Advanced Development,
Space Programs Summary 37-62, Vol. III, pp. 53-56,
April 30, 1970

For abstract, see Williams, W.

T019 Electron Scattering by H₂ With and Without Vibrational Excitation: II. Experimental and Theoretical Study of Elastic Scattering

S. Trajmar, D. G. Truhlar (California Institute of Technology), and J. K. Rice (California Institute of Technology)
J. Chem. Phys., Vol. 52, No. 9, pp. 4502-4515, May 1, 1970

Elastic scattering of electrons by the hydrogen molecule has been studied. The differential elastic cross sections have been determined experimentally from 10 to 80 deg at seven impact energies ranging from 7 to 81.6 eV. The experimental methods for measuring the relative elastic scattering intensities, the transformation of these intensities into relative cross sections, and their normalization to the absolute scale are presented. The elastic differential and integral cross sections have also been calculated in this energy range by the quantum-mechanical method described in Part I of this report. A comparison is made between the experimental and calculated cross sections and, whenever possible, with the results of other investigators. It is found that, in the energy and angular ranges investigated here, polarized Born and polarized Born-Ochkur-Rudge approximations using the theoretically most justified potential give better agreement with experiment than any previous calculation and that the inclusion of polarization is necessary to obtain accurate cross sections at low scattering angles.

T020 Electron Scattering by H₂ With and Without Vibrational Excitation: III. Experimental and Theoretical Study of Inelastic Scattering

S. Trajmar, D. G. Truhlar (California Institute of Technology), J. K. Rice (California Institute of Technology), and A. Kuppermann (California Institute of Technology)
J. Chem. Phys., Vol. 52, No. 9, pp. 4516-4533, May 1, 1970

The ratios of the differential cross sections (DCSs) for excitation of the first, second, and third vibrational states of H₂ in its ground electronic state to the elastic DCS have been measured as a function of scattering angle in the 10- to 80-deg range and impact energy in the 7- to 81.6-eV range. From these ratios, the DCSs corresponding to transitions from the ground to the first two vibrationally excited levels (fundamental and first overtone bands) were obtained by utilizing the elastic cross sections determined in Part II of this report. In addition, the DCS for excitation of the second overtone band was determined for an impact energy of 10 eV. By angular extrapolation and integration of the DCSs, the integral cross sections for the vibrational excitations were also determined. In addition, all these cross sections have been calculated using a quantum-mechanical method based on potential scattering in a plane wave scattering approximation, which was described in Part I of this report. The present experimental and theoretical cross sections are compared and previous measurements and calculations are compared. The calculated DCS ratios and the DCSs themselves for the fundamental excitation are in good agreement with experiment at 7 and 10 eV; however, at higher energies, the calculated DCSs are generally larger than the experimental ones, at some angles by as much as a factor of 10. The calculated ratio of the DCS for the fundamental excitation to the elastic DCS shows a minimum as a function of angle, in qualitative agreement with the experimental results in the 13.6- to 81.6-eV energy range. The experimental DCSs for vibrational excitation also show a deep minimum. For excitation of the first overtone vibration, the experimental ratios are an order of magnitude larger than the calculated ones at low energy, but in better agreement for the magnitude at higher energy. This discrepancy at low energies is explained in terms of resonance scattering. These experiments are in good agreement with others reported elsewhere in the few (low-energy) cases where comparison is possible.

TRUBERT, M. R.

T021 A Frequency Domain Solution for the Linear Attitude-Control Problem of Spacecraft With Flexible Appendages

M. R. Trubert
Technical Report 32-1478, November 15, 1970

The three-dimensional linear interaction problem between attitude control of spacecraft and the flexibility of spacecraft is solved in the frequency domain by using the concept of Fourier transform. The transfer-function matrix of the system formed by the linear structure and the linear control circuit is determined from the modal characteristics of the structure, using the modal combination concept and the electrical characteristics of the control loop. A large number of elastic modes can be used for the structure. Time histories are obtained by inverse Fourier transformation. The three angles of the attitude of the spacecraft with respect to an inertial frame of reference are computed for any disturbance torques applied about the three axes of the spacecraft. A stability study is made by direct inspection of the responses to unit impulse for the three attitude angles or, alternatively, by the display of a determinant. A computer program has been written to compute all of the necessary transfer functions, and the last Fourier transform algorithm has been used to compute Fourier transforms. The program is used on a teletype terminal.

TRUHLAR, D. G.

T022 Vibrational Excitation of H₂ by Low- and Medium-Energy Electrons

S. Trajmar, D. G. Truhlar (California Institute of Technology), J. K. Rice (California Institute of Technology), and A. Kuppermann (California Institute of Technology), *Supporting Research and Advanced Development, Space Programs Summary 37-62, Vol. III, pp. 36-43, April 30, 1970*

For abstract, see Trajmar, S.

T023 Electron Scattering by H₂ With and Without Vibrational Excitation: II. Experimental and Theoretical Study of Elastic Scattering

S. Trajmar, D. G. Truhlar (California Institute of Technology), and J. K. Rice (California Institute of Technology), *J. Chem. Phys., Vol. 52, No. 9, pp. 4502-4515, May 1, 1970*

For abstract, see Trajmar, S.

T024 Electron Scattering by H₂ With and Without Vibrational Excitation: III. Experimental and Theoretical Study of Inelastic Scattering

S. Trajmar, D. G. Truhlar (California Institute of Technology), J. K. Rice (California Institute of Technology), and A. Kuppermann (California Institute of Technology), *J. Chem. Phys., Vol. 52, No. 9, pp. 4516-4533, May 1, 1970*

For abstract, see Trajmar, S.

TRUSCELLO, V. C.

T025 Interactions Between Radiation Fields From Radioisotope Thermoelectric Generators and Scientific Experiments on Spacecraft

C. G. Miller and V. C. Truscello
Nucl. Appl. Technol., Vol. 9, No. 5, pp. 722-735, November 1970

For abstract, see Miller, C. G.

TUSTIN, D. G.

T026 Network Allocation Schedules

D. G. Tustin
The Deep Space Network, Space Programs Summary 37-64, Vol. II, pp. 105-106, August 31, 1970

This article describes the network allocation scheduling method currently used by the Deep Space Network to provide for long-range planning, network resource sizing, detailed user commitment generation, and operational scheduling. Each of the various levels of scheduling and the means by which these levels fit together to function as an integrated system are discussed.

UDLOCK, D.

U001 Low-Modulus Propellant for Case-Bonded, End-Burning Motors

H. E. Marsh, Jr., and D. Udlock
Supporting Research and Advanced Development, Space Programs Summary 37-63, Vol. III, pp. 184-188, June 30, 1970

For abstract, see Marsh, H. E., Jr.

UNTI, T.

U002 Magnetospheric Flows and Their Time Dependence

T. Unti and G. Atkinson
Supporting Research and Advanced Development, Space Programs Summary 37-62, Vol. III, p. 53, April 30, 1970

A two-dimensional model of the magnetosphere, incorporating a magnetic tail and perfect neutral sheet, has been used to study magnetospheric flows. In this article, the model is used to determine the response of the magnetosphere to fluctuations in the solar wind. The results of this study indicate that: (1) the large-scale flow is usually determined by the rate at which field lines are carried into the tail, (2) reconnection of tail field lines at the neutral sheet significantly affects the flow only if it occurs in bursts, and (3)

changes in solar wind momentum flux produce a significant flow only if they are of an order of magnitude ≤ 10 min. The magnetosphere response to solar wind "signals" depends on two time constants of the magnetosphere.

URECH, J. M.

U003 Telemetry Improvement Proposal for the 85-ft Antenna Network

J. M. Urech

The Deep Space Network, Space Programs Summary 37-63, Vol. II, pp. 116-120, May 31, 1970

Since most of the spacecraft currently being tracked at the Madrid stations are either near or below the telemetry threshold, studies and tests have been carried out to ascertain the possibility of combining two or more stations to improve telemetry performance. The studies show that telemetry performance can be improved by several decibels, depending on which of the proposed methods of combination is selected. An increase of 3 dB over a normal two-way tracking station can be obtained with the combined tracking of two identical stations—one in normal two-way (acting as prime) and the other in three-way (acting as booster). With the configuration of one station in a *receive only* mode (with diplexer bypass) acting as the "booster station," a 4.75-dB improvement may be obtained.

VOLKOFF, J. J.

V001 Irradiance Required to Cause Damage to Developed Photographic Film

J. J. Volkoff

The Deep Space Network, Space Programs Summary 37-63, Vol. II, pp. 47-52, May 31, 1970

A noticeable change in the photometric and physical properties of a developed photographic film is found to be a function of the irradiance level and the period of exposure imposed upon the film. Results show that developed black and white film may be irradiated up to an energy density of 10^5 W-s/cm² without causing an apparent photometric degradation.

V002 Contrast Ratio Determination for the SFOF Video Image Display

J. J. Volkoff

The Deep Space Network, Space Programs Summary 37-65, Vol. II, pp. 91-93, September 30, 1970

The Space Flight Operations Facility (SFOF) Mark III central processing system will include a video image display subsystem that will display and print tonal images through video processing of digital image data.

The images will be displayed on high-resolution monitors having the capability to display a large number of discernible grayshades requiring a minimum contrast ratio for a given monitor configuration and ambient light condition. This article is concerned with the effect of ambient light upon the contrast ratio and upon the output light of the display.

WALKER, B.

W001 Aerodynamics of Vehicles in Tubes

B. Walker and B. Dayman, Jr.

Supporting Research and Advanced Development, Space Programs Summary 37-62, Vol. III, pp. 216-218, April 30, 1970

Many transportation systems are currently being studied that require vehicles to operate in tunnels (tubes) under conditions of high blockage. An understanding of the aerodynamic characteristics of such transportation systems is necessary to design systems that utilize vehicles in tunnels, which in turn will make it possible to select an optimum transportation system. This article describes a facility in which aerodynamic studies of vehicles in tubes can be performed.

WALMSLEY, D. E.

W002 Investigation of Sterilizable Battery Separator Membranes [June-July 1970]

E. F. Cuddihy, D. E. Walmsley, and J. Moacanin

Supporting Research and Advanced Development, Space Programs Summary 37-64, Vol. III, pp. 136-138, August 31, 1970

For abstract, see Cuddihy, E. F.

WARD, S. C.

W003 A Time-Synchronized VLF Phase-Tracking Receiver

S. C. Ward

The Deep Space Network, Space Programs Summary 37-63, Vol. II, pp. 108-112, May 31, 1970

Frequency offset and stability information is achieved directly through the phase tracking of very low frequency (VLF) transmissions. Time synchronization is indirectly maintained using these data. At present, keyed VLF transmissions contain both primary time and frequency information; however the VLF receiver presently used by the Deep Space Network cannot be used on keyed broadcasts in areas of high interference or low signal level. More meaningful time data and a great improvement in signal-to-noise ratio of primary frequency data can be achieved by time-code-keying the VLF receiver while tracking WWVL

transmissions. This article discusses the exploitation of WWVL as a worldwide source of a frequency reference.

WARD, S. H.

W004 Dipole Antenna Radiation in a Compressible, Anisotropic Electron Plasma Overlying an Imperfectly Conducting Half-Space—Lunar Applications: 1. Formulation of the Solution; 2. Integration and Results

R. J. Phillips and S. H. Ward (University of California, Berkeley)

Radio Sci., Vol. 5, No. 5, pp. 821–839, May 1970

For abstract, see Phillips, R. J.

WEBER, R. L.

W005 Canberra Microwave Link Relocation

R. L. Weber

The Deep Space Network, Space Programs Summary 37-63, Vol. II, pp. 61–63, May 31, 1970

Construction of the new 210-ft antenna at the Tidbinbilla Deep Space Station (Australia) has caused blockage of the radio frequency path of the Manned Space Flight Network (MSFN) backup wing to the prime site microwave link. MSFN backup wing tracking commitments for future *Apollo* missions, such as *Apollo 13* in mid-April, presented an urgent need to replace or relocate the existing microwave link. The link relocation was completed in the required time-span by relocating the equipment at the Tidbinbilla Deep Space Station end of the microwave link.

WEBER, W. J.

W006 Preliminary System Testing of the Proposed TOPS All-Digital Command Detection Algorithm

J. C. Springett and W. J. Weber

Supporting Research and Advanced Development, Space Programs Summary 37-62, Vol. III, pp. 93–99, April 30, 1970

For abstract, see Springett, J. C.

WELLS, R. A.

W007 Diagnostics for the SFOF Mark IIIA Central Processing System: Standalone Acceptance and Maintenance Routines

R. A. Wells

The Deep Space Network, Space Programs Summary 37-65, Vol. II, pp. 97–99, September 30, 1970

This article summarizes the history and current status of diagnostic development for Space Flight Operations Facility (SFOF) central-processing-system subsystems having main processors that can be operated independently of the 360/75 computers. These routines are employed for hardware checkout and equipment acceptance where vendor-furnished diagnostics are unavailable. Particular attention is given to the digital TV assembly, the mission display board, the simulation center, and the SFOF/Ground-Communications-Facility high-speed/wideband data interfaces.

WENGERT, R.

W008 Multiple Mission Telemetry 1971 Configuration

W. Frey, R. Petrie, R. Greenberg, J. McInnis, and R. Wengert
The Deep Space Network, Space Programs Summary 37-63, Vol. II, pp. 63–77, May 31, 1970

For abstract, see Frey, W.

WICK, H.

W009 Design of a Thick-Film Microcircuit DC-to-DC Converter

H. Wick and S. Capodici (General Electric Co.)

Supporting Research and Advanced Development, Space Programs Summary 37-64, Vol. III, pp. 64–67, August 31, 1970

Thick-film microcircuit techniques have been utilized in the electronic portion of a dc-to-dc converter. This packaging approach for the converter electronics reduced the weight by 70%, the volume by 80%, and the number of external interconnections with the remaining converter piece parts by 75%. Additionally, the uniform manufacturing procedures and in-process controls lead to an inherently more reliable device, protected from contamination by a hermetic seal. The close piece-part spacing allowed short interconnections, lower dissipation, and reduced the opportunity for noise coupling into adjacent circuitry. The developed microcircuit was applied to handle total power levels from 1 to approximately 25 W, requiring a change in the discrete values of only 7 piece-parts for an output power level change.

WIEBE, E. R.

W010 Low Noise Receivers: Microwave Maser Development [July–August 1970]

E. R. Wiebe

The Deep Space Network, Space Programs Summary 37-65, Vol. II, pp. 62–63, September 30, 1970

An instrument for automatically recording the reserve heat capacity of maser closed-cycle refrigerators that

has been built and tested at JPL is described. Using this device, the overall health of closed-cycle refrigerator systems in the field can easily be monitored between tracking periods. The measurement of reserve heat capacity is performed with higher accuracy and greater speed than is possible with the manual methods generally in use.

WIGGINS, C. P.

W011 Transmitter Phase Modulation as a Result of Beam Voltage Ripple

C. P. Wiggins, E. B. Jackson, and T. W. Rathbun
The Deep Space Network, Space Programs Summary 37-64, Vol. II, pp. 96-97, August 31, 1970

As described in this article, spectrographic analysis at the Venus Deep Space Station of the *Mariner VII* spacecraft down-link on April 27, 1970 showed 9.9-Hz phase modulation sidebands 16 dB below the carrier. This was attributed to up-link modulation of the 200-kW carrier from the high-power transmitter at the Mars Deep Space Station. A corresponding amplitude modulation of the transmitter high-voltage power supply was observed in data collected the previous week as part of a program to optimize the power supply feedback loop. The power supply modulation was reduced by frequency compensation of the feedback loop, thus removing the spurious phase modulation of the *Mariner VII* down-link, as verified by spectrographic analysis on April 29, 1970.

WILCHER, J.

W012 DSIF Multiple-Mission Command System

R. Crow, S. Friesema, J. Wilcher, and J. Woo
The Deep Space Network, Space Programs Summary 37-63, Vol. II, pp. 77-94, May 31, 1970

For abstract, see Crow, R.

WILLIAMS, W.

W013 Vibrational Excitation of N₂ and CO by Electron Impact

W. Williams and S. Trajmar
Supporting Research and Advanced Development, Space Programs Summary 37-62, Vol. III, pp. 53-56, April 30, 1970

Pure N₂ and CO vibrational excitation has been studied by electron impact as a function of scattering angle in the 10- to 50-eV energy range. The CO and N₂ vibrational-to-elastic intensity ratios as functions of scattering angle were compared at 20 eV. The

normalization of e-CO elastic and vibrational excitation cross sections at 20-eV impact energy to the absolute scale was performed, and the results compared with absolute results on H₂. The elastic scattering cross sections for CO and H₂ are quite comparable, while the vibrational excitation cross sections differ by a factor of 10.

WILLIAMSON, R. E.

W014 Support Equipment for a Strapdown Navigator

R. E. Williamson
Supporting Research and Advanced Development, Space Programs Summary 37-62, Vol. III, pp. 149-151, April 30, 1970

This article describes the equipment provided to support the operation, test, and evaluation of a strapdown electrostatic gyro aerospace navigator. The support equipment includes a test van system; analog, digital, and photographic data acquisition systems; portable power systems; and an altimeter.

WILSON, R. K.

W015 The 1982 Jupiter Orbiter Mission

R. K. Wilson
Supporting Research and Advanced Development, Space Programs Summary 37-62, Vol. III, pp. 290-295, April 30, 1970

Results are presented of a preliminary study of the trajectory considerations for a 1982 Jupiter orbiter mission. Minimum launch energies for the 1975-2000 period are shown to place the 1982 opportunity in perspective. A trajectory design chart is given for the 1981-1982 launch opportunity in the form of launch and arrival date plots, with pertinent trajectory parameters overlaid. With the use of this design chart, a launch period and interplanetary trajectory were selected. Also included are the Jupiter orbiter trajectory considerations. Plots of orbit position for natural satellite encounters and occultation periods throughout the active orbit life of 3 yr are given.

WILSON, S.

W016 An Improved Newton-Raphson Algorithm for Finding the Roots of Equations for Solid Propellant Combustion Studies

R. L. Klaus and S. Wilson
Supporting Research and Advanced Development, Space Programs Summary 37-63, Vol. III, pp. 173-175, June 30, 1970

For abstract, see Klaus, R. L.

WILSON, S. K.

W017 Comparative Performance of Double Focused and Quadrupole Mass Spectrometers

S. K. Wilson

Technical Memorandum 33-456, September 1, 1970

A comparison is made of double focused and quadrupole mass spectrometers by analytical means. The analysis considers size, weight, and power for both types of instruments at identical resolutions and sensitivity for the same mass number. In the analysis, both instruments are used with equivalent ion sources having a 10-V voltage spread. It is shown that with weight and power the bases for comparison, the double-focused mass spectrometer is the better.

WOLF, F.

W018 Nuclear Radiation Mapping of Thermoelectric Outer Planet Spacecraft

F. Wolf

Supporting Research and Advanced Development,
Space Programs Summary 37-64, Vol. III, pp. 88-91,
August 31, 1970

The radiation environment of the Thermoelectric Outer-Planet Spacecraft (TOPS) due to the radioisotope thermoelectric power plant aboard the spacecraft is being determined. A radiation transport program of the Monte Carlo type is applied to find solutions for the gamma and neutron flux in locations suitable for the sensors and scientific experiments of the payload and the electronics compartment of the bus. A preliminary map of these areas was obtained for TOPS version 12j.

WOO, J.

W019 DSIF Multiple-Mission Command System

R. Crow, S. Friesema, J. Wilcher, and J. Woo

The Deep Space Network, Space Programs Summary 37-63,
Vol. II, pp. 77-94, May 31, 1970

For abstract, see Crow, R.

WOO, K.

W020 Spacecraft Antenna Research: Further RF Test Results of Reflector Surface Materials for Spacecraft Antennas

K. Woo

Supporting Research and Advanced Development,
Space Programs Summary 37-63, Vol. III, pp. 46-47,
June 30, 1970

Radio frequency test results of reflector surface materials for spacecraft antennas are presented. The RF reflectivity loss of an improved gold-plated Chromel-R mesh is found to be of the order of 0.07 dB or better at 8448 MHz; the RF reflectivity loss of Emfoil (copper-clad glass epoxy laminate) is of the order of 0.04 dB or better at the same frequency.

WOO, R.

W021 Final Report on RF Voltage Breakdown in Coaxial Transmission Lines

R. Woo

Technical Report 32-1500, October 1, 1970

Because of its occurrence in components designed for operation in space, RF voltage breakdown has attracted considerable interest in recent years. Extensive studies have been made of RF voltage breakdown in the coaxial transmission line geometry; the results are summarized in this report. Using the principle of similarity and a minimum of experimental data, universal curves are constructed covering a wide range of experimental parameters. These data are sufficient to determine the power handling capability of any coaxial transmission lines likely to be encountered by a spacecraft design engineer.

W022 Spacecraft Antenna Research: Voltage Breakdown in Monopole Antennas at S-band

R. Woo

Supporting Research and Advanced Development,
Space Programs Summary 37-63, Vol. III, pp. 47-50,
June 30, 1970

Voltage breakdown in $\lambda/4$ monopole antennas has been studied. The breakdown power levels are found to increase rapidly when either monopole diameter or frequency is increased. When voltage breakdown is a problem, dielectrics may be used to significantly improve the power-handling capability of monopole antennas.

W023 Large Spacecraft Antennas: Slotted Lens Antenna Study

R. Woo

Supporting Research and Advanced Development,
Space Programs Summary 37-64, Vol. III, pp. 44-47,
August 31, 1970

A slotted lens antenna is proposed as a spacecraft antenna. It is shown that the potential efficiency of the slotted lens offers an improvement over the zone-plate lens.

WUEST, W. S.

W024 TOPS Pyrotechnics Switching

W. S. Wuest

Supporting Research and Advanced Development,
Space Programs Summary 37-62, Vol. III, pp. 233-234,
April 30, 1970

A series-redundant, power-switching arrangement has been devised for the Thermoelectric Outer-Planet Spacecraft (TOPS) pyrotechnic subsystem. A solid-state switch and an electromechanical stepping switch in series form a squib-firing circuit that is immune to switch failure or random command. This circuit also decreases the number of commands required in a system that has many pyrotechnic events.

WYATT, M. E.

W025 DSS Control Room Reconfiguration in Support of Future Project Requirements

M. E. Wyatt

The Deep Space Network, Space Programs Summary 37-63,
Vol. II, pp. 60-61, May 31, 1970

The Deep Space Instrumentation Facility (DSIF), in 1970, will greatly increase its capabilities to meet the requirements of future spacecraft projects. Consequently, the DSIF will realize a significant increase in the amount of equipment located within the deep space station (DSS) control rooms throughout the DSIF. This article describes the new equipment and the philosophy utilized in location of the new equipment within the control rooms.

W026 CTA 21 to TRW Passive Microwave Link

M. E. Wyatt

The Deep Space Network, Space Programs Summary 37-65,
Vol. II, pp. 104-105, September 30, 1970

To establish compatibility between the Deep Space Network and various spacecraft prior to launch, Compatibility Test Area 21 (CTA 21) was implemented at JPL to represent a standard Deep Space Instrumentation Facility station. However, the *Pioneer* Project has determined it impractical to bring the *Pioneer F* and *G* spacecraft to JPL for the necessary compatibility tests. Therefore, it has been proposed that an S-band microwave link be established between CTA 21 and TRW Systems, Inc. in Redondo Beach so that the compatibility tests may be integrated with the presently scheduled tests at TRW. The preliminary work towards establishing such a link is the subject of this article.

YANG, J.-N.

Y001 Optimum Structural Design Based on Reliability Analysis

M. Shinozuka (Columbia University), J.-N. Yang, and E. Heer
Technical Report 32-1496 (Reprinted from *Proceedings of the Eighth International Symposium on Space Technology and Science, Tokyo, Japan, August 25-30, 1969,* pp. 245-258)

For abstract, see Shinozuka, M.

Y002 On the Maximum Dynamic Response of Structures and Proof Testing

J.-N. Yang and E. Heer

Supporting Research and Advanced Development,
Space Programs Summary 37-64, Vol. III, pp. 91-95,
August 31, 1970

Based on the information of the excitation energy and the excitation envelope, respectively, upper bounds of the dynamic structural response are derived. Two proof testing forcing functions, which produce the derived upper bounds, are also obtained.

YANG, L. C.

Y003 Initiation of Explosives by Laser Energy

V. J. Menichelli and L. C. Yang

Supporting Research and Advanced Development,
Space Programs Summary 37-63, Vol. III, pp. 167-169,
June 30, 1970

For abstract, see Menichelli, V. J.

YASUI, R. K.

Y004 Lightweight Integrated Silicon Solar Cell Array

R. K. Yasui

Supporting Research and Advanced Development,
Space Programs Summary 37-62, Vol. III, pp. 132-133,
April 30, 1970

The design and fabrication of an advanced-concept solar cell module are described. The solar cell module is comprised of 19 cells in parallel by 20 cells in series and wraparound flexible interconnectors. The module has been tested and delivered to General Electric for mounting on their 30-W/lb roll-up solar array for further testing. Also described are thermal cycling and flexure/tensile experimental tests to evaluate analytical modeling techniques developed earlier in this program.

YATES, B. C.

Y005 Comparisons of Waveguide Losses Calibrated by the DC Potentiometer, AC Ratio Transformer, and Reflectometer Techniques

T. Y. Otoshi, C. T. Stelzried, B. C. Yates (National Bureau of Standards), and R. W. Beatty (National Bureau of Standards)
IEEE Trans. Microwave Theory and Techniques, Vol. MTT-18, No. 7, pp. 406–409, July 1970

For abstract, see Otoshi, T. Y.

YEN, S. P. S.

Y006 Synthesis and Properties of a New Class of Potential Biomedical Polymers

A. Rembaum, S. P. S. Yen, R. F. Landel, and M. Shen (University of California, Berkeley)
J. Macromol. Sci.—Chem., Vol. A4, No. 3, pp. 715–738, May 1970

For abstract, see Rembaum, A.

Y007 Electronic Conductivity of Elastomeric Ionenenes

R. Somoano, S. P. S. Yen, and A. Rembaum
J. Polym. Sci., Pt. B: Polym. Lett., Vol. 8, No. 7, pp. 467–479, July 1970

For abstract, see Somoano, R.

YEN, T. F.

Y008 Potentialities of a New Class of Anticlotting and Antihemorrhagic Polymers

T. F. Yen (University of Southern California, California State College), M. Davar (University of Southern California, California State College), and A. Rembaum
J. Macromol. Sci.—Chem., Vol. A4, No. 3, pp. 693–714, May 1970

Major blood anticlotting agents may be grouped into two classes: (1) heparin and heparin analogs, and (2) coumarin and coumarin analogs. The first class of compounds interferes with the formation of thrombin and thromboplastin, whereas the second inhibits the formation of prothrombin. Both classes have their own antagonists, namely, protamine sulfate types and vitamin K types exhibiting antihemorrhagic properties. On a molecular level, the heparinlike structures and their antagonists may be regarded as polyanions and polycations, respectively, whereas the coumarinlike structures and their antagonists as electron donors and acceptors, respectively, which may form charge transfer complexes.

Heparin belongs to the class of mucopolysaccharides consisting of repeating units of glucosamine and glucuronic acid. It can either be grafted on a plastic surface or it can be incorporated into functional cellulose derivatives. This polyanion combines in effective group ratios with other cationic compounds such as basic dyes (Azure A) or other dications; i.e., compounds such as nitro blue tetrazolium chloride. It also forms complexes with polycations, e.g., ionenes, which are known antihemorrhagic reagents. Structural analogs of heparin such as dextran sulfate or chitin sulfate behave similarly.

A polymer consisting of repeating units of bishydroxycoumarin units was prepared. The antagonist, a polymer with repeating units of menadione, was also prepared. The properties and potential uses of such systems are discussed.

Y009 Fluorometric Examination of the Returned Lunar Fines From Apollo 11

J. H. Rho, A. J. Bauman, T. F. Yen (University of Southern California), and J. Bonner (California Institute of Technology)
Proceedings of the Apollo 11 Lunar Science Conference, Houston, Texas, January 5–8, 1970, Vol. 2, pp. 1929–1932

For abstract, see Rho, J. H.

YOUNG, A. T.

Y010 Photometric Error Analysis. X: Enriched Energy (Total Illuminance) Calculations for Annular Apertures

A. T. Young
Appl. Opt., Vol. 9, No. 8, pp. 1874–1878, August 1970

Encircled energy calculations show the effects of focus errors, spherical aberration, and a central stop on image contrast. The complementary quantity (excluded energy) gives the illumination at the center of a dark spot on an incoherent background and is useful in some photometric situations. A simple formula is given for the approximate calculation of the excluded energy at large distances from the center of the diffraction pattern.

YOUNG, L. G.

Y011 Interpretation of High-Resolution Spectra of Mars: I. CO₂ Abundance and Surface Pressure Derived From the Curve of Growth

L. G. Young
Icarus: Int. J. Sol. Sys., Vol. 11, No. 3, pp. 386–389, November 1969

High-resolution spectra of Mars obtained by Pierre and Janine Connes have been used to obtain a curve of growth for CO₂ and CO lines formed in the Martian atmosphere. A rotational temperature of 201 ± 6 °K is found for the CO₂ lines, while the CO lines indicate a temperature of 203 ± 8 °K. By a nonlinear least-squares fit to the curve of growth, for an air mass $\eta = 3.5$, an approximate CO₂ abundance of 70 m-atm and a surface pressure of 5 mbar are found. This surface pressure is approximately equal to the CO₂ partial pressure.

Y012 High-Dispersion Spectroscopic Observations of Venus: VI. The Carbon Dioxide Band at 10 362 Å

R. A. Schorn and L. G. Young
Icarus: Int. J. Sol. Sys., Vol. 12, No. 3, pp 391–401,
May 1970

For abstract, see Schorn, R. A.

ZANTESON, R.

Z001 Multiple Primary Feed Cone Installation and Alignment

R. Zanteson
The Deep Space Network, Space Programs Summary 37-63,
Vol. II, pp. 56–60, May 31, 1970

The installation and alignment phases of the multiple primary feed system have been completed at the Mars Deep Space Station. This involved removal of the original single cone system, structural modifications to accept larger and heavier components, and the installation of new structure. Subsequent alignment and gravity deflection testing phases indicate that design criteria have been met or exceeded.

ZELDIN, B.

Z002 Calibrating a Hot Film Anemometer for Low Velocity Measurement in Nonisothermal Flow

B. Zeldin and F. W. Schmidt (Pennsylvania State University)
Rev. Sci. Instr., Vol. 41, No. 9, pp. 1373–1374,
September 1970

A modification of King's law is presented that can be used to accurately correlate calibration data for a constant-temperature, hot film anemometer for low-velocity, nonisothermal, laminar air flow. By determining certain calibration parameters, a mathematical relationship is obtained that may be used to predict velocity as a function of measured anemometer bridge voltage and local air temperature.

ZOHAR, S.

Z003 Digital Acquisition and Detection: Solution of a Toeplitz Set of Linear Homogeneous Equations

S. Zohar
The Deep Space Network, Space Programs Summary 37-64,
Vol. II, pp. 38–41, August 31, 1970

In this article, a fast algorithm is derived for the solution of a homogeneous set of linear equations in which the associated matrix has a Toeplitz structure. When this matrix is Hermitian, this algorithm is twice as fast as the one for the non-homogeneous case.

ZWEBEN, C.

Z004 Tensile Strength of Fiber-Reinforced Composite Materials

C. Zweben
Supporting Research and Advanced Development,
Space Programs Summary 37-62, Vol. III, pp. 195–198,
April 30, 1970

The tensile strengths of a variety of filamentary composite materials are compared with theoretical, statistical bounds. The experimental data generally fall within the bounds, tending to verify the validity of the theoretical approach. This provides useful insights into the fracture behavior of composite materials.

Z005 Fiber-Reinforced Composite Materials for Spacecraft Antenna Structures

C. Zweben
Supporting Research and Advanced Development,
Space Programs Summary 37-64, Vol. III, pp. 106–108,
August 31, 1970

Advanced composite materials consisting of high-strength, high-stiffness, lightweight fibers in resin and metal matrices provide the engineer with the ability to tailor materials to a particular mission requirement. It has been shown that it is possible to make materials having extremely small, and even zero, coefficients of thermal expansion. The application of these materials to antenna structures is being studied.

Z006 A Statistical Theory of Material Strength With Application to Composite Materials

C. Zweben and B. W. Rosen (Materials Sciences Corporation)
J. Mech. Phys. Solids, Vol. 18, No. 3, pp. 189–206,
June 1970

A statistical theory of material strength is proposed. Materials are considered to be imperfect heterogeneous continua composed of discrete volume elements whose characteristics are related to material structure and

imperfections. The strength of the elements is assumed to be a statistical quantity, and, as the material is loaded, elements fracture randomly throughout the body, causing localized stress concentrations. The accumulation of these breaks results in overall failure. By relating strength to material structure, this theory attempts to bridge the gap between the microscopic and continuum approaches to fracture mechanics. The theory is applied to composite materials reinforced with whiskers and continuous fibers. Comparisons with experimental data show good agreement. Results for whisker-reinforced composites appear to provide a good prediction of strength and an explanation of the disparity between the strength of individual whiskers and the strength of the composites made from them.

ZYGIELBAUM, A.

Z007 Information Systems: Multiple-Mission Sequential Decoder Interface Buffer

A. Zygielbaum

The Deep Space Network, Space Programs Summary 37-64, Vol. II, pp. 53-55, August 31, 1970

This article describes a computer buffer that has been built to interface the multiple-mission sequential decoder with XDS 900-series computers. The buffer operation is compatible with standard *Pioneer* spacecraft telemetry and command processing decommutation software. Design considerations, programming, and hardware are discussed.

Publication Index

Technical Reports

Number	Entry	Number	Entry
32-1401	S062	32-1484	K016
32-1438	G006	32-1486	A007
32-1439	L039	32-1487	H033
32-1443	J009	32-1488	H041
32-1451	S016	32-1490	M015
32-1460, Vol. I	J010	32-1494	R038
32-1461	A001	32-1496	S026
32-1469	N014	32-1498	G027
32-1470	S060	32-1500	W021
32-1475	J011	32-1501	H042
32-1476	A021	32-1502	C036
32-1478	T021	32-1504	M010
32-1480	P006	32-1505	H024
32-1481	G005	32-1506	K013
32-1483	M009	32-1507	A006

Technical Memorandums

Number	Entry	Number	Entry
33-341	G021	33-455	B015
33-426, Vol. III	R018	33-456	W017
33-426, Vol. IV	R019	33-458	C028
33-439	G004	33-461	M002
33-452, Vol. I	F008	33-462	B021
33-453	Q001	33-463	A015
33-454	R011		

Space Programs Summaries 37-63 Through 37-65, Vol. I

JPL Technical Section	Entry	JPL Technical Section	Entry
210 Mariner Mars 71 Project	J027 J028 J029	344 Spacecraft Control	J020 J022 J023 J024 J025 J026
220 Viking Orbiter	J039 J040 J041	350 Engineering Mechanics Division	J017 J018
250 Mariner Venus-Mercury 73 Project	J030 J031	351 Materials	J016
314 Computation and Analysis	J013 J014	352 Spacecraft Structure	J015 J016 J018
315 Flight Operations and DSN Programming	J013	353 Applied Mechanics	J015 J016
321 Space Photography	J037	354 Electronic Parts Engineering	J015
323 Space Instruments	J035	355 Advanced Projects Development	J015
324 Science Data Analysis	J036	362 Spacecraft Measurements	J012
336 Spacecraft Radio	J038	375 Space Simulation	J019
339 Spacecraft Telecommunications Systems	J038	382 Polymer Research	J034
342 Spacecraft Power	J020 J021 J025 J026	384 Liquid Propulsion	J032 J033 J034

Space Programs Summaries 37-63 Through 37-65, Vol. II

JPL Technical Section	Entry	JPL Technical Section	Entry
315 Flight Operations and DSN Programming	H037	331 Communications Systems Research (contd)	L012 L013 M033 M044 M048 S009 S010 S011 S019 S075 T006 Z003 Z007
316 SFOF/GCF Operations	H010		
318 SFOF/GCF Development	M017 M058 P018 S045 V001 V002 W007	332 DSIF Engineering	C011 C012
331 Communications Systems Research	A013 B037 E002 G007 L011		

Space Programs Summaries 37-63 Through 37-65, Vol. II (contd)

JPL Technical Section	Entry	JPL Technical Section	Entry
332 DSIF Engineering (contd)	K008 K018 L017 L018 L019 L027 L028 L030 M022 W005 W025 W026 Z001	337 DSIF Operations (contd)	R028 S006 S007 U003 W003
333 Communications Elements Research	B008 N013 O008 O009 O010 R008 W010	338 DSIF Digital Systems Development	C043 F012 G001 H001 L016
335 R. F. Systems Development	B040 B041 B042 C042 J001 J002 J004 K029 K030 W011	373 Aerophysics	K034
		391 Tracking and Orbit Determination	M053 M054 M055 M056 O003 O004 O005
		392 Navigation and Mission Design	D001
		401 DSN Engineering and Operations	A008 A010 C007 H008 H017 K014 R007 T026
337 DSIF Operations	B017 B024 F014 P019	420 Mission Support	L001 L002 L003 L024 M051 S030

Space Programs Summaries 37-62 Through 37-64, Vol. III

JPL Technical Section	Entry	JPL Technical Section	Entry
131 Advanced Studies	B031 B032 B033	323 Space Instruments	C009 H034 L020
294 Environmental Requirements	H009	324 Science Data Analysis	B027 R032 S071
314 Computation and Analysis	D014 N006		

Space Programs Summaries 37-62 Through 37-64, Vol. III (contd)

JPL Technical Section	Entry	JPL Technical Section	Entry
325 Lunar and Planetary Sciences	C029 C034	342 Spacecraft Power (contd)	C006 D018 G019 J044 J045 K031 L014 L015 L038 M024 P005 R001 R010 T001 W009 Y004
326 Bioscience	B020		
328 Physics	B025 B035 D009 H006 K011 T016 U002 W013		
331 Communications Systems Research	B045 B046 B048 B049 H027 H028 K023 K024 L004 L010 M018 M020 P020 T013	343 Guidance and Control Analysis and Integration	A003 D021 S025 S070 W014
333 Communications Elements Research	C037 L036 L037 W020 W022 W023	344 Spacecraft Control	B013 C038 C039 D019 F003 G012 H003 H026 L022 M007 R036 S015 S020 S050 S051
336 Spacecraft Radio	D012		
339 Spacecraft Telecommunications Systems	C008 C014 C015 H032 J006 K028 L023 S040 S041 S042 S049 S058 S059	351 Materials	A004 C040 C041 F005 F006 R035
342 Spacecraft Power	B005 B018 C003	353 Applied Mechanics	C020 C021 C022 H038 K025

Space Programs Summaries 37-62 Through 37-64, Vol. III (contd)

JPL Technical Section	Entry	JPL Technical Section	Entry
353 Applied Mechanics (contd)	K026 M049 P013 S002 S069 W018 Y002 Z004 Z005	381 Solid Propellant Engineering (contd)	S072 W024
355 Advanced Projects Development	S001	382 Polymer Research	C044 I001 K003 K006 M040 R002 R003 R012 R021 R022
357 Electronic Packaging and Cabling	B043 D006	383 Research and Advanced Concepts	C045 G023 G024 M003 M045 P002 P007 P008 P017
361 Spacecraft Computer	R034	384 Liquid Propulsion	C026 H015 H016 R027 S044
362 Spacecraft Measurements	H030	391 Systems Analysis Research	G014 M025
363 Spacecraft Data Systems	A018 E001 H020 H022 P012	391 Tracking and Orbit Determination	G003 M057
364 Astrionics Research	M012	392 Navigation and Mission Design	C017 S061
373 Aerophysics	H018 J005 W001	392 Systems Analysis	W015
375 Space Simulation	M035 M036		
381 Solid Propellant Engineering	K020 K021 K022 M008 M028 M029 S021		

JPL Reporting in the Open Literature

Advances in Astronomy and Astrophysics	Entry	AIAA Guidance, Control, and Flight Mechanics Conference	Entry
Vol. 7, pp. 83-145	L041	Paper 69-868	B014
AIAA/ASTM/IES 4th Space Simulation Conference	Entry	AIAA J.	Entry
Paper 69-994	D002	Vol. 8, No. 4, pp. 794-802	B001

JPL Reporting in the Open Literature (contd)

Anal. Chem.	Entry	Comm. ACM	Entry
Vol. 42, No. 8, pp. 881–885	S037	Vol. 13, No. 7, p. 449	N008
Vol. 42, No. 9, pp. 969–973	L035		
Vol. 42, No. 11, pp. 1214–1222	G025	Icarus: Int. J. Sol. Sys.	Entry
		Vol. 11, No. 3, pp. 283–288	S017
Antarctic Ecology: Volume 2	Entry	Vol. 11, No. 3, pp. 386–389	Y011
pp. 702–716	C001	Vol. 12, No. 1, pp. 78–81	L033
		Vol. 12, No. 1, pp. 118–127	C004
Appl. Microbiol.	Entry	Vol. 12, No. 3, pp. 391–401	S018
Vol. 20, No. 4, pp. 567–572	S039		
		IEEE Trans. Communication Technology	Entry
Appl. Opt.	Entry	Vol. COM-18, No. 2, pp. 119–126	H029
Vol. 9, No. 5, pp. 1056–1067	G013		
Vol. 9, No. 5, pp. 1068–1074	B007	IEEE Trans. Information Theory	Entry
Vol. 9, No. 5, pp. 1075–1081	F015	Vol. IT-16, No. 3, pp. 348–351	B051
Vol. 9, No. 5, pp. 1082–1091	K012	Vol. IT-16, No. 5, pp. 581–587	T014
Vol. 9, No. 6, pp. 1289–1303	M032	Vol. IT-16, No. 5, pp. 609–611	M021
Vol. 9, No. 8, pp. 1874–1878	Y010	Vol. IT-16, No. 5, pp. 640–641	C016
		Vol. IT-16, No. 6, pp. 692–699	T015
Astron. Astrophys.	Entry	IEEE Trans. Instrumentation and Measurement	Entry
Vol. 6, No. 2, pp. 173–182	B038	Vol. IM-19, No. 1, pp. 23–25	S066
Astronaut. Aeronaut.	Entry	IEEE Trans. Microwave Theory and Techniques	Entry
Vol. 7, No. 5, pp. 26–29	C047	Vol. MTT-18, No. 7, pp. 406–409	O011
Vol. 7, No. 5, pp. 30–36	C048		
Vol. 7, No. 5, pp. 38–43	M026	Int. J. Heat Mass Transfer	Entry
Vol. 7, No. 5, pp. 44–49	B029	Vol. 13, No. 6, pp. 1029–1047	B002
Vol. 7, No. 5, pp. 50–55	D020	Vol. 13, No. 8, pp. 1293–1297	H011
Vol. 7, No. 5, pp. 56–64	M046		
Vol. 7, No. 5, pp. 66–70	H002	J. Am. Chem. Soc.	Entry
		Vol. 92, No. 12, pp. 3565–3573	H039
Astrophys. J.	Entry	Vol. 92, No. 15, pp. 4646–4652	C032
Vol. 161, No. 3, pp. 803–809	K009		
		J. Appl. Phys.	Entry
Canad. J. Phys.	Entry	Vol. 41, No. 8, pp. 3442–3445	S073
Vol. 48, No. 12, pp. 1472–1479	L031		
Celest. Mech.	Entry		
Vol. 2, No. 1, pp. 9–20	B039		

JPL Reporting in the Open Literature (contd)

J. Astronaut. Sci.	Entry	J. Quant. Spectrosc. Radiat. Transfer	Entry
Vol. XVII, No. 4, pp. 185-217	L026	Vol. 10, No. 7, pp. 755-773	N004
J. Bacteriol.	Entry	J. SMPTE	Entry
Vol. 102, No. 3, pp. 677-681	H035	Vol. 79, No. 7, pp. 607-615	S003
		Vol. 79, No. 7, pp. 615-620	A009
J. Chem. Phys.	Entry	J. Spacecraft Rockets	Entry
Vol. 52, No. 9, pp. 4502-4515	T019	Vol. 7, No. 4, pp. 398-404	N012
Vol. 52, No. 9, pp. 4516-4533	T020	Vol. 7, No. 5, pp. 634-636	K007
Vol. 52, No. 10, pp. 5044-5056	F010	Vol. 7, No. 6, pp. 684-689	D016
Vol. 53, No. 1, pp. 462-463	M050	Vol. 7, No. 7, pp. 837-842	M052
Vol. 53, No. 5, pp. 1899-1905	B011	Vol. 7, No. 8, pp. 928-933	D023
Vol. 53, No. 6, pp. 2343-2352	C033	Vol. 7, No. 8, pp. 968-976	P010
J. Geophys. Res., Space Phys.	Entry	Nature	Entry
Vol. 75, No. 19, pp. 3735-3750	S012	Vol. 225, No. 5239, pp. 1234-1236	B044
Vol. 75, No. 25, pp. 4746-4755	A020	Nucl. Appl. Technol.	Entry
Vol. 75, No. 25, pp. 4898-4899	D010	Vol. 9, No. 5, pp. 722-735	M038
J. Macromol. Sci.—Chem.	Entry	Phys. Fluids	Entry
Vol. A4, No. 3, pp. 693-714	Y008	Vol. 13, No. 7, pp. 1883-1885	N010
Vol. A4, No. 3, pp. 715-738	R014	Vol. 13, No. 9, pp. 2420-2422	N011
J. Mater.	Entry	Phys. Rev., Pt. D: Part. Fields	Entry
Vol. 5, No. 3, pp. 666-683	H012	Vol. 1, No. 8, pp. 2269-2271	H007
J. Mech. Phys. Solids	Entry	Planet. Space Sci.	Entry
Vol. 18, No. 3, pp. 189-206	Z006	Vol. 18, No. 4, pp. 449-478	B036
J. Opt. Soc. Am.	Entry	Proceedings of the Apollo 11 Lunar Science Conference, Houston, Texas, January 5-8, 1970	Entry
Vol. 60, No. 9, pp. 1204-1208	C024	Vol. 2, pp. 1929-1932	R023
J. Phys. Chem.	Entry	Vol. 3, pp. 2013-2023	C031
Vol. 74, No. 13, pp. 2583-2589	B026	Vol. 3, pp. 2341-2350	N002
Vol. 74, No. 13, pp. 2621-2625	D011	Pub. Astron. Soc. Pacific	Entry
J. Polym. Sci., Pt. B: Polym. Lett.	Entry	Vol. 82, No. 484, pp. 122-125	J042
Vol. 8, No. 7, pp. 457-466	R015		
Vol. 8, No. 7, pp. 467-479	S055		

JPL Reporting in the Open Literature (contd)

Radio Sci.	Entry	Sol. Energy	Entry
Vol. 5, No. 5, pp. 821-839	P016	Vol. 13, No. 1, pp. 43-57	L008
Recent Advances in Engineering Science: Volume 5	Entry	Solid-State Electron.	Entry
pp. 359-383	O007	Vol. 13, No. 6, pp. 751-754	S029
Rev. Sci. Instr.	Entry	Space Research X	Entry
Vol. 41, No. 9, pp. 1373-1374	Z002	pp. 975-983	M060
Science	Entry	Trans. Am. Microsc. Soc.	Entry
Vol. 169, No. 3949, pp. 974-977	G009	Vol. 89, No. 2, pp. 264-273	C002

Major Categories Used in Subject Index

Antennas and Transmission Lines	<i>Lunar Orbiter Project</i>	Propulsion, Liquid
<i>Apollo Project</i>	Lunar Surface	Propulsion, Solid
Atmospheric Entry		Pyrotechnics
	Management Systems	
Bioengineering	<i>Mariner Mars 1964 Project</i>	Quality Assurance and Reliability
Biology	<i>Mariner Mars 1969 Project</i>	
	<i>Mariner Mars 1971 Project</i>	Radar
Chemistry	<i>Mariner Venus 67 Project</i>	Radio Astronomy
Computer Applications and Equipment	<i>Mariner Venus-Mercury 1973 Project</i>	Relativity
Computer Programs	Masers and Lasers	Scientific Instruments
Control and Guidance	Materials, Metallic	Shielding
	Materials, Nonmetallic	Soil Sciences
Earth Atmosphere	Mathematical Sciences	Solar Phenomena
Earth Interior	Mechanics	Solid-State Physics
Earth Motion	Mechanisms	Spectrometry
Earth Surface	Meteors	Standards, Reference
Electricity and Magnetism		Sterilization
Electronic Components and Circuits	Optics	Structural Engineering
Energy Storage		<i>Surveyor Project</i>
	Packaging and Cabling	
Facility Engineering	Particle Physics	Telemetry and Command
Fluid Mechanics	Photography	Temperature Control
	<i>Pioneer Project</i>	Test Facilities and Equipment
	Planetary Atmospheres	Thermodynamics
Industrial Processes and Equipment	Planetary Exploration, Advanced	Thermoelectric Outer-Planet Spacecraft (TOPS)
Information Theory	Planetary Interiors	Tracking
	Planetary Motion	Trajectory Analysis/Orbit Determination
Launch Operations	Planetary Quarantine	
Launch Vehicles	Planetary Spacecraft, Advanced	
Lunar Exploration, Advanced	Planetary Surfaces	<i>Viking Project</i>
Lunar Interior	Plasma Physics	Voice Communications
Lunar Motion	Power Sources	
	Propulsion, Electric	Wave Propagation

Subject Index

Subject	Entry	Subject	Entry
Antennas and Transmission Lines		Antennas and Transmission Lines (contd)	
polarization converter	B041	multiple primary feed cone installation and alignment	Z001
Johannesburg Deep Space Station antenna mechanical subsystem upgrade	C011	fiber-reinforced composite materials for spacecraft antenna structures	Z005
overseas 210-ft-diam antenna project	C012		
comparison of focal point and cassegrain antennas for spacecraft	C037	Apollo Project	
mesh materials for deployable antennas	F005	automated post-missions for lunar roving vehicle	B032
conical-gregorian high-gain antenna	F006	Deep Space Network support	F008 H008
antennas used for Deep Space Network support of Manned Space Flight Network for <i>Apollo</i> Project	F008	gamma ray spectrometer for <i>Apollo 16</i>	L020
<i>Mariner</i> Mars 1969 spacecraft antennas	J010	gamma ray spectrometer thermal model tests	P013
120-ft-diam radar antenna at Haystack	J011	fluorometric examination of bulk fine lunar sample from <i>Apollo 11</i>	R023
<i>Mariner</i> Mars 1971 medium-gain antenna RF plug assembly	J018		
30-ft-diam antenna upgrade	K008	Atmospheric Entry	
clock-sync antenna installation at U.S. Naval Observatory	K018	reverse Goddard problem	B014
210-ft-diam antenna wind loading measurements	K034	heat-sterilizable capsule spin motors	N014
wind tunnel coefficients for parabolic reflectors	L017	hypersonic blunt-body flow of a radiating gas at low density	S016
30-deg reflector mockup study: comparisons of measured and predicted deflections	L018		
method of selecting antenna rigging angles to improve performance	L019	Bioengineering	
deep space station antenna repairs	L028	man-machine interaction in post-1971 Space Flight Operations Facility	H037
low-frequency, low-level stress reversals on an assembly of antenna bolted joint specimens	L030		
use of efficiency program to calculate feed defocusing loss in spacecraft antennas	L036	Biology	
test of conical gregorian antenna	L037	identification of products from nucleotide pyrolysis by high resolution mass spectrometry	B020
new cable wrap-up system for 210-ft-diam antenna	M022	microbiology, ecology, and microclimatology of soil sites in dry valleys of southern Victoria Land, Antarctica	C001
correction factors for near field horn antenna gain measurements	N013	nature of inactivation of isocitrate dehydrogenase from obligate halophile	H035
precision compact rotary vane attenuator	O008 O009	synthesis and properties of a new class of potential biomedical polymers	R014
comparisons of waveguide losses calibrated by dc potentiometer, ac ratio transformer, and reflectometer techniques	O011	fluorometric search for porphyrins, essential components of life, in bulk fine lunar sample from <i>Apollo 11</i>	R023
system operating noise temperature calibrations of low noise cones	R008	whole microorganisms studied by pyrolysis-gas chromatography-mass spectrometry	S039
precision microwave waveguide loss calibrations	S066	potential of a new class of anticlotting and antihemorrhagic polymers	Y008
test results of reflector surface materials	W020		
radio frequency voltage breakdown in coaxial transmission lines	W021	Chemistry	
voltage breakdown in monopole antennas at S-band	W022	skeletal molecular structure of <i>closo</i> -2,3-dicarbahexaborane(6) from microwave spectral studies	B011
slotted lens antenna	W023	identification of products from nucleotide pyrolysis by high resolution mass spectrometry	B020

Subject	Entry
Chemistry (contd)	
ion cyclotron resonance study of ion-molecule reactions in hydrogen-methane mixtures	B025
analysis of ion-molecule reactions in allene and propyne by ion cyclotron resonance	B026
new method for determining SiO ₂ abundance in silicate glass from powder film transmission measurements in the infrared	C030
effect of steric compression on proton-proton, spin-spin coupling constants	C032
proton nuclear magnetic resonance coupling constants between vinyl protons in <i>cisoid</i> -dienes	C033
rates and mechanism of alkyne ozonation	D009
efficiency of CO ₃ formation in Mars and Venus atmospheres	D010
pressure dependence of carbon trioxide formation in the gas-phase reaction of O(¹ D) with carbon dioxide	D011
multi-phase ammonia-water system	H009
nature of inactivation of isocitrate dehydrogenase from obligate halophile	H035
ion cyclotron resonance study of the ion-molecule reactions in methane-ammonia mixtures	H039
functionality of isobutylene prepolymers	I001
palladium generator-separator: a combined electrolytic source and sink for hydrogen in closed circuit gas chromatography	L035 S037
reaction of O ⁺ with CO ₂	M050
long-term aging of elastomers: kinetics of oxidation of styrene-butadiene rubber studied by infrared spectrometry	R003
kinetics of formation of high-charge-density ionene polymers	R012 R015
synthesis and properties of a new class of potential biomedical polymers	R014
determination of molecular weight distribution of poly(isobutylene) by gel permeation chromatography	R021
molecular-sieve catalyzed polymerization of isobutylene	R022
whole microorganisms studied by pyrolysis-gas chromatography-mass spectrometry	S039
electronic conductivity of elastomeric ionenes	S055
electron scattering by H ₂ with and without vibrational excitation	T019 T020
new class of ant clotting and antihemorrhagic polymers	Y008

Subject	Entry
Computer Applications and Equipment	
television image processing for navigation	A003
automatic input data generation scheme for a finite-element method	A007
Deep Space Network Monitor System	A008
quasi-linearity of digital record/reproduce process on magnetic tape recorders	A018
digital fault diagnosis by low-cost arithmetical coding techniques	A021
Polaroid quick-look system for digital prints	B025
numerical interactive controller for digital video display system	B037
Deep Space Network Simulation System	C007 P018
Deep Space Instrumentation Facility multiple-mission command system	C043
reliable interface circuit for driving field effect transistor switching trees	E001
Deep Space Instrumentation Facility multiple-mission telemetry 1971 configuration	F012
telemetry simulation conversion assembly	G001
average access times for a magnetic disk storage device	G014
reactor simulator runs with thermionic diode kinetics experiment	G024
matching of mass spectra when peak height is encoded to one bit	G025
recording of subcarrier demodulator assembly outputs for <i>Mariner</i> Mars 1971 missions	H001
evaluation of spacecraft magnetic recording tapes	H022 K003 K006
man-machine interaction in post-1971 Space Flight Operations Facility	H037
<i>Mariner</i> Mars 1969 Project computer applications	J010
binary coded sequential acquisition ranging system	J011
data processing for Haystack planetary ranging radar	J011
<i>Mariner</i> Mars 1971 mission-and-test computer system	J013
<i>Mariner</i> Mars 1971 mission-and-test video system	J014
modifications to logic mechanization of <i>Mariner</i> Mars 1971 attitude-control subsystem	J020
<i>Mariner</i> Mars 1971 television data acquisition for image processing	J036
real-time selection and validation of telemetry data in the Space Flight Operations Facility	K014

Subject	Entry	Subject	Entry
Computer Applications and Equipment (contd)		Computer Programs (contd)	
dual-mode routing algorithm for autonomous roving vehicle	K016	dynamic programming approach to optimal stochastic orbital transfer strategy	N012
Deep Space Instrumentation Facility monitor system development	L016	computerized receiver and telemetry signal-to-noise ratio predictions program	P019
reliability analysis and architecture of a hybrid-redundant digital system: generalized triple modular redundancy with self-repair	M015	synthesis of a binary system	R007
Ground Communications Facility wideband digital data system	M017	program for determination of molecular weight distribution of poly(isobutylene) by gel permeation chromatography	R021
Deep Space Network simulation center development	P018	software for self testing and repairing (STAR) computer	R034
computerized receiver and telemetry signal-to-noise ratio predictions program	P019	testing of proposed all-digital command detection algorithm	S058
digital removal of noise from video imagery	R032	program used to measure Faraday rotation of signal from <i>Pioneer VI</i>	S062
effective computing power of computer memory	S010	Control and Guidance	
computational complexity	S011	attitude control and structural response interaction	A001
computer-assisted acquisition	S019	television image processing for navigation	A003
Space Flight Operations Facility digital television assembly	S045	state determination for disturbed limit cycle operations in attitude-control via nonlinear filtering	B013
diagnostics for Space Flight Operations Facility central processing system standalone acceptance and maintenance routines	W007	reverse Goddard problem encountered in atmospheric entry	B014
multiple-mission sequential decoder interface buffer	Z007	definition of spacecraft-based navigation system	B029
Computer Programs		solar-electric spacecraft thrust vector control system mechanization	C038
automatic input data generation scheme for a finite-element method	A007	<i>Mariner</i> limit cycles and self-disturbance torques	D016
set of programs constructed to perform the literal series expansions of the two-body problem	B039	attitude control for an outer planet orbiter spacecraft	D019
general-purpose simulation system (GPSS) program used for Deep Space Network system simulation models	C007	strategies and systems for navigation corrections	D020
program used for Chebyshev polynomial expansions of Emden functions	D014	<i>Mariner</i> Mars 1969 approach guidance demonstration	D021
program for plotting probability density function of a hardware performance parameter	G004	spacecraft-based navigation instrument for outer planet missions	D023
program used for high-impact dynamic response analysis of nonlinear structures	G027	evaluation of attitude-control nitrogen-gas-system valves	F003
<i>Mariner</i> Mars 1969 Project computer programs	J010	electrostatic image dissector for star tracker	G012
Mission Operations System software for <i>Mariner</i> Mars 1971 Project	J013	<i>Mariner</i> spacecraft star sensors	G013
solar panel shadow analysis program for <i>Mariner</i> Mars 1971 Project	J020	Thermoelectric Outer-Planet Spacecraft (TOPS) inertial reference unit	H003
use of efficiency program to calculate feed defocusing loss in spacecraft antennas	L036	techniques for selecting auxiliary propulsion systems	H024
algorithm 385 (S13) exponential integral $Ei(x)$ tested against reference subprogram QE1EI	N008	minimum redundancy transformation between body and inertial frame for typical strapped-down inertial navigation system	H026
		<i>Mariner</i> Mars 1969 spacecraft control and guidance	J010
		integration testing of <i>Mariner</i> Mars 1971 attitude-control subsystem	J020

Subject	Entry
Control and Guidance (contd)	
modifications to logic mechanization of <i>Mariner</i> Mars 1971 attitude-control subsystem	J020
scan platform motion effects on <i>Mariner</i> Mars 1971 attitude-control subsystem	J020
stabilization of <i>Mariner</i> Mars 1971 autopilot in nonflight environment	J020
proposed <i>Viking</i> attitude-control roll-reacquisition logic	J022
<i>Viking</i> attitude-control subsystem status register	J022
<i>Mariner</i> Mars 1971 attitude-control performance in commanded turn mode of operation	J023
<i>Mariner</i> Mars 1971 Canopus tracker	J023
<i>Mariner</i> Mars 1971 sun sensors	J023
automatic sun occultation-sun acquisition control for <i>Viking</i> orbiter system	J024
<i>Mariner</i> Mars 1971 gimbal actuator	J025
<i>Mariner</i> Mars 1971 reaction control assembly	J025
<i>Mariner</i> Mars 1971 sun acquisition performance with latched solar panels	J025
<i>Viking</i> orbiter system inertial reference unit integrator redesign	J026
<i>Viking</i> orbiter system reaction control assembly	J026
<i>Mariner</i> Mars 1971 propulsion subsystem sequence failure mode analysis	J032
Thermoelectric Outer-Planet Spacecraft (TOPS) attitude-control reliability study	L022
nonlinear equations of motion for a solar-electric spacecraft	M007
sizing of a solar-electric thrust subsystem for thrust-vector control	M010
control analysis of ion thruster with programmed thrust	M052
dynamic programming approach to optimal stochastic orbital transfer strategy	N012
solar-electric propulsion system thrust vector control tests	P006
evaluation of thrust vector control for solar-electric propulsion system	P010
Thermoelectric Outer-Planet Spacecraft (TOPS) digital sun sensor	S015
Thermoelectric Outer-Planet Spacecraft (TOPS) attitude-control single-axis simulator momentum-wheel tachometer circuit	S050
Thermoelectric Outer-Planet Spacecraft (TOPS) attitude-control single-axis simulator command telemetry link	S051
frequency domain solution for the linear attitude-control problem of spacecraft with flexible appendages	T021

Subject	Entry
Control and Guidance (contd)	
support equipment for strapdown, electrically suspended gyro, aerospace navigation system	W014
Earth Atmosphere	
theory of auroral arc formation	A020
new tropospheric range refraction model	B017
ion cyclotron resonance study of ion-molecule reactions in hydrogen-methane mixtures, as in earth's early atmosphere	B025
electron impact excitation of N ₂	B035
departures from Jeans' escape rate for H and He	B036
measurements of earth from <i>Surveyor</i> spacecraft	J009
measurement of solar spectral irradiance at different terrestrial elevations	L008
charged-particle calibration system analysis	M053
ionospheric electron content determined from faraday rotation measurements of an earth satellite and a deep-space probe	M054
evaluation of ionospheric model	M055
effect of diurnal variation of earth ionosphere on interplanetary navigation	M056
solution for tropospheric zenith range correction using a single pass of differenced doppler data	O003
effects of a variable h_{\max} on the mapping of zenith ionospheric corrections to lower elevation angles	O004
variations in zenith tropospheric range effect computed from radiosonde balloon data	O005
vibrational excitation of H ₂ by low- and medium-energy electrons	T016
magnetospheric flows and their time dependence	U002
vibrational excitation of N ₂ and CO by electron impact	W013
Earth Interior	
structures of terrestrial planets	L041
Earth Motion	
<i>Mariner</i> Mars 1971 celestial mechanics experiment	L033
Earth Surface	
desert stream channels resembling lunar sinuous rills	B044
photometry and polarimetry of earth by <i>Surveyor VII</i>	J009

Subject	Entry	Subject	Entry
Earth Surface (contd)		Electronic Components and Circuits (contd)	
proposed measurement of continental drift by very long baseline interferometry	J011	switched-carrier experiments	K029
multispectral remote sensing of an exposed volcanic province	Q001	waveguide switch protector	K030
Electricity and Magnetism		solid-state switching matrix for solar-electric propulsion	M002
theory of auroral arc formation	A020	fabrication of Josephson junctions	M012
thermal noise in space-charge-limited solid-state diodes	S029	integrated toggle relay driver	M024
magnetospheric flows and their time dependence	U001	digital frequency doubler	M048
radio frequency voltage breakdown in coaxial transmission lines	W021	solar-electric propulsion system tests	P006
Electronic Components and Circuits		evaluation of power conditioner for solar-electric propulsion system	P010
improved solar cell contact-interconnect feasibility	A004	Deep Space Network simulation center development	P018
evaluation of 26- to 32-AWG (American wire gauge) wire	A015	fixed high-power directional couplers and high- power microwave power divider used for low transmitted power operation	R028
noise-adding radiometer	B008	thermal noise in space-charge-limited solid-state diodes	S029
planetary ranging demodulator	B040	Space Flight Operations Facility digital television assembly	S045
functional checking of hybrid layouts prior to processing	B043	Thermoelectric Outer-Planet Spacecraft (TOPS) attitude-control single-axis simulator momentum-wheel tachometer circuit	S050
solar-electric propulsion system technology (SEPST) project thrust vector control electronics	C039	analysis of random modulation in amplifier circuits	S075
1.0002-MHz frequency synthesizer	C042	angle demodulation using state-variable techniques to design a receiver system	T006
multiple-cathode electron gun	D012	contrast ratio determination for Space Flight Operations Facility video image display	V002
reliable interface circuit for driving field effect transistor switching trees	E001	design of a thick-film microcircuit dc-to-dc converter	W009
Deep Space Network equipment for support of Manned Space Flight Network for <i>Apollo</i> Project	F008	multiple-mission sequential decoder interface buffer	Z007
electrostatic image dissector for star tracker	G012	Energy Storage	
evaluation of spacecraft magnetic recording tapes	H022 K006	sterilizable battery development	B005 C044 L038
<i>Mariner</i> Mars 1969 spacecraft electronics	J010	battery storage optimization and design studies	B021
<i>Mariner</i> Mars 1971 flight telemetry subsystem	J012	impact analysis of battery components for hard landers	G027
integrated circuit procurement for <i>Mariner</i> Mars 1971 Project	J015	<i>Mariner</i> Mars 1969 batteries	J010
<i>Viking</i> attitude-control subsystem status register	J022	solar panel-battery power analysis for <i>Mariner</i> Mars 1971 Project	J020
<i>Mariner</i> Mars 1971 Canopus tracker	J023	<i>Mariner</i> Mars 1971 power subsystem design	J025
<i>Mariner</i> Mars 1971 sun sensors	J023	<i>Viking</i> orbiter power subsystem design	J026
<i>Mariner</i> Mars 1971 scan actuator	J025	model pore electrode studies	J044
<i>Viking</i> orbiter system inertial reference unit integrator redesign	J026	electrochemical cells with liquid amalgam electrodes	J045
testing and selection of vidicons for <i>Mariner</i> Mars 1971 television subsystem	J037	long term life test of spare <i>Mariner</i> Venus 67 power subsystem hardware	K031
<i>Viking</i> orbiter radio frequency subsystem	J038	development of a long-life, high-cycle-life, 30-A-h, sealed AgO-Zn battery	P005
<i>Mariner</i> Mars 1969 spacecraft scan control subsystem design and analysis	K013		

Subject	Entry
Facility Engineering	
overseas 210-ft-diam antenna project	C012
Space Flight Operations Facility	
mission support area for	
<i>Mariner</i> Mars 1971 Project	H010
Venus Deep Space Station operations	J001
	J002
	J004
Tidbinbilla Deep Space Station	
microwave link relocation	W005
deep space station control room	
reconfiguration in support of future	
project requirements	W025
passive microwave link from JPL Compatibility	
Test Area to TRW Systems, Inc.	W026
Fluid Mechanics	
acceleration and cooling effects in laminar	
boundary layers	B001
effect of wall cooling on mean structure	
of turbulent boundary layer in	
low-speed gas flow	B002
injector hydrodynamics effects on	
baffled-engine stability	C026
performance of supersonic nozzle with 75-deg	
convergent half-angle and a small	
throat radius of curvature	C045
thrust and plume measurements taken on	
miniature nozzles in a vacuum chamber	H018
optimum mixing of hypergolic propellants	
in an unlike doublet injector element	H033
nonplanar wind tunnel testing	J005
<i>Mariner</i> Mars 1971 pressurant relief	
plume flow field definition	J033
supersonic boundary layer transition studies	K011
instantaneous burning rate during	
depressurization of rocket motor	K020
basic equations in the mathematical	
modeling of the gas phase of a	
burning solid propellant	K022
two-dimensional molecular gas leakage flow	R036
hypersonic blunt-body flow of a radiating	
gas at low density	S016
nozzle exhaust plumes in a space environment	S044
aerodynamics of vehicles in tubes	W001
Industrial Processes and Equipment	
improved solar cell contact-interconnect	
fabrication	A004
functional checking of hybrid layouts	
prior to processing	B043
fabrication of Josephson junctions	M012

Subject	Entry
Information Theory	
minimum switching network for generating	
the weight, in binary notation, of a	
binary vector	A013
digital fault diagnosis by low-cost	
arithmetical coding techniques	A021
automatic carrier acquisition	B042
an efficient two-channel telemetry	
system for space exploration	B045
optimization of acquisition time for	
sequential ranging system	B046
efficient multichannel space telemetry	B048
decision rules for a two-channel	
deep-space telemetry system	B049
rank-order statistics for optimum detection	
of binary signals in the presence of	
white noise and dc drift	B051
approximate analysis of command lock	
detector performance	C008
estimating phase of sampled signal with	
minimum mean-square error	C014
error probability of wide-band binary	
frequency-shift-keyed receiver	
in presence of multipath fading	C015
equivalence of rank permutation codes to a	
new class of binary codes	C016
finite-sample quantile estimation	E002
matching of mass spectra when peak	
height is encoded to one bit	G025
first-order digital phase-locked loop	H027
all-digital command system timing loop	H028
solution to the second-order phase-locked loop	H029
cyclic search algorithms for synchronizing	
maximal length linear shift register sequences	H032
digital transition tracking symbol	
synchronizer for low signal-to-noise	
ratio coded systems	H041
coding for multiple demand access	
satellite systems for speech	
communications in remote areas	H042
method for finding exact power spectrums	
of pseudonoise codes	J006
binary coded sequential acquisition	
ranging system	J011
coding scheme used by Haystack planetary	
radar system for making range measurements	J011
simple sequence permutation method	K023
uniform permutation of sequences	K024
analysis of effect of predemodulation filtering	
on the correlation and error signals in	
a pseudonoise receiver	K028
optimum modulation indexes and maximum	
data rates for interplex modem	L004

Subject	Entry	Subject	Entry
Information Theory (contd)		Lunar Exploration, Advanced	
upper bound on free distance of tree code	L010	mission objectives for a lunar roving vehicle	B033
performance of short constraint length		dual-mode routing algorithm for	
convolutional codes and a heuristic		autonomous roving vehicle	K016
code-construction algorithm	L011	vehicle mobility tests: soft soil slopes	K025
synchronizability of convolutional codes	L012	dipole antenna radiation in a compressible,	
comparing performance of three rate $\frac{1}{2}$,		anisotropic electron plasma overlaying	
$K = 32$ codes	L013	an imperfectly conducting half-space:	
hybrid carrier and modulation tracking loops	L023	lunar applications	P016
Ramsey bounds for coefficients of		tests of devices proposed for science	
internal stability of graph products	M018	payload of lunar rover	S071
relationship between games of search and			
optimum storage of information	M020		
arbitrarily long binary block codes that are			
preserved under very large permutation			
groups and that satisfy the Gilbert bound	M021		
mean-square error and bias of phase			
estimator for sequential ranging system	M044		
linear m -ary feedback shift registers	P012		
epsilon entropy and data compression	P020		
asymptotic complexity of the Green			
decoding procedure	S009		
effective computing power of computer			
memory	S010		
computational complexity	S011		
optimum receiver structure for single-channel,			
phase-coherent communication system	S040		
optimum modulation index for a data-aided			
phase-coherent communication system	S041		
effect of limiter suppression on			
command detection performance	S042		
analysis of phase coherent-incoherent			
output of bandpass limiter	S059		
suppressed-carrier two-channel interplex			
modulation system	T013		
design of signals for analog communication	T014		
upper bound on estimation error in			
threshold region for nonlinear			
pulse modulation systems	T015		
digital acquisition and detection:			
solution of a Toeplitz set of linear			
homogeneous equations	Z003		
Launch Operations		Lunar Interior	
<i>Mariner</i> Mars 1969 launch operations	J010	high resolution lunar gravimetry from	
<i>Viking</i> orbiter system ground handling	J017	<i>Lunar Orbiter</i> radio tracking data	M060
Deep Space Network support of <i>Pioneer VIII</i>	R018	dipole antenna radiation in a compressible,	
Tracking and Data System support		anisotropic electron plasma overlaying	
of <i>Pioneer</i> Project	R019	an imperfectly conducting half-space:	
		lunar subsurface soundings	P016
Launch Vehicles		Lunar Motion	
<i>Mariner</i> Mars 1969 <i>Atlas/Centaur</i>		quantitative confirmation of planetary defects	
launch vehicle	J010	in lunar theory by spectral decomposition	M057
<i>Pioneer IX</i> launch vehicle	R019		
		Lunar Orbiter Project	
		error analysis of extraterrestrial convergent	
		photogrammetric mapping system with	
		<i>Lunar Orbiter</i> results	B015
		high resolution lunar gravimetry from	
		<i>Lunar Orbiter</i> radio tracking data	M060
		Lunar Surface	
		automated post-missions for <i>Apollo</i>	
		lunar roving vehicle	B032
		desert stream channels resembling lunar	
		sinuous rills	B044
		coloring of synthetic and natural lunar	
		glass by titanium and iron	C029
		spectral reflectance and albedo of	
		<i>Apollo 11</i> lunar samples	C031
		moon soil properties determined from	
		<i>Surveyor</i> data and laboratory tests	J009
		radar studies of moon	J011
		luminescence properties of <i>Apollo 11</i>	
		lunar samples	N002
			R023
		Management Systems	
		Deep Space Network Monitor System	A008
		Deep Space Network Telemetry System	A010
		Deep Space Network Simulation System	C007
			P018
		consensus of individual preferences	C017
		probability density function of a	
		hardware performance parameter	G004

Subject	Entry
Management Systems (contd)	
techniques for selecting auxiliary propulsion systems	H024
<i>Mariner</i> Mars 1969 Project management	J010
Deep Space Network allocation schedules	T026
<i>Mariner</i> Mars 1964 Project	
limit cycles and self-disturbance torques	D016
star sensor	G013
microwave occultation data used to infer neutral atmospheric parameters	J011
<i>Mariner</i> Mars 1969 Project	
television image processing for navigation	A003
multilayer insulation thermal shield	C041
environmental testing and calibration of television system	D002
limit cycles and self-disturbance torques	D016
approach guidance demonstration	D021
star sensor	G013
Venus Deep Space Station support of extended mission project	J002
<i>Atlas/Centaur</i> launch vehicle	J010
attitude-control subsystem	J010
cabling system	J010
central computer and sequencer subsystem	J010
computer applications	J010
computer programs	J010
data automation subsystem	J010
data storage subsystem	J010
flight command subsystem	J010
flight telemetry subsystem	J010
infrared radiometer subsystem	J010
infrared spectrometer subsystem	J010
launch operations	J010
mechanical devices subsystem	J010
planetary quarantine requirements	J010
power subsystem	J010
project management	J010
propulsion subsystem	J010
pyrotechnic subsystem	J010
radio frequency subsystem	J010
scan control subsystem	J010
	K013
spacecraft development, design, and test	J010
spacecraft reliability studies	J010
spacecraft sterilization	J010
spacecraft trajectory analysis	J010
structure subsystem	J010
system test and prelaunch operations	J010
television subsystem	J010
temperature-control subsystem	J010
test facilities and equipment	J010
tracking	J010

Subject	Entry
<i>Mariner</i> Mars 1969 Project (contd)	
ultraviolet spectrometer subsystem	J010
Deep Space Network extended operations mission support	L024
transmitter phase modulation as a result of beam voltage ripple in <i>Mariner VII</i> signal	W011
<i>Mariner</i> Mars 1971 Project	
multilayer insulation thermal shield	C041
recording of subcarrier demodulator assembly outputs	H001
Space Flight Operations Facility mission support area	H010
flight telemetry subsystem	J012
mission and test computer system	J013
Mission Operations System software	J013
mission-and-test video system	J014
developmental test model forced vibration test	J015
integrated circuit procurement	J015
solar panel deployment/damper mechanism	J015
	J018
temperature control model testing	J015
flight loads analysis	J016
improved television camera shutter	J016
cracked solder joints	J018
medium-gain antenna RF plug assembly	J018
propellant tank fluid dynamics tests	J018
propulsion support structure	J018
integration testing of attitude-control subsystem	J020
modifications to logic mechanization of attitude-control subsystem	J020
scan platform motion effects on attitude-control subsystem	J020
solar panel shadow analysis program	J020
stabilization of autopilot in nonflight environment	J020
attitude control performance in commanded turn mode of operation	J023
Canopus tracker	J023
sun sensors	J023
gimbal actuator	J025
power subsystem design	J025
reaction control assembly	J025
scan actuator	J025
sun acquisition performance with latched solar panels	J025
project description and status	J027
	J028
	J029
propulsion subsystem sequence failure mode analysis	J032
pressurant relief assembly	J033

Subject	Entry	Subject	Entry
Mariner Mars 1971 Project (contd)		Materials, Metallic (contd)	
analysis of pressurant gas solubility in propellant tanks	J034	thermoelectric properties of 80-at.% silicon-20-at.% germanium alloy as a function of time and temperature	R001
effects of solvent on liquid propellant expulsion Teflon bladder bags	J034	test results of antenna reflector surface materials	W020
pressurant relief valve component testing	J034		
propulsion subsystem design	J034		
scan latch manifold assembly	J034		
television data acquisition for image processing	J036		
testing and selection of vidicons for television subsystem	J037		
evaluation of three spacecraft magnetic recording tapes	K003		
Deep Space Network support	L001		
	L002		
	L003		
celestial mechanics experiment	L033		
Mariner Venus 67 Project		Materials, Nonmetallic	
limit cycles and self-disturbance torques	D016	radiation damage in lithium-doped silicon	B018
star sensor	G013	mesh materials for deployable antennas	F005
long term life test of spare power subsystem hardware	K031	effects of strain energy and size on material fracture characteristics	G006
ionospheric effect on <i>Mariner V</i> mission	M055	effects of solvent on <i>Mariner Mars 1971</i> liquid propellant expulsion Teflon bladder bags	J034
		effects of simulated Venus atmosphere on polymeric materials	K007
		composite filament-wound pressure vessels	K026
		low-modulus propellant for case-bonded end-burning solid rocket motors	M008
		long-term aging of elastomers: stress relaxation of styrene-butadiene rubber	R002
		kinetics of formation of high charge density ionene polymers	R012
		spacecraft adhesives for long life and extreme environments	R035
		tensile strength of fiber-reinforced composite materials	Z004
		fiber-reinforced composite materials for spacecraft antenna structures	Z005
		statistical theory of material strength with application to composite materials	Z006
Mariner Venus-Mercury 1973 Project		Mathematical Sciences	
high-intensity solar simulation	J019	analysis of attitude control and structural response interaction	A001
power subsystem design	J021	second-order artificial satellite theory based on an intermediate orbit	A006
project description and status	J030	automatic input data generation scheme for a finite-element method	A007
	J031	digital fault diagnosis by low-cost arithmetical coding techniques	A021
		state determination for disturbed limit cycle operations via nonlinear filtering	B013
		calculus of variations applied to reverse Goddard problem	B014
		error analysis of extraterrestrial convergent photogrammetric mapping system	B015
		new tropospheric range refraction model	B017
		Monte Carlo calculations as used for correction to Jeans' escape rate	B036
		matrizant of the two-body problem	B038
		set of computer programs constructed to perform the literal series expansions of the two-body problem	B039
Masers and Lasers			
holographic interferometry for studying shell structures	C022		
masers used by Deep Space Network in support of Manned Space Flight Network for <i>Apollo</i> Project	F008		
optical systems and station procedures for <i>Surveyor VII</i> laser pointing test	J009		
ignition of explosives by laser energy	M029		
holography for pressure vessel flaw detection	M049		
microwave maser development	W010		
Materials, Metallic			
heat pipe materials compatibility	C040		
mesh materials for deployable antennas	F005		
effects of strain energy and size on material fracture characteristics	G006		
surface damage to metals from high-velocity flow of liquid lithium	H012		
<i>Mariner Mars 1971</i> improved television camera shutter materials	J016		
zinc coating for antenna	L030		
uranium nitride-tungsten compatibility	P017		

Subject	Entry
Mathematical Sciences (contd)	
analysis of automatic carrier acquisition in spacecraft telemetry	B042
analysis for optimization of acquisition time for sequential ranging system	B046
analysis of multichannel space telemetry	B048
decision rules for a two-channel deep-space telemetry system	B049
rank-order statistics for optimum detection of binary signals in the presence of white noise and dc drift	B051
approximate analysis of command lock detector performance	C008
technique for estimating phase of sampled signal with minimum mean-square error	C014
error probability of wide-band binary frequency-shift-keyed receiver in presence of multipath fading	C015
consensus of individual preferences	C017
analysis of nonlinear vibration of an infinite long circular cylinder	C020 C021
derivation of equations describing effects of scattering in radiative transfer	C028
differential equations of motion for a satellite after many revolutions	D001
Chebyshev polynomial expansions of Emden functions	D014
finite-sample quantile estimation	E002
construction of tetrahedral harmonics	F010
interferometric analysis for measurement of optical polarization	F015
analytic expressions for the partial derivatives of observables with respect to Robertson's relativistic parameters	G003
probability density function of a hardware performance parameter	G004
analysis of average access times for a magnetic disk storage device	G014
matching of mass spectra when peak height is encoded to one bit	G025
finite element matrix displacement using quadrilateral shell elements with step-by-step integration using Runge-Kutta extrapolation for high-impact dynamic response analysis of nonlinear structures	G027
mathematical treatment of self gravitation of rotating dense bodies	H006
simplified equations for relativistic rotating perfect fluids with axial symmetry	H007
minimum redundancy transformation between body and inertial frame for typical strapped-down inertial navigation system	H026

Subject	Entry
Mathematical Sciences (contd)	
analysis of performance of first-order digital phase-locked loop	H027
solution to the second-order phase-locked loop	H029
pattern recognition: invariant stochastic feature extraction and classification by the sequential ratio test	H030
cyclic search algorithms for synchronizing maximal length linear shift register sequences	H032
analysis and simulation of phase detector used for digital telemetry	H041
method for finding exact power spectrums of pseudonoise codes	J006
parameter estimation from sets of two-dimensional maps	J011
application of discriminant analysis to validation of telemetry data in the Space Flight Operations Facility	K014
dual-mode routing algorithm for autonomous roving vehicle	K016
improved Newton-Raphson algorithm for finding the roots of equations for solid propellant combustion studies	K021
basic equations in the mathematical modeling of the gas phase of a burning solid propellant	K022
simple sequence permutation method	K023
uniform permutation of sequences	K024
analysis of effect of predemodulation filtering on the correlation and error signals in a pseudonoise receiver	K028
analysis of interplex modem	L004
upper bound on free distance of tree code	L010
theorems for synchronizability of convolutional codes	L012
equations for closed-form computations for selecting antenna rigging angles to improve performance	L019
Markov process approach used in Thermoelectric Outer-Planet Spacecraft (TOPS) attitude control reliability study	L022
cross spectrum generalized harmonic analysis of hybrid carrier and modulation tracking loops	L023
variational equations derived from Herrick variation of parameters method	L026
nonlinear equations of motion for a solar-electric spacecraft	M007
reliability analysis and architecture of a hybrid-redundant digital system: generalized triple modular redundancy with self-repair	M015
Ramsey bounds for coefficients of internal stability of graph products	M018

Subject	Entry	Subject	Entry
Mathematical Sciences (contd)		Mathematical Sciences (contd)	
finite sets and compact metric spaces in relationship between games of search and optimum storage of information	M020	analytical calculation of neutron yield from (α, n) reactions of low-Z impurities in a plutonium heat source	T001
arbitrarily long binary block codes that are preserved under very large permutation groups and that satisfy the Gilbert bound	M021	analysis of tracking loop with noise in suppressed-carrier two-channel interplex modulation system	T013
brute-force least-squares estimation	M025	mathematical analyses relative to design of signals for analog communication	T014
generalization of Boltzmann superposition principle	M040	upper bound on estimation error in threshold region for nonlinear pulse modulation systems	T015
mathematical and computational properties for the incomplete gamma functions	N006	frequency domain solution for the linear attitude-control problem of spacecraft with flexible appendages	T021
certification of algorithm 385 (S13) exponential integral $Ei(x)$	N008	analysis of comparative performance of double focused and quadrupole mass spectrometers	W017
dynamic programming approach to optimal stochastic orbital transfer strategy	N012	analysis of maximum dynamic response of structures	Y002
solution for tropospheric zenith range correction using a single pass of differenced doppler data	O003	solution of a Toeplitz set of linear homogeneous equations	Z003
effects of a variable h_{\max} on the mapping of zenith ionospheric corrections to lower elevation angles	O004	statistical theory of material strength with application to composite materials	Z006
linear m -ary feedback shift registers	P012		
Fourier-Bessel integrals used to study dipole antenna radiation in a compressible, anisotropic electron plasma overlaying an imperfectly conducting half-space	P016	Mechanics	
epsilon entropy and data compression	P020	attitude control and structural response interaction	A001
formulation of optimum shell design	S002	second-order artificial satellite theory based on an intermediate orbit	A006
computational complexity	S011	state determination for disturbed limit cycle operations in spacecraft attitude-control via nonlinear filtering	B013
rate equations for emission in hypersonic blunt-body flow of a radiating gas at low density	S016	matrizant of the two-body problem	B038
optimum structural design based on reliability analysis	S026	set of computer programs constructed to perform the literal series expansions of the two-body problem	B039
derivation of optimum receiver structure for single-channel, phase-coherent communication system	S040	nonlinear vibration of an infinite long circular cylinder	C020 C021
transponder-receiver system model and loop parameters in terms of system design point	S042	solar-electric spacecraft thrust vector control system mechanization	C038
probability of error from synchronization jitter in relay performance	S049	differential equations of motion for a satellite after many revolutions	D001
testing of proposed all-digital command detection algorithm	S058	<i>Mariner</i> limit cycles and self-disturbance torques	D016
analysis of phase coherent-incoherent output of bandpass limiter	S059	construction of tetrahedral harmonics	F010
calculation of Faraday rotation of 13-cm signal from <i>Pioneer VI</i> passing through solar corona	S062	high-impact dynamic response analysis of nonlinear structures	G027
analysis of random modulation in amplifier circuits	S075	<i>Mariner</i> Mars 1971 flight loads analysis	J016
		<i>Mariner</i> Mars 1971 propellant tank fluid dynamics tests	J018
		nonlinear equations of motion for a solar-electric spacecraft	M007

Subject	Entry	Subject	Entry
Mechanics (contd)		Packaging and Cabling	
frequency domain solution for the linear attitude-control problem of spacecraft with flexible appendages	T021	Thermoelectric Outer-Planet Spacecraft (TOPS) packaging and cabling	D006
maximum dynamic response of structures	Y002	<i>Mariner</i> Mars 1969 packaging and cabling	J010
		new cable wrap-up system for 210-ft-diam antenna	M022
Mechanisms		Particle Physics	
<i>Mariner</i> Mars 1969 spacecraft mechanisms	J010	ion cyclotron resonance study of ion-molecule reactions in hydrogen-methane mixtures	B025
<i>Mariner</i> Mars 1971 solar panel deployment/damper mechanism	J015	electron impact excitation of N ₂	B035
	J018	effect of steric compression on proton-proton, spin-spin coupling constants	C032
<i>Mariner</i> Mars 1971 improved television camera shutter	J016	proton nuclear magnetic resonance spectra of <i>cisoid</i> -dienes	C033
<i>Mariner</i> Mars 1971 medium-gain antenna RF plug assembly	J018	gamma ray and neutron analysis for a 15-W(th) Pu ²³⁸ O ₂ isotopic heater	D018
<i>Mariner</i> Mars 1971 gimbal actuator	J025	gamma radiation characteristics of plutonium dioxide fuel	G005
<i>Mariner</i> Mars 1971 scan actuator	J025	ion cyclotron resonance study of the ion-molecule reactions in methane-ammonia mixtures	H039
<i>Mariner</i> Mars 1971 pressurant relief valve component testing	J034	retention coefficients and thermal release profiles of ion-injected argon from silicates and iron	L031
<i>Mariner</i> Mars 1971 scan latch manifold assembly	J034	absolute gamma ray intensity measurements of a SNAP-15A (System for Nuclear Auxiliary Power 15A)	R010
thermomechanical pump for Thermoelectric Outer-Planet Spacecraft (TOPS)	S001	analytical calculation of neutron yield from (α , n) reactions of low-Z impurities in a plutonium heat source	T001
electromechanical pyrotechnics switching for Thermoelectric Outer-Planet Spacecraft (TOPS)	W024	vibration excitation of H ₂ by low- and medium-energy electrons	T016
		electron scattering by H ₂ with and without vibrational excitation	T019
Meteors			T020
retention coefficients and thermal release profiles of ion-injected argon from meteoric materials	L031	vibrational excitation of N ₂ and CO by electron impact	W013
Optics		comparative performance of double focused and quadrupole mass spectrometers	W017
error analysis of extraterrestrial convergent photogrammetric mapping system	B015	nuclear radiation mapping of Thermoelectric Outer-Planet Spacecraft (TOPS)	W018
interferometric approach to measurement of optical polarization	F015		
polarizers and retardation plates for a vector helium magnetometer	H034	Photography	
colorimetric measurements of solar eclipse and earth from <i>Surveyor III</i>	J009	operation of <i>Surveyor</i> television system in photon-integration mode	A009
optical systems and station procedures for <i>Surveyor VII</i> laser pointing test	J009	television image processing for navigation	A033
photometry and polarimetry of earth by <i>Surveyor VII</i>	J009	error analysis of extraterrestrial convergent photogrammetric mapping system	B015
<i>Mariner</i> Mars 1969 optical systems	J010	Polaroid quick-look system for digital prints	B025
uniform variable light sources for instrument calibration	S060	holographic interferometry for studying shell structures	C022
photometric error analysis: enriched energy (total illuminance) calculations for annular apertures	Y010	environmental testing and calibration of <i>Mariner</i> Mars 1969 television system	D002
		<i>Mariner</i> Mars 1969 television equipment	J010

Subject	Entry	Subject	Entry
Photography (contd)		Planetary Atmospheres (contd)	
<i>Mariner</i> Mars 1971 mission-and-test video system	J014	high-dispersion spectroscopic studies of Mars: water-vapor	S017
<i>Mariner</i> Mars 1971 improved television camera shutter	J016	high-dispersion spectroscopic observations of Venus	S018
scan subsystem mechanization	J022	vibrational excitation of H ₂ by low- and medium-energy electrons	T016
<i>Mariner</i> Mars 1971 television data acquisition for image processing	J036	vibrational excitation of N ₂ and CO by electron impact	W013
testing and selection of vidicons for <i>Mariner</i> Mars 1971 television subsystem	J037	high-resolution spectra of Mars: CO ₂ abundance and surface pressure derived from curve of growth	Y011
holography for pressure vessel flaw detection	M049		
multispectral remote sensing of an exposed volcanic province	Q001	Planetary Exploration, Advanced	
scientific objectives for imaging experiments at outer planets	R011	error analysis of extraterrestrial convergent photogrammetric mapping system	B015
digital removal of noise from video imagery	R032	identification of products from nucleotide pyrolysis by high resolution mass spectrometry for detection of life	B020
applications of slow-scan television systems to planetary exploration	S003	advanced planetary navigation	B029
uniform variable light sources for instrument calibration	S060		C047
irradiance required to cause damage to developed photographic film	V001		C048
			D020
			H002
			M026
			M046
Pioneer Project		microbiology, ecology, and microclimatology of soil sites in dry valleys of southern Victoria Land, Antarctica, in preparation for detection of life in extraterrestrial environments	C001
Deep Space Network support	R018	attitude control for an outer planet orbiter spacecraft	D019
	S030	high-impact dynamic response analysis of nonlinear structures such as hard landers	G027
Tracking and Data System support	R019	effects of simulated Venus atmosphere on polymeric materials	K007
Faraday rotation measurement of signal from <i>Pioneer</i> VI	S062	dual-mode routing algorithm for autonomous roving vehicle	K016
		proposed gamma ray spectroscopic measurements of Mars to be made from Mars orbiter	M032
Planetary Atmospheres		scientific objectives for imaging experiments at outer planets	R011
ion cyclotron resonance study of ion-molecule reactions in hydrogen-methane mixtures, as in Jupiter atmosphere	B025	spacecraft adhesives for long life and extreme environments	R035
electron impact excitation of N ₂	B035	applications of slow-scan television systems to planetary exploration	S003
departures from Jeans' escape rate for H and He	B036	whole microorganisms studied by pyrolysis-gas chromatography-mass spectrometry: extraterrestrial life detection experiments	S039
Martian blue-clearing during 1967 apparition	C004	possible 1975 Jupiter-Pluto gravity assist trajectories	S061
efficiency of CO ₃ formation in Mars and Venus atmospheres	D010	1982 Jupiter orbiter mission	W015
multi-phase ammonia-water system to be used for modeling Jupiter and Saturn atmospheres	H009		
profile inversion processing of radio occultation data for the determination of planetary atmospheres	J011		
spectrum of Jupiter at 18.5-24.0 GHz	J042		
effects of simulated Venus atmosphere on polymeric materials	K007		
<i>Mariner</i> Mars 1971 occultation experiment	L001		
scientific objectives for imaging experiments at outer planets	R011		

Subject	Entry	Subject	Entry
Planetary Interiors		Plasma Physics (contd)	
Chebyshev polynomial expansions of Emden functions used to determine density, mass and temperature of stars and planets	D014	Faraday rotation measurement of 13-cm signal in solar corona	S062
mass of Mercury, Venus, and Mars from radar data	J011	drift velocities of electrons in the positive column of a neon discharge	S073
internal structures of Mercury and Venus	L039		
structures of terrestrial planets	L041	Power Sources	
Planetary Motion		improved solar cell contact-interconnect feasibility	A004
motion and mass of Mercury, Venus, and Mars from radar doppler residuals	J011	radiation damage in lithium-doped silicon	B018
rotation period and direction of spin axis of Venus determined from anomalous backscattering of UHF radar waves	J011	radioisotope thermoelectric generator test laboratory	C003
<i>Mariner</i> Mars 1971 celestial mechanics experiment	L033	multi-hundred-watt radioisotope thermoelectric generator thermal environment	C006
Planetary Quarantine		performance and weight of large roll-up solar arrays	C036
<i>Mariner</i> Mars 1969 Project planetary quarantine requirements	J010	gamma radiation characteristics of plutonium dioxide fuel	G005
Planetary Spacecraft, Advanced		solar cell standardization	G019
spacecraft-based navigation instrument for outer planet missions	D023	design of reactor simulator for thermionic diode kinetics experiment	G023
70-kWe thermionic reactor electric propulsion spacecraft	M045	reactor simulator runs with thermionic diode kinetics experiment	G024
Planetary Surfaces		thermal conductance at elevated temperatures of alumina-nickel interfaces usable in magnetohydrodynamic generators	H011
radar brightness map of Venus	G009	surface damage to metals from high-velocity flow of liquid lithium, as in a magnetohydrodynamic generator	H012
Venus radar backscatter at 70-cm wavelength	J011	<i>Mariner</i> Mars 1969 solar panels	J010
<i>Mariner</i> Mars 1971 radio experiment	L001	<i>Mariner</i> Mars 1971 solar panel deployment/damper mechanism	J015
gamma ray spectroscopic measurements of Mars	M032		J018
Plasma Physics		<i>Mariner</i> Mars 1971 solar panel shadow analysis program	J020
theory of auroral arc formation	A020	<i>Mariner</i> Venus-Mercury 1973 power subsystem design	J021
curves of growth of autoionizing spectral lines with application to the 3s-4p transition in argon	C024	<i>Mariner</i> Mars 1971 power subsystem design	J025
plasma properties and performance of mercury ion thrusters	M009	<i>Viking</i> orbiter power subsystem design	J026
numerical study of collisional effects on spatial ion-wave echoes	N010	long term life test of spare <i>Mariner</i> Venus 67 power subsystem hardware	K031
second-order perturbed distribution associated with the plasma wave echo	N011	thermal interface of radioisotope thermoelectric generators with spacecraft	L014
dipole antenna radiation in a compressible, anisotropic electron plasma overlaying an imperfectly conducting half-space: lunar applications	P016	multi-hundred-watt radioisotope thermoelectric generator transient performance	L015
<i>Orbiting Geophysical Observatory 5</i> observations of quasi-trapped electromagnetic waves in the solar wind	S012	electric propulsion power conditioning	M003
		interactions between radiation fields from radioisotope thermoelectric generators and scientific experiments on spacecraft	M038
		nuclear criticality studies for a thermionic reactor with uninsulated externally fueled diodes	P002
		uranium nitride-tungsten compatibility for in-pile thermionic diode fuel	P017

Subject	Entry	Subject	Entry
Power Sources (contd)		Propulsion, Liquid (contd)	
thermoelectric properties of 80-at.% silicon-20-at.% germanium alloy as a function of time and temperature	R001	<i>Mariner</i> Mars 1971 pressurant relief assembly	J033
absolute gamma ray intensity measurements of a SNAP-I5A (System for Nuclear Auxiliary Power 15A)	R010	analysis of pressurant gas solubility in <i>Mariner</i> Mars 1971 propellant tanks	J034
analytical calculation of neutron yield from (α , n) reactions of low-Z impurities in a plutonium heat source	T001	effects of solvent on <i>Mariner</i> Mars 1971 liquid propellant expulsion Teflon bladder bags	J034
nuclear radiation mapping of Thermoelectric Outer-Planet Spacecraft (TOPS)	W018	<i>Mariner</i> Mars 1971 pressurant relief valve component testing	J034
lightweight integrated silicon solar cell array	Y004	<i>Mariner</i> Mars 1971 propulsion subsystem	J034
Propulsion, Electric		composite filament-wound pressure vessels	K026
solar-electric spacecraft thrust vector control system mechanization	C038	advanced combustion device development	R027
solar-electric propulsion system technology (SEPST) project thrust vector control electronics	C039	Propulsion, Solid	
auxiliary propulsion systems	H024	design, fabrication, and testing of the applications technology satellite	G021
solid-state switching matrix for solar-electric propulsion	M002	apogee motor insulation	G021
power conditioning	M003	auxiliary propulsion systems	H024
nonlinear equations of a motion for a solar-electric spacecraft	M007	functionality of isobutylene prepolymers	I001
plasma properties and performance of mercury ion thrusters	M009	instantaneous burning rate during depressurization of rocket motor	K020
sizing of a solar-electric thrust subsystem	M010	improved Newton-Raphson algorithm for finding the roots of equations for solid propellant combustion studies	K021
70-kWe thermionic reactor electric propulsion spacecraft	M045	basic equations in the mathematical modeling of the gas phase of a burning solid propellant	K022
control analysis of ion thruster with programmed thrust	M052	low-modulus propellant for case-bonded end-burning motors	M008
solar-electric propulsion system tests	P006	ignition of explosives by laser energy	M029
ion thruster control loop sensitivity	P007	generalization of Boltzmann superposition principle to determine stress-relaxation behavior of an elastomer undergoing scission reactions	M040
ion thruster hollow cathode studies	P008	heat-sterilizable capsule spin motors	N014
solar-electric propulsion system evaluation	P010	long-term aging of elastomers: stress relaxation of styrene-butadiene rubber	R002
Propulsion, Liquid		long-term aging of elastomers: kinetics of oxidation of styrene-butadiene rubber studied by infrared spectrometry	R003
injector hydrodynamics effects on baffled-engine stability	C026	molecular-sieve catalyzed polymerization of isobutylene for solid fuel	R022
Thermoelectric Outer-Planet Spacecraft (TOPS) trajectory correction engine	H015	case-bonded end-burning rocket motors	S021
Thermoelectric Outer-Planet Spacecraft (TOPS) trajectory correction engine testing	H016	electronic conductivity of elastomeric ionenes	S055
auxiliary propulsion systems	H024	effects of heat sterilization and vacuum storage on ignition of solid propellant rockets	S072
optimum mixing of hypergolic propellants in an unlike doublet injector element	H033	Pyrotechnics	
<i>Mariner</i> Mars 1969 propulsion subsystem design	J010	<i>Mariner</i> Mars 1969 pyrotechnic devices	J010
<i>Mariner</i> Mars 1971 propellant tank fluid dynamics tests	J018	nondestructive testing of electro-explosive devices	M028
<i>Mariner</i> Mars 1971 propulsion subsystem sequence failure mode analysis	J032	ignition of explosives by laser energy	M029
		pyrotechnics switching for Thermoelectric Outer-Planet Spacecraft (TOPS)	W024

Subject	Entry	Subject	Entry
Quality Assurance and Reliability		Radio Astronomy	
Deep Space Network Monitor System	A008	noise-adding radiometer for using telemetry	
evaluation of 26- to 32-AWG (American wire		system for radio astronomy	B008
gauge) wire	A015	Venus Deep Space Station experiments	J001
radiation damage in lithium-doped silicon	B018	spectrum of Jupiter at 18.5–24.0 GHz	J042
reliable interface circuit for driving		high-resolution observations of compact	
field effect transistor switching trees	E001	radio sources at 13 cm	K009
probability density function of a		Deep Space Network radio science support	S006
hardware performance parameter	G004		S007
evaluation of spacecraft magnetic		Faraday rotation measurement of 13-cm	
recording tapes	H022	signal in solar corona	S062
	K003		
	K006	Relativity	
techniques for selecting auxiliary propulsion		analytic expressions for the partial derivatives	
systems	H024	of observables with respect to	
reliability in man-machine interaction in		Robertson's relativistic parameters	G003
post-1971 Space Flight Operations Facility	H037	general relativistic axially symmetric	
<i>Mariner</i> Mars 1969 spacecraft reliability studies.....	J010	rotating perfect fluids	H006
integrated circuit procurement for			H007
<i>Mariner</i> Mars 1971 Project	J015	potential of interplanetary spacecraft data	
<i>Mariner</i> Mars 1971 spacecraft cracked		for testing gravity theories	J011
solder joints	J018	<i>Mariner</i> Mars 1971 celestial mechanics	
<i>Mariner</i> Mars 1971 propulsion subsystem		experiment	L033
sequence failure mode analysis	J032	generalization of Boltzmann superposition	
long term life test of spare <i>Mariner</i>		principle	M040
Venus 67 power subsystem hardware	K031	Scientific Instruments	
Thermoelectric Outer-Planet Spacecraft		miniaturized absolute gravimeter	B031
(TOPS) attitude control reliability		near infrared multidetector grating	
study	L022	spectrometer	C009
welded joint integrity study	L027	<i>Mariner</i> spacecraft star sensors	G013
nondestructive testing of		polarizers and retardance plates for a	
electro-explosive devices	M028	vector helium magnetometer	H034
	R038	<i>Mariner</i> Mars 1969 science subsystem	J010
diagnostics for Space Flight Operations Facility		optimal optical design for Mars atmospheric	
central processing system standalone		water detection spectrometer on	
acceptance and maintenance routines	W007	<i>Viking</i> orbiter system	J035
Radar		two accurate blackbody radiometers	K012
radar brightness map of Venus	G009	multichannel radiometer for measurement of	
Venus Deep Space Station		solar spectral irradiance at	
planetary radar experiments	J001	different terrestrial elevations	L008
	J002	gamma ray spectrometer for <i>Apollo 16</i>	L020
	J004	gamma ray spectrometer to orbit Mars	M032
application of model fitting procedure to		interactions between radiation fields from	
determination of unknown parameters in		radioisotope thermoelectric generators	
several theoretical backscatter models		and scientific experiments on spacecraft	M038
of Venus at 70-cm wavelength	J011	<i>Apollo</i> gamma ray spectrometer thermal	
design of Haystack planetary radar system	J011	model tests	P013
multispectral remote sensing of an		<i>Pioneer IX</i> scientific instruments	R019
exposed volcanic province	Q001	palladium-hydrogen system: efficient interface	
Deep Space Network planetary radar		for gas chromatography-mass	
experiments	S007	spectrometry	S037
		uniform variable light sources for	
		instrument calibration	S060

Subject	Entry	Subject	Entry
Scientific Instruments (contd)		Solid-State Physics	
cooling of infrared-radiometer for outer-planet missions	S069	radiation damage in lithium-doped silicon	B018
electron impact spectrometer	T019	microwave emission from granular silicates: determination of the absorption coefficient from plate measurements and the effects of scattering	C028
comparative performance of double focused and quadrupole mass spectrometers	W017	effects of strain energy and size on material fracture characteristics	G006
calibration of hot film anemometer for low velocity measurement in nonisothermal flow	Z002	thermal conductance of alumina-nickel interfaces at elevated temperatures	H011
Shielding		thermal joint conductance	H038
multilayer insulation testing	C040	retention coefficients and thermal release profiles of ion-injected argon from silicates and iron	L031
<i>Mariner</i> Mars 1969 spacecraft shielding	J010	generalization of Boltzmann superposition principle representing stress-relaxation behavior of an elastomer undergoing scission reactions	M040
shielding for scientific experiments on spacecraft having radioisotope thermoelectric generators	M038	thermoelectric properties of 80-at.% silicon-20-at.% germanium alloy as a function of time and temperature	R001
nuclear radiation mapping of Thermoelectric Outer-Planet Spacecraft (TOPS)	W018	optimum shell design	S002
Soil Sciences		thermal noise in space-charge-limited solid-state diodes	S029
microbiology, ecology, and microclimatology of soil sites in dry valleys of southern Victoria Land, Antarctica	C001	electronic conductivity of elastomeric ionenes	S055
scanning electron and optical microscope study of Antarctic soil algal crusts	C002	metal-cadmium sulphide work functions at non-zero current densities	S070
microwave emission from granular silicates: determination of the absorption coefficient from plate measurements and the effects of scattering	C028	maximum dynamic response of structures	Y002
moon soil properties determined from <i>Surveyor</i> data and laboratory tests	J009	tensile strength of fiber-reinforced composite materials	Z004
vehicle mobility tests: soft soil slopes	K025	statistical theory of material strength with application to composite materials	Z006
multispectral remote sensing of an exposed volcanic province	Q001	Spectrometry	
fluorometric examination of bulk fine lunar sample from <i>Apollo 11</i>	R023	skeletal molecular structure of <i>closo</i> -2,3-dicarbahexaborane (6) from microwave spectral studies	B011
Solar Phenomena		identification of products from nucleotide pyrolysis by high resolution mass spectrometry	B020
colorimetric measurements of solar eclipse from <i>Surveyor III</i>	J009	ion cyclotron resonance study of ion-molecule reactions in hydrogen-methane mixtures	B025
radar studies of sun	J011	analysis of ion-molecule reactions in allene and propyne by ion cyclotron resonance	B026
high-intensity solar simulation for <i>Mariner</i> Venus-Mercury 1973 spacecraft	J019	near infrared multidetector grating spectrometer	C009
measurement of solar spectral irradiance at different terrestrial elevations	L008	curves of growth of autoionizing spectral lines with application to the 3s-4p transition in argon	C024
charged-particle calibration system analysis	M053	determining SiO ₂ abundance in silicate glass from powder film transmission measurements in the infrared	C030
luminescence properties of <i>Apollo 11</i> lunar samples: solar-excited lunar luminescence	N002	spectral reflectance and albedo of <i>Apollo 11</i> lunar samples	C031
<i>Orbiting Geophysical Observatory 5</i> observations of quasi-trapped electro- magnetic waves in the solar wind	S012		
Faraday rotation measurement of 13-cm signal in solar corona	S062		

Subject	Entry
Spectrometry (contd)	
effect of steric compression on proton–proton, spin–spin coupling constants determined from spectra	C032
proton nuclear magnetic resonance spectra of <i>cisoid</i> -dienes	C033
determination of rates and mechanism of alkyne ozonation	D009
interferometric approach to measurement of optical polarization	F015
matching of mass spectra when peak height is encoded to one bit	G025
ion cyclotron resonance study of the ion–molecule reactions in methane–ammonia mixtures	H039
<i>Mariner</i> Mars 1969 science subsystem spectrometers	J010
spectrum of Jupiter at 18.5–24.0 GHz	J042
measurement of solar spectral irradiance at different terrestrial elevations	L008
gamma ray spectrometer for <i>Apollo 16</i>	L020
gamma ray spectroscopic measurements of Mars	M032
quantitative confirmation of planetary defects in lunar theory by spectral decomposition	M057
luminescence properties of <i>Apollo 11</i> lunar samples	N002
experimental measurements of some ArII transition probabilities and a comparison of published values	N004
long-term aging of elastomers: kinetics of oxidation of styrene–butadiene rubber studied by infrared spectrometry	R003
linear-energy spectrophotofluorometric examination of bulk fine lunar sample from <i>Apollo 11</i>	R023
high-dispersion spectroscopic studies of Mars	S017
high-dispersion spectroscopic observations of Venus	S018
palladium–hydrogen system: efficient interface for gas chromatography–mass spectrometry	S037
whole microorganisms studied by pyrolysis–gas chromatography–mass spectrometry	S039
electron impact spectrometer	T019
electron impact spectrometry used to measure electron scattering by H ₂	T019 T020
comparative performance of double focused and quadrupole mass spectrometers	W017
high-resolution spectra of Mars: CO ₂ abundance and surface pressure derived from curve of growth	Y011

Subject	Entry
Standards, Reference	
Deep Space Instrumentation Facility network maintenance facility: reference standards frequency and timing laboratory	F014
solar cell standardization	G019
Venus Deep Space Station clock synchronization transmissions	J001
very long baseline interferometry for more accurate measurement of time and location	J011
clock-sync antenna installation at U.S. Naval Observatory	K018
celestial mechanics experiment for improved ephemerides of earth and Mars to be performed by <i>Mariner</i> Mars 1971	L033
improved planetary ephemerides required for future planetary navigation	M026
quantitative confirmation of planetary defects in lunar theory by spectral decomposition	M057
uniform variable light sources for instrument calibration	S060
time-synchronized very-low frequency phase-tracking receiver	W003
calibration of hot film anemometer	Z002
Sterilization	
<i>Mariner</i> Mars 1969 spacecraft sterilization	J010
heat-sterilizable capsule spin motors	N014
effects of heat sterilization and vacuum storage on ignition of solid propellant rockets	S072
Structural Engineering	
attitude control and structural response interaction	A001
nonlinear vibration of an infinite long circular cylinder	C020 C021
design of large roll-up solar arrays	C036
effects of strain energy and size on material fracture characteristics	G006
high-impact dynamic response analysis of nonlinear structures	G027
<i>Mariner</i> Mars 1969 spacecraft structure	J010
<i>Mariner</i> Mars 1971 flight loads analysis	J016
<i>Mariner</i> Mars 1971 propellant tank fluid dynamics tests	J018
<i>Mariner</i> Mars 1971 propulsion support structure	J018
30-ft-diam antenna upgrade	K008
method for selecting antenna rigging angles to improve performance	L019
welded joint integrity study	L027
deep space station antenna repairs	L028
low-frequency, low-level stress reversals on an assembly of bolted joint specimens	L030

Subject	Entry	Subject	Entry
Structural Engineering (contd)		Telemetry and Command (contd)	
optimum shell design	S002	telemetry simulation conversion assembly	G001
optimum structural design based		loop stress diminution	G007
on reliability analysis	S026	recording of subcarrier demodulator assembly	
frequency domain solution for the linear		outputs for <i>Mariner</i> Mars 1971 Project	H001
attitude-control problem of spacecraft		Deep Space Network support of	
with flexible appendages	T021	<i>Apollo</i> Project	H008
maximum dynamic response of structures	Y002	performance of a first-order digital	
fiber-reinforced composite materials for		phase-locked loop	H027
spacecraft antenna structures	Z005	performance of all-digital command system	
Surveyor Project		timing loop	H028
operation of television system		solution to the second-order phase-locked loop	H029
in photon-integration mode	A009	cyclic search algorithms for synchronizing	
colorimetric measurements of solar eclipse		maximal length linear shift register	
and earth from <i>Surveyor III</i>	J009	sequences	H032
moon soil properties determined from		digital transition tracking symbol	
<i>Surveyor</i> data and laboratory tests	J009	synchronizer for low signal-to-noise	
optical systems and station procedures for		ratio coded systems	H041
<i>Surveyor VII</i> laser pointing test	J009	method for finding exact power spectrums	
photometry and polarimetry of earth by		of pseudonoise codes	J006
<i>Surveyor VII</i>	J009	<i>Mariner</i> Mars 1969 telemetry and	
environmental testing of <i>Surveyor</i> spacecraft		command subsystems	J010
at JPL Environmental Test Laboratory	O007	<i>Mariner</i> Mars 1971 flight telemetry subsystem	J012
Telemetry and Command		<i>Viking</i> orbiter relay system	J038
Deep Space Network Telemetry System	A010	real-time selection and validation of telemetry	
minimum switching network for generating		data in the Space Flight Operations Facility	K014
the weight, in binary notation,		effect of predemodulation filtering on the	
of a binary vector	A013	correlation and error signals in a	
an efficient two-channel telemetry		pseudonoise receiver	K028
system for space exploration	B045	switched-carrier experiments	K029
	B049	Deep Space Network support	
optimization of acquisition time for		of <i>Mariner</i> Mars 1971 Project	L001
sequential ranging system	B046		L002
efficient multichannel space telemetry	B048		L003
rank-order statistics for optimum detection		space station unified communication: optimum	
of binary signals in the presence of		modulation indexes and maximum data	
white noise and dc drift	B051	rates for the interplex modem	L004
approximate analysis of command lock		performance of short constraint length	
detector performance	C008	convolutional codes and a heuristic	
estimating phase of sampled signal with		code-construction algorithm	L011
minimum mean-square error	C014	synchronizability of convolutional codes	L012
error probability of wide-band binary		comparing performance of three rate $\frac{1}{2}$,	
frequency-shift-keyed receiver in		$K = 32$ codes for multiple-mission	
presence of multipath fading	C015	sequential decoder	L013
Deep Space Instrumentation Facility		hybrid carrier and modulation tracking loops	L023
multiple-mission command system	C043	Deep Space Network extended operations	
Deep Space Network support of Manned		mission support of <i>Mariner</i> Mars 1969 Project	L024
Space Flight Network for <i>Apollo</i> Project	F008	Ground Communications Facility wideband	
Deep Space Instrumentation Facility		digital data system	M017
multiple mission telemetry 1971		frequency generation and control:	
configuration	F012	measurement of phase jitter	M033
		mean-square error and bias of phase	
		estimator for sequential ranging system	M044

Subject	Entry
Telemetry and Command (contd)	
Deep Space Network support of <i>Viking</i> Project	M051
charged-particle calibration system analysis	M053
Space Flight Operations Facility high-speed data transmission	M058
linear <i>m</i> -ary feedback shift registers	P012
computerized receiver and telemetry signal-to- noise ratio predictions program	P019
Deep Space Network support of <i>Pioneer</i> Project	R018
	S030
Tracking and Data System support of <i>Pioneer</i> Project	R019
the asymptotic complexity of the Green decoding procedure	S009
computational complexity in telemetry and command	S011
computer-assisted acquisition	S019
optimum receiver structure for single-channel, phase-coherent communication system	S040
optimum modulation index for a data-aided, phase-coherent communication system	S041
effect of limiter suppression on command detection performance	S042
Space Flight Operations Facility digital television assembly	S045
effects of synchronizer jitter on relay performance	S049
testing of proposed all-digital command detection algorithm	S058
analysis of phase coherent-incoherent output of bandpass limiter	S059
suppressed-carrier two-channel interplex modulation system	T013
upper bound on estimation error in threshold region for nonlinear pulse modulation systems	T015
telemetry improvement proposal for the 85-ft antenna network	U003
contrast ratio determination for Space Flight Operations Facility video image display	V002
digital acquisition and detection: solution of a Toeplitz set of linear homogeneous equations	Z003
Temperature Control	
multi-hundred-watt radioisotope thermoelectric generator thermal environment	C006
heat pipe materials compatibility	C040
multilayer insulation testing	C040
	C041
gamma ray and neutron analysis for a 15-W(th) Pu ²³⁸ O ₂ isotopic heater	D018

Subject	Entry
Temperature Control (contd)	
design, fabrication, and testing of the applications technology satellite apogee motor insulation	G021
thermal joint conductance	H038
<i>Mariner</i> Mars 1969 temperature control	J010
<i>Mariner</i> Mars 1971 temperature control model testing	J015
thermal design for <i>Viking</i> orbiter system	J017
thermal interface of radioisotope thermoelectric generators with spacecraft	L014
<i>Apollo</i> gamma ray spectrometer thermal model tests	P013
thermomechanical pump for Thermoelectric Outer-Planet Spacecraft (TOPS)	S001
cooling of infrared-radiometer for outer-planet missions	S069
temperature control of microwave maser	W010
Test Facilities and Equipment	
JPL solar simulators	B007
radioisotope thermoelectric generator test laboratory	C003
holographic interferometry for testing shell structures	C022
facility for testing injector hydrodynamics effects on baffled-engine stability	C026
multilayer insulation test facility	C040
telemetry simulation conversion assembly	G001
design of reactor simulator for thermionic diode kinetics experiment	G023
equipment for testing surface damage to metals from high-velocity flow of liquid lithium	H012
Thermoelectric Outer-Planet Spacecraft (TOPS) trajectory correction engine testing	H016
thrust and plume measurements taken on miniature nozzles in a vacuum chamber	H018
nonplanar wind tunnel capability	J005
penetrometer used in laboratory to compare lunar soil to standard samples	J009
test arrangement to determine moon soil erosion by <i>Surveyor</i> spacecraft attitude-control jets	J009
<i>Mariner</i> Mars 1969 Project test facilities and equipment	J010
<i>Mariner</i> Mars 1971 developmental test model forced vibration test	J015
<i>Mariner</i> Mars 1971 temperature control model testing	J015
<i>Viking</i> orbiter system test equipment	J017
high-intensity solar simulation for <i>Mariner</i> Venus-Mercury 1973 spacecraft	J019

Subject	Entry	Subject	Entry
Test Facilities and Equipment (contd)		Thermodynamics (contd)	
stabilization circuit for <i>Mariner</i> Mars 1971 autopilot in nonflight environment	J020	instantaneous burning rate during depressurization of rocket motor	K020
testing and selection of vidicons for <i>Mariner</i> Mars 1971 television subsystem	J037	improved Newton–Raphson algorithm for finding roots of equations for solid propellant combustion studies	K021
apparatus for testing effects of simulated Venus atmosphere on polymeric materials	K007	basic equations in the mathematical modeling of the gas phase of a burning solid propellant	K022
210-ft antenna wind loading measurements	K034	thermomechanical pump for Thermoelectric Outer-Planet Spacecraft (TOPS)	S001
wind tunnel coefficients for parabolic reflectors	L017	hypersonic blunt-body flow of a radiating gas at low density	S016
thirty-degree reflector mockup	L018		
welded joint integrity test equipment	L027	Thermoelectric Outer-Planet Spacecraft (TOPS)	
nondestructive testing of electro-explosive devices	M028 R038	evaluation of 26- to 32-AWG (American wire gauge) wire for potential TOPS use	A015
design considerations for accelerated radiation tests	M035	multi-hundred-watt radioisotope thermoelectric generator thermal environment	C006
application of imposed magnetic fields to compact-arc lamps in solar simulator	M036	electronic packaging and cabling	D006
holography for pressure vessel flaw detection	M049	attitude control of a TOPS-based outer-planet orbiter spacecraft	D019
environmental testing of <i>Surveyor</i> spacecraft at JPL Environmental Test Laboratory	O007	spacecraft-based navigation instrument for outer-planet missions	D023
comparisons of waveguide losses calibrated by dc potentiometer, ac ratio transformer, and reflectometer techniques	O011	reliable interface circuit for driving field effect transistor switching trees in data handling subsystem	E001
solar–electric propulsion system tests	P006	mesh materials for deployable antenna	F005
<i>Apollo</i> gamma ray spectrometer thermal model tests	P013	inertial reference unit	H003
plasma-immersion-probe tube in metal–ceramic envelope	S025	trajectory correction engine	H015 H016
facility for testing nozzle exhaust plumes in a space environment	S044	selection of auxiliary propulsion system	H024
Thermoelectric Outer-Planet Spacecraft (TOPS) attitude-control single-axis simulator momentum-wheel tachometer circuit	S050	first-order digital phase-locked loop command system	H027
facility for testing aerodynamics of vehicles in tubes	W001	performance of all-digital command system timing loop to be used by TOPS	H028
test equipment for strapdown electrostatic aerospace navigator (SEAN) system	W014	thermal interface of radioisotope thermoelectric generators with spacecraft	L014
passive microwave link from JPL Compatibility Test Area to TRW Systems, Inc.	W026	multi-hundred-watt radioisotope thermoelectric generator transient performance	L015
		attitude control reliability study	L022
Thermodynamics		use of efficiency program to calculate feed defocusing effect in antenna	L036
acceleration and cooling effects in laminar boundary layers	B001	thermomechanical pump	S001
effect of wall cooling on mean structure of turbulent boundary layer in low-speed gas flow	B002	digital sun sensor	S015
thermal environment of multi-hundred-watt radioisotope thermoelectric generator	C006	analysis of science package pointing error due to structural vibration of supporting booms	S020
thermal conductance of alumina–nickel interfaces at elevated temperatures	H011	attitude-control single-axis simulator momentum-wheel tachometer circuit	S050
		attitude-control single-axis simulator command telemetry link	S051

Subject	Entry
Thermoelectric Outer-Planet Spacecraft (TOPS) (contd)	
cooling of infrared-radiometer	S069
analytical calculation of neutron yield from (α, n) reactions of low-Z impurities in a plutonium heat source such as TOPS'	T001
design of a thick-film microcircuit dc-to-dc converter for TOPS	W009
nuclear radiation mapping for spacecraft	W018
pyrotechnics switching	W024
Tracking	
new tropospheric range refraction model	B017
proposed method of counting doppler with the digital tracking system	B024
automatic carrier acquisition	B042
optimization of acquisition time for sequential ranging system	B046
error probability of wide-band binary frequency-shift-keyed receiver in presence of multipath fading	C015
1.0002-MHz frequency synthesizer	C042
earth based tracking for advanced planetary navigation	C048
Deep Space Network support of <i>Apollo</i> Project	F008
	H008
Deep Space Network Tracking System operations	H017
<i>Mariner</i> Mars 1969 tracking operations	J010
Deep Space Network support of <i>Mariner</i> Mars 1971 Project	L001
	L002
	L003
hybrid carrier and modulation tracking loops	L023
Deep Space Network extended operations mission support of <i>Mariner</i> Mars 1969 Project	L024
radio tracking data to be used for celestial mechanics experiment for <i>Mariner</i> Mars 1971	L033
mean-square error and bias of phase estimator for sequential ranging system	M044
Deep Space Network support of <i>Viking</i> Project	M051
charged-particle calibration system analysis	M053
effect of diurnal variation of earth ionosphere on interplanetary navigation	M056
high resolution lunar gravimetry from <i>Lunar Orbiter</i> radio tracking data	M060
solution for tropospheric zenith range correction using a single pass of differenced doppler data	O003
effects of a variable h_{\max} on the mapping of zenith ionospheric corrections to lower elevation angles	O004

Subject	Entry
Tracking (contd)	
variations in zenith tropospheric range effect computed from radiosonde balloon data	O005
Tracking and Data System support of <i>Pioneer</i> Project	R018
	R019
Deep Space Network support of <i>Pioneer</i> Project	S030
Trajectory Analysis/Orbit Determination	
second-order artificial satellite theory based on an intermediate orbit	A006
advanced planetary navigation	B029
	C047
	C048
	D020
	H002
	M026
	M046
matrizant of the two-body problem	B038
set of computer programs constructed to perform the literal series expansions of the two-body problem	B039
prediction of position and velocity of a satellite after many revolutions	D001
<i>Mariner</i> Mars 1969 approach guidance demonstration	D021
analytic expressions for the partial derivatives of observables with respect to Robertson's relativistic parameters	G003
<i>Mariner</i> Mars 1969 spacecraft trajectory analysis	J010
potential of interplanetary spacecraft data for testing gravity theories	J011
variational equations derived from Herrick variation of parameters method for obtaining partial derivatives of position and velocity of spacecraft	L026
dynamic programming approach to optimal stochastic orbital transfer strategy	N012
possible 1975 Jupiter-Pluto gravity assist trajectories	S061
Viking Project	
thermal design for orbiter system	J017
orbiter system ground handling and assembly equipment	J017
orbiter attitude-control subsystem status register	J022
proposed orbiter system attitude-control roll-reacquisition logic	J022
orbiter scan subsystem mechanization	J022
automatic sun occultation-sun acquisition control for orbiter system	J024
orbiter system inertial reference unit integrator redesign	J026

Subject	Entry	Subject	Entry
Viking Project (contd)		Wave Propagation (contd)	
orbiter system power subsystem design	J026	effect of predemodulation filtering on the correlation and error signals in a pseudonoise receiver	K028
orbiter system reaction control assembly	J026	optimum modulation indexes and maximum data rates for interplex modem	L004
optimal optical design for Mars atmospheric water detection spectrometer on orbiter system	J035	test of conical gregorian antenna	L037
orbiter relay system	J038	frequency generation and control: measurement of phase jitter	M033
orbiter radio frequency subsystem	J038	effect of diurnal variation of earth ionosphere on interplanetary navigation	M056
project description and status	J039	correction factors for near field horn antenna gain measurements	N013
	J040	variations in zenith tropospheric range effect computed from radiosonde balloon data	O005
	J041	realizability conditions on reflection coefficients of unsymmetrical, passive, reciprocal 2-port networks	O010
Deep Space Network support	M051	dipole antenna radiation in a compressible, anisotropic electron plasma overlaying an imperfectly conducting half-space: lunar applications	P016
Voice Communications		low transmitted power operation of a transmitter	R028
multiple demand access satellite systems for speech communications in remote areas	H042	<i>Orbiting Geophysical Observatory 5</i> observations of quasi-trapped electro- magnetic waves in the solar wind	S012
permutation of sequences for scrambling	K023	analysis of phase coherent-incoherent output of bandpass limiter	S059
	K024	Faraday rotation measurement of 13-cm signal in solar corona	S062
Wave Propagation		analysis of random modulation in amplifier circuits	S075
noise-adding radiometer for gain compensation	B008	angle demodulation using state-variable techniques	T006
new tropospheric range refraction model	B017	design of signals for analog communication	T014
polarization converter	B041	transmitter phase modulation as a result of beam voltage ripple	W011
approximate analysis of command lock detector performance in spacecraft telecommunications	C008	slotted lens antenna analysis	W023
microwave emission from granular silicates: determination of the absorption coefficient from plate measurements and the effects of scattering	C028		
1.0002-MHz frequency synthesizer	C042		
loop stress diminution	G007		
cyclic search algorithms for synchronizing maximal length linear shift register sequences	H032		
multiple demand access satellite systems for speech communications in remote areas	H042		